Organic geochemical study of the Upper Cretaceous to Paleogene - Neogene mudstones and coals, Central Myanmar Basin, Myanmar

By

EI MON HAN

S119705

A dissertation submitted to the Geoscience department in partial fulfilment of the requirement for the Degree of Doctor of Science (D. Sc.) at the Interdisciplinary Graduate School of Science and Engineering, Shimane University, JAPAN

March, 2014

Thesis Supervisor

Professor Dr. Yoshikazu Sampei

CONTENTS

ACKNOWLEDGEMENTS

First of all I would like to thank our Union Minister, U Than Htay, from Ministry of Energy in Myanmar, who gave permission to undertake a doctoral study and to conduct this work in Japan.

I am deeply thankful my supervisor, Prof. Yoshikazu Sampei, for sharing his limitless knowledge and guidance me a lot during his scarce time throughout the course of my research.

I would like to express my thanks to Dr. B.P. Roser for his comments and reviewing to improve the manuscript.

I am also thankful to the other members of my thesis committee (Prof. Dr. T. Irisuki, Dr. T. Sakai, and Dr. A. Takasu) for their valuable suggessions and review to improve this study.

Great thanks go to U Myint Oo (Director, Exploration and development department, Myanma Oil and Gas Enterprise), U Lynn Myint (Chief Geologist, MOGE), and U Kyin Sein (Development Geologist, MOGE), for their permissions me to take samples supporting this research.

My sincere thanks go to U Kyi Soe (Senior Executive Geologist, MOGE), U Aung Kyaw Htoo, Deputy Director from Ministry of Energy for their fruitful ideas and invaluable advice and also U Tun Nyunt Oo (Assistant Executive Geologist, leader of Field party, MOGE) and U Win Naing (Assistant Geologist, MOGE) for their help and advice during fieldwork.

I would like to express my appreciation to the Japanese Government (MEXT) for providing me financial support and generous scholarships.

Many thanks also go to all of my friends in the Science and Engineering Faculty of Shimane University for their help and kind understandings.

Last but not least I wish to express my deepest thanks to my beloved family- my parents, sisters and husband. Their love and encouragement gave me plenty of power.

ABSTRACT

Upper Cretaceous to Tertiary clastic sediments from the western margin of Central Myanmar succession have been investigated to evaluate source of organic matter (OM), maturity, hydrocarbon potential, paleo-depositional environment, and paleoclimate based on CNS elemental analysis, vitrinite reflectance, Rock-Eval pyrolysis, and gas-chromatography─mass spectrometry (GC─MS).

Ninety-four outcrop samples including coals, coaly shales, mudstones and sandstones were collected from different stratigraphic units throughout the western margin of the Central Myanmar Basin (CMB) in Upper Cretaceous and Paleogene - Neogene period. The CMB succession includes Upper Cretaceous (Kabaw Formation), Paleocene (Paunggyi Formation), Eocene (Laungshe, Tilin, Tabyin, Pondaung, and Yaw Formations), Pegu Group (Shwezetaw, Padaung, Okhmintaung, Pyawbwe, Kyaukkok, and Obogon Formations) in ascending order. Total organic carbon contents (TOC) in the western margin of Central Myanmar Basin are low containing oxidized organic matter. Sulfur contents are low in most mudstones with the exception of two coal and coaly shale, and three mudstones. The C/S ratios imply an alternating marine and non-marine related with oxic to oxygen-poor environmental conditions.

Upper Eocene coals and coaly shales show terrestrial higher land plants with lesser aquatic plants and bacteria. These sediments were deposited under freshwater oxic to oxygen poor environments such as peat swamp, estuary, lacustrine, which are influenced by marine water due to sea level rises. As the Rock-Eval pyrolysis results for unweathered coals and coaly shales, modarate hydrogen indices (HI) values (100-191 mg HC/g TOC), T_{max} values (413 – 429˚C), production indices (S_1/ (S_1+S_2) < 0.1) provided that Upper Eocene carbonaceous sediments indicate an immature in the OM. It is consistent with the vitrinite reflectance values (Ro<0.5%). The $\delta^{13}C$ values in the coals and coaly shale have been considered to be the less contributions of resinous conifers (i.e.gymnosperms) in the coaly shales. Mid-and long- chain

n-alkanes are mostly enrichment along the Central Myanmar succession. On the other hand, short chain *n*-alkanes are relatively dominant in the Upper Cretaceous to Plaeocene, Lower to middle Eocene but less in the Upper Eocene and Oligocene mudstones. Similarly, the distributions of sterane $C_{29}/(C_{27}+C_{28}+C_{29})$ values are abundant throughout the Central Myanmar succession, while the sterane $C_{27}/ (C_{27}+C_{28}+C_{29})$ are slightly enrichment in the Upper Cretaceous, Lower to Upper Eocene (Laungshe, Tilin and Yaw Formations), and Pegu Group (Padaung, Okhmintaung, Pyawbwe, and Kyaukkok Formations). The Carbon Preference Index (CPI) values are predominant in the middle to Upper Eocene (Tabyin, Pondaung, and Yaw Formations), and Pegu Group (Shwezetaw and Pyawbwe Formations), showing strongly inputs of higher plant wax. The relatively abundant distributions of oleanane/C_{30} hopane ratios along the CM succession indicate higher land plants, mainly inputs of angiosperm vegatations. The enrichment of hopane/sterane ratios throughout the CM succession shows extensive inputs of bacterial organisms.

The various combustion-derived unsubstituted PAHs (i.e non-alkylated) compounds such as, cadalene (Cad), phenanthrene (Phe), anthracene (An), pyrene (Py), fluoranthene (Fla), benzo[a]anthracene (BaAn), chrysene/triphenylene (Chry+Tpn), benzofluoranthenes (Bflas), benzo[e]pyrenes (BePy), benzo[a]pyrenes (BaPy), indeo[1,2,3-*cd*] pyrene (InPy), and benzo (ghi)perylene (BghiP), and coronene (cor) were detected all mudstone samples. The distributions of methyl derivatives compounds such as methylphenanthrenes (3-MP, 2-MP, (9+4)-MP, 1-MP) were detected in the Upper Cretaceous, Lower to Upper Eocene (Laungshe, Tabyin, Pondaung, and Yaw Formations), and Pegu Group (Shwezetaw Fm.), showing immature OM due to significant isomers of (9+4) MP and 1 MP. Upper Cretaceous samples are relatively predominance of 2- and 3- MP isomers, indicating early mature stage. It can be aggrement with the sterane C_{29} 20S/(20S+20R) with values of greater than 0.5.

Similarly, the relatively abundant concentration of pimathrene (1,7 DMP) compound in the above formations can suggest a partly contribution of resinous conifers, especially gymnosperms. Gymnosperm marker retene is more significant in the middle Eocene (Tabyin Fm.) and Pegu Group (Shwezetaw, Padaung, and Okhmintaung Formations), suggesting an influence of gymnosperm vegetations at that time. Upper Cretaceous to Paleocene, Lower to Upper Eocene (Laungshe, Tilin, Pondaung, and Yaw Foramtions), and Pegu Group (Pyawbwe, Kyaukkok, and Obogon Foramtions) mudstones have less abundant contributions of retene, showing a small distributions of gymnosperms. Similarly, Upper Eocene coals and coaly shales show a contribution of resinous conifers. Fungi-derived Perylene contents are more dominant in the middle to Upper Eocene and Pegu Group mudstones, indicating humid climatic condition and oxygen-poor environments.

The WMCMB has been classified into three phases based on biological markers. In the first phase (Upper Cretaceous to Paleocene) mudstones, the OM was sourced from terrestrial land plants including angiosperms with a minor amount of aquatic plants accumulated under oxic to oxygen-poor conditions with periodically marine water influences. Aquatic materials are more significant in the Upper Cretaceous mudstones. Gymnosperms are less contributions in the first phase. Lesser contents of perylene show dry condition. The second phase (Lower to Upper Eocene) mudstones consists of abundant inputs of terrestrial land plants with lesser amount of aquatic plants and bacteria, deposited in the freshwater oxic to anoxic conditions with frequent marine water fluctuation due to sea level rises. Lower Eocene (Laungshe Fm.) and middle to Upper Eocene (Tilin and Yaw Formations) contains more aquatic materials. Gymnosperms are more predominant in the middle Eocene mudstones, while less abundance in the other mudstones. Low to high contents of perylene indicate dry (warm) to wet (humid) climatic conditions. The third phase (Pegu Group: Oligocene to Miocene) mudstones contain mixing inputs of terrestrial higher plants including angiosperms and gymnosperms and aquatic

plants accumulated under oxic to anoxic conditions with periodic sea water influence according to eustatic sea level changes. Aquatic materials are more abundant in the middle to Upper Oligocene (Padaung and Okhmintaung Formations) and middle Miocene mudstones (Pyawbwe and Kyaukkok Formations). Oligocene mudstones (Shwezetaw, Padaung, and Okhmintaung Formations) show abundant contributions of gymnosperm vegetations. Perylene contents are relatively higher in the third phase indicating wet (humid) climatic conditions. Various maturity parameters for mudstones in the western margin of Central Myanmar succession (WMCMS) showed an immature to very early mature in the OM. According to the Hydrogen Index (HI~ 200 mg HC/g TOC) values of the Upper Eocene coals and coaly shales in the CMB, potential of hydrocarbon generation is reasonably good, mostly gas prone.

Based on inorganic geochemical data of the mudstones and sandstones, Upper Cretaceous to Eocene deposits were mostly generated from intermediate sources and the Pegu Group is from recycled materials associated with continental island arc. Upper Cretaceous and Paleocene mudstones would be mainly sourced from both tectonically stable Eurasia Plate and active continental margins. Eocene and Oligocene mudstones have been generated from active continental margins such as uplifted Myanmar margins and Himalaya and partly from passive margin (i.e. Eurasia Plate). Some Oligocene and Miocene mudstones are sourced from both passive margin and Himalaya during active tectonism. Upper Cretaceous to Eocene materials are also partly originated from Myanmar magmatic arc as mafic source. The Pegu Group (Oligocene and Miocene) mudstones and sandstones were probably generated from both Myanmar margins and Himalayan detritus. The Pegu Group shows recycled quartzose materials and Eocene sediments indicate partly inputs of recycled materials. Chemical Index of Alteration (CIA) values indicate moderate to high source weathering in the Upper Cretaceous to Miocene mudstones may exhibit alternating shifts of dry (hot) and wet (humid/seasonal) climatic conditions.

LIST OF FIGURES

LIST OF TABLES

CHAPTER 1. INTRODUCTION

1.1 Objectives

In order to improve the overall organic and inorganic geochemical information available for the Central Myanmar Basin, the present study emphasized to investigate the origin and type of OM, thermal maturity; to reconstruct the records of marine and non-marine environments; to evaluate hydrocarbon potential of upper Eocene coals and mudstones; to identity the paleoclimates and paleowildfires; to determine provenance, tectonic setting and source weathering history throughout the Late Cretaceous to Miocene succession in the Western margin of the Central Myanmar Basin (WMCMB), Myanmar. These factors will be identified using mudstone, coals and sandstone samples throughout the different stratigraphic units from the WMCMB.

1.2 Significance

The Central Myanmar Basin (CMB) has been reported in geological, sedimentological, hydrocarbon prospects and geochemical studies (Chhibber, H.L. 1934; Maung Lwin, K., 1972; Aung et al., 1974; Myint et al., 1977; Bender, F. 1983; Khin, J.A., 1991; J.A. Curial et al., 1994; Pivnick et al., 1998). Previous work emphasized by J.A. Curial *et al*. discussed the oil family including chemical composition of oil and possible source rocks of CMB. The present study will specifically identify the origin of OM, thermal maturity, depositional environment, and paleoclimates of the CMB using organic geochemical results.

Geochemical compositions of the Central Myanmar sedimentary rocks have been partially used to investigate tectonic setting using Paleogene and Neogene sediments of Indo-Myanmar Ranges (Allen, 2008; Mitchell, 1993) and upper Eocene sediments from Chindwin Basin which forms north of the CMB and eastern flank of CMB (Licht et al., 2013). The present study will identify source rock composition, tectonic setting, weathering history, and

paleoclimates using the geochemical compositions of sedimentary rocks from the WMCMB. In this study, geochemical data will contribute a better understanding on the geological processes of provenance, tectonic setting and weathering history of the Central Myanmar succession which is a part of Inner-Myanmar Tertiary Basin (IMTB).

1.3 Location and Background

The Central Myanmar Basin (CMB) is one of the sub-basins of the Inner- Myanmar (Burman) Tertiary Basin (IMTB) in Myanmar. The IMTB is located between the Shan Plateau to the east and a right lateral strike-slip fault (also known as Sagaing fault) to the west (Fig. 1.1). This basin has been filled with fluvio-deltaic sediments transported by the numerous Asia's great rivers systems including Irrawaddy River (Fig. 1.2). Sediments derived from the continents in N and NE, were deposited in the northern mountains of Myanmar (Hadden, 2008) and continuing southwards in the present day Irrawaddy deltaic system and Gulf of Martaban (Chhibber, 1934). Sedimentation of the north-to-south prograding continental deposits in the marine environments was until the end of Miocene (Bender et al., 1983).

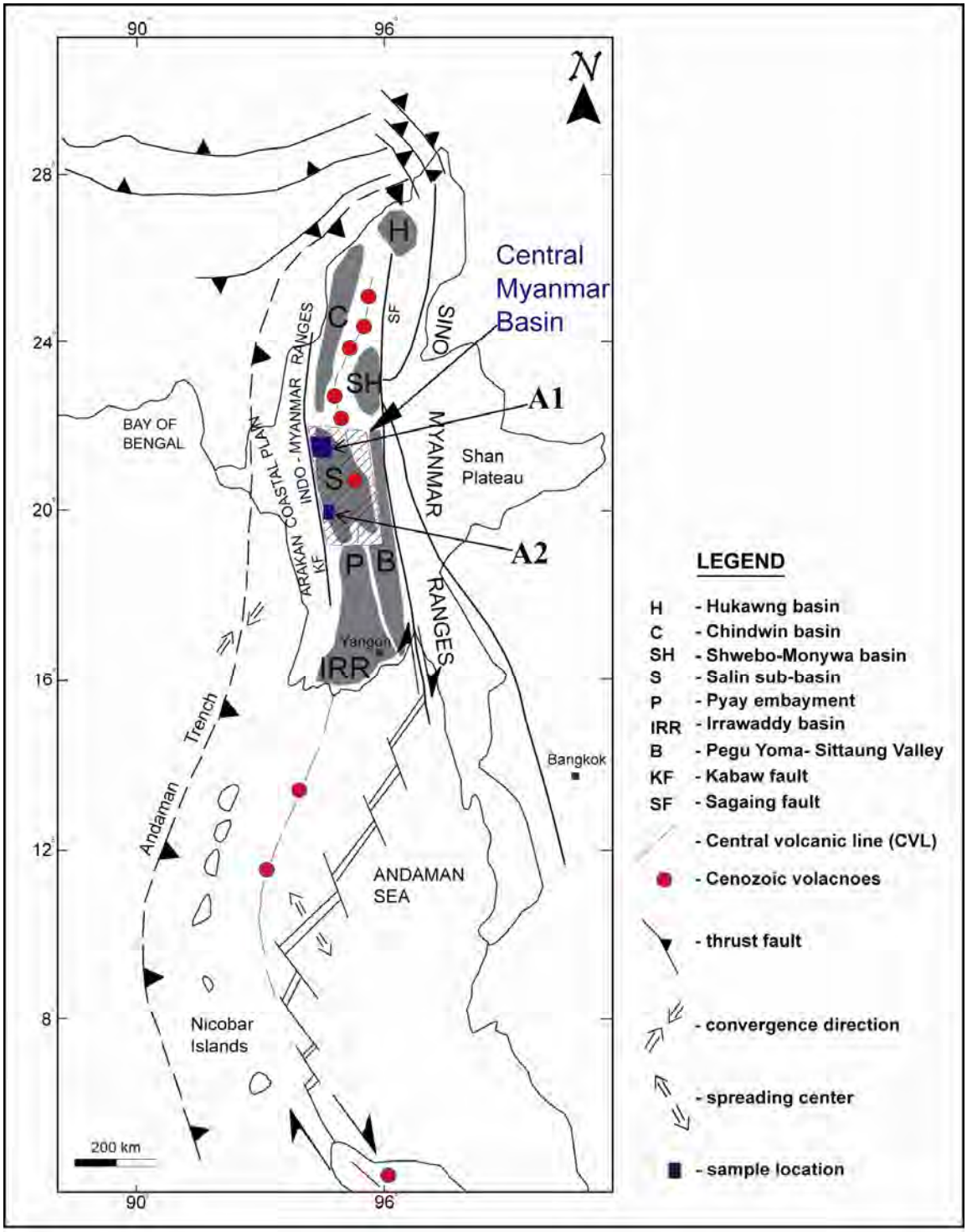

Fig. 1.1. Map showing study areas in the western margin of the Central Myanmar Basin and other sub-basins, Myanmar. (modified from Pivnik et al., 1998)

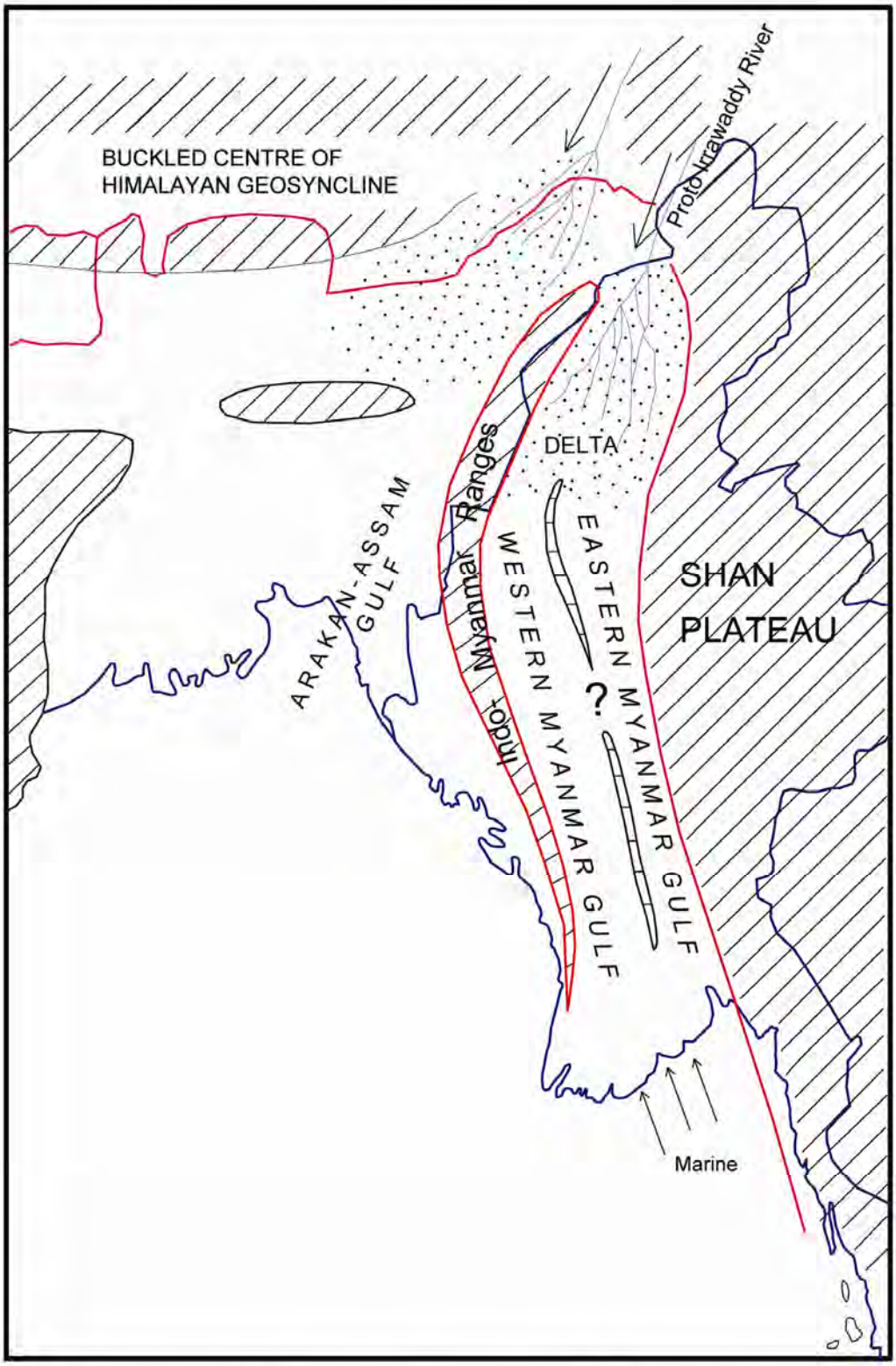

Fig.1.2. Map showing Myanmar (Burmese) Gulf with the position of the Irrawaddy River in the early Tertiary Period (Chhibber, 1934)

1.3.1 Central Myanmar Basin (CMB)

The CMB is a complex fore-arc/back-arc basin, and is situated between a major right-lateral strike slip fault in the east, and the obliquely converging India plate beneath the Myanmar (Burma) micro-plate to the west (Pivnik et al., 1998). It is one of the largest petroliferous onshore sub-basins within the IMTB.

The IMTB was occupied by the sea until the Miocene period, by which time it had filled with Tertiary clastic sediments underlain by Mesozoic deep-water sediments and older metamorphic basements (Chhibber, 1934; Bender, 1983). The IBTB is divided into a number of individual onshore sub-basins: Irrawaddy Delta, Pegu Yoma- Sitaung valley, Pyay Embayment, Central Myanmar, Shwebo- Monywa, Chindwin, and Hukawng (Bender, 1968; Khin J.A., 1991)

The Central Myanmar Basin (CMB) formed as a subsiding sub-basin within the IMTB. The CMB has been well-known as the Salin sub-basin or Minbu sub-basin. However, the CMB is loosely wider than the Salin sub-basin (Fig. 1.1). The total stratigraphic thickness of the CMB succession is very high, reaching about 19 km (Tun, 1968; Myint and Soe, 1977). The large depth of the CMB is considered to be due to tectonic subsidence (i.e. oblique subduction of Indian oceanic plate underneath the Myanmar micro-plate) by sediment loading (Hall and Morley, 2004).

Curiale et al. (1994) suggested that Eocene and lower Oligocene source rocks reached the minimum maturity for hydrocarbon generation. The tectonic and volcanic activity would be favourable to increase temperatures and have affected little on regional maturation (Wandrey, 2006).

Bender (1983) mentioned that rocks of Miocene age in the Gulf of Martaban indicate that it was sufficiently mature to generate hydrocarbons. Burial depths in the Inner-Myanmar (Burman) Tertiary Basin were generally increasing from north to south, with the youngest

Miocene source rocks found in the Gulf of Martaban and northern Andaman Sea (Matthews, et al., 2000).

Khin (1991) suggested that the source rocks in the CMB must be deeper because samples taken from depths of 3 km in the Basin yield 0.5 % Rm.

Tertiary coal seams are widely distributed in the CMB and other sub-basins of the IMTB. Coals of Eocene age can be found in Kyaukset Village in the Minbu district, and in Tazu and Letpanhla Villages in the Pakokku district within the CMB. Coal seams in this district generally vary from 1.2 and 2.1 m in thickness (Bender, 1983).

Curial et al. (1994) speculated that Eocene coals in the CMB could be one of the source rocks for the oils/gas found in the CMB based on composition of hydrocarbon compositions.

This basin has been divided by the Central Volcanic line (CVL) into the Eastern Trough (ET) and Western Trough (WT) (Mitchell, 1993). The ET contains a series of en echelon, elongated anticline features. Current hydrocarbon production in Myanmar is associated with this structure. Similarly, several hydrocarbon seepages and hand-dug wells have been found throughout the WT (Bender et al., 1983; Trevena et al., 1991; Curial et al., 1994).

The Late Mesozoic to Paleogene sediments are well-outcropped along the eastern flank of the Indo-Myanmar Ranges (Bender, 1983) and western margin of the CMB. The CMB has been reported in geological, sedimentological, hydrocarbon prospects and geochemical studies (Chhibber, 1934; Bender, 1983; Khin, 1991; Curial et al., 1994; Pivnick et al., 1998; Hadden, 2008). However, organic and inorganic geochemical studies of sedimentary rocks in the Central Myanmar Basin have been limited.

1.4 Definition of kerogen, bitumen and types of Kerogen

Kerogen is the most important structure of organic carbon on earth (Tissot and Welte, 1984). The term “kerogen” has been well known as the organic constituent of the sedimentary

rocks which is insoluble in aqueous alkaline solvents or organic solvents. It is composed of different basic materials with variable proportions and some of them can be defined as macerals. Kerogen contains no bitumen that is soluble organic matter separated from kerogen by extraction with organic solvents. Bitumen is composed of asphaltenes, resins, and hydrocarbons (aromatic HC and saturated HC).

Types of kerogen can be classified as Type-I, Type-II, and Type-III kerogens. Three types of kerogen can be identified by their respective evolution path in the van Krevelen (H/C, O/C) diagram (Tissot and Welte, 1984). The van Krevelen diagram was first proposed by van Krevelan (1961) to characterize coals and colification paths of different macerals based on H/C and O/C ratios.

Type-I kerogen comprises many aliphatic chains, and few polyaromatic nuclei. This type of kerogen yields high initial H/C atomic (ca. 1.5 or more) and low initial O/C atomic (generally <0.1) (Tissot and Welte, 1984). The organic matter is mainly sourced from algae.

Type-II kerogen is particularly frequent in many petroleum source rocks and oil shales, with relatively high H/C and low O/C ratios and comprises more aromatic rings. It is likely associated with marine OM, sourced from phytoplankton, zooplankton and microorganisms (i.e bacteria), has been accumulated in an anaerobic environment, with medium to high sulphur content. (Tissot and Welte, 1984)

Type-III kerogen yields low initial H/C atomic (<1.0) and high initial O/C atomic ratios (≥0.2 or 0.3) and comprises mostly condensed polyaromatics, minor constituents of aliphatic groups and oxygen-containing groups, but no ester group. The organic matter in the kerogen is made up mostly of terrestrial higher plants. Although this type of kerogen is generally less favourable for liquid hydrocarbon generation than types I and II, it may provide to occur gas source rocks if burial depth is sufficient. (Tissot and Welte, 1984)

CHAPTER 2. GENERAL GEOLOGY

2.1 Inner-Myanmar Tertiary Basin or Central Lowlands

Myanmar can be divided into four provinces: the Eastern Highlands (EH), the Central Lowlands (CL), and the Western Fold belt (WFB), and Arakan Coastal Plain (ACP) (Fig. 2.1). Eastern Highlands on the east and Arakan Yoma comprising WFB on the west, were uplifted into land masses at the beginning of the Tertiary or end of Cretaceous period. A low and narrow barrier was occurred between these two land masses, was known as Burmese Gulf. This Burmese Gulf has been occupied by the sea until very Late Tertiary period. It was gradually subsiding while the Arakan Yoma was ever uplifting throughout the Tertiary period and filled with Tertiary sediments (Chhibber, 1934). The latter, it was known as the Central lowlands or Inner-Myanmar Tertiary Basin.

The collision of Indian Plate relative to the rest of Asia Plate took place the northward movement of Myanmar (Burma) micro-plate, which was rotated to 90˚ of clockwise direction to reach present position (LeDain et al., 1984; Everett et al., 1990). The Myanmar micro-plate is composed of Mesozoic metamorphic basement rocks, Tertiary materials, volcanic and magmatic rocks (Bender, 1983; Pivnik et al., 1998). This plate has experienced with a complex tectonic activities such as collision of India with the margin of Asian in the Paleocene (~ 55–49 Ma, Bender, 1983; Zhu et al., 2005), Eocene (50 Ma, Najman et al., 2010; Meng et al., 2012) and northeastward subduction of oceanic plate underneath the Myanmar micro-plate (Win Swe, 1981a). This subduction generated a Late Cretaceous magmatic arc (presently known as Central Volcanic Line) in Myanmar micro-plate (Mitchell, 1993). The interrupted occurrence of magmatism during latest Cretaceous to Mid-Eocene (Mitchell, 1993) may indicate shallow subduction of oceanic plate. The collision of Indian plate with Eurasia plate occurs uplifts of the IMRs, Eastern Himalayas regions and Tibet during the Oligocene-Miocene (Chhibber, 1934; Aitchison et al., 2007).

Licht et al. (2013) reported that the IMRs were not uplifted until early Oligocene and the IMTB connected with the Indian Ocean at that time.

The progressive occurrence of the strong collision of Indian Plate relative to Myanmar micro-plate after middle Eocene (Alam et al., 2003) might be responsible to induce a little uplifting areas along the Arakan Yoma in the west as long narrow islands.

Myanmar micro-plate includes the CL and Indo-Myanmar Ranges (IMRs). The Central Lowland (CL) is developed parallel to the subduction of marine and continental boundaries.

The Inner- Burman Tertiary Basin (also known as CL) was progressively deposited in the south by transgressive shallow marine shales, argillaceous sands and carbonatic sediments of the Tertiary, which interfinger towards the N and NE with fluvio-deltaic non-marine deposits of the same age (Bender, 1983).

The IMTB contains a series of pull-apart sub-basins, which were affected by the oblique subduction of the Indian oceanic Plate underneath the Myanmar micro-plate during early Eocene (Tankard et al., 1994). The formations of local sub-basins in the IMTB could be identified after the middle Miocene (Bender, 1983). The CMB is one of the sub-basins formed in the IMTB. This basin developed parallel to the converging oceanic and continental boundaries (Wandrey, 2006).

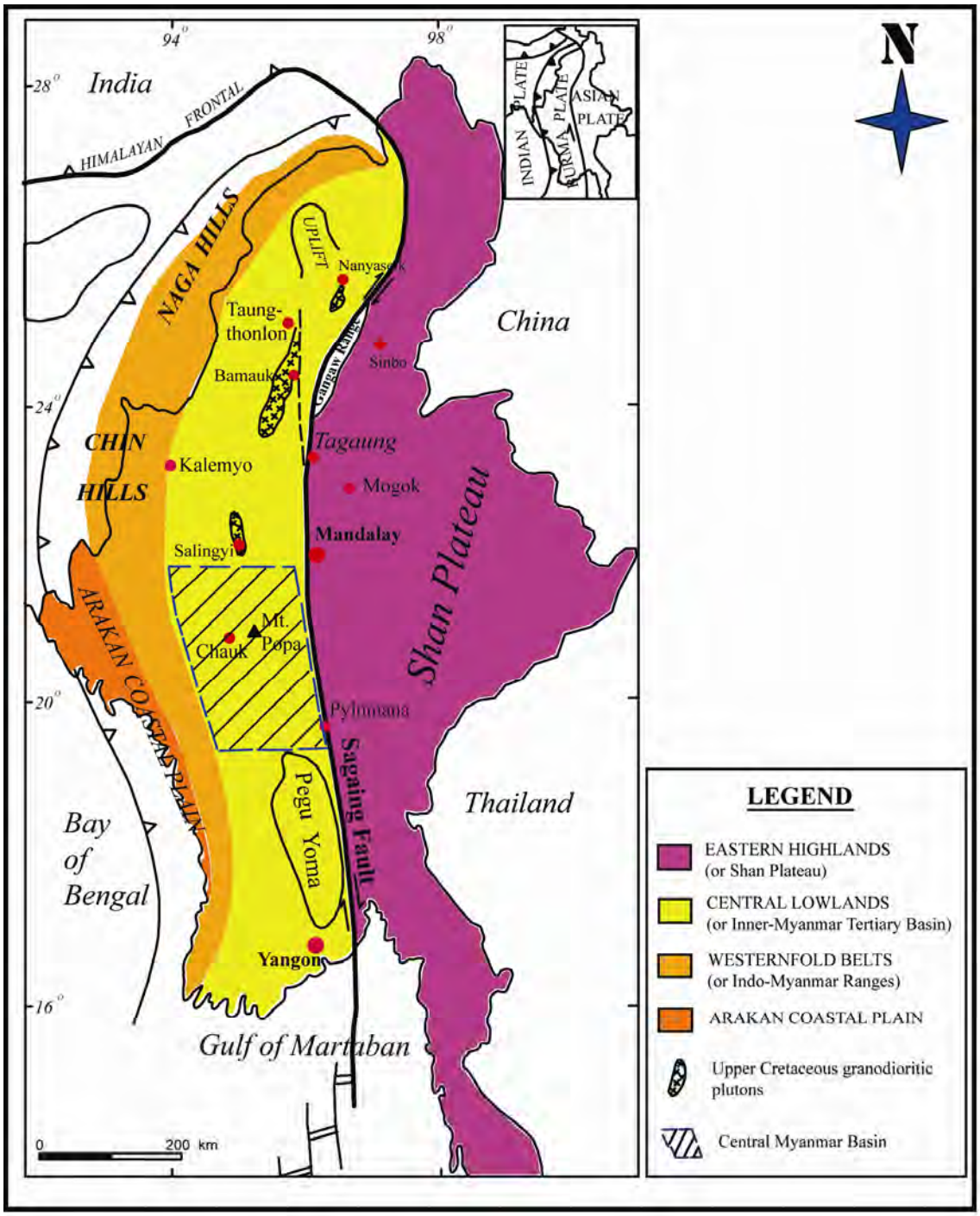

Fig. 2.1. Geolomorphological and structural Map of Myanmar (Burma). (modified from Chhibber, 1934, Mitchell, 1993, Pivnik et al., 1998)

2.2 Central Myanmar Basin (CMB)

2.2.1 Stratigraphy

The Cenozoic and Cretaceous deposits are well exposed along the western margin of the Central Myanmar Basin (CMB). During Cretaceous, only Upper Cretaceous Kabaw Formation was exposed in the study area. Upper Cretaceous sediments were overlain by conglomeratic sediments of Paleocene age in Tertiary period (Tun, 1968, F. Bender, 1983). The general sedimentary stratigraphic succession and associated formations of the basin are illustrated in Table 2.1.

The Eocene sequence in the CMB is divided into five major stratigraphic units, which are Laungshe Formation (Early), Tilin Formation (earliest Middle), Tabyin Formation (latest Middle), Pondaung Formation (earliest Late), Yaw Formation (latest Late) in ascending order. The Oligocene sequence is divided into the Shwezetaw Formation (Early to Middle), Padaung Formation (Middle) and Okhmintaung Formation (Late).

The Miocene unit is divided into three lithologic units: Pyawbwe Formation (Early), Kyaukkok Formation (Middle), and Obogon Formation (Late).The Pyawbwe Formation is composed mainly of light-grey mudstone.

2.2.1.1 Upper Cretaceous

(a) Kabaw Formation

The Kabaw Formation was underlain by older metamorphic sediments. The contact between the metamorphic sediments and the kabaw Formation is highly disturbed by faulting and metamorphosed in the study area (Fig. 2.2), The Kabaw Formation was estimated about 1000–2500 m in thick and became thinnly southwards. In the study area, due to incompetent nature and highly affected by tectonic (variable dip and strike), it is difficult to estimate the exact stratigraphic thickness.

The Kabaw Formation consists of grey to dark-brown, bluish-grey, thin-bedded, moderately hard, nodular, carbonaceous shale, interbedded with fine-grained, sandstones. The tuffaceous sandstones (ca.5–10 ft; Fig. 2.3), and limestones are found in some places. It was deposited on continental slope under marine environment as indicated by sedimentary features and lithological characters (Tun, 1968; Bender, 1983), and suggested that deposition under deeper marine environment based on evidence of fossils (Myint and Soe, 1977).

Fig. 2.2. Faulted contact between older metamorphic rocks and the Kabaw Formation (Upper Cretaceous) in the A2 study area.

Fig. 2.3. Tuffaceous sandstone in the Kabaw Formation (Late Cretaceous) in the A2 study area.

2.2.1.2 Paleocene

(a) Paunggyi Formation

In the present study area, the contact with the underlying Kabaw Formation is unconformable. The thickness of the Paunggyi Formation varies from 900-1800 m according to its position in the study area. It consists mainly of yellowish brown sandstones, interbedded with gritty to conglomeratic sandstones, and tuff beds (ca.3–5 ft) in the lower part of this formation. The tuff beds suggest that volcanic eruption occurred during deposition. (Myint and Soe,1977; Bender, 1983). The bluish-grey, thinly bedded, soft shales are alternating with above gritty sandstones.

The gritty sandstones and conglomerates increase in the northern part and decrease in amount southwards as the shale contents gradually increase in the study area. During the deposition of this Formation, it was considered to be deposited under shore line (Tun, 1968).

Table 2.1. Generalized lithostratigraphic succession of the U-Cretaceous to Miocene in the western margin of the CMB, Myanmar (After Bender, 1983; T. Htut, 2008). Sampling formations are shaded.

Age			Group	Formation	Lithology	no: of samples	Depositional Environments
QUATERNARY			Pegu Group	Irrawaddy	Sandstone, siltstone, clay, comglomerates		Fluvial, non-marine[e]
NEOGENE	PLIOCENE						
	MIOCENE	Upper		Obogon	Shale, sandstone	4	shallow marine[c,e]
		Middle		Kyaukkok	Sandstone, shale	4	near shore, deltaic[c,e]
		Lower		Pyawbwe	Shale, sandstone	3	shallow marine[e]
PALEOGENE	OLIGOCENE	Upper		Okhmintaung	Sandstone, shale, silt	6	near shore[c]
		Middle		Padaung	Shale, sandstone	7	shallow marine[c]
		Lower		Shwezetaw	Sandstone, shale, silt, minor lignites	9	Swamp, deltaic[c]
	EOCENE	Upper		Yaw	Shale, sandstone, silt, minor coal	10	shallow marine, lagoon[a.h]
				Pondaung	Sandstone, shale, minor coal	4	near shore, delta plain[c,g]
		Middle		Tabyin	Shale, sandstone	8	shallow marine[d,e]
				Tilin	Sandstone, shale	4	near shore[d,e]
		Lower		Laungshe	Shale, sandstone	11	shallow marine[e]
	PALEOCENE			Paunggyi	Conglomerates, shale, sandstone	4	Alluvial or shore line[e]
	UPPER CRETACEOUS			Kabaw	Shale, sandstone, minor Lst.	13	shallow marine[b,e]

[a]Chhibber, 1934; [b]Tun, 1968; [c]Aung and Myint, 1974; [d]Myint and Soe, 1977; [e]Bender, 1983; [f]Aung and Myint, 1974; [g]A.N.Soe et al., 2002; [h]Wandrey, 2006

2.2.1.3 Lower Eocene

(a) Laungshe Formation

The Laungshe Formation is conformable contact with the underlying Paunggyi Formation. The stratigraphic thickness of the Laungshe shales is approximately 900–5000 m. This formation is characterised by grey to dark-grey, bluish-grey, nodular in places, moderately hard, carbonaceous shales. The yellowish-brown, tuffaceous, argillaceous sandstones are interbedded with the above shales. This Formation was deposited under shallow marine condition as evidenced by sedimentary features (Tun, 1968; Bender, 1983).

2.2.1.4 Middle Eocene

(a) Tilin Formation (Lowermost Middle Eocene)

The contact with the underlying Laungshe Formation was found to be conformable. The thickness of the Tilin sandstones is approximately 500–1000 m in the present study. This Formation consists of thin-bedded to well-bedded, yellowish brown sandstones and alternating with thin-bedded, light-grey, soft shales. This Formation is poorly exposed along the section in the southern part of the present area. It was accumulated near shore condition as evidenced by fossils and sedimentary features. Alteration of marine shales and thin-bedded to well-bedded sandstones suggest that transgression and regression frequently occurred during deposition (Tun, 1968).

(b) Tabyin Formation (Uppermost Middle Eocene)

The Tabyin Formation is composed mainly of light-bluish-grey to grey shales, nodular structure in places, interbedded with yellowish-brown, thin-bedded, argillaceous sandstone.

The thickness of this formation is approximately 2000–4000 m. It was deposited under shallow marine environments which may be shallower than Laungshe Formation (Tun, 1968).

2.2.1.5 Upper Eocene

(a) Pondaung Formation (Earliest Upper Eocene)

The Pondaung Formation is composed mainly of yellowish-brown, well-bedded to massive sandstones, coal seams in some places, alternating with light-grey, thinly bedded, and carbonaceous, sandy shales. This formation is approximately 1500 m in thick.

It was accumulated partly under brackish swampy water condition and near shore fluvial environments as evidenced by fossils and sedimentary features (Myint and Soe, 1977).

(b) Yaw Formation (Latest Upper Eocene)

The Yaw Formation is extensively exposed in the Western ourtcrops. It comprises mainly nodular, bluish-grey shale, fine-grained sandstones with coal seams in places, and occasionally limestone beds in top of the Formation. The thickness of this formation is approximately 500–1500 m. Generally, this formation is more arenaceous around the Mann chaung.

It was deposited under shallow marine environment as evidenced by fossils. (Chhibber, 1934; Myint and Soe, 1977; Bender, 1983)

2.2.1.6 Oligocene

(a) Shwezetaw Formation (Lower to Middle Oligocene)

The Shwezetaw Formation is composed of yellowish-brown sandstone, interbedded with laminated light-grey shale, and some small coal seams in places. This formation attains a maximum thickness of 500 m in the study area.

(b) Padaung Formation (Middle Oligocene)

The Padaung Formation consists mainly of grey shale, interbedded with fossiliferous marl bands, gluconitic sandstone layers in the basal part of this formation, and with minor limestone (approximately 3 feet) in the upper part. It has a maximum thickness of 300 m in the study area.

(c) Okhmintaung Formation (Upper Oligocene)

The Okhmintaung Formation is characterised by well-bedded, yellowish-brown sandstones, and interbedded with thinly bedded grey shale. Generally, this formation become more arenaceous around the Mann chaung.

The contact between the Oligocene unit and the overlying Upper Miocene is unconformable.

2.2.1.7 Miocene

(a) Pyawbwe Formation (Lower Miocene)

The Pyawbwe Formation consists mainly of arenaceous, thin-bedded grey shales. The stratigraphic thickness is approximately 200–300 m. This formation is absent in the northern part of the study area.

(b) Kyaukkok Formation (Middle Miocene)

The Kyaukkok Formation consists mainly of medium-bedded, grey sandstones, interbedded with shaly and silty beds. It is approximately 300m in thick.

(c) Obogon Formation (Upper Miocene)

The Obogon Formation comprises arenaceous shale, clays, siltstones and sandstones, deposited in shallow marine or beach. This thickness of the formation is estimated approximately 200m. It is not exposed in the northern part of the study area.

Bender (1983) mentioned that Miocene strata in the Irrawaddy delta sub-basin, which is formed in the south of CMB, were deposited under marine condition, whereas they were under non-marine condition in the Chindwin basin, which is formed in the north of CMB. In the CMB, Miocene strata were locally formed under non-marine.

2.2.2 Structure

The Mesozoic-Tertiary Basin was divided by Central Volcanic line (CVL) into the back-arc and fore-arc basins (Mitchell, 1993). The present study area is located in the fore-arc basin. North-south running Sagaing fault (Fig. 2.1) separates the Shan Plateau (Eastern Highlands) from the Central Lowlands. The Kabaw fault (KF; Fig 1.1), which forms along the eastern foot of the Indo-Myanmar Ranges, delimits the Central Lowlands from the Indo-Myanmar (Burman) Ranges. Major faults are N-S trending and cross-faults are found in places. The Salin synclinorium is the prominent structural feature in the CMB. It is an asymmetrical syncline with a steeper eastern flank of the basin. The axial trend is generally N-S but in some parts it slightly deviates to NNW-SSE direction. The eastern flank of the Salin syncline, which is associated with the elongated asymmetrical anticline, is being currently produced oil and gas in Myanmar.

In contrast, hydrocarbon seepages are very common and the stratigraphic units are generally east-dipping in the western flank of the Salin syncline. The western flank of the Central Myanmar basin is well-knowns as “Western outcrops”. Structurally, it is a broad monocline, dipping towards the east, in which local sporadic folds were developed. The present study area is located in the western flank of the Salin syncline.

CHAPTER 3. MATERIALS AND METHODS

3.1 Materials

3.1.1 Outcrop samples

The present study was based on 100 outcrops samples including coals, coaly shales, mudstones, and sandstones from upper Cretaceous to Miocene age throughout the western margin of the Central Myanmar Basin. The thickness of each lignite seam from Upper Eocene is ranging from 5 to 150 cm. Late Cretaceous to Late Eocene sediments were collected along the Padan- Gokkyi, Tilin-Akyiban road section. Middle Eocene to Miocene samples were collected from the Mann Chaung river section, Ngape township, Pauk- Yebyu, Pauk-Tilin road sections. The outcrop photographs for upper Cretaceous to Miocene samples are shown in Figs 3.1 to 3.13.

Fig. 3.1. Outcrop photo of A2-26 from Obogon Formation (Upper Miocene).

Fig. 3.2. Outcrop photo of A2-20 from Kyaukkok Formation (Middle Miocene).

Fig. 3.3. Outcrop photo of A2-9 from Pyawbwe Formation (Lower Miocene).

Fig.3.4. Outcrop photo of A2-7 from Okhmintaung Formation (Upper Oligocene).

Fig.3.5. Outcrop photo of A1-103 from Padaung Formation (Middle Oligocene).

Fig.3.6. Outcrop photo of A1-109 from Shwezetaw Formation (Lower to Middle Oligocene).

Fig.3.7. Outcrop photo of A1-99 from Yaw Formation (Upper Eocene).

Fig.3.8. Outcrop photo of A1-115 from Pondaung Formation (Upper Eocene).

Fig.3.9. Outcrop photo of A1-129 from Tabyin Formation (Middle Eocene).

Fig.3.10. Outcrop photo of A1-164 from Tilin Formation (Middle Eocene).

Fig.3.11. Outcrop photo of A1-157 from Laungshe Formation (Lower Eocene).

Fig.3.12. Outcrop photo of A1-137 from Paunggyi Formation (Paleocene).

Fig.3.13. Outcrop photo of A2-71 from Kabaw Formation (Upper Cretaceous).

3.2 Methods

3.2.1 CHNS elemental analysis

Eight coal and coaly shale samples, and 86 mudstone and sandstone samples from Late Cretaceous to Miocene age were analysed by EA1108 Elemental Analyzer (FISONS Co. Ltd) to determine total organic carbon (TOC), total nitrogen (TN), and total sulphur (TS) contents. Each sample was prepared by air drying, cleaned with ethanol to remove any surface contamination, and powdered in an iron pestle. Each powdered samples were weighed ca. 5 mg for coal and coaly shale samples, ca.10 mg for mudstones and then were placed in silver capsules, pre-treated with 1M HCL to remove carbonate, and then dried at room temperature. Samples dried at 110°C for 45 min. were then placed in tin capsules and sealed. Ash contents of the coals were determined by heating in a muffle furnace at 850˚C for 2 hours. BBOT standard [2,5-bis-(5-tert-gutyl-benzoxazol-2-yl)-thiopene] was used as calibration for this analysis.

3.2.2 Rock-Eval pyrolysis

Eight coal and coaly shale samples were selected to determine for Rock-Eval analysis. Rock–Eval analysis was carried out to evaluate the potential hydrocarbon generation and maturity of the Late Eocene samples, using a Rock-Eval 6 instrument. Powdered samples (ca. 100 mg) were heated from 300ºC to 600ºC (300–650ºC for kerogen) in a helium flow. The amounts of hydrocarbons released from organic matter were then used to determine hydrogen index (HI mg HC/g TOC), oxygen index (OI mg HC/g TOC) and maximum temperature of hydrocarbon generation (T_{max}). This analysis was performed by the JAPEX Research Center.

3.2.3 Microscopic observation and vitrinite reflectance (R_o)

Vitrinite reflectance (R_o) measurements were made of 8 samples including coals and coaly shales. Coal and coaly shale chips (ca. 2 mm) were embedded in an epoxy resin which was allowed to set for 24 hrs. The mounts were then polished using water-lubricated silicon carbide paper of different meshs (320, 600), and finished to a highly reflecting surface using a mesh of 0.05 μm and finer grade alumina polishing powders.

For upper Cretaceous to Miocene samples, the manually crushed sandstone samples were treated with HF for (7) days prior to microscopic analysis.

Reflectance measurements were made on coals, coaly shales and sandstones with oil immersion in 546 nm reflected light, using a Lambda Vision-OLYMPUS microscope equipped with a TFCAM7000F-LA100USW spectrograph system.

3.2.4 Carbon isotopes of the OM

Eight coal and coaly shale samples were measured for carbon isotopes ($\delta^{13}C$). Pulverized samples and oxidized copper were placed in quartz tubes and vacuumed, then heated at 900˚C

for 2 hours. The CO_2 from the samples was analyzed by Geoscience Laboratory Inc. (Chikyu Kagaku Kenkyusho).

3.2.5 Fourier transform infrared (FT-IR) spectroscopy

Functional groups of the kerogens and bitumens in the coals and coaly shale samples were identified by means of FT-IR spectroscopy. FT-IR is well established as a useful technique for the identifying chemical characteristics of maceral in coals and kerogen in source rocks (Fujii et al., 1970; Painter et al., 1978; Blob et al., 1988; Rochdi and Landais, 1991), and to determine the different structures of coals during oxidation (Mae et al., 2000). Furthermore, it has also been known as a useful tool to determine maturity stage and types of kerogens (Wang et al., 1983; Ganz and Kalkreuth, 1987)

The kerogens and bitumens were measured by FT-IR at Shimane University, using a JASCO FT/IR- 660 spectrometer. We measured the infrared spectra in the 400 – 4000 cm^{-1} wave number range. Extracted samples ca. 1 mg in weight were powdered in an agate mortar with 100 mg potassium bromide (KBr) for 2 min, and then pressed into pellets.

3.2.6 Pyrolysis-Gas chromatography and Mass spectrometry (GC-MS)

Coal and coaly shale samples were pyrolysed at 600ºC after removal of free hydrocarbons and non-hydrocarbons using the 9:1 DCM-methanol solvent, using a double-shot pyrolyser (PY-2020D) connected to a GC-17A gas chromatograph coupled with a mass spectrometer (*m/z* 35–600; Shimadzu GC-MS QP5050A). The GC oven was operated with a 30 m fused silica column (DB 5MS, 0.25 mm i.d., 0.25 μm film thickness). Helium was used as the carrier gas. The GC oven temperature stepped from 40 to 300ºC (held for 12 min) at 15ºC min^{-1}. The interface was set at 280ºC.

Same samples with acid-treatment (ca. 1 mg for kerogens and ca. 0.5 mg for bitumens) were analyzed at pyrolysis temperatures of 600ºC, using a double-shot pyrolyser (PY-2020D: small SUS cup slide-down system for 30 sec.) connected to a GC-17A gas chromatograph coupled with a mass spectrometer (*m/z* 50–850; Shimadzu GC-MSQP5050A) using electron impact ionization (70 eV). The GC was equipped with an automatic programmable-temperature system and a capillary column (30 m × 0.25 mm i.d.) coated with 5% phenyl-methylpolysiloxane (DB-5MS: Agilent Tec.). Helium was used as the carrier gas. The GC oven temperature was held at 40ºC for 2 minutes and programmed from 40 to 300ºC at 15ºC min^{-1} (held for 12 min at 300ºC). The interface was set at 280ºC. The identification of individual compounds was performed by ion chromatography, and comparison with published and NIST library data.

3.2.7 Biomarker analyses

Extractions were made of coals and coaly shale samples weighing ca. 1.5–5 g, and mudstone samples weighting ca. 30–45 g, depending on their total organic carbon contents. Extracts were made in a Soxhlet extractor, using a 9:1 mixture of dichloromethane (DCM) and methanol (CH_3OH) for 120 hrs for the coals (23.1–57.6 wt% TOC) and 72 hrs for the coaly shales and mudstones (0.01–8.58 wt% TOC). Activated copper was used to remove the elemental sulphur during the extraction. After a first evaporation of the solvent, the extracts were transferred from the flask to a beaker by dissolution with a little DCM-methanol solvent, and then dried overnight in a draft hood at room temperature. The dried extracts were then dissolved in *n*-hexane and placed on a thin layer chromatogram (TLC). The aliphatic and aromatic fractions on the TLC were analyzed using a GC-MS (GC-MS Shimadzu- QP2010) equipped with a 30 m capillary column (*m/z* 50–850; DB-5MS, 0.25 mm i.d., 0.25 μm film (5% phenyl methylpolysiloxane) thickness: Agilent Technologies), using electron impact

ionization (70 eV). The GC oven temperature was held at 50˚C for 5 min, stepped from 50 to 300˚C at a rate of 8˚C min^{-1}, and then held at 300˚C for 30 min. Helium was used as the carrier gas. *n*-Tetracosane, cholestane and PAHs Solution Mix (Accu Standard Inc., Z-013-17) were used as internal standards for differing compound groups in the hydrocarbon fractions. Individual compounds were identified by comparison of retention times with standard mixtures and mass spectra with previous literature and published work from our laboratory. Identification of PAHs was performed by comparison of GC retention times, mass spectra with published data and standard PAH. In this study, the PAHs quantified were Anthracene (A), phenanthrene (Phe), fluoranthene (Fla), pyrene (Py), benzo (a) anthracene (BaAn), chrysene/triphenylene (Chry+Tpn), benzofluoranthenes (Bflas), benzo[e]pyrenes (BePy), benzo[a]pyrenes (BaPy), perylene (Pery), indeo[1,2,3-*cd*] pyrene (InPy), benzo (ghi) perylene (BghiP), coronene (Cor) and retene (Ret). Selected PAHs were monitored at *m/z* = 183 (Cad), *m/z* = 178 (P, An), *m/z* = 202 (Fla, Py), *m/z* = 291 (Ret), *m/z* = 228 (BaAn, Chry), *m/z* = 252 (Bflas, BePy, BaPy, Pery), *m/z* = 276 (InPy, BghiP), and *m/z* = 300 (Cor). Relative abundances (%) and concentrations (μg/g TOC) were calculated by comparing the TIC (total ion current) chromatogram area to the standard area.

3.2.8 X-ray fluorescence (XRF) analysis

For geochemical analysis, 94 mudstones and sandstones were chipped and crushed in a tungsten-carbide ring mill, with mill times of 25–30 seconds. Loss on ignition (LOI) determination was performed by lignition of powdered samples (ca. 8–10 g) in a muffle furnace at 1020˚C for at least three hours. The ignited sample was prepared to make glass fusion beads for X-ray fluorescence (XRF) analysis. Major and trace elements were determined using a Rigaku RIX 2000 instrument in Shimane University. Analytical processes followed methods of Kimura and Yamada (1996).

CHAPTER 4. RESULTS

4.1 Organic Geochemistry

4.1.1 CNS elemental analysis

Ninety four samples were measured by CNS elemental analysis to determine total organic carbon (TOC), total nitrogen, and total sulphur (TS) contents.

(a) Coal and coaly shale (Upper Eocene)

Total organic carbon contents (TOC) of the upper Eocene coals and coaly shales range from 2.08 wt% to 57.56 wt% (Table 4.1a, Fig. 4.1a). Sulphur contents are slightly elevated in coaly shale A2-52 and in the coal samples A1-92, at 1.14 wt% and 3.95 wt%, respectively (Fig. 4.1b), but the remainder of samples are sulphur-poor (<0.47 wt%). All C/N ratios are high, with a range from 30.6 to 66.8 (Fig. 4.1c), as are C/S ratios (range 7.52 – 662) (Fig. 4.1d).

We analysed same samples which is HF-HCL acid treatment to remove carbonate minerals. All elemental results are shown in Table 4.1b. TOC contents are higher in the kerogens (32.2 – 70.3%) than those from rock samples (without acid treatment). C/N ratios are slightly higher in the kerogens.

Table 4.1. CNS elemental, vitrinite reflectance, and Rock-Eval pyrolysis data for Upper Eocene coals and coaly shales from the Central Myanmar Basin, Myanmar. (a) Rock data (b) Kerogen data

a. Rock data

Formation	Yaw	Pondaung	Pondaung	Pondaung	Pondaung	Pondaung	Pondaung	Pondaung
Sample	A1-92	A1-113	A1-114	A2-55	A2-54	A2-52	A2-52A	A1-120
TOC (%)	26.26	23.13	57.56	31.33	7.36	8.58	2.08	7.18
TS(%)	3.95	0.47	0.09	0.19	0.48	1.14	0.13	0.08
C/N	49.66	39.29	66.83	39.90	26.32	30.57	16.03	19.79
C/S	6.65	48.97	611.59	166.92	15.48	7.52	16.14	95.38
Ro (%)	0.29	0.28	0.26	0.42	0.33	0.39	0.30	0.36
HI	142	141	100	166	20	191	12	26
OI	73	107	40	44	137	28	212	144
S1	1.92	3.86	0.36	0.71	0.03	0.23	0.01	0.07
S2	37.35	32.64	57.33	52.01	1.46	16.39	0.25	1.87
S3	19.1	24.68	22.84	13.88	10.05	2.41	4.4	10.32
Tmax	422	421	413	429	435	425	451	442
PI	0.05	0.11	0.01	0.01	0.02	0.01	0.04	0.04
$\delta^{13}C$	-26.5	-26.5	-24.8	-25.5	-24.5	-26.0	-25.7	-24.6

b. Kerogen data

Formation	Yaw	Pondaung	Pondaung	Pondaung	Pondaung	Pondaung	Pondaung	Pondaung
Sample	A1-92	A1-113	A1-114	A2-55	A2-54	A2-52	A2-52A	A1-120
TOC (%)	32.3	67.40	56.60	61.40	45.30	70.30	43.80	51.80
TS(%)	0.00	0.58	0.19	0.08	0.14	0.37	0.15	0.13
C/N	46.39	52.58	56.83	51.90	33.49	52.68	36.47	31.88
Ash (%)	1.11	0.59	1.56	1.20	2.12	2.95	23.37	24.47
HI	178	86	96	186	36	250	42	29
OI	115	94	37	52	168	25	102	96
S1(300°C)	1.88	2.39	1.85	1.61	0.91	2.02	0.87	0.8
S2 (300-650°C)	57.5	57.74	54.04	114.28	16.3	175.61	18.42	15.17
S3 (300-400°C)	37.1	63.42	20.89	32.18	76.25	17.31	44.79	49.66
S3´(400-650°C)	34	51.2	23.5	29.9	80.4	17.8	47.1	58.8
Tmax	420	417	420	426	426	426	424	425
S_1+S_2	59.38	60.13	55.89	115.89	17.21	177.63	19.29	15.97
S_2/S_3	1.55	0.91	2.59	3.55	0.21	10.15	0.41	0.31

Note: HI= (S2*100/TOC: mg HC/g TOC); OI= (S3*100/TOC: mg CO2/g TOC); S1 (mg/g rock); S2 (mg/g rock); S3 (mg/g rock)

(b) Mudstones (Upper Cretaceous to Miocene)

Total organic carbon contents (TOC) of mudstone samples throughout the Upper Cretaceous to Miocene successions are mostly low to very low, ranging from 0.11 to 0.92% in the Late Cretaceous, 0.22 to 0.34% in the Paleocene, 0.08 to 0.66% in the Eocene, and 0.10 to 8.09% in the Pegu Group. (Table 4.2; Fig. 4.2a)

Generally, Upper Cretaceous Kabaw Formation shows slightly high TOC contents (>0.5). Most mudstones are low in TS (<0.001-0.41%) ratios. (Fig. 4.2b)

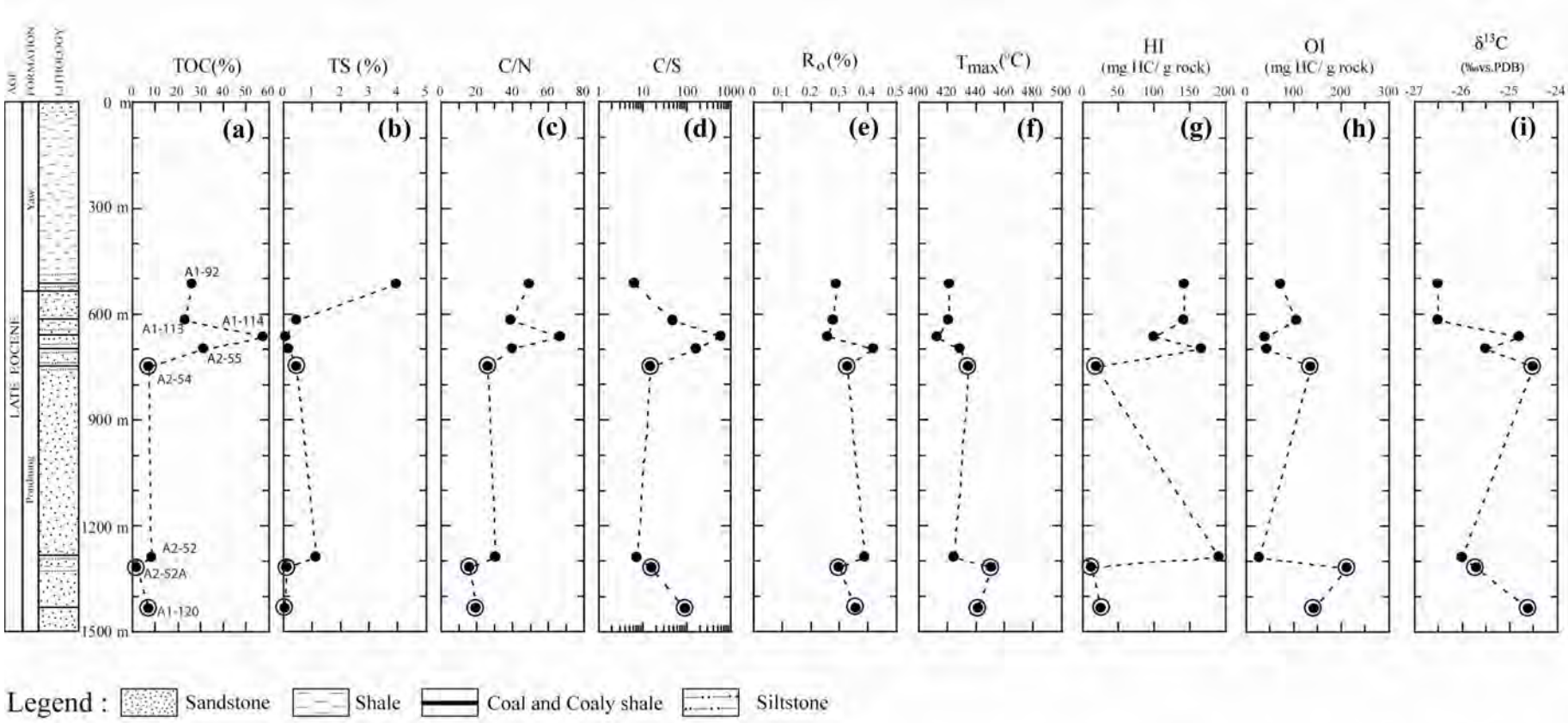

Fig. 4.1. CNS elemental, vitrinite reflectance, and Rock-Eval pyrolysis data for the Upper Eocene coals and coaly shales. Circled data points indicate weathered samples.

Two Laungshe mudstones (Early Eocene) and one Shwezetaw carbonaceous mudstone (early to middle Oligocene) have exceptionally high TS with 1.46%, 1.94%, and 3.42% respectively. C/N values are less than 11 in the Upper Cretaceous to Eocene and ranging from 2 to 55 in the Pegu Group (Fig. 4.2c). The C/S ratios are varying from 5 to < 1000 in the Upper Cretaceous, 9 to >500 in the Paleocene, 0.3 to >600 in Eocene, 1 to >600 in the Pegu Group (Fig. 4.2d). (Table 4.2)

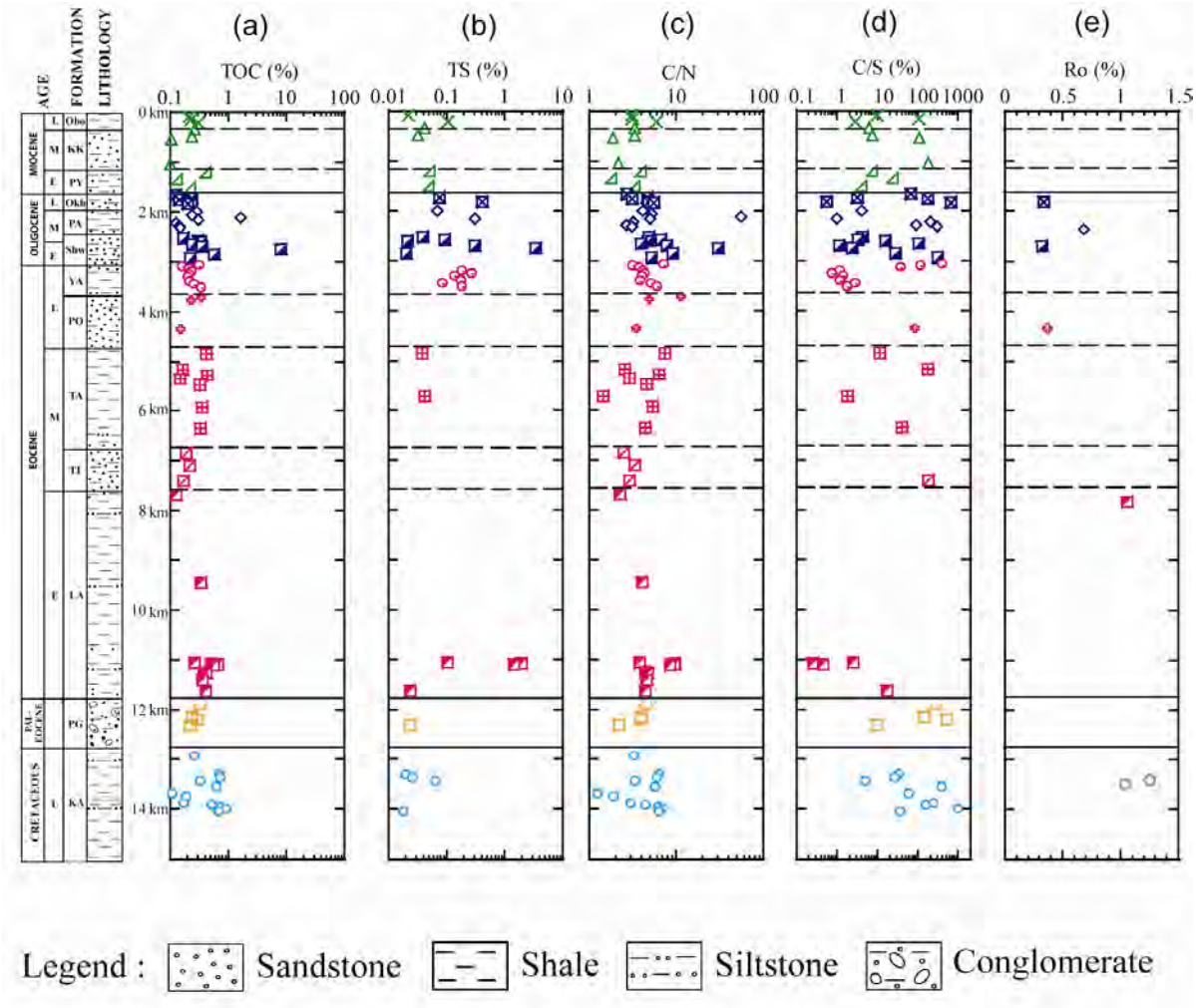

Fig. 4.2. CNS elemental data for Upper Cretaceous to Miocene mudstones from the western margin of CMB, Myanmar.

Table 4.2. CNS elemental, and vitrinite reflectance data for Late Cretaceous to Miocene mudstones from the Central Myanmar Basin, Myanmar.

No.	Formation	Lithology	Sample	TOC (%)	TN (%)	TS (%)	C/N	C/S
1	Obogon	mudstone	A2-22	0.21	0.07	0.022	3.06	9.72
2	Obogon	mudstone	A2-24	0.22	0.07	0.002	3.11	103.18
3	Obogon	sandstone	A2-25	-0.03	0.02	-0.012	-1.47	2.37
4	Obogon	mudstone	A2-26	0.31	0.05	0.106	5.92	2.89
5	Kyaukkok	mudstone	A2-28	0.26	0.08	0.042	3.32	6.27
6	Kyaukkok	mudstone	A2-29	0.24	0.07	0.032	3.33	7.62
7	Kyaukkok	mudstone	A2-21	0.11	0.06	0.001	1.89	106.44
8	Kyaukkok	mudstone	A2-20	0.10	0.05	0.001	2.15	183.60
9	Pyawbwe	mudstone	A2-16	0.44	0.11	0.054	4.13	8.12
10	Pyawbwe	mudstone	A2-12	0.14	0.08	0.005	1.89	26.24
11	Pyawbwe	mudstone	A2-9	0.24	0.07	0.052	3.45	4.54
12	Okhmintaung	mudstone	A1-89	0.13	0.05	0.002	2.70	65.96
13	Okhmintaung	mudstone	A2-7	0.24	0.05	0.076	4.63	3.20
14	Okhmintaung	mudstone	A2-6	0.14	0.05	0.001	3.12	176.25
15	Okhmintaung	mudstone	A2-5	0.23	0.05	0.413	4.81	0.56
16	Okhmintaung	mudstone	A2-3	0.21	0.04	0.000	5.57	662.77
17	Okhmintaung	sandstone	A2-2	0.07	0.03	-0.011	2.60	-6.80
18	Padaung	mudstone	A2-38	0.28	0.07	0.069	4.14	4.12
19	Padaung	mudstone	A2-36	0.24	0.05	n.a.	5.30	n.a.
20	Padaung	mudstone	A2-34	1.65	0.03	n.a.	55.22	n.a.
21	Padaung	mudstone	A2-33	0.31	0.06	0.308	5.00	0.99
22	Padaung	mudstone	A1-103	0.13	0.04	0.001	3.19	207.30
23	Padaung	mudstone	A1-105	0.14	0.05	0.002	2.67	88.27
24	Padaung	mudstone	A1-107	0.15	0.05	0.000	3.11	297.80
25	Shwezetaw	mudstone	A2-39	0.17	0.03	0.039	4.91	4.30
26	Shwezetaw	mudstone	A2-42	0.31	0.05	0.093	6.71	3.35
27	Shwezetaw	mudstone	A2-43	0.34	0.07	0.022	4.72	15.84
28	Shwezetaw	mudstone	A2-41	0.24	0.06	0.002	3.97	101.68
29	Shwezetaw	mudstone	A2-45	0.35	0.04	0.312	7.91	1.14
30	Shwezetaw	mudstone	A2-46	0.47	0.05	0.724	8.84	0.65
31	Shwezetaw	mudstone	A1-109	8.09	0.26	3.435	30.66	2.36
32	Shwezetaw	mudstone	A1-111	0.57	0.06	0.020	9.27	28.21
33	Shwezetaw	mudstone	A1-112	0.23	0.04	0.001	5.22	310.77
34	Yaw	mudstone	A2-58	0.33	0.04	0.001	7.37	421.96
35	Yaw	mudstone	A2-60	0.16	0.05	0.001	3.20	120.12
36	Yaw	mudstone	A2-59	0.22	0.06	0.006	3.85	39.66
37	Yaw	mudstone	A1-100	0.24	0.06	0.188	4.22	1.26
38	Yaw	mudstone	A1-99	0.22	0.05	0.275	4.41	0.79
39	Yaw	mudstone	A1-98	0.21	0.05	0.139	4.12	1.51
40	Yaw	mudstone	A2-57	0.00	0.02	-0.011	n.a.	n.a.
41	Yaw	mudstone	A1-96	0.23	0.06	0.181	3.93	1.24
42	Yaw	mudstone	A1-95	0.26	0.05	0.088	5.30	2.98
43	Yaw	mudstone	A1-93	0.35	0.06	0.189	6.16	1.86

Note: n.a, not analysed

Table 4.2. continued-

Table 4.2. CNS elemental, and vitrinite reflectance data for Late Cretaceous to Miocene mudstones from the Central Myanmar Basin, Myanmar.

No.	Formation	Lithology	Sample	TOC (%)	TN (%)	TS (%)	C/N	C/S
44	Pondaung	mudstone	A1-115	0.35	0.03	n.a.	11.33	n.a.
45	Pondaung	mudstone	A1-117	0.23	0.05	n.a.	4.95	n.a.
46	Pondaung	mudstone	A2-50	0.15	0.04	0.002	3.49	82.72
47	Tabyin	mudstone	A2-48	0.43	0.06	0.038	7.42	11.19
48	Tabyin	mudstone	A1-123	0.16	0.06	0.001	2.59	177.69
49	Tabyin	mudstone	A1-125	0.44	0.07	n.a.	6.42	n.a.
50	Tabyin	mudstone	A1-126	0.15	0.05	n.a.	2.90	n.a.
51	Tabyin	mudstone	A1-127	0.33	0.07	n.a.	4.57	n.a.
52	Tabyin	mudstone	A2-62	0.08	0.05	0.042	1.46	1.77
53	Tabyin	mudstone	A1-129	0.35	0.06	n.a.	5.39	n.a.
54	Tabyin	mudstone	A1-131	0.34	0.08	0.008	4.42	40.23
55	Tilin	mudstone	A1-165	0.19	0.08	n.a.	2.47	n.a.
56	Tilin	mudstone	A1-164	0.22	0.07	n.a.	3.34	n.a.
57	Tilin	sandstone	A2-82	-0.07	0.01	-0.010	-4.94	6.81
58	Tilin	mudstone	A2-84	0.17	0.06	0.001	2.88	180.26
59	Laungshe	mudstone	A2-65	0.13	0.06	n.a.	2.25	n.a.
60	Laungshe	sandstone	A2-67	-0.10	<0.001	-0.01	-107.85	8.89
61	Laungshe	mudstone	A1-162	0.34	0.08	n.a.	4.02	n.a.
62	Laungshe	mudstone	A1-134	0.26	0.07	0.104	3.76	2.51
63	Laungshe	mudstone	A1-135	0.51	0.05	1.942	9.65	0.26
64	Laungshe	mudstone	A1-136	0.66	0.07	1.4561	9.55	0.45
65	Laungshe	mudstone	A1-160	0.57	0.07	n.a.	8.63	n.a.
66	Laungshe	mudstone	A1-158	0.38	0.09	n.a.	4.40	n.a.
67	Laungshe	mudstone	A1-157	0.42	0.09	n.a.	4.71	n.a.
68	Laungshe	mudstone	A1-156	0.36	0.08	n.a.	4.58	n.a.
69	Laungshe	mudstone	A1-153	0.42	0.09	0.024	4.45	17.44
70	Paunggyi	mudstone	A1-137	0.34	0.08	0.001	4.47	279.96
71	Paunggyi	mudstone	A1-140	0.24	0.06	0.002	3.94	137.71
72	Paunggyi	mudstone	A2-69	0.30	0.08	0.001	3.93	537.60
73	Paunggyi	mudstone	A1-152	0.22	0.10	0.024	2.18	9.35
74	Kabaw	mudstone	A1-142	0.27	0.08	n.a.	3.36	n.a.
75	Kabaw	mudstone	A2-77	0.73	0.11	0.021	6.47	35.44
76	Kabaw	mudstone	A2-78	0.74	0.12	0.026	6.16	28.06
77	Kabaw	sandstone	A2-79	-0.03	0.02	0.046	-1.68	-0.67
78	Kabaw	mudstone	A2-74	0.34	0.10	0.066	3.45	5.25
79	Kabaw	mudstone	A1-149	0.64	0.11	0.002	5.88	405.83
80	Kabaw	mudstone	A1-145	0.11	0.09	0.002	1.28	62.12
81	Kabaw	mudstone	A1-146	0.19	0.10	n.a.	1.95	n.a.
82	Kabaw	mudstone	A1-150	0.18	0.06	0.001	3.08	255.50
83	Kabaw	mudstone	A2-80	0.53	0.12	0.003	4.60	164.49
84	Kabaw	mudstone	A2-72	0.77	0.12	n.a.	6.33	n.a.
85	Kabaw	mudstone	A2-71	0.92	0.13	0.001	7.13	1017.06
86	Kabaw	mudstone	A2-70	0.71	0.11	0.019	6.43	37.93

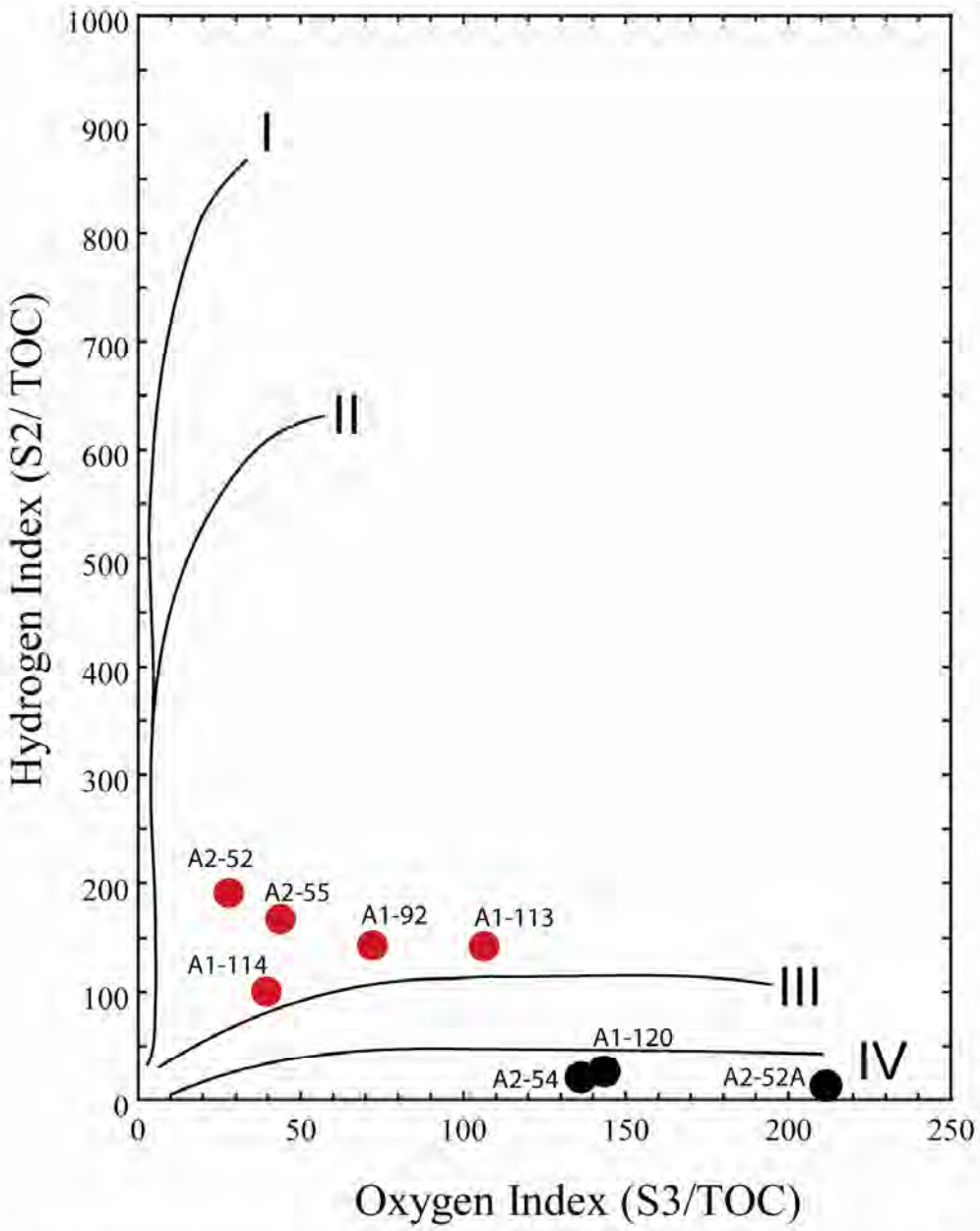

Fig. 4.3. Van Krevenlan-type diagram showing mixed Type II and III kerogens in the Upper Eocene coals and coaly shales, mostly gas-prone. Black circles indicate weathered coaly shale samples.

4.1.2 Rock-Eval pyrolysis

(a) Coal and coaly shale (Upper Eocene)

On the basis of pyrolysis analysis, free hydrocarbon contents (S_1), the amount of hydrocarbon yields (S_2), and organic carbon dioxide (S_3) expelled during pyrolysis are determined and summarized in Table 4.1a.

According to Peters (1986), we evaluated the amount of hydrocarbon yields (S2) to determine the potential hydrocarbons generated source rocks. Upper Eocene coals and coaly shales comprise elevated pyrolysis S_2 yields with a varying from 16.39 to 57.33 mg HC/g rock.

Coal samples (A1-92, A1-113, A1-114, A2-55) are characterized by moderate Hydrogen index (HI) values of 100 – 166 mg HC/g TOC, whereas coaly shale samples have higher and more variable HI of 12 –191mg HC/g TOC (Table 4.1; Fig. 4.1g). The oxygen index (OI) values are low to moderately high (28–107 mg CO_2/g TOC) in all coal and coaly shale samples (Fig. 4.1h). T_{max} (temperature at maximum evolution of S2 hydrocarbons) values range between 413˚C and 451˚C (Fig. 4.1f). Production Index (PI) values vary from 0.01 to 0.11 (Table 4.1a). The diagrams of the HI versus OI values (Fig. 4.3) is illustrated to determine the type of organic matter (i.e. oil, gas prone of mixed) for Upper Eocene samples.

Furthermore, we analysed same samples by HF-HCL acid treatment. Results are shown in Table 4.1b. The plot of HI versus OI is shown in Fig. 4.4 (open symbols indicate data of the whole-rocks), where we compare results for the equivalent whole-rock data for the same samples. Results for the whole-rocks and kerogens indicate a contrast. HI values of three of the unweathered rock samples are lower than those of their corresponding kerogens (A2-52, A2-55 and A1-92). In contrast, OI values of the weathered rocks A2-52A and A1-120 are greater than those of their corresponding unweathered kerogen. The unweathered kerogens show a mixture of type II-III (Fig. 4.4), and clearly differ from the weathered kerogens, which

lie in type IV, with high OI values (90–170 mg CO_2/g TOC). This trend can be considered that effect of weathering reflects a decrease in HI value with increase in OI value.

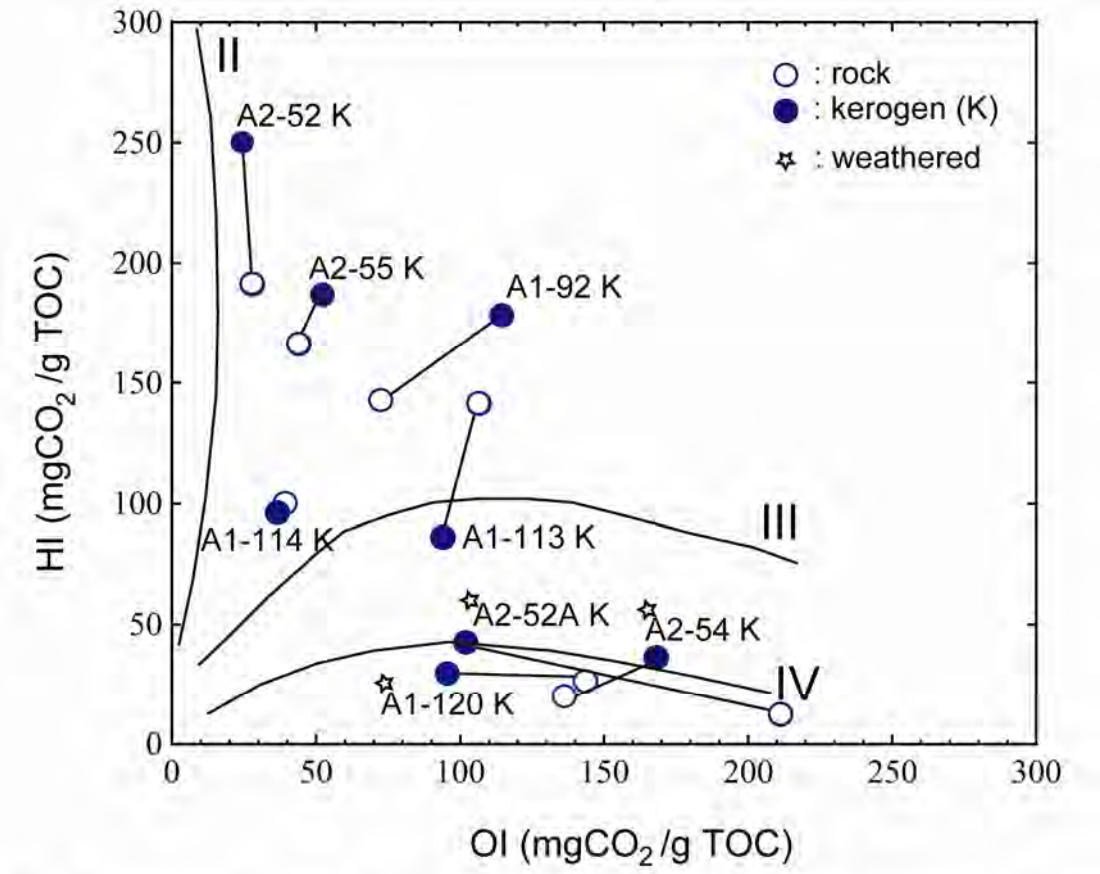

Fig. 4.4. HI versus OI diagram showing types of kerogen for rock and kerogen of coals and coaly shales. Tie lines join whole-rock and kerogen analyses from the same sample.

The measurement of original CO_2 in the kerogen is shown in Fig 4.5. This method is similar to the temperature-elevation Py-GC-MS with monitoring m/z = 44 (e.g. Wang et al., 2013). The OI value is calculated from the ratio of S_3 (Fig. 4.5 and Table 4.1b) between 300 and 400˚C and the TOC content. Two peaks are evident between 300 and 400˚C, suggesting the presence of both weak-bonding and strong-bonding CO_2 in the kerogen.

The former is presumed to originate from carboxyl units and the latter from oxygen-containg units (Christiansen et al., 1995; Cervantes-Uc et al., 2006), according to their respective bonding energies. The S_3 and S_3' peaks are consistently higher in the weathered kerogens (A2-54, A2-52A and A1-120) at 300–400˚C than in the unweathered group.

The CO_2 releasing area expands into the high temperature area above 400˚C (Fig. 4.5). The range from 400 – 650˚C yields the S_3'values (Table 4.1b, Fig. 4.6). The S_3 value shows strong correlation with S_3' (Fig. 4.6): $S_3' = 0.976\ S_3 + 6.574$ ($R^2 = 0.957$) in the weathered samples and $S_3' = 0.695\ S_3 + 7.512$ ($R^2 = 0.991$) in the unweathered samples. The S_3 and S_3' values and the ratio of S_3' to S_3 are higher in the weathered samples (Fig. 4.6). This can be speculated that strong-bonding oxygen compounds to kerogen are predominant in the weathered group more than unweathered samples, suggesting an increase in S_3' or a decrease in S_3 values.

The variation of HI and OI for unweathered kerogen is mainly associated with the characters of kerogen (e.g. Katz, 1983). Low organic carbon contents of the weathered rock samples (Table 4.1a) seems to give high OI.

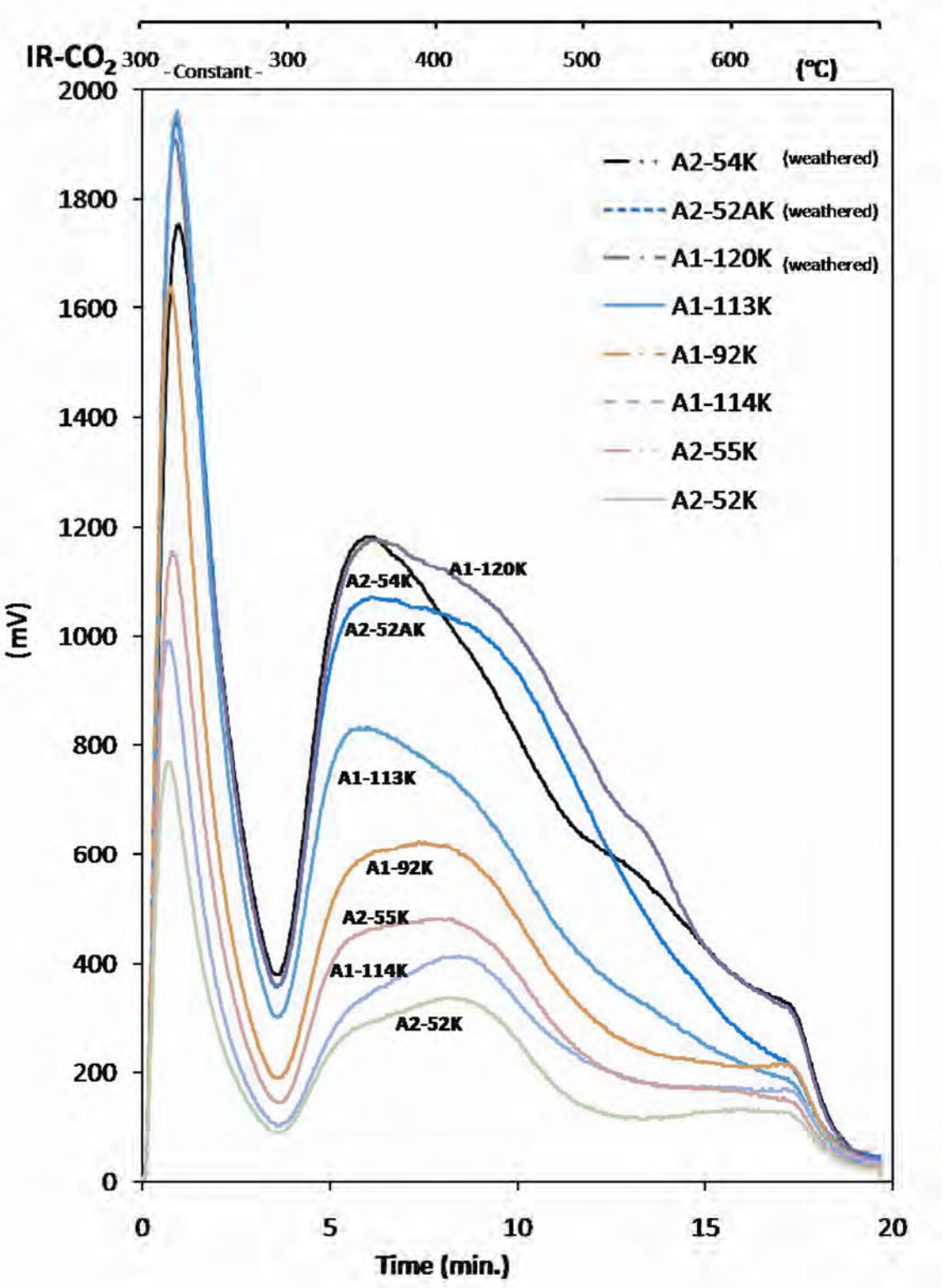

Fig. 4.5. Rock-Eval pyrograms (S3 and S3′) for kerogen from the coals and coaly shales.

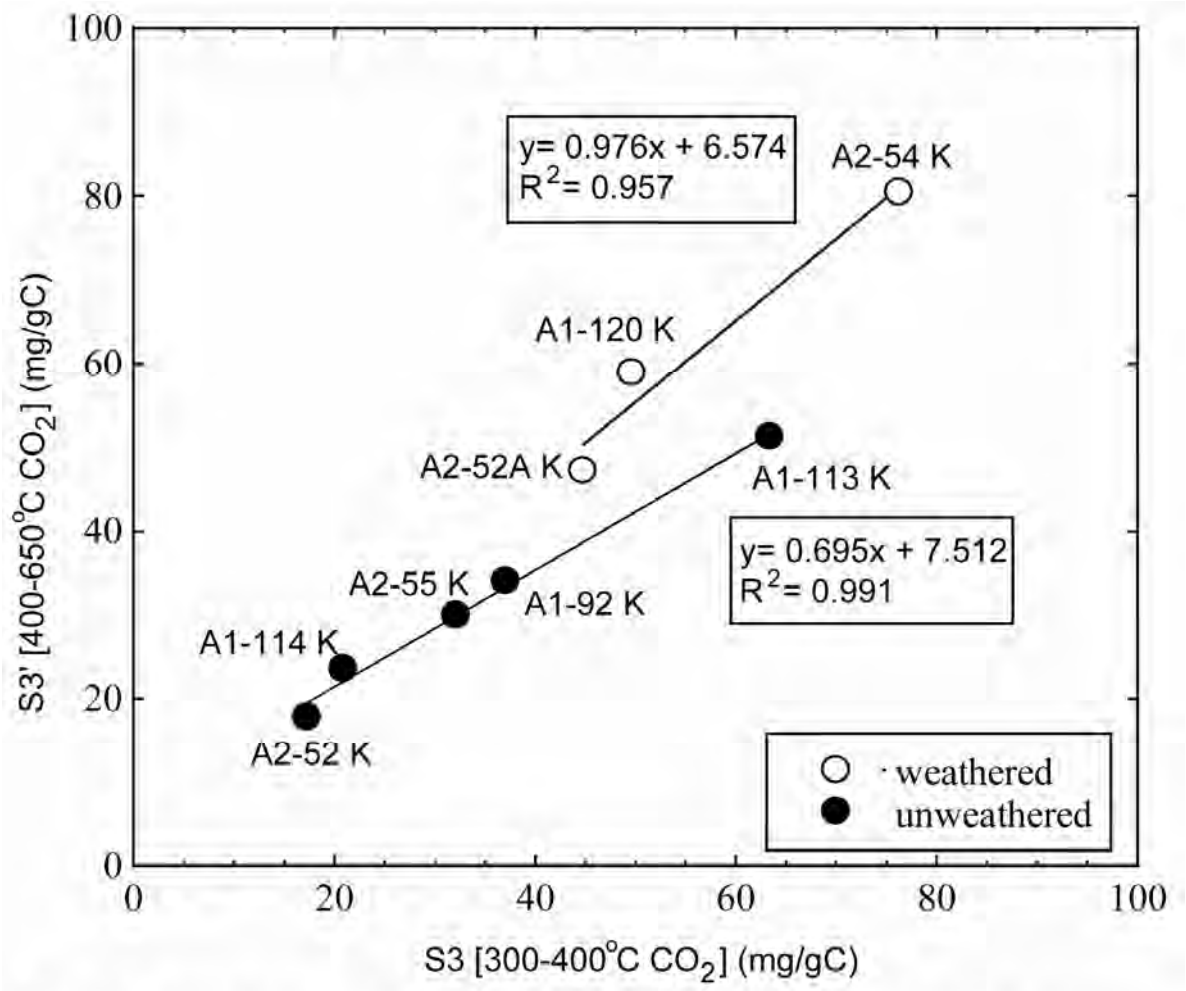

Fig. 4.6. Correlation of Rock-Eval pyrolysis data (S3 and S3') for kerogen from the coals and coaly shales.

4.1.3 Vitrinite reflectance (R_o)

(a) Coal and coaly shale (Upper Eocene)

Representative outcrop photographs of coals and coaly shales are shown in the Fig. 4.7. Vitrinite reflectance (*Ro*) values are relatively uniform, ranging from 0.26 to 0.41% (Fig. 4.1e; Table 4.1).

Fig. 4.7 Outcrop photographs of coals (A1-92 and A2-55) and coaly shales (A2-54 and A2-52) from the Upper Eocene, CMB.

(b) Mudstones (Upper Cretaceous to Miocene)

Eight sandstones (A2-79, A1-147, A2-67, A2-51, A2-45, A2-30, A2-15, and A2-4) are measured by vitrinite reflectance. Vitrinite reflectance (*Ro*) values are ranging from 0.32 to 1.25% (Fig. 4.2e).

4.1.4 Carbon isotopes ($\delta^{13}C$) of the OM

(a) Coal and coaly shale (Upper Eocene)

Coaly shales have $\delta^{13}C$ values varying from -24.5 to -26‰ and coals vary from -24.8 to -26.5‰ (Table 4.1; Fig. 4.1i). Gymnosperm vegetation yields average carbon isotopic composition between -22.7‰ and -25.1‰, whereas angiosperms are of between -25.5‰ and -26.6 (Bechtel et al., 2003).

4.1.5 Fourier transform infrared (FT-IR) spectroscopy

The micro-FTIR spectra for kerogens and bitumens in all samples are illustrated in Figures 4.8a &b. The aliphatic (C-H) stretching bands for all studied samples occur at 2925 and 2850 cm^{-1}, CH_2 stretching at 1375 and 1383cm^{-1}, and CH_3 at 1455 and 1457 cm^{-1} (Takeda and Asakawa, 1988; Ibarra et al., 1996; Faure et al., 1999).

Aliphatic bonds are decreased in the weathered kerogens (Fig. 4.8a). It can be suggesting that some parts of alkyl chains in functional group might be probably reduced by weathering. The aliphatic oxygen-containing bond (C=O) is detected at 1716 cm^{-1} in the weathered samples, and in one unweathered sample (A1-113).

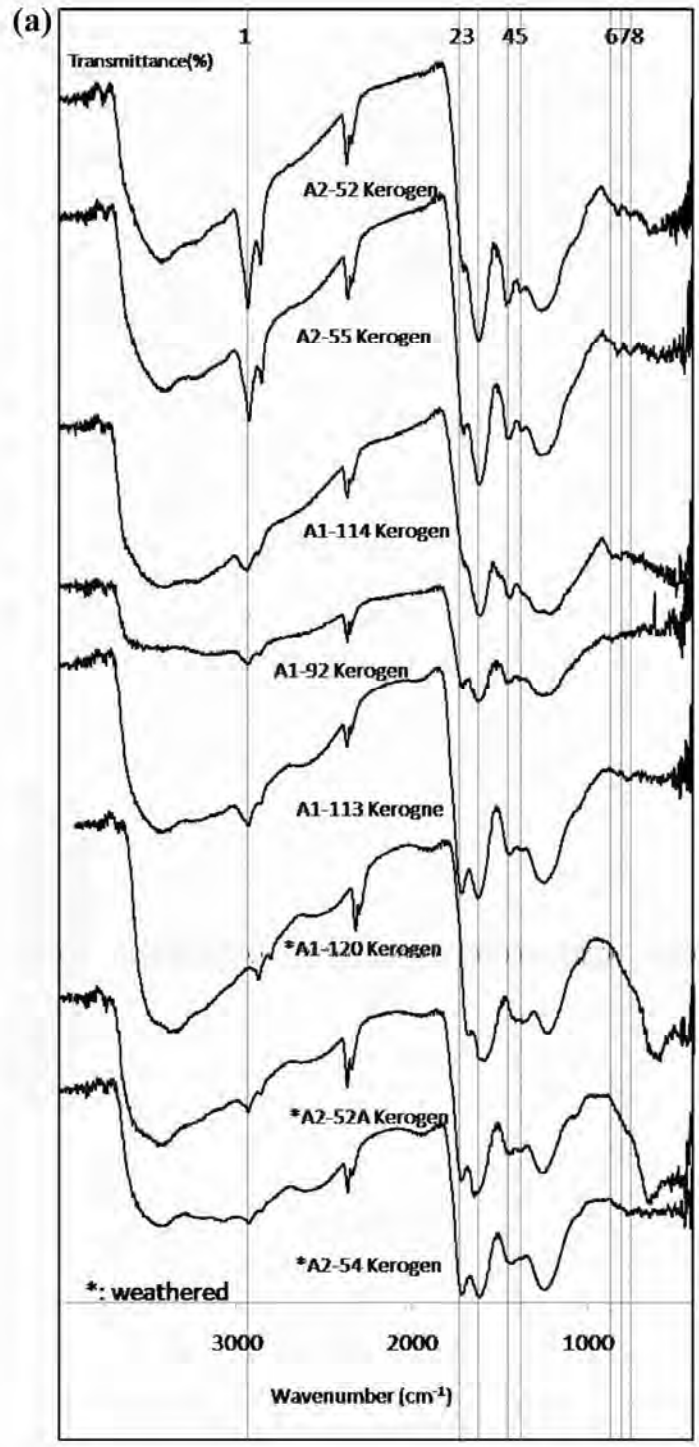

Fig. 4.8 (a) FT-IR measurements showing chemical characteristics of kerogen from the coals and coaly shales. 1: 2925 and 2850 cm^{-1} to C-H stretching (aliphatic methylene groups); 2: 1716 cm^{-1} to aliphatic C=O stretching group; 3: 1617 cm^{-1} to aromatic nucleus C=C stretching; 4-5: 1455 and 1457 cm^{-1} to aliphatic C-H deformation; 6-7-8: 702, 751 and 819 cm^{-1} toaromatic C-H out-of-plane bending, and 1000-1300 cm^{-1} to C-O bonds.
(b) FT-IR data showing chemical structure of bitumen from the coals and coaly shales.

Fig. 4.8 continued—

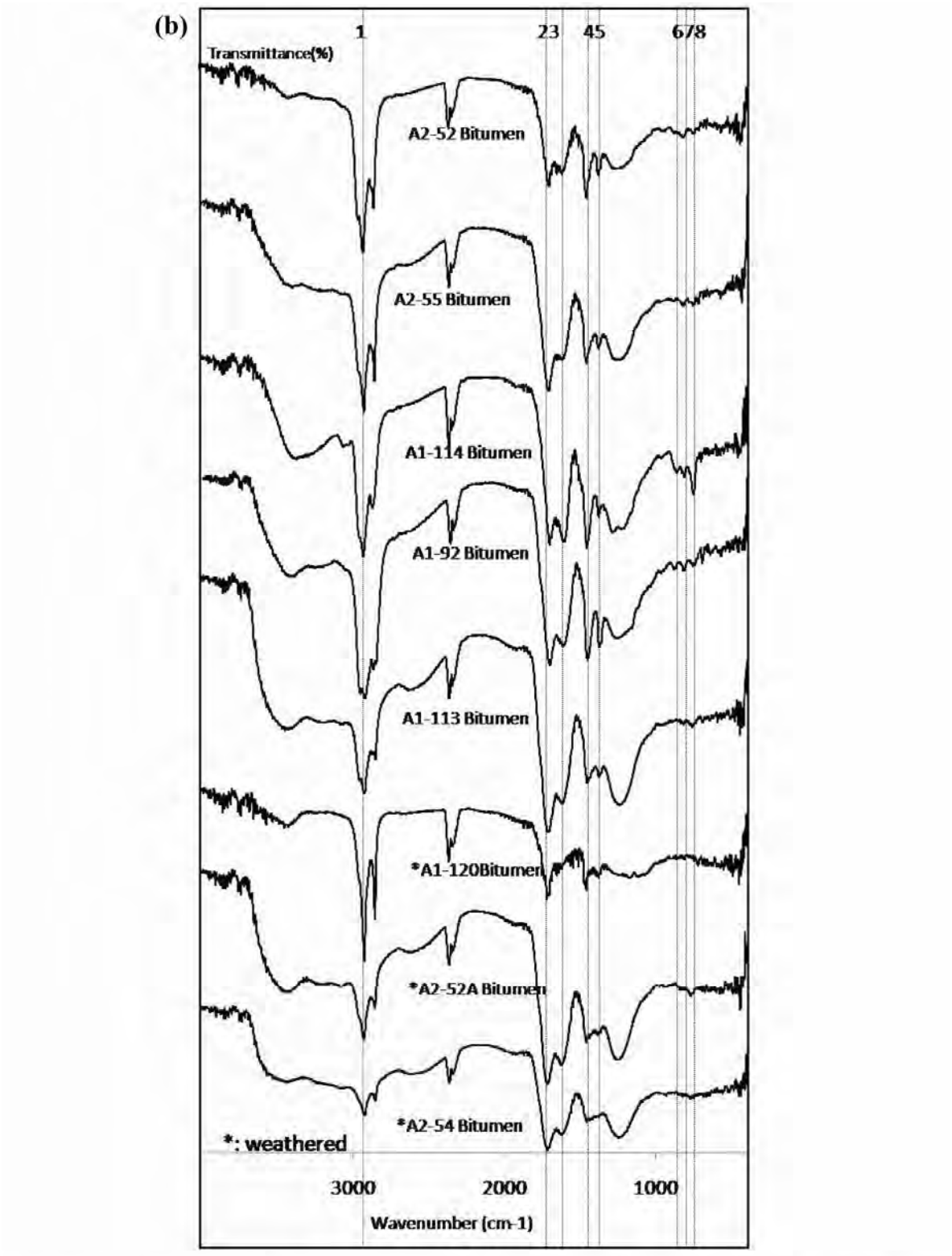

(b) FT-IR data showing chemical structure of bitumen from the coals and coaly shales.

The intensity of C-O bands at 1000–1300 cm^{-1} yield a higher frequency compared to C-H bands (Fig. 4.8a), indicating that carboxylic and/or ester groups are predominant in the weathered samples. The weathered kerogen and bitumen in Fig. 4.8 a & b show significant and clear decrease in aliphatic groups because C=O/C-O bonds possibly indicate significant occurrence of esters or ether formation (e.g. Jackson et al., 1996; Faure et al., 1999) and aliphatic side chains are readily oxidized to occur the aliphatic acid or ester C=O groups (e.g. Guo and Bustin, 1998). Furthermore, rather abundant of ester bonds (e.g. C=O or –COOR) may indicate type II kerogen (e.g. Tissot and Welte, 1984).

The aromatic C=C stretching band at 1617 cm^{-1} is similarly high in all samples. The aromatic (C-H) stretching bands at 702 cm^{-1}, 751 cm^{-1}, and 819 cm^{-1} also seem to differ little between kerogen and bitumen samples.

Bitumen samples (Fig. 4.8b) illustrate that functional groups such as aliphatic stretching groups (C-H, CH_2, CH_3), aromatic bonds (C-H, C=C) and aliphatic stretching C=O groups (e.g. COOH, ester, ketones) are more predominant than those in the kerogens.

4.1.6 Pyrolysis-Gas chromatography and Mass Spectrometry (GC-MS)

The *n*-alkenes and *n*-alkanes doublets are clearly performed by pyrolysis, in both the weathered and unweathered kerogens (Fig. 4.9). The *n*-C_7– *n*-C_{27} homologous series are clearly detected in all samples. The unweathered kerogens contain dominant aromatics such as benzene, toluene, indane, and p-xylene and phenolic materials (Fig. 4.9). Unweathered kerogens show significant light hydrocarbons (less than *n*-C_{10}). It is considered to be weathering, rather than maturity as the T_{max} is constant and immature (417– 426 °C in Table 1).

Phenol is relatively predominant in the weathered group (Peaks 3 in Fig. 5). Phenol is known to be generated from hydroxybenzoic acids (Kuder et al., 1998). On the other hand,

methyl phenols (Peaks 4 and 6) and dimethyl phenols (Peaks 7 and 8) seem to decrease in the weathered kerogens. This indicates that methyl/dimethyl phenolic moiety in the kerogen has been decomposed by the weathering. Although oxidized kerogen has been reported to be abundant in oxygen bonds linking to benzene compounds (Christiansen et al., 1995), the above relationship between phenol and methyl/dimethyl phenols suggests that decomposition rate of the methylene groups is faster than that of forming organic oxygen structures by the weathering.

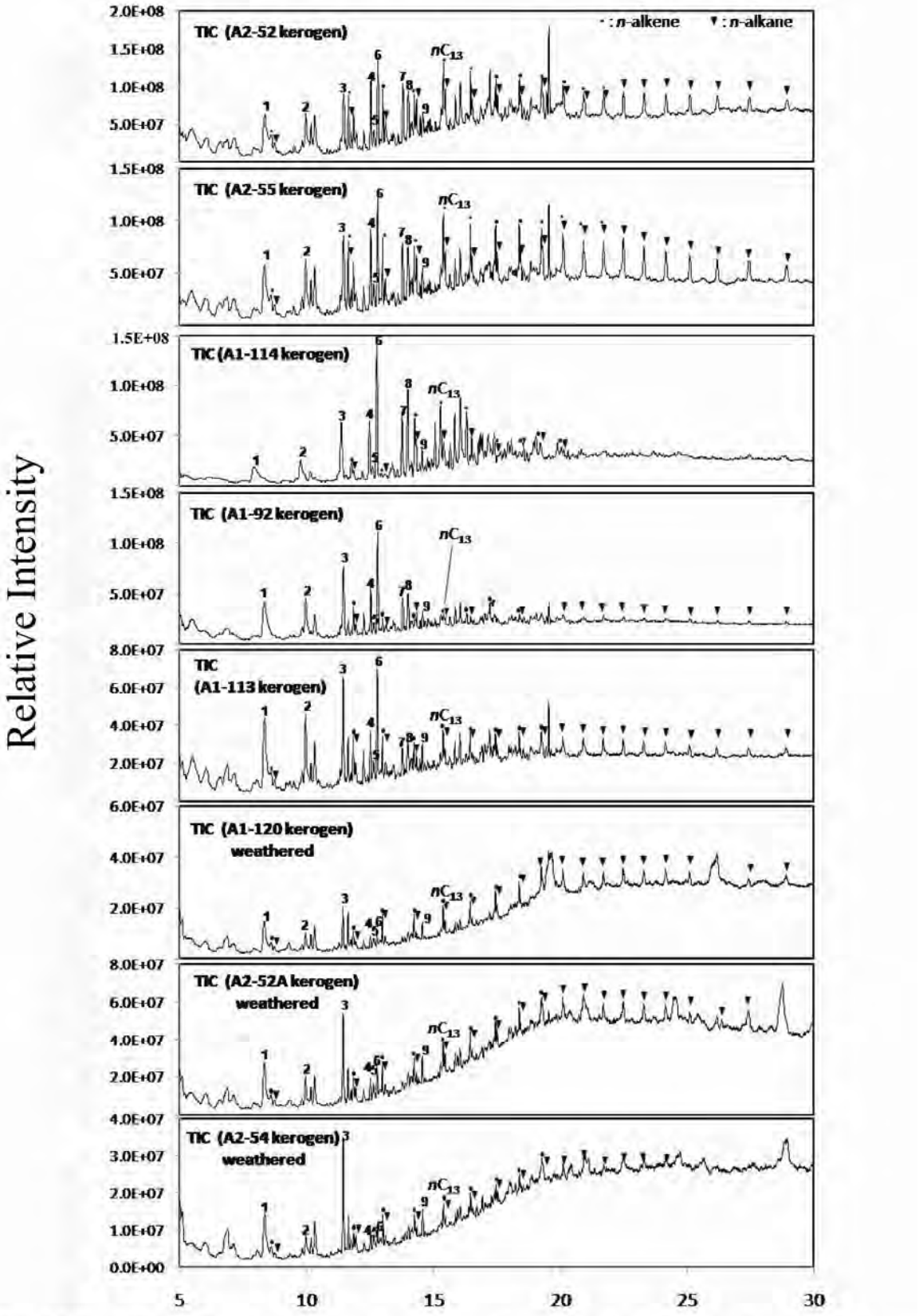

Fig. 4.9 Py-GC-MS data for kerogen from the coals and coaly shales. 1:toluene; 2:xylene; 3:phenol; 4 and 6:methyl phenol; 5:indene; 7 and 8:dimethyl phenol; 9: naphthalene.

4.1.7 Biomarker analyses

Biomarker has been useful as source indicators to distinguish between marine and continental land plants, and for reconstruction of paleoenvironments (Peters and Moldowan, 1993; Meyers, 1997).

4.1.7.1 Saturated hydrocarbons

(a) Coal and coaly shale (Upper Eocene)

(i) *n*-Alkanes and Acyclic isoprenoids (Pr/Ph, Pr/*n*-C_{17}, Ph/*n*-C_{18})

The distributions of *n*-alkanes in the Upper Eocene coals and coaly shales from the Yaw and Pondaung Formations were identified in the range *n*-C_{17}–*n*-C_{33} (Fig. 4.10a). The *n*-alkanes have been classified as short- (<*n*-C_{20}), mid- (*n*-C_{21} – *n*-C_{26}), and long chain (*n*-C_{27} – *n*-C_{33}) homologues. Mid-chain (n-$C_{21\text{-}25}$) *n*-alkanes with a maximum intensity at *n*-C_{22} are dominant in the coal sample A1-92, while most other samples show predominance in both mid-chain (*n*-$C_{21\text{-}25}$) and long-chain (*n*-$C_{27\text{-}32}$) *n*-alkanes (Table 4.3).

Carbon preference index (CPI) values were calculated based on the formula [0.5*(C_{25}+C_{27}+C_{29}+C_{31}+C_{33})/(C_{24}+C_{26}+C_{28}+C_{30}+C_{32})+(C_{25}+C_{27}+C_{29}+C_{31}+C_{33})/(C_{26}+C_{28}+ C_{30}+C_{32}+C_{34})] (Peters and Moldwan, 1993). All CPI values are greater than 1, with a range of 1.16–2.25 (Table 4.3; Fig. 4.11d). With one exception, the samples show a range of quite low to high concentrations of pristine (Pr) and phytane (Ph), from 0.002–5.37 and 0.01–1.96 μg/g TOC respectively. Coaly shale (A2-52) has significantly higher values of Pr (17.85 μg/g TOC) and Ph (1.96 μg/g TOC).

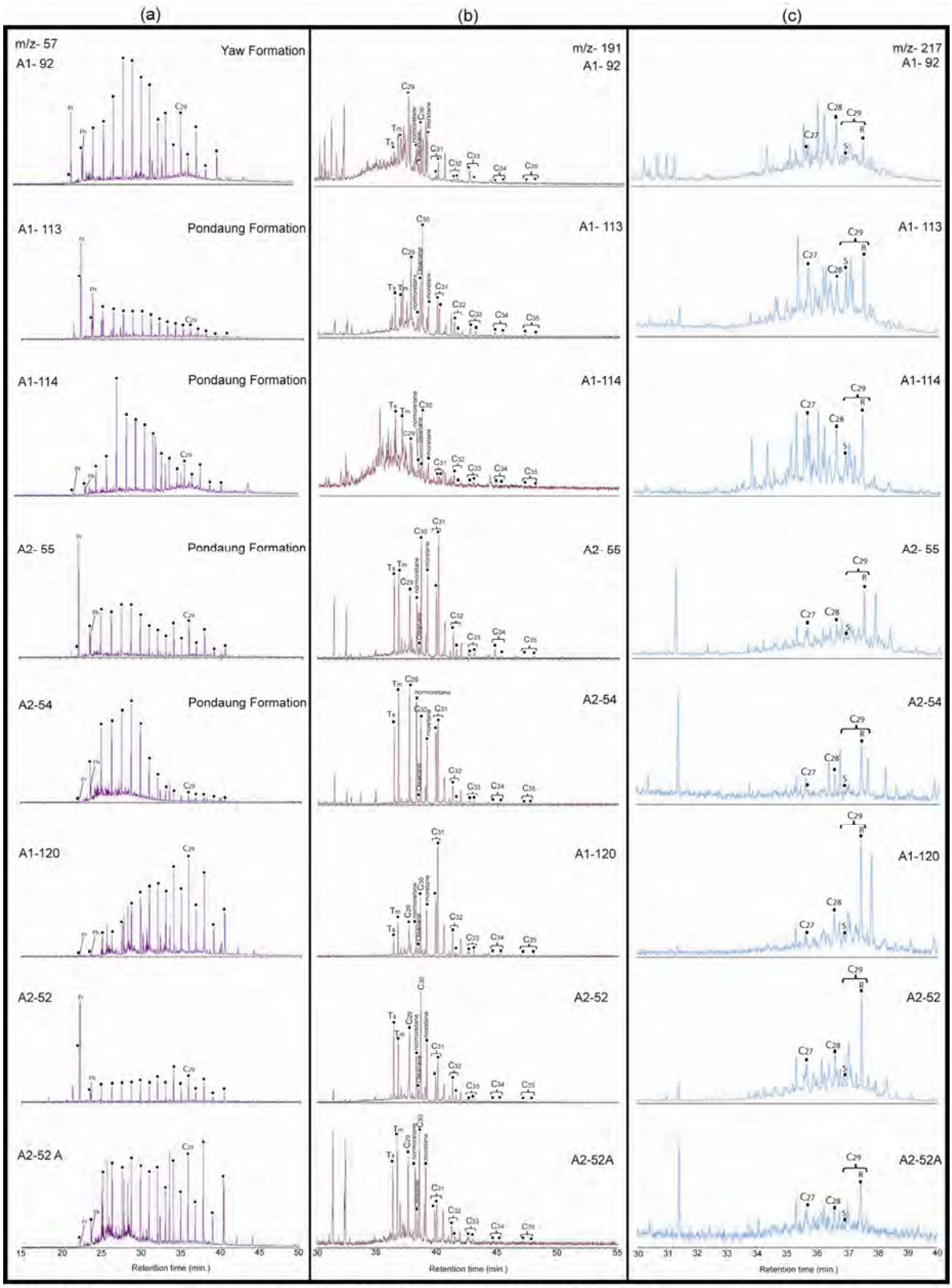

Fig. 4.10. GC/MS chromatograms of (a) n-alkanes (m/z 57), (b) Hopanes (m/z 191), and (c) Steranes (m/z 217) for Upper Eocene coal and coaly shale samples from the western margin of the Central Myanmar Basin.

Pr/Ph ratios thus range from 0.23 to 9.09 (Table 4.3; Fig 4.11a). The Pr/*n*-C_{17} values are high (1.87 – 9.86) and Ph/*n*-C_{18} values are relatively low (0.48 – 2.96) in all samples (Table 4.3; Fig. 4.11b). The ratios of mid-chain to long chain *n*-alkanes [P_{aq} = (C_{23}+C_{25})/ (C_{23}+C_{25}+C_{29}+C_{31})] are ranging from 0.40 to 0.89 (Table 4.3). The values of P_{wax} [P_{wax}= (C_{27}+C_{29}+C_{31})/ (C_{23}+C_{25} +C_{27}+C_{29}+C_{31})] which is a proxy of vascular plant waxes are higher in the coaly shale samples than in the coals (Table 4.3).

(ii) Hopanes (Pentacyclic triterpanes)

Pentacyclic triterpanes (*m/z* 191) originating from bacteria/land plants are significantly enriched in the Upper Eocene coals and coaly shales. The hopane distributions are illustrated in the Fig. 4.10b. In five samples (A1-92, A2-55, A2-54, A2-52A, and A1-120) Tm (17α(H)-22,29,30-trisnohopane) is dominant over Ts (18α(H)-22,29,30-trisnorneohopane), whereas in two coal samples (A1-113, A1-114) and one coaly shale sample (A2-52), Ts predominates over Tm. Oleanane/C_{30} hopane ratios are higher in the coals than in coaly shales (Table 4.3; Fig. 4.11c). Oleanane is highly enriched in Phase-II coal A1-113, at 1.56 µg/g TOC (Table 4.3). C_{30} 17β,21α (H)-hopane is most abundant amongst the homohopanes in most samples, with the exception of coal A1-92, which has a high C_{29} 17β,21α (H)-hopane content. Contents of C_{31}-C_{33} homologues are high in all samples, whereas values of the C_{35} homohopane index are very low (<0.05), except for a value of 0.24 in one Phase-II coal (Table 4.3; Fig. 4.11g). Hopane/sterane ratios are generally higher in the coaly shales than in the coals (Table 4.3; Fig. 4.11h). Values of C_{31} 22S/(22S+22R), C_{32} 22S/(22S+22R), moretane/C_{30} hopane, Ts/Tm and Ts/(Ts+Tm) range between 0.23 and 0.56, 0.54 and 0.86, 0.32 and 0.87, 0.50 and 1.86, and 0.33 and 0.65, respectively (Table 4.3; Fig. 4.11e & f).

(iii) Steranes

Regular steranes are dominant and are illustrated in the Fig. 4.10 c. The ergostane (C_{28}) concentration is significantly greater (63%) than cholestane (C_{27}) and stigmastane (C_{29}) in Phase-II coal A1-92, while the other coals show predominance of C_{29} steranes (42% – 58%) (Table 4.3). Most coaly shales are enriched in C_{29} steranes (63% – 74%).

Regular sterane C_{29}- 20S/(20S+20R) values range from 0.03 to 0.37 overall, and sterane $C_{29}/(C_{27}+C_{28}+C_{29})$ ratios are uniformly greater (0.63 – 0.74) in the coaly shales than in the coals (0.27 – 0.58) (Table 4.3).

(b) Mudstones (Upper Cretaceous to Miocene)

(i) *n*-Alkanes and Acyclic isoprenoids (Pr/Ph, Pr/*n*-C_{17}, Ph/*n*-C_{18})

The presence of n-alkanes were identified in the range of C_{15}-C_{39} (Fig. 4.12 (i-a, ii-a, iii-a, iv-a)). Short-chain n-alkanes (<*n*-C_{20}) (Table 4.4) are relatively enrichment in mudstones of the upper Cretaceous and lower to middle Eocene and lesser in the upper Eocene and Pegu Group (Shwezetaw Fm., Padaung Fm., and Okhmintaung Fm.). Generally, Upper Cretaceous to Miocene succession is characterized by predominance of both mid-chain (*n*-$C_{21\text{-}25}$) (Fig. 4.13b) and long-chain (*n*-$C_{27\text{-}32}$) (Fig. 4.13c) compounds with a maximum intensity at *n*-C_{23}, *n*-C_{29}, and *n*-C_{31}. The carbon preference index (CPI) values are ranging from 1.06 to 1.89 in the upper Cretaceous to Paleocene; 1.41 to 3.75 in the Eocene; and 1.49 to 4.65 in the Pegu group (Table 4.4; Fig. 4. 13h).

Table 4.3. Biomarker data for Upper Eocene coal and coaly shale from the Central Myanmar Basin, Myanmar.

Formation	Yaw	Pondaung	Pondaung	Pondaung	Pondaung	Pondaung	Pondaung	Pondaung
Sample	A1-92	A1-113	A1-114	A2-55	A2-54	A2-52	A2-52A	A1-120
<*n*-C_{20}/total *n*-alkanes	0.08	0.31	0.06	0.18	0.22	0.21	0.06	0.02
<*n*-C_{20-25}/total *n*-alkanes	0.55	0.48	0.65	0.47	0.69	0.32	0.37	0.32
<*n*-C_{26-39}/total *n*-alkanes	0.37	0.22	0.29	0.34	0.09	0.47	0.57	0.66
CPI	2.11	1.16	1.46	2.09	1.29	2.22	2.25	1.76
Pr/Ph	2.37	3.16	0.71	4.63	0.23	9.09	0.69	0.24
Pr/*n*-C_{17}	7.03	7.81	4.80	9.86	1.87	5.44	7.34	4.75
Pr/*n*-C_{18}	1.05	2.96	0.69	1.07	0.48	2.76	1.02	1.02
P_{aq}	0.63	0.68	0.70	0.50	0.89	0.47	0.37	0.40
P_{wax}	0.48	0.41	0.40	0.59	0.19	0.66	0.69	0.69
Sterane 20R (%) C_{28}	62.54	20.41	28.22	21.89	30.57	19.22	10.98	18.29
Sterane 20R (%) C_{27}	10.57	34.75	29.74	19.83	5.26	18.04	21.10	7.23
Sterane 20R (%) C_{29}	26.89	44.84	42.04	58.27	64.17	62.74	67.92	74.48
Sterane C_{29} 20S/(20S+20R)	0.27	0.37	0.28	0.07	0.06	0.17	0.12	0.03
Sterane C_{27}/ (C_{27}R+C_{29}R)	0.28	0.44	0.41	0.25	0.08	0.22	0.24	0.09
Olean./ C_{30} Hopane	0.17	0.84	0.20	0.06	0.05	0.10	0.20	0.12
sterane C_{27}/ (C_{27}+C_{28}+C_{29})	0.11	0.35	0.30	0.20	0.05	0.18	0.21	0.07
sterane C_{28}/(C_{27}+C_{28}+C_{29})	0.63	0.20	0.28	0.22	0.31	0.19	0.11	0.18
sterane C_{29}/ (C_{27}+C_{28}+C_{29})	0.27	0.45	0.42	0.58	0.64	0.63	0.68	0.74
Ts/Tm	0.59	1.86	1.15	0.83	0.69	1.26	0.84	0.50
Ts/ (Ts+Tm)	0.37	0.65	0.54	0.45	0.41	0.56	0.46	0.33
C_{31} 22S/ (22S+22R)	0.23	0.56	0.51	0.38	0.49	0.37	0.41	0.35
C_{32} 22S/ (22S+22R)	0.54	0.76	0.70	0.74	0.80	0.74	0.68	0.86
Homohopane index	0.05	0.04	0.24	0.01	0.01	0.01	0.04	0.01
oleanane (µg/g TOC)	0.06	1.56	0.01	0.20	0.08	0.82	0.15	0.15
hopanes/steranes	6.03	15.65	1.55	64.91	185.71	26.80	43.69	66.66
steranes/ hopanes	0.17	0.06	0.65	0.02	0.01	0.04	0.02	0.02

total n-alkanes=sum of n-alkanes C_{16}–C_{39}

CPI= carbon preference index

Pr/Ph= pristane/phytane

Paq = (C_{23}+C_{25})/(C_{23}+C_{25}+C_{29}+C_{31})

Pwax = (C_{27}+C_{29}+C_{31})/(C_{23}+C_{25}+C_{27}+C_{29}+C_{31})

Ts/Tm= 18α (H)-22,20,30-trisnorneohopane/ 17α (H)-22,20,30-trisnohopane

Homohopane index=hopane C_{35} (S+R)/hopane [C_{31} (S+R) – C_{35} (S+R)]

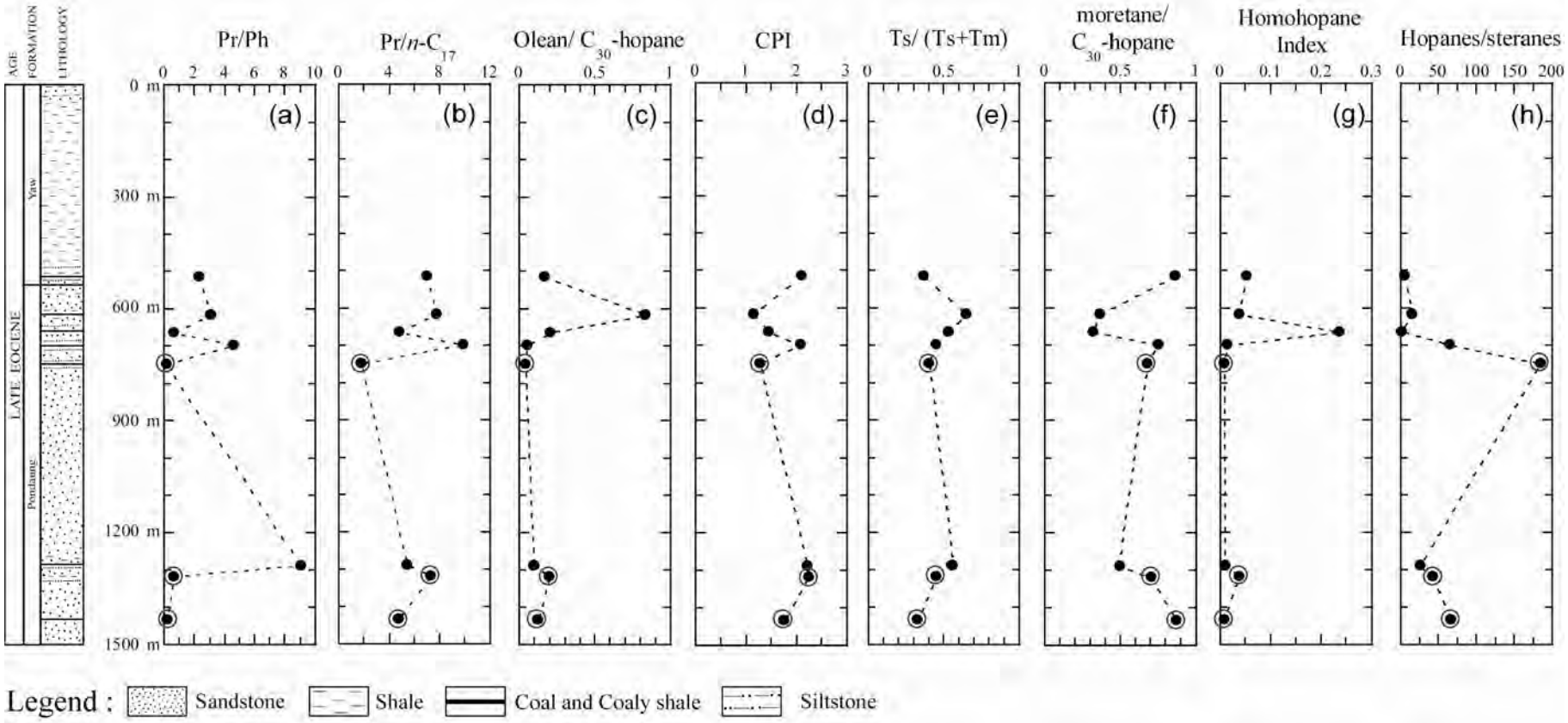

Fig. 4.11. Biomarker compositions of the Upper Eocene coals and coaly shales from the Central Myanmar Basin, Myanmar. Circled data points indicate weathered coaly shale samples.

Pr/Ph values are ranging between 0.1 and 4.1 in the upper Cretaceous to Paleocene; 0.1 and 1.8 in the Eocene; 0.1 and 0.9 in Oligocene mudstone samples (Table 4.4; Fig. 4.13f). These values are under very limited detection in the Miocene mudstones.

The Pr/*n*-C_{17} and Ph/*n*-C_{18} values range from 0.74 - 16.19 and 0.19 to 5.19 in the upper Cretaceous to Paleocene; 0.53 - 11.8 and 0.32 - 4.51 in the Eocene; 0.53 to 8.04 and 0.39 to 1.76 in the Pegu Group mudstones (Table 4.4; Fig. 4.13g).

(ii) Hopanes (Pentacyclic triterpanes)

The distributions of hopanes in the mudstones are illustrated in Fig. 4.12 (i-b, ii-b, iii-b, iv-b)). Ts (18α (H)-22,29,30-trisnorhopane) is dominant over Tm (17α (H)-22,29,30-trisnorhopane) in the upper Cretaceous to middle Eocene and late Eocene (Pondaung Fm.). Ts/Tm values are higher in the upper Cretaceous to middle Eocene (Table 4.5).

The Ts/(Ts+Tm) ratios are varying from 0.64 to 0.92 in the upper Cretaceous to Paleocene, 0.19 to 0.84 in the Eocene, and 0.16 to 0.65 in the Pegu group (Table 4.5; Fig. 4.14d). The concentration of oleanane is varying from 0.26 to 15.03 μg/g TOC in the upper Cretaceous to Paleocene; 0.05 to 9.76 in the Eocene; and 0.02 to 3.44 in the Pegu group (Table 4.5).

The oleanane/C_{30} hopane values are varying from 0.07 to 0.59; 0.02 to 1.72; and 0.05 to 1.04; in the upper Cretaceous to Paleocene, Eocene, and Pegu Group mudstones, respectively (Table 4.5; Fig. 4.14a).

The values of moretane/C_{30}-hopane range from 0.10 to 0.52 in the upper Cretaceous; 0.36 to 0.63 in the Paleocene, 0.26 to 3.35 in the Eocene, and 0.21 to 2.11 in the Pegu Group, respectively (Table 4.5). The extended homohopanes (C_{31}-C_{35}) are predominant in all mudstone samples. All mudstones indicate very low C_{35} homohopane index with a varying from 0.01 to 0.23 (Table 4.5; Fig. 4.14b).

The values of hopane/sterane ratio are ranging between 7.25 and 49.37 in the upper Cretaceous to Paleocene; 5.51 and 43.95 in the Eocene; 0.49 and 24.05 in the Pegu Group mudstones (Table 4.5; Fig. 4.14c). Contents of hopane concentration are widely ranging from 4.61 to 191.62; 7.47 to 209.24; 0.95 to 29.32 in the upper Cretaceous to Paleocene, Eocene, and Pegu Group respectively.

The distribution of moretane is more predominant in Miocene mudstones, while 17α, 21β C_{30}-hopane is significant in upper Cretaceous to Oligocene mudstones.The concentration of oleanane is varying from 0.26 to 15.03 μg/g TOC in the upper Cretaceous to Paleocene; 0.05 to 9.76 in the Eocene; and 0.02 to 3.44 in the Pegu group (Table 4.5). The oleanane/C_{30} hopane values are varying from 0.07 to 0.59; 0.02 to 1.72; and 0.05 to 1.04; in the upper Cretaceous to Paleocene, Eocene, and Pegu Group mudstones, respectively (Table 4.5; Fig. 4.14a).

(iii) Steranes

The distributions of the regular steranes in the m/z 217 mass chromatogram are shown in Fig. 4.12 (i-c, ii-c, iii-c, iv-c)). The stigmastane (C_{29}) concentration is mostly higher than cholestane (C_{27}) and ergostane (C_{28}) in upper Cretaceous to Eocene mudstones.

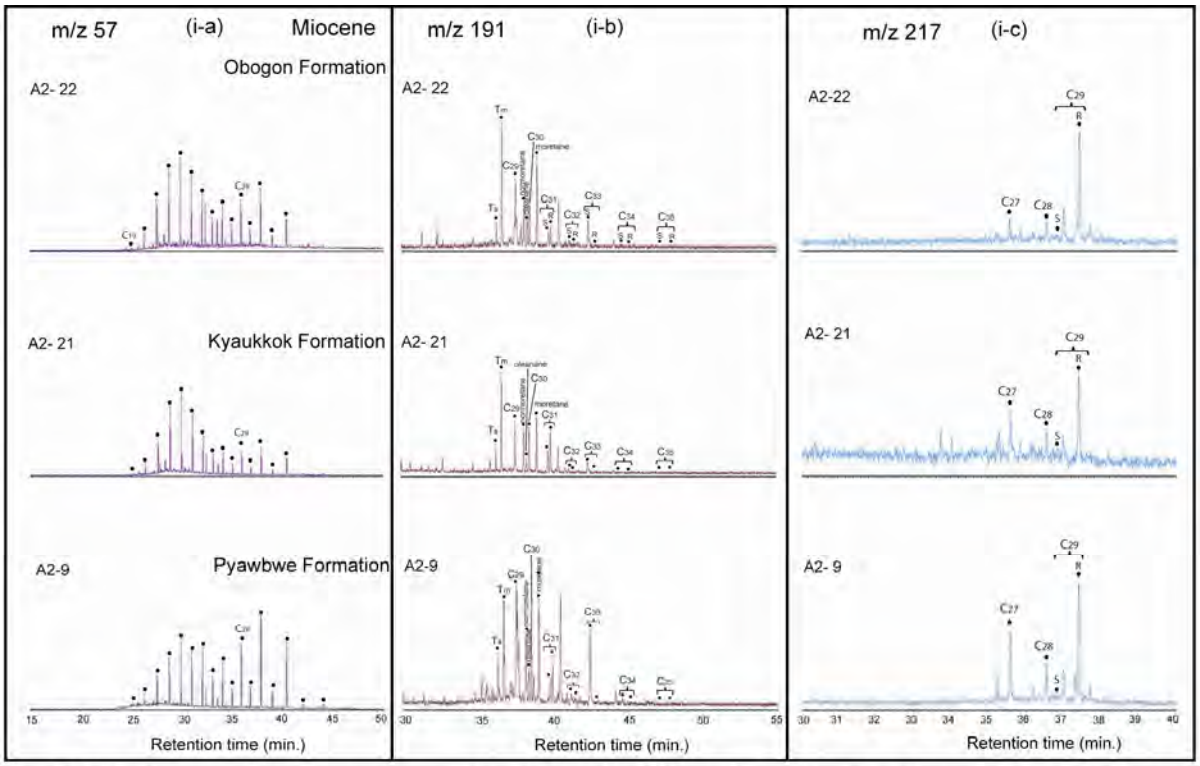

Fig. 4.12 (i). Representatives chromatograms of mudstones for Miocene Formation (a) n-alkanes (m/z 57), (b) Hopanes (m/z 191), and (c) Steranes (m/z 217) from the western margin of the Central Myanmar Basin.

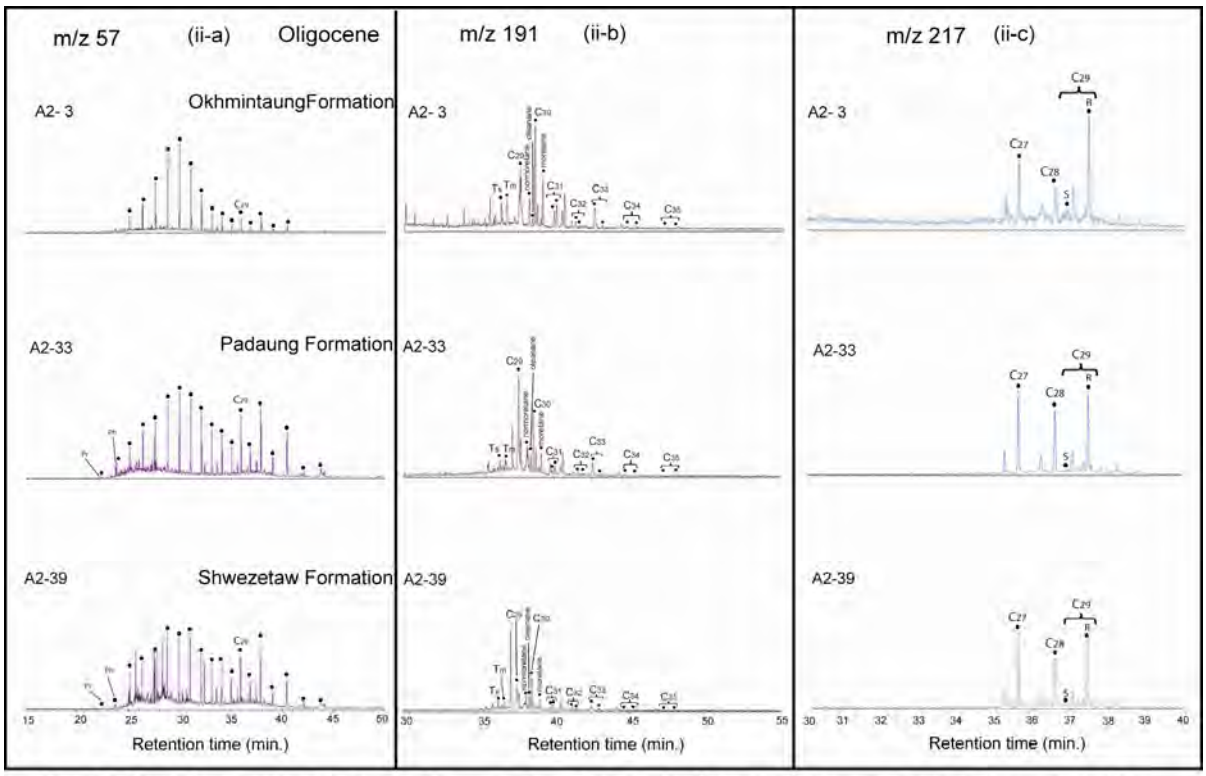

Fig. 4.12 (ii). Representatives chromatograms of mudstones for Oligocene Formation (a) n-alkanes (m/z 57), (b) Hopanes (m/z 191), and (c) Steranes (m/z 217) from the western margin of the Central Myanmar Basin.

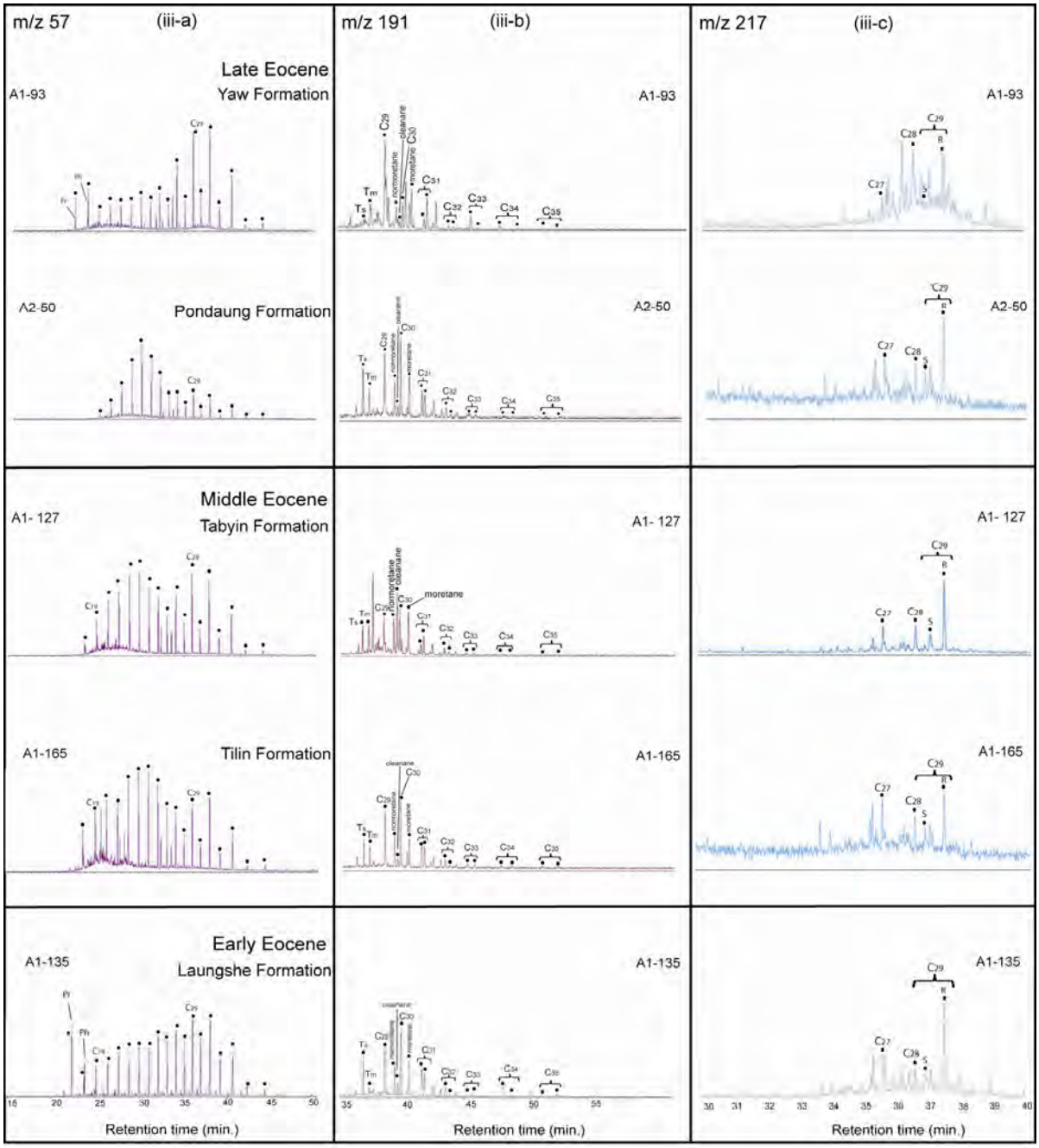

Fig. 4.12 (iii). Representatives chromatograms of mudstones for Eocene Formation (a) n-alkanes (m/z 57), (b) Hopanes (m/z 191), and (c) Steranes (m/z 217) from the western margin of the Central Myanmar Basin.

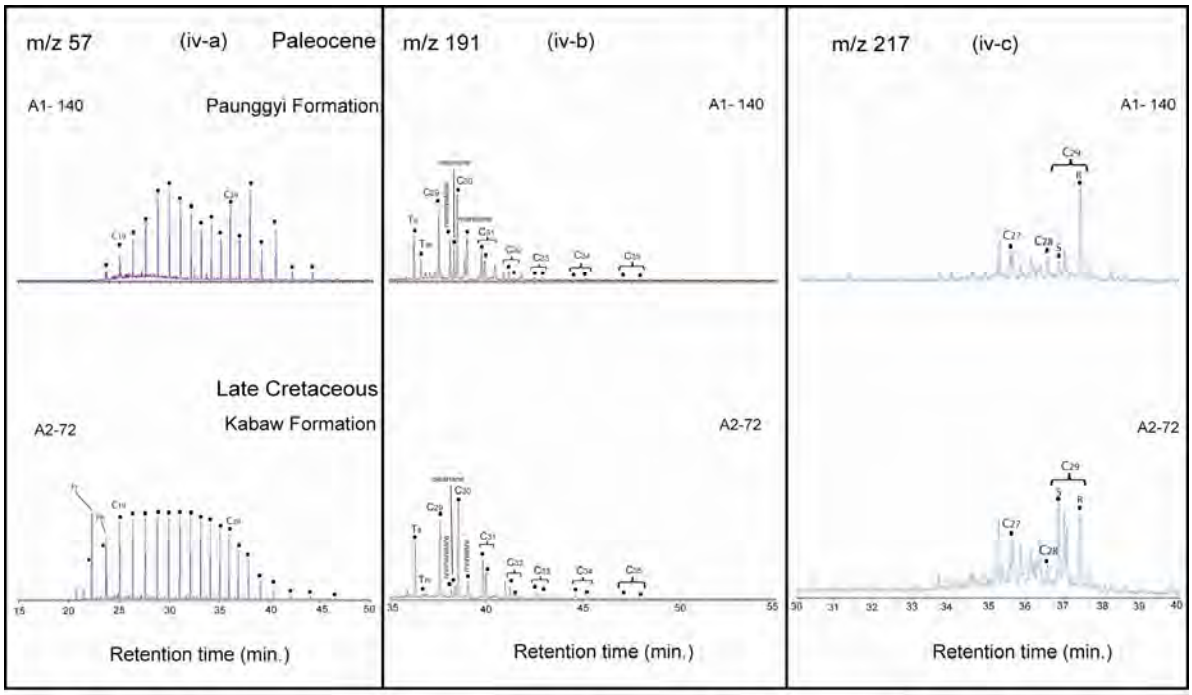

Fig. 4.12 (iv). Representatives chromatograms of mudstones for Paleocene and Upper Cretaceous Formations (a) n-alkanes (m/z 57), (b) Hopanes (m/z 191), and (c) Steranes (m/z 217) from the western margin of the Central Myanmar Basin.

The C_{27} sterane is relatively abundant in the upper Cretaceous, Eocene (Laungshe, Tilin, Yaw), and Pegu Group (Padaung, Okhmintaung, Pyawbwe, and Kyaukkok) mudstones. The values of sterane $C_{29}/(C_{27}+C_{28}+C_{29})$ are varying from 0.39 to 0.76 in the upper Cretaceous to Eocene and from 0.36 to 0.78 in the Pegu Group mudstones, while that of sterane $C_{27}/(C_{27}+C_{28}+C_{29})$ ratio are slightly enrichment in the upper Cretaceous, early to middle Eocene (Tilin Fm.) and Pegu Group (Padaung, Okhmintaung, Pyawbwe, Kyaukkok) mudstones (Table 4.6; Fig. 4.14 f & g). The sterane C_{29} 20S/(20S+20R) values in all mudstones are less than 0.5. These values are close to 0.5 in most late Cretaceous mudstones (0.1-0.49). (Table 4.6; Fig. 4.14e)

Table 4.4. Biomarker data (*n* -alkanes, iso-prenoids) for Upper Cretaceous to Miocene mudstones from the Central Myanmar Basin, Myanmar. (n.d, not detected)

Formation	Sample	$<n\text{-}C_{20}$/ total *n* -alkanes	$<n\text{-}C_{20\text{-}25}$/ total *n* -alkanes	$<n\text{-}C_{26\text{-}39}$/ total *n* -alkanes	$n\text{-}C_{29}/n\text{-}C_{19}$	$n\text{-}C_{23}/n\text{-}C_{29}$	Pr/Ph	CPI	$Pr/n\text{-}C_{17}$	$Pr/n\text{-}C_{18}$	P_{aq}	P_{wax}
Obogon	A2-22	0.002	0.54	0.46	28.74	2.20	n.d	2.32	n.d	n.d	0.54	0.54
Obogon	A2-24	0.000	0.41	0.59	n.d	1.00	n.d	1.69	n.d	n.d	0.49	0.59
Obogon	A2-26	0.007	0.56	0.43	8.66	2.17	n.d	2.41	n.d	n.d	0.57	0.50
Kyaukkok	A2-28	0.002	0.64	0.36	22.27	3.39	n.d	1.82	n.d	n.d	0.70	0.38
Kyaukkok	A2-29	0.003	0.54	0.45	28.49	2.04	n.d	2.37	n.d	n.d	0.58	0.49
Kyaukkok	A2-21	0.003	0.63	0.37	18.47	3.04	n.d	2.27	n.d	n.d	0.65	0.42
Kyaukkok	A2-20	0.001	0.51	0.49	50.33	2.11	n.d	1.86	n.d	n.d	0.60	0.49
Pyawbwe	A2-16	0.001	0.69	0.30	36.61	4.62	n.d	1.79	n.d	n.d	0.77	0.31
Pyawbwe	A2-12	0.002	0.54	0.46	49.93	2.14	n.d	2.20	n.d	n.d	0.60	0.48
Pyawbwe	A2-9	0.004	0.37	0.62	35.00	1.08	0.03	3.18	0.22	0.83	0.40	0.65
Okhmintaung	A1-89	0.019	0.72	0.27	1.88	5.14	0.48	1.62	4.24	1.04	0.77	0.32
Okhmintaung	A2-7	0.034	0.59	0.37	2.07	2.40	0.32	2.17	1.75	0.91	0.61	0.45
Okhmintaung	A2-6	0.073	0.68	0.25	0.78	3.17	0.24	1.69	2.27	0.48	0.69	0.38
Okhmintaung	A2-5	0.017	0.39	0.59	6.89	0.85	0.29	2.33	0.53	0.79	0.38	0.67
Okhmintaung	A2-3	0.039	0.74	0.22	0.90	6.36	0.08	1.75	0.91	0.88	0.80	0.27
Padaung	A2-38	0.031	0.53	0.44	2.56	2.03	0.09	2.51	1.14	1.08	0.54	0.52
Padaung	A2-36	0.061	0.71	0.23	0.75	3.84	0.14	1.74	1.66	1.00	0.73	0.35
Padaung	A2-34	0.008	0.55	0.44	9.82	1.85	0.30	1.96	1.07	0.60	0.54	0.52
Padaung	A2-33	0.044	0.44	0.51	2.13	1.37	0.10	1.89	0.89	1.64	0.49	0.58
Padaung	A1-103	0.035	0.63	0.34	1.99	2.80	0.22	2.25	1.43	0.39	0.63	0.44
Padaung	A1-105	0.012	0.39	0.60	10.47	0.72	0.90	1.82	3.03	0.62	0.42	0.66
Padaung	A1-107	0.039	0.55	0.41	2.13	2.04	0.13	2.43	1.41	0.84	0.55	0.52
Shwezetaw	A2-39	0.029	0.49	0.48	2.84	1.36	0.09	1.82	0.87	1.15	0.48	0.59
Shwezetaw	A2-42	0.038	0.36	0.61	3.18	0.66	0.35	2.48	1.69	1.09	0.31	0.72
Shwezetaw	A2-43	0.019	0.25	0.73	6.75	0.47	0.32	2.08	4.84	1.76	0.27	0.77
Shwezetaw	A2-41	0.019	0.39	0.59	5.08	0.74	0.46	1.88	1.36	0.57	0.33	0.72
Shwezetaw	A2-45	0.071	0.57	0.36	1.23	2.22	0.61	1.49	3.11	0.80	0.62	0.46
Shwezetaw	A1-109	0.074	0.44	0.48	1.39	1.00	0.83	3.82	8.04	1.50	0.50	0.63
Shwezetaw	A1-111	0.015	0.13	0.85	14.35	0.19	0.27	4.65	5.91	1.56	0.13	0.89
Shwezetaw	A1-112	0.055	0.60	0.35	1.26	2.80	0.23	1.99	1.47	0.60	0.62	0.44
Yaw	A2-58	0.056	0.45	0.49	1.74	1.35	0.32	1.53	1.97	0.70	0.52	0.56
Yaw	A2-60	0.042	0.53	0.43	1.99	1.84	0.09	2.30	1.44	0.66	0.52	0.54
Yaw	A2-59	0.027	0.52	0.45	2.52	2.41	0.25	2.15	10.35	0.44	0.56	0.50
Yaw	A1-100	0.024	0.30	0.68	5.41	0.60	0.13	2.77	1.18	0.88	0.33	0.73
Yaw	A1-99	0.030	0.42	0.55	3.76	1.03	0.06	2.65	1.17	1.96	0.43	0.63
Yaw	A1-98	0.066	0.58	0.36	1.31	2.24	0.19	2.15	1.96	1.41	0.59	0.48
Yaw	A1-96	0.026	0.22	0.76	6.97	0.32	0.27	2.86	6.68	4.51	0.23	0.81
Yaw	A1-95	0.015	0.23	0.76	11.83	0.33	0.39	3.09	4.03	1.85	0.24	0.80
Yaw	A1-93	0.043	0.20	0.75	5.98	0.27	0.78	3.03	7.67	3.66	0.21	0.83

Table 4.4. continued-

Formation	Sample	$<n$-C_{20}/ total n-alkanes	$<n$-$C_{20\text{-}25}$/ total n-alkanes	$<n$-$C_{26\text{-}39}$/ total n-alkanes	n-C_{29}/n-C_{19}	n-C_{23}/n-C_{29}	Pr/Ph	CPI	Pr/n-C_{17}	Pr/n-C_{18}	P_{aq}	P_{wax}
Pondaung	A1-115	0.038	0.36	0.60	2.50	1.11	0.58	3.07	8.34	1.27	0.36	0.67
Pondaung	A1-117	0.029	0.20	0.77	6.55	0.33	0.63	3.75	11.80	2.69	0.19	0.83
Pondaung	A2-50	0.010	0.63	0.36	6.38	3.04	0.71	1.76	3.22	0.36	0.69	0.40
Tabyin	A2-48	0.010	0.33	0.66	14.06	0.63	0.30	2.57	2.09	2.08	0.34	0.71
Tabyin	A1-123	0.072	0.59	0.34	0.96	2.71	0.24	1.93	3.35	1.10	0.63	0.44
Tabyin	A1-125	0.026	0.25	0.72	8.00	0.33	0.25	3.03	4.02	1.58	0.26	0.79
Tabyin	A1-126	0.040	0.52	0.44	2.31	1.41	0.23	2.22	1.57	0.55	0.47	0.59
Tabyin	A1-127	0.052	0.44	0.51	2.51	0.94	0.09	2.51	0.60	0.62	0.43	0.64
Tabyin	A2-62	0.083	0.77	0.15	0.30	12.00	0.39	1.41	3.61	0.46	0.90	0.17
Tabyin	A1-129	0.089	0.47	0.44	1.13	1.38	0.23	1.94	9.76	0.69	0.52	0.56
Tabyin	A1-131	0.102	0.41	0.49	1.47	1.07	0.17	2.07	0.80	1.26	0.46	0.61
Tilin	A1-165	0.087	0.47	0.44	1.05	1.67	0.40	2.04	7.74	0.53	0.54	0.54
Tilin	A1-164	0.081	0.58	0.33	0.97	2.43	0.35	1.75	8.41	0.68	0.63	0.45
Tilin	A2-84	0.002	0.56	0.44	54.07	2.60	1.17	1.45	0.93	0.43	0.69	0.41
Laungshe	A2-65	0.052	0.30	0.65	2.59	0.71	0.95	1.91	5.19	0.53	0.31	0.73
Laungshe	A1-162	0.022	0.45	0.53	4.03	1.23	0.43	1.73	7.60	0.39	0.52	0.57
Laungshe	A1-134	0.005	0.50	0.50	18.37	1.49	1.45	1.57	9.78	0.80	0.57	0.53
Laungshe	A1-135	0.111	0.23	0.66	3.57	0.46	1.06	1.86	0.53	2.19	0.29	0.76
Laungshe	A1-136	0.088	0.24	0.67	5.22	0.46	1.81	1.92	0.99	1.97	0.30	0.76
Laungshe	A1-160	0.034	0.22	0.74	7.12	0.26	0.68	2.35	3.74	1.52	0.22	0.82
Laungshe	A1-158	0.068	0.45	0.49	2.07	1.15	0.50	1.93	0.87	0.56	0.49	0.60
Laungshe	A1-157	0.039	0.42	0.54	3.16	0.97	0.15	1.95	2.36	0.77	0.46	0.62
Laungshe	A1-156	0.005	0.41	0.59	23.68	0.99	0.24	1.66	3.40	1.50	0.48	0.60
Laungshe	A1-153	0.018	0.46	0.52	5.35	1.16	0.32	1.60	2.39	0.32	0.52	0.58
Paunggyi	A1-137	0.003	0.23	0.76	47.42	0.49	0.31	1.80	4.48	2.76	0.30	0.75
Paunggyi	A1-140	0.030	0.40	0.57	3.29	1.25	0.16	1.89	1.41	1.16	0.45	0.62
Paunggyi	A2-69	0.003	0.59	0.41	37.88	2.73	0.55	1.35	1.32	1.10	0.71	0.38
Paunggyi	A1-152	0.096	0.58	0.32	0.75	2.59	0.14	1.32	0.83	0.66	0.68	0.42
Kabaw	A1-142	0.122	0.54	0.34	0.65	2.28	1.35	1.66	1.98	0.37	0.62	0.46
Kabaw	A2-77	0.082	0.56	0.36	0.77	2.41	1.04	1.07	2.12	0.22	0.71	0.43
Kabaw	A2-78	0.114	0.45	0.44	1.10	1.30	3.52	1.10	2.12	0.32	0.59	0.54
Kabaw	A2-74	0.049	0.56	0.39	1.31	2.12	0.68	1.06	4.77	0.19	0.70	0.44
Kabaw	A1-149	0.023	0.32	0.66	6.15	0.58	0.51	1.77	16.19	0.88	0.36	0.70
Kabaw	A1-145	0.003	0.61	0.39	17.30	3.18	0.42	1.53	0.74	5.19	0.72	0.39
Kabaw	A1-146	0.002	0.67	0.33	115.29	3.18	1.34	1.78	0.93	0.51	0.84	0.29
Kabaw	A1-150	0.105	0.38	0.51	1.32	0.85	0.82	1.66	2.31	0.51	0.43	0.65
Kabaw	A2-80	0.025	0.62	0.36	2.10	2.58	0.33	1.18	7.30	0.31	0.76	0.38
Kabaw	A2-72	0.158	0.45	0.39	0.92	1.35	4.08	1.16	2.09	0.40	0.61	0.53
Kabaw	A2-71	0.085	0.45	0.47	1.36	1.26	3.18	1.11	3.22	0.40	0.59	0.55
Kabaw	A2-70	0.197	0.37	0.43	1.07	1.12	3.97	1.07	1.56	0.49	0.55	0.58

4.1.7.2 Aromatic hydrocarbons

The various unsubstituted PAHs such as cadalene (Cad), phenanthrene (Phe), fluoranthene (Fla), pyrene (Py), benzo[a]anthracene(BaAn), chrysene/triphenylene (Chry+Tpn), benzofluoranthrenes (Bflas), benzo [e]pyrene (BePy), benzo [a] pyrene (BaPy), perylene (Pery), benzo [ghi] perylene (BghiP), indeo[1,2,3-*cd*] pyrene (InPy), coronene (Cor) and retene (Ret) show abundant distribution in all studied samples.

(a) Coal and coaly shale (Upper Eocene)

Aromatic compounds comprising combustion-derived polycyclic aromatic hydrocarbons (PAHs) (Table 4.7; Fig. 4.15) and their alkylated hydrocarbons are relatively abundant. Concentrations of two to five-ring PAHs are relatively high in all samples. Six-ring PAHs such as InPy and BghiP were present at low levels in the coal A1-114 (Fig. 4.15), but were not detected in any other coal or in the coaly shale A2-54 (Table 4.7). Total combustion-derived PAHs concentration is greatest in the coaly shale A2-52 (Table 4.7; Fig. 4.16e).

Methyl derivative compounds such as methylphenanthrenes (3-MP, 2-MP, (9+4)-MP, 1-MP) and dimethylphenanthrenes (DMP) were detected in the coals and the unweathered coaly shale A2-52. Pimarane (1,7 DMP) is more abundant (0.53 μg/g TOC) in A2-52 than in the coals (0.03–0.21 μg/g TOC), but was not detected in the other three coaly shales (Table 4.7; Fig. 4.16c). The same pattern is seen for perylene, which is abundant in A2-52 (9.86 μg/g TOC), present at lower levels in all coals (0.15–0.66 μg/g TOC), but was not detected in the remaining coaly shales (Table 4.7; Fig. 4.16d).

Table 4.5. Biomarker data (hopanes) for Late Cretaceous to Miocene mudstones from the Central Myanmar Basin, Myanmar.

Formation	Sample	Olean./ C_{30} Hopane	Ts/Tm	Ts/ (Ts+Tm)	C_{31} 22S/ (22S+22R)	C_{32} 22S/ (22S+22R)	Moretane/ C_{30} hopane	Homohopane index	oleanane (µg/g TOC)	hopanes/steranes
Obogon	A2-22	0.73	0.18	0.16	0.44	0.62	1.79	0.04	1.38	7.83
Obogon	A2-24	0.52	1.83	0.65	0.37	0.60	0.48	0.23	0.06	15.02
Obogon	A2-26	1.04	1.49	0.60	0.44	0.63	2.11	0.01	1.48	6.29
Kyaukkok	A2-28	0.31	0.62	0.38	0.43	0.65	1.39	0.08	0.42	14.88
Kyaukkok	A2-29	0.33	0.46	0.31	0.40	0.88	1.47	0.01	0.69	24.05
Kyaukkok	A2-21	0.33	0.26	0.21	0.33	0.74	1.49	0.02	1.01	15.52
Kyaukkok	A2-20	0.49	0.51	0.34	0.41	0.52	0.85	0.11	0.79	17.15
Pyawbwe	A2-16	0.27	0.53	0.35	0.56	0.61	0.49	0.06	0.15	12.43
Pyawbwe	A2-12	0.19	0.60	0.38	0.45	0.42	0.34	0.13	0.28	6.03
Pyawbwe	A2-9	0.35	0.45	0.31	0.39	0.46	1.23	0.04	0.86	4.19
Okhmintaung	A1-89	0.24	0.51	0.34	0.48	0.58	0.34	0.17	0.07	17.21
Okhmintaung	A2-7	0.11	0.66	0.40	0.30	0.50	1.95	0.02	0.11	5.28
Okhmintaung	A2-6	0.11	1.02	0.50	0.47	0.59	0.21	0.13	0.28	6.23
Okhmintaung	A2-5	0.22	0.74	0.43	0.31	0.32	1.45	0.04	0.54	3.60
Okhmintaung	A2-3	0.08	0.74	0.43	0.35	0.51	0.43	0.07	0.15	3.60
Padaung	A2-38	0.14	0.69	0.41	0.32	0.53	1.42	0.04	0.26	6.56
Padaung	A2-36	0.20	0.65	0.39	0.37	0.43	1.15	0.06	0.24	1.56
Padaung	A2-34	0.19	0.32	0.24	0.29	0.44	0.86	0.08	0.03	2.34
Padaung	A2-33	0.33	0.75	0.43	0.39	0.48	0.29	0.05	1.66	0.69
Padaung	A1-103	0.28	0.40	0.29	0.43	0.47	0.66	0.14	0.17	15.36
Padaung	A1-105	0.05	0.48	0.32	0.31	0.65	0.61	0.09	0.02	10.96
Padaung	A1-107	0.60	0.59	0.37	0.42	0.56	0.70	0.13	1.72	14.06
Shwezetaw	A2-39	0.38	1.06	0.51	0.48	0.54	0.29	0.07	2.61	0.49
Shwezetaw	A2-42	0.56	0.52	0.34	0.33	0.55	0.61	0.05	3.44	4.88
Shwezetaw	A2-43	0.21	0.46	0.31	0.30	0.57	0.57	0.05	1.10	4.80
Shwezetaw	A2-41	0.21	0.53	0.35	0.32	0.59	0.66	0.08	0.89	6.03
Shwezetaw	A2-45	0.47	0.69	0.41	0.29	0.63	0.63	0.05	1.45	1.54
Shwezetaw	A1-109	0.07	0.26	0.20	0.31	0.41	0.21	0.05	0.18	20.82
Shwezetaw	A1-111	0.14	0.29	0.22	0.28	0.52	1.99	0.03	0.13	22.25
Shwezetaw	A1-112	0.15	0.33	0.25	0.55	0.72	0.86	0.09	0.56	12.32
Yaw	A2-58	0.82	0.43	0.30	0.39	0.60	0.59	0.07	1.08	7.16
Yaw	A2-60	0.79	0.58	0.37	0.33	0.60	0.70	0.07	9.76	5.89
Yaw	A2-59	0.37	0.80	0.44	0.43	0.70	0.67	0.13	0.51	8.59
Yaw	A1-100	0.09	0.33	0.25	0.22	0.59	3.35	0.03	0.32	31.43
Yaw	A1-99	0.11	0.56	0.36	0.24	0.52	2.21	0.02	0.33	31.55
Yaw	A1-98	0.18	0.40	0.29	0.28	0.58	2.38	0.07	0.97	23.70
Yaw	A1-96	0.14	0.44	0.31	0.26	0.54	1.38	0.02	0.66	18.36
Yaw	A1-95	0.07	0.47	0.32	0.21	0.54	2.64	0.01	0.25	43.95
Yaw	A1-93	0.29	0.31	0.24	0.26	0.54	1.97	0.01	4.45	18.75

Table 4.5 continued-

Formation	Sample	Olean./ C_{30} Hopane	Ts/Tm	Ts/ (Ts+Tm)	C_{31} 22S/ (22S+22R)	C_{32} 22S/ (22S+22R)	Moretane/ C_{30} hopane	Homohopane index	oleanane (µg/g TOC)	hopanes/steranes
Pondaung	A1-115	0.29	0.24	0.19	0.50	0.83	0.57	0.04	2.23	11.28
Pondaung	A1-117	0.17	0.32	0.24	0.38	0.54	0.52	0.06	1.41	6.67
Pondaung	A2-50	0.11	1.60	0.61	0.66	0.43	0.53	0.05	0.16	10.71
Tabyin	A2-48	0.58	0.65	0.39	0.23	0.63	1.47	0.07	1.03	13.35
Tabyin	A1-123	0.18	1.18	0.54	0.44	0.61	0.63	0.06	1.06	6.14
Tabyin	A1-125	0.22	1.01	0.50	0.35	0.66	0.85	0.04	1.17	6.52
Tabyin	A1-126	0.29	0.86	0.46	0.44	0.55	0.69	0.08	0.52	6.24
Tabyin	A1-127	1.72	0.83	0.45	0.34	0.68	1.12	0.05	7.21	7.72
Tabyin	A2-62	0.21	1.21	0.55	0.53	0.68	0.26	0.19	0.57	12.47
Tabyin	A1-129	0.02	2.28	0.69	0.55	0.80	0.74	0.06	0.09	16.29
Tabyin	A1-131	0.02	2.17	0.68	0.57	0.64	0.83	0.09	0.05	15.64
Tilin	A1-165	0.12	1.13	0.53	0.49	0.61	0.44	0.12	0.46	15.15
Tilin	A1-164	0.06	1.81	0.64	0.52	0.82	0.68	0.04	0.56	17.71
Tilin	A2-84	0.31	3.70	0.79	0.60	0.77	0.64	0.11	1.15	23.36
Laungshe	A2-65	0.38	1.01	0.50	0.47	0.71	0.51	0.05	4.20	10.72
Laungshe	A1-162	0.08	1.87	0.65	0.57	0.88	0.69	0.03	0.86	16.41
Laungshe	A1-134	0.04	5.26	0.84	0.59	0.76	0.67	0.05	0.54	17.68
Laungshe	A1-135	0.19	5.16	0.84	0.55	0.78	0.54	0.07	8.13	15.91
Laungshe	A1-136	0.36	3.75	0.79	0.52	0.78	0.48	0.06	8.64	9.54
Laungshe	A1-160	0.57	0.79	0.44	0.33	0.70	0.96	0.02	4.36	5.51
Laungshe	A1-158	0.08	1.99	0.67	0.51	0.86	0.71	0.03	1.04	13.74
Laungshe	A1-157	0.07	1.66	0.62	0.47	0.84	0.76	0.02	0.38	15.57
Laungshe	A1-156	0.08	3.15	0.76	0.59	0.69	0.67	0.05	0.39	14.61
Laungshe	A1-153	0.03	4.28	0.81	0.56	0.80	0.69	0.05	0.32	14.79
Paunggyi	A1-137	0.32	1.98	0.66	0.52	0.78	0.63	0.03	3.87	15.17
Paunggyi	A1-140	0.38	1.75	0.64	0.56	0.78	0.53	0.03	15.03	17.04
Paunggyi	A2-69	0.33	2.61	0.72	0.55	0.48	0.53	0.14	0.26	14.15
Paunggyi	A1-152	0.09	6.40	0.86	0.60	0.88	0.36	0.04	1.42	26.51
Kabaw	A1-142	0.21	2.33	0.70	0.59	0.69	0.52	0.08	0.62	15.06
Kabaw	A2-77	0.10	9.68	0.91	0.61	0.84	0.13	0.03	1.96	49.37
Kabaw	A2-78	0.25	6.88	0.87	0.61	0.87	0.22	0.04	8.88	18.06
Kabaw	A2-74	0.29	6.29	0.86	0.60	0.74	0.10	0.07	0.90	32.38
Kabaw	A1-149	0.16	6.80	0.87	0.60	0.81	0.52	0.03	1.27	7.25
Kabaw	A1-145	0.59	2.74	0.73	0.61	0.58	0.29	0.17	1.22	29.33
Kabaw	A1-146	0.20	3.60	0.78	0.71	0.58	0.48	0.11	0.64	46.52
Kabaw	A1-150	0.29	3.90	0.80	0.60	0.69	0.51	0.09	0.33	12.24
Kabaw	A2-80	0.07	11.77	0.92	0.61	0.88	0.15	0.03	0.55	36.53
Kabaw	A2-72	0.14	9.75	0.91	0.61	0.88	0.15	0.02	0.81	19.88
Kabaw	A2-71	0.28	8.54	0.90	0.64	0.88	0.16	0.03	2.94	8.77
Kabaw	A2-70	0.17	10.95	0.92	0.60	0.89	0.26	0.03	3.09	12.56

Table 4.6. Biomarker data (steranes) for Late Cretaceous to Miocene mudstones from the Central Myanmar Basin, Myanmar.

Formation	Sample	Sterane 20R (%)			Sterane C_{29}	Sterane C_{27}/	sterane C_{27}/	sterane C_{28}/	sterane C_{29}/	steranes/ hopanes
		C28	C27	C29	20S/(20S+20R)	(C_{27}R+C_{29}R)	(C_{27}+C_{28}+C_{29})	(C_{27}+C_{28}+C_{29})	(C_{27}+C_{28}+C_{29})	
Obogon	A2-22	14	9	76	0.03	0.11	0.09	0.14	0.76	0.13
Obogon	A2-24	27	28	44	0.22	0.39	0.28	0.27	0.44	0.07
Obogon	A2-26	12	13	75	0.02	0.15	0.13	0.12	0.75	0.16
Kyaukkok	A2-28	6	51	43	0.19	0.54	0.51	0.06	0.43	0.07
Kyaukkok	A2-29	18	26	56	0.06	0.32	0.26	0.18	0.56	0.04
Kyaukkok	A2-21	17	21	62	0.10	0.25	0.21	0.17	0.62	0.06
Kyaukkok	A2-20	12	47	41	0.15	0.53	0.47	0.12	0.41	0.06
Pyawbwe	A2-16	14	31	55	0.18	0.36	0.31	0.14	0.55	0.08
Pyawbwe	A2-12	21	34	45	0.30	0.43	0.34	0.21	0.45	0.17
Pyawbwe	A2-9	11	32	56	0.02	0.37	0.32	0.11	0.56	0.24
Okhmintaung	A1-89	18	39	43	0.26	0.48	0.39	0.18	0.43	0.06
Okhmintaung	A2-7	24	12	64	0.04	0.16	0.12	0.24	0.64	0.19
Okhmintaung	A2-6	22	36	42	0.04	0.46	0.36	0.22	0.42	0.16
Okhmintaung	A2-5	12	10	78	0.03	0.12	0.10	0.12	0.78	0.28
Okhmintaung	A2-3	27	23	49	0.10	0.32	0.23	0.27	0.49	0.28
Padaung	A2-38	19	23	58	0.03	0.29	0.23	0.19	0.58	0.15
Padaung	A2-36	30	34	36	0.01	0.48	0.34	0.30	0.36	0.64
Padaung	A2-34	30	31	39	0.05	0.44	0.31	0.30	0.39	0.43
Padaung	A2-33	32	30	38	0.02	0.44	0.30	0.32	0.38	1.44
Padaung	A1-103	16	44	40	0.27	0.52	0.44	0.16	0.40	0.07
Padaung	A1-105	13	35	52	0.34	0.40	0.35	0.13	0.52	0.09
Padaung	A1-107	12	33	55	0.16	0.38	0.33	0.12	0.55	0.07
Shwezetaw	A2-39	30	33	37	0.03	0.47	0.33	0.30	0.37	2.05
Shwezetaw	A2-42	32	4	63	0.11	0.07	0.04	0.32	0.63	0.21
Shwezetaw	A2-43	19	12	69	0.02	0.15	0.12	0.19	0.69	0.21
Shwezetaw	A2-41	16	9	75	0.04	0.11	0.09	0.16	0.75	0.17
Shwezetaw	A2-45	17	8	74	0.03	0.10	0.08	0.17	0.74	0.65
Shwezetaw	A1-109	31	21	48	0.15	0.31	0.21	0.31	0.48	0.05
Shwezetaw	A1-111	25	13	62	0.17	0.17	0.13	0.25	0.62	0.04
Shwezetaw	A1-112	22	14	64	0.16	0.18	0.14	0.22	0.64	0.08
Yaw	A2-58	23	5	72	0.02	0.06	0.05	0.23	0.72	0.14
Yaw	A2-60	19	13	69	0.08	0.15	0.13	0.19	0.69	0.17
Yaw	A2-59	20	19	61	0.09	0.23	0.19	0.20	0.61	0.12
Yaw	A1-100	17	36	47	0.05	0.43	0.36	0.17	0.47	0.03
Yaw	A1-99	25	28	47	0.10	0.37	0.28	0.25	0.47	0.03
Yaw	A1-98	23	28	49	0.15	0.36	0.28	0.23	0.49	0.04
Yaw	A1-96	25	19	56	0.10	0.25	0.19	0.25	0.56	0.05
Yaw	A1-95	23	18	58	0.19	0.24	0.18	0.23	0.58	0.02
Yaw	A1-93	43	11	45	0.08	0.20	0.11	0.43	0.45	0.05

Table 4.6. continued-

Formation	Sample	Sterane 20R (%)			Sterane C_{29} 20S/(20S+20R)	Sterane C_{27}/ (C_{27}R+C_{29}R)	sterane C_{27}/ (C_{27}+C_{28}+C_{29})	sterane C_{28}/ (C_{27}+C_{28}+C_{29})	sterane C_{29}/ (C_{27}+C_{28}+C_{29})	steranes/ hopanes
		C28	C27	C29						
Pondaung	A1-115	29	21	50	0.24	0.29	0.21	0.29	0.50	0.09
Pondaung	A1-117	19	8	73	0.10	0.10	0.08	0.19	0.73	0.15
Pondaung	A2-50	27	23	50	0.21	0.31	0.23	0.27	0.50	0.09
Tabyin	A2-48	19	13	68	0.08	0.16	0.13	0.19	0.68	0.07
Tabyin	A1-123	19	19	62	0.08	0.23	0.19	0.19	0.62	0.16
Tabyin	A1-125	25	18	58	0.08	0.24	0.18	0.25	0.58	0.15
Tabyin	A1-126	22	19	58	0.13	0.25	0.19	0.22	0.58	0.16
Tabyin	A1-127	21	18	60	0.03	0.23	0.18	0.21	0.60	0.13
Tabyin	A2-62	32	15	52	0.11	0.23	0.15	0.32	0.52	0.08
Tabyin	A1-129	24	18	59	0.20	0.23	0.18	0.24	0.59	0.06
Tabyin	A1-131	7	17	76	0.15	0.18	0.17	0.07	0.76	0.06
Tilin	A1-165	28	32	40	0.23	0.44	0.32	0.28	0.40	0.07
Tilin	A1-164	21	30	48	0.20	0.39	0.30	0.21	0.48	0.06
Tilin	A2-84	21	33	46	0.14	0.41	0.33	0.21	0.46	0.04
Laungshe	A2-65	19	25	55	0.03	0.32	0.25	0.19	0.55	0.09
Laungshe	A1-162	25	19	57	0.12	0.25	0.19	0.25	0.57	0.06
Laungshe	A1-134	17	27	57	0.13	0.32	0.27	0.17	0.57	0.06
Laungshe	A1-135	17	23	59	0.12	0.28	0.23	0.17	0.59	0.06
Laungshe	A1-136	16	16	68	0.14	0.19	0.16	0.16	0.68	0.10
Laungshe	A1-160	23	15	62	0.07	0.20	0.15	0.23	0.62	0.18
Laungshe	A1-158	23	20	57	0.15	0.26	0.20	0.23	0.57	0.07
Laungshe	A1-157	22	21	57	0.17	0.27	0.21	0.22	0.57	0.06
Laungshe	A1-156	20	12	68	0.16	0.15	0.12	0.20	0.68	0.07
Laungshe	A1-153	25	19	56	0.21	0.26	0.19	0.25	0.56	0.07
Paunggyi	A1-137	21	17	63	0.12	0.21	0.17	0.21	0.63	0.07
Paunggyi	A1-140	17	15	68	0.13	0.18	0.15	0.17	0.68	0.06
Paunggyi	A2-69	6	24	69	0.06	0.26	0.24	0.06	0.69	0.07
Paunggyi	A1-152	18	28	54	0.35	0.35	0.28	0.18	0.54	0.04
Kabaw	A1-142	20	21	58	0.15	0.27	0.21	0.20	0.58	0.07
Kabaw	A2-77	32	14	54	0.51	0.21	0.14	0.32	0.54	0.02
Kabaw	A2-78	10	47	43	0.48	0.52	0.47	0.10	0.43	0.06
Kabaw	A2-74	13	16	70	0.40	0.19	0.16	0.13	0.70	0.03
Kabaw	A1-149	18	9	73	0.35	0.11	0.09	0.18	0.73	0.14
Kabaw	A1-145	27	34	39	0.17	0.47	0.34	0.27	0.39	0.03
Kabaw	A1-146	10	27	63	0.10	0.30	0.27	0.10	0.63	0.02
Kabaw	A1-150	13	12	75	0.14	0.14	0.12	0.13	0.75	0.08
Kabaw	A2-80	23	26	51	0.47	0.34	0.26	0.23	0.51	0.03
Kabaw	A2-72	15	21	63	0.47	0.25	0.21	0.15	0.63	0.05
Kabaw	A2-71	13	20	68	0.49	0.23	0.20	0.13	0.68	0.11
Kabaw	A2-70	16	15	69	0.44	0.18	0.15	0.16	0.69	0.08

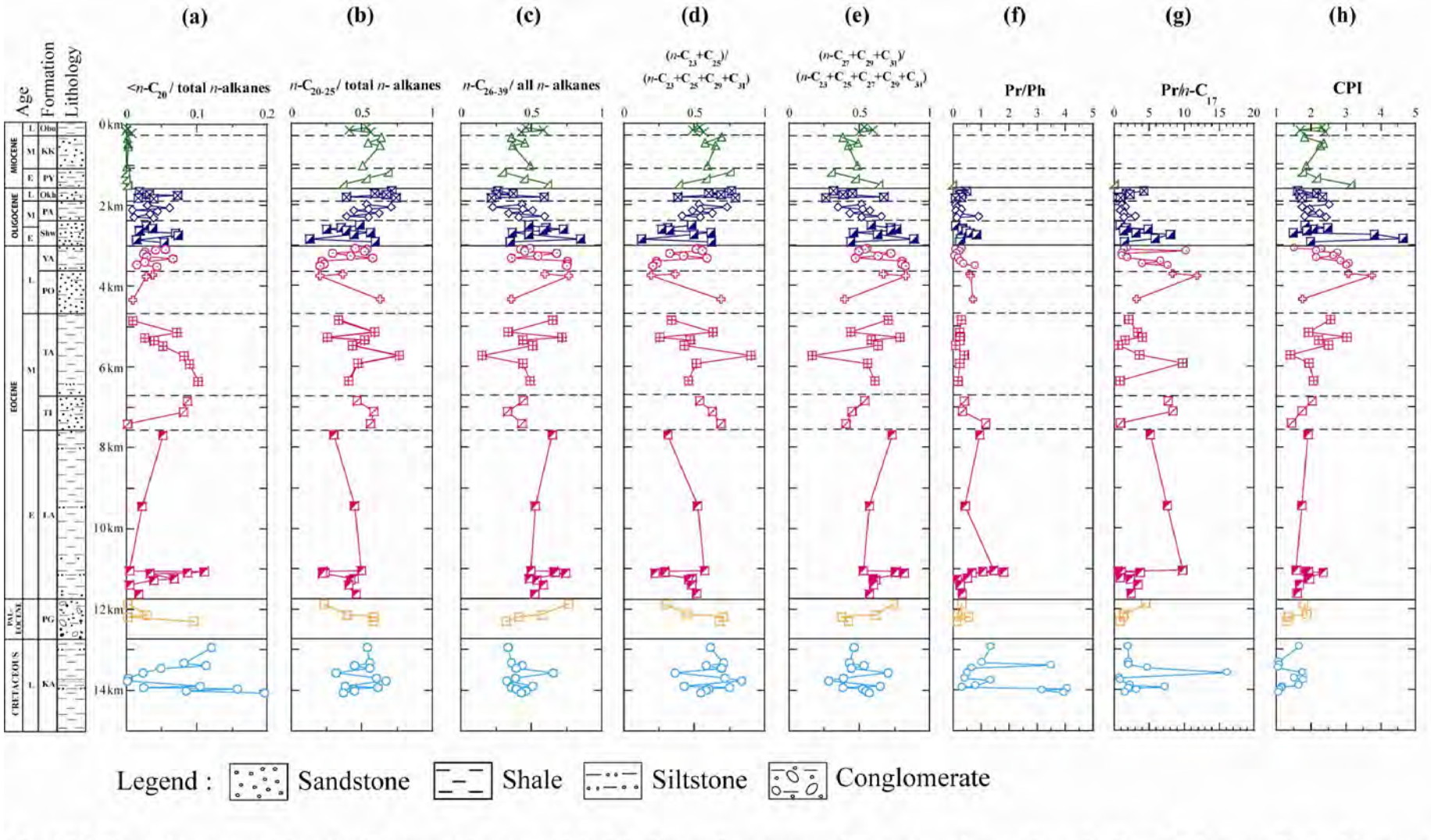

Fig. 4.13. Biomarker compositions (n-alkanes and iso-prenoids) of the Upper Cretaceous to Miocene mudstones from the Central Myanmar Basin, Myanmar.

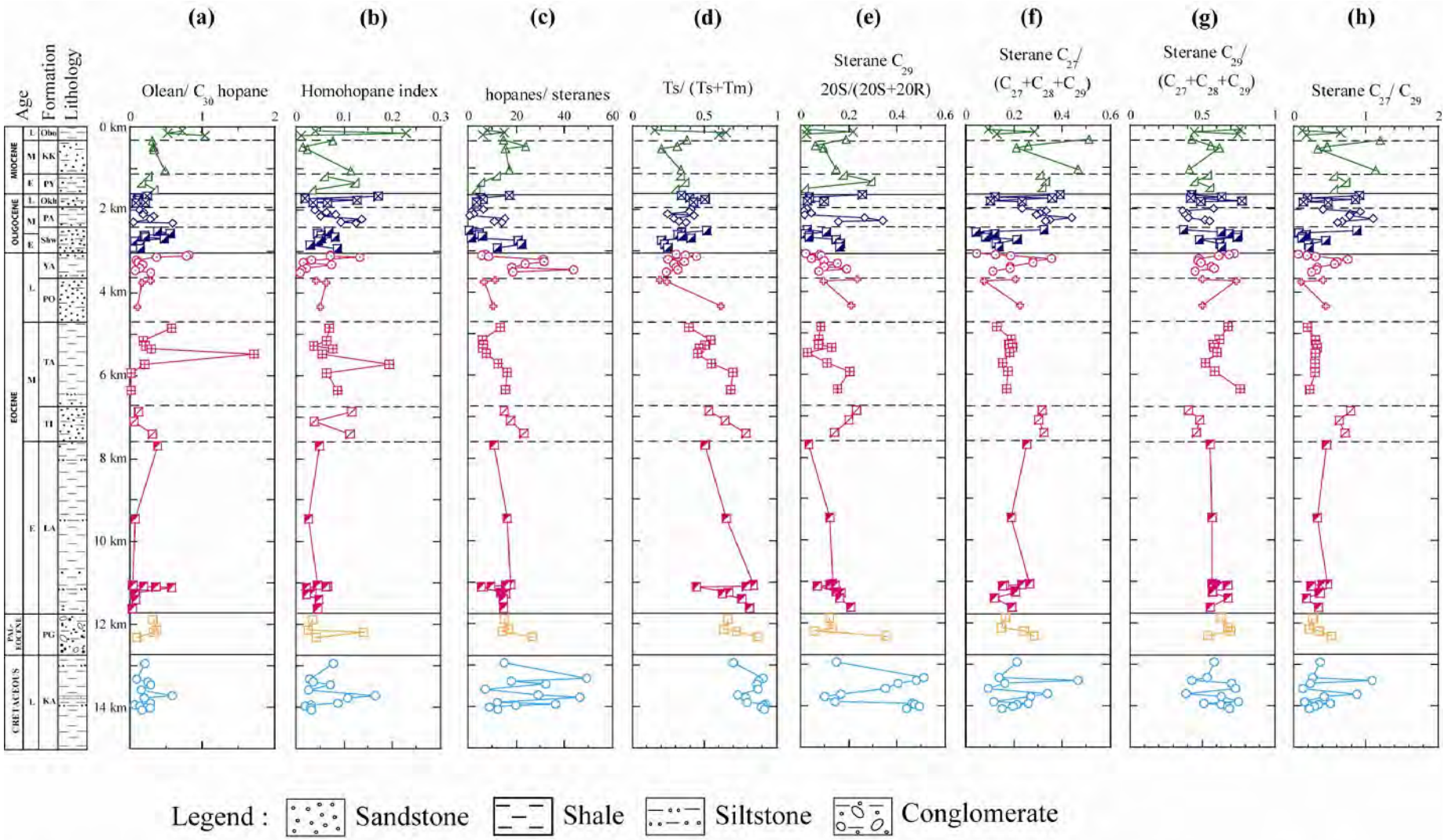

Fig. 4.14. Biomarker compositions (hopanes and steranes) of the Upper Cretaceous to Miocene mudstones from the Central Myanmar Basin, Myanmar.

Sesquiterpenoid-derived cadalene ($C_{15}H_{18}$) is abundant in coaly shale A2-52 and coal A1-92, present in coals A1-113, A2-55, and not detected in the remaining samples (Table 4.7; Fig. 4.16a). Aromatic diterpenoids such as retene (*m/z* 219) concentration were detected in trace amounts in most samples (Table 4.7; Fig. 4.16e).

(a) Mudstones (Upper Cretaceous to Miocene)

Generally, the distributions of 3- to 5- rings combustion-derived PAHs (Phe, Fla, Py, BaAn, Chry, Bflas, BePy, BaPy) are predominant throughout the Central Myanmar succession (Table 4.8; Fig 4.17). The high marker of combustion-derived PAHs (Cor) is more significant in the upper Cretaceous to Paleocene (3-18%), and Eocene mudstones (1-22%), and slightly decreased in the upper Eocene (Yaw Fm.) to Pegu Group mudstones (2-15%) (Table 4.8;Fig. 4.18f).

Retene derived from abietic acid in resinous conifers (Laflamme et al., 1978) is more significant in the Paleocene, middle Eocene (Tabyin Fm.), and Oligocene mudstones, while lesser amounts in the upper Cretaceous, lower Eocene, middle to upper Eocene (Tilin, Pondaung, and Yaw Fm.), and Miocene mudstones (Table 4.8; Fig. 4.18a).

Table 4.7. Concentrations of polycyclic aromatic hydrocarbons (μg/g TOC) in the Upper Eocene coals and coaly shales of the Central Myanmar Basin, Myanmar. Abbreviations are: BaAn, benzo[a]anthracene; Chry+Tpn, chrysene/triphenylene; Bflas, benzofluoranthenes; BePy, benzo[e]pyrene; BaPy, benzo[a]pyrene; Pery, perylene; InPy, indeo[1,2,3-cd] pyrene; BghiP, benzo (ghi) perylene; Cor, coronene; 1,7 DMP, 1,7-dimethylphenanthrene or pimanthrene; MP, methyl phenanthrene; n.d., not detected.

Lithology	Coals				Coaly shales			
Sample	A1-92	A1-113	A1-114	A2-55	*A2-54	A2-52	*A2-52A	*A1-120
Cadalene (Cad)	3.10	0.02	n.d.	0.32	n.d.	9.12	n.d.	n.d.
Anthracene (A)	1.97	n.d.	n.d.	0.05	n.d.	0.24	n.d.	n.d.
Phenanthene (P)	0.64	0.03	0.42	0.08	n.d.	0.16	n.d.	n.d.
Fluoranthene (Fla)	1.05	0.11	0.81	0.16	0.04	0.20	n.d.	n.d.
Pyrene (Py)	0.37	0.17	1.24	0.37	0.01	0.93	n.d.	n.d.
Retene (Ret)	n.d.	0.02	n.d.	0.16	0.12	0.03	0.05	0.01
BaAn	0.17	0.48	0.40	0.25	0.04	1.76	n.d.	n.d.
Chry+Tpn	2.25	0.17	0.74	0.32	0.01	0.84	n.d.	n.d.
Bflas	0.49	0.98	0.85	0.11	0.05	1.81	n.d.	n.d.
BePy	0.86	0.91	1.16	0.10	0.08	5.50	n.d.	n.d.
BaPy	0.56	n.d.	0.29	0.04	0.02	1.85	n.d.	n.d.
Perylene	0.66	0.15	0.26	0.49	n.d.	9.86	n.d.	n.d.
InPy	n.d.	n.d.	0.13	n.d.	0.06	n.d.	n.d.	n.d.
BghiP	n.d.	n.d.	0.14	n.d.	0.10	n.d.	n.d.	n.d.
Cor	n.d.	n.d.	n.d.	n.d.	n.d.	n.d.	n.d.	n.d.
1,7 DMP	0.09	0.03	0.21	0.19	n.d.	0.53	n.d.	n.d.
3-MP	0.26	0.02	0.29	0.06	n.d.	0.32	n.d.	n.d.
2-MP	0.70	0.07	0.37	0.09	n.d.	0.41	n.d.	n.d.
9-MP	1.51	0.03	0.93	0.13	n.d.	0.46	n.d.	n.d.
1-MP	0.87	0.05	0.60	0.14	n.d.	0.75	n.d.	n.d.
Fla/(Fla+Py)	0.74	0.38	0.40	0.31	0.73	0.18	n.d.	n.d.
Non-alkylated PAHs[a]	8.37	2.83	6.17	1.49	0.42	13.28	n.d.	n.d.
Total PAHs[b]	15.56	3.22	8.83	3.07	0.54	34.76	0.05	0.01

[a] Non-alkylated PAHs=(A+P+Fla+Py+BaAn+Chry+Tpn+Bflas+BePy+BaPy+InPy+BghiP)

[b] Total PAHs=(Cad+A+P+Fla+Py+Ret+BaAn+Chry+Tpn+Bflas+BePy+BaPy+Pery+InPy+BghiP+1,7 DMP+3 MP+2 MP+9 MP+1 MP)

* weathered samples

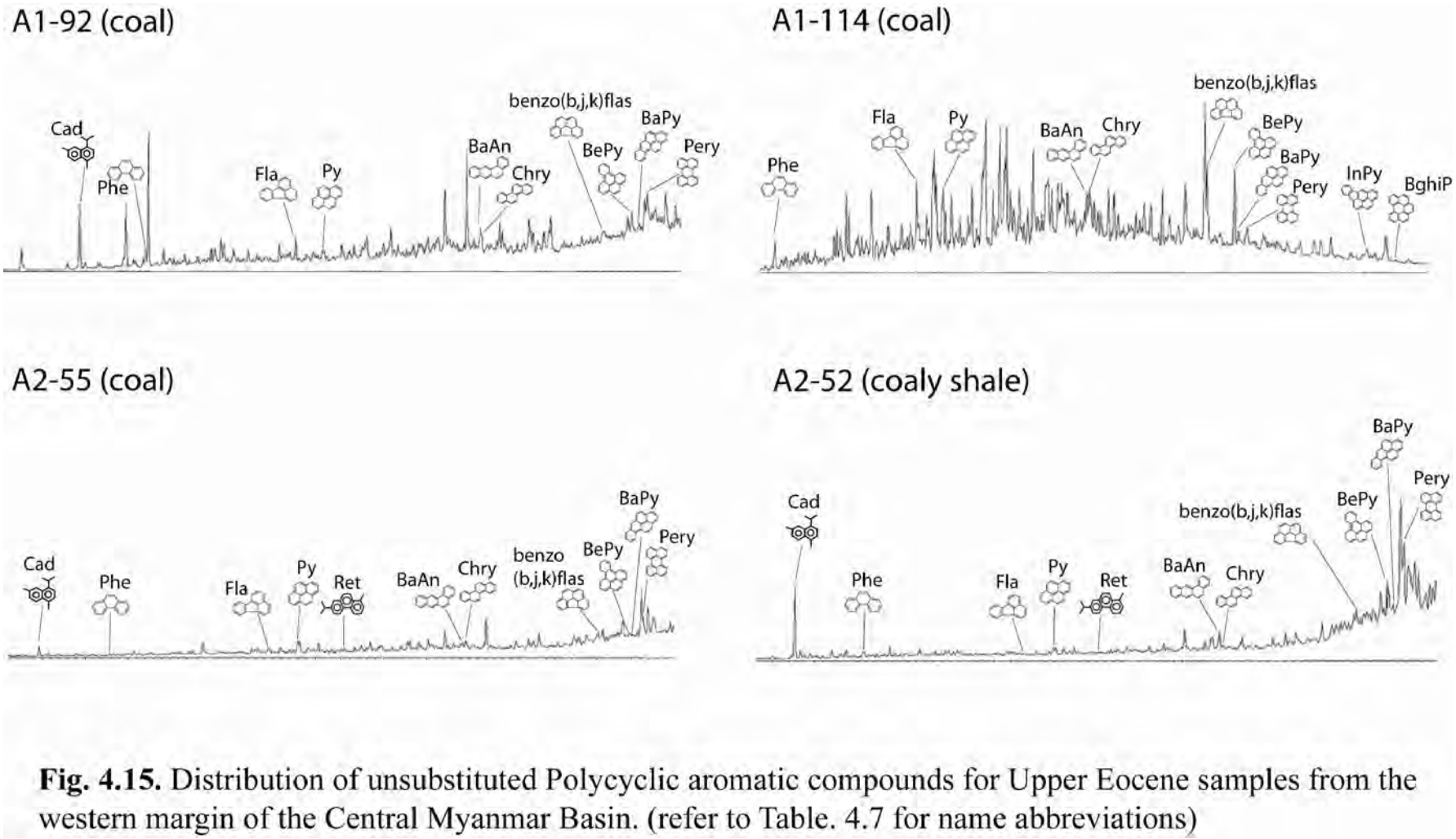

Fig. 4.15. Distribution of unsubstituted Polycyclic aromatic compounds for Upper Eocene samples from the western margin of the Central Myanmar Basin. (refer to Table. 4.7 for name abbreviations)

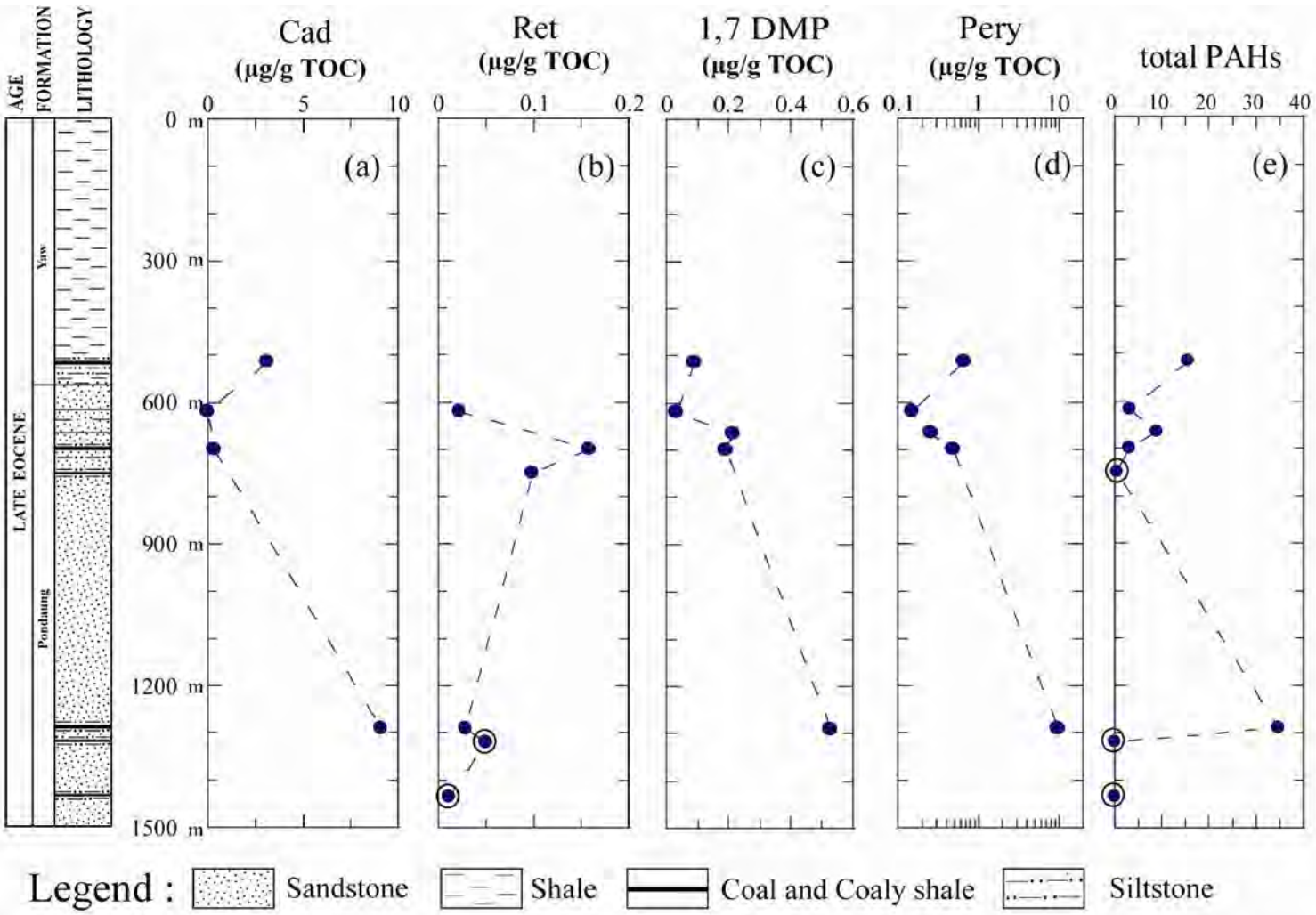

Fig. 4.16. Showing higher land plant marker cadalene (Cad), gymnosperm (i.e. conifers) marker retene (Ret), pimanthrene (1,7 DMP) and fungi-derived marker perylene (Pery), and total polycyclic aromatic hydrocarbons (PAHs) for Upper Eocene coals and coaly shales from CMB.Circled data points indicate weathered coaly shale samples.

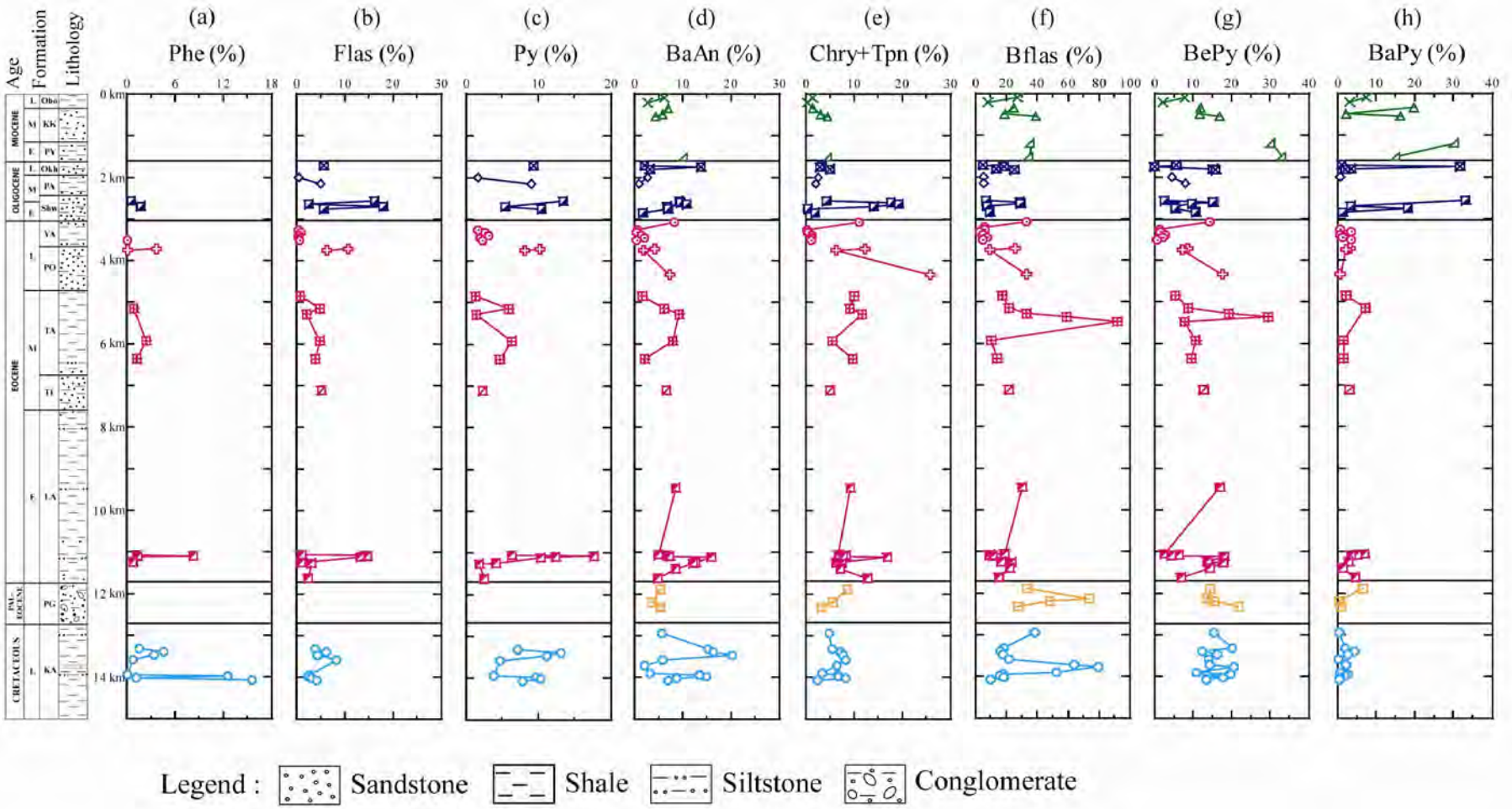

Fig. 4.17. Relative distributions of 3- to 5- rings polycyclic aromatic hydrocarbons (PAHs) for Upper Cretaceous to Miocene mudstones from the Central Myanmar Basin (CMB), Myanmar.

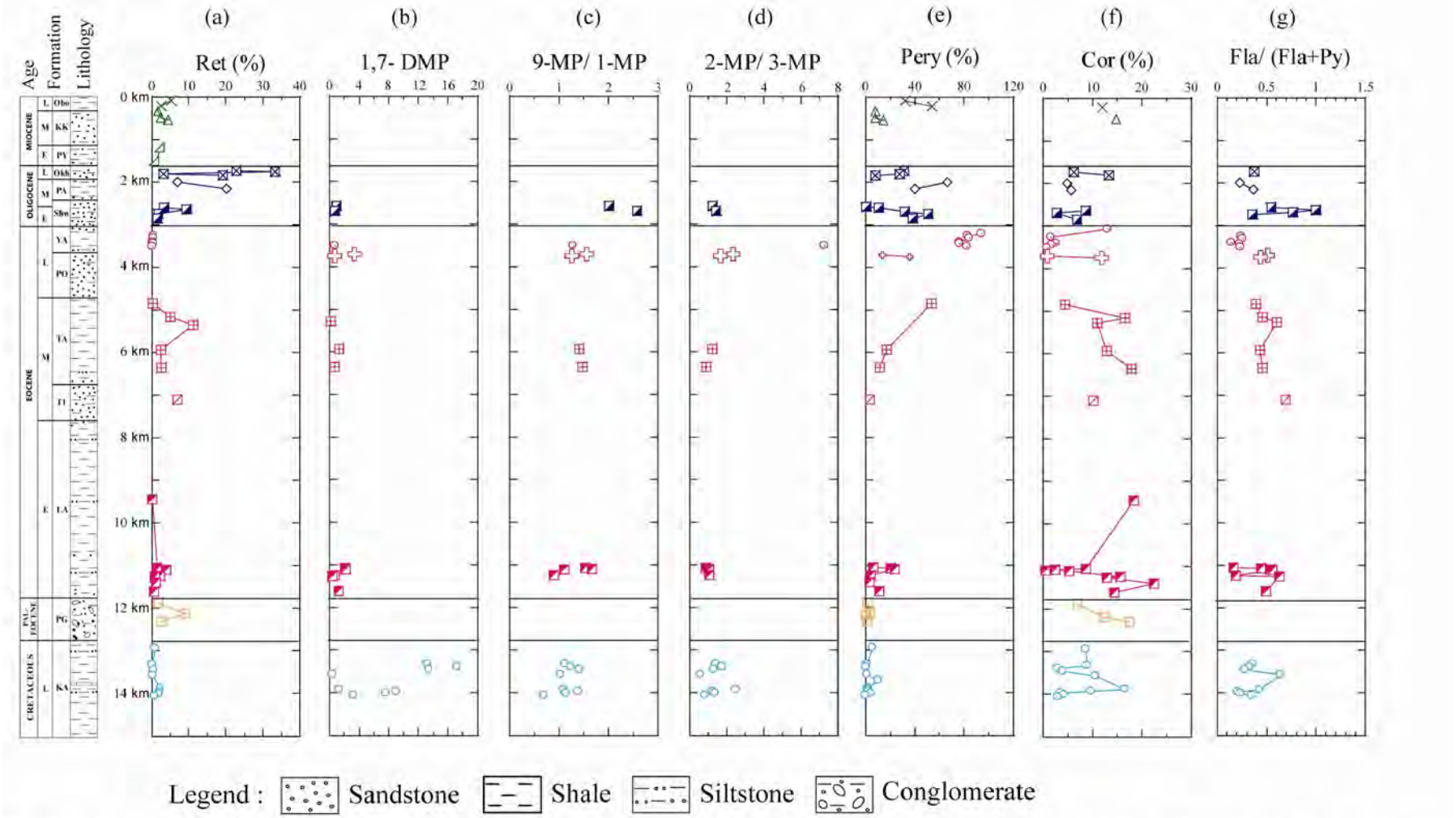

Fig. 4.18. Retene (Ret), dimethyl phenanthrenes (1,7 DMP, 9-MP,1-MP, 2-MP, 3-MP), perylene (Pery), coronene (Cor) and fluoranthene/ fluoranthene and pyrene (Fla/(Fla+Py), showing paleovegetation, maturity of OM, paleoclimate, and source of PAHs for Upper Cretaceous to Miocene mudstones from CMB.

The distribution of fungi-derived perylene (Grice et al., 2009; Suzuki et al., 2010) is less abundant in the upper Cretaceous to lower Eocene (0.1-23.5%), and significantly increasing in the middle Eocene (Tabyin Fm.) and Pegu Group mudstones (1.1-94.25%) (Table 4.8; Fig. 4.18e).

The distribution of methylphenanthrene (MP) isomers was defined from m/z 192 chromatograms and shown in the figure 4.18 b, c, and d. The values of methyl phenanthrene index (MPI 3) are varying from 0.43 to 2.17 in the upper Cretaceous; 0.32 to 1.56 in the Eocene; and 0.22 to 0.62 in the Oligocene (Table 4.8).

Pimarane (1,7 Dimethyl phenanthrene) is significant in the upper Cretaceous and less abundant in the Eocene (Laungshe, Tabyin, Pondaung, Yaw) to lower -middle Oligocene (Shwezetaw) and scarce in the other formations (Table 4.8; Fig. 4.18 b).

Table 4.8. Relative proportion (%) of polycyclic aromatic hydrocarbons in the Late Cretaceous to Miocene mudstones of the Central Myanmar Basin, Myanmar.

Abbreviations are: Cad, cadalene; P, phenanthrene; Fla, fluoranthene; Py, pyrene; Ret, retene; BaAn, benzo[a]anthracene; Chry+Tpn, Chrysene/triphenylene; Bflas, benzofluoranthenes; BePy, benzo[e]pyrene; BaPy, benzo[a]pyrene; Pery, perylene; InPy, indeo[1,2,3-cd]pyrene; BghiP, benzo[ghi]perylene; Cor, coronene; n.d., not detected.

Formation	Sample	Cad	P	Fla	Py	Ret	BaAn	Chry	Bflas	BePy	BaPy	Pery	InPy	BghiP	Cor	Fla/(Fla+Py)	3-MP	2-MP	9-MP	1-MP	1,7 DMP	MPI-3
Obogon	A2-22	n.d	n.d	n.d	n.d	5.31	6.23	1.53	27.35	7.75	7.40	32.53	3.93	7.97	n.d	n.d	n.d	n.d	n.d	n.d	n.d	n.d
Obogon	A2-26	n.d	n.d	n.d	n.d	2.62	2.84	0.39	7.95	2.21	3.04	54.22	5.38	9.36	11.99	n.d	n.d	n.d	n.d	n.d	n.d	n.d
Kyaukkok	A2-28	n.d	n.d	n.d	n.d	1.60	6.93	1.43	25.10	11.99	19.68	8.27	n.d	25.00	n.d	n.d	n.d	n.d	n.d	n.d	n.d	n.d
Kyaukkok	A2-29	n.d	n.d	n.d	n.d	2.41	5.79	3.11	19.07	11.80	2.18	8.17	6.96	25.71	14.81	n.d	n.d	n.d	n.d	n.d	n.d	n.d
Kyaukkok	A2-21	n.d	n.d	n.d	n.d	4.48	4.38	4.50	39.10	16.86	16.24	14.44	n.d	n.d	n.d	n.d	n.d	n.d	n.d	n.d	n.d	n.d
Pyawbwe	A2-16	n.d	n.d	n.d	n.d	2.65	n.d	n.d	36.37	30.42	30.56	n.d	n.d	n.d	n.d	n.d	n.d	n.d	n.d	n.d	n.d	n.d
Pyawbwe	A2-9	n.d	n.d	n.d	n.d	1.01	10.46	4.92	35.05	33.17	15.39	n.d	n.d	n.d	n.d	n.d	n.d	n.d	n.d	n.d	n.d	n.d
Okhmintaung	A2-7	n.d	n.d	5.66	9.33	22.89	2.14	3.39	5.13	5.67	1.17	31.35	1.21	5.79	6.26	0.38	n.d	n.d	n.d	n.d	n.d	n.d
Okhmintaung	A2-6	n.d	n.d	n.d	n.d	33.32	13.84	2.97	18.27	0.00	31.59	n.d	n.d	n.d	n.d	n.d	n.d	n.d	n.d	n.d	n.d	n.d
Okhmintaung	A2-5	n.d	n.d	n.d	n.d	3.26	3.27	4.99	13.56	15.28	3.52	27.85	n.d	14.93	13.34	n.d	n.d	n.d	n.d	n.d	n.d	n.d
Okhmintaung	A2-3	n.d	n.d	n.d	n.d	19.31	n.d	n.d	25.35	15.91	1.87	8.06	n.d	29.50	n.d	n.d	n.d	n.d	n.d	n.d	n.d	n.d
Padaung	A2-38	n.d	n.d	0.48	1.63	7.04	2.76	2.56	5.28	4.53	0.76	66.33	0.82	2.88	4.94	0.23	n.d	n.d	n.d	n.d	n.d	n.d
Padaung	A2-33	n.d	n.d	5.13	8.96	20.18	0.97	2.14	5.45	8.02	n.d	39.93	n.d	3.55	5.69	0.36	n.d	n.d	n.d	n.d	n.d	n.d
Shwezetaw	A2-42	n.d	0.55	16.27	13.40	n.d	9.19	4.47	7.19	2.64	33.10	1.05	6.23	5.90	n.d	0.55	0.98	1.22	2.38	1.18	0.90	0.62
Shwezetaw	A2-43	n.d	n.d	n.d	n.d	3.41	9.56	17.69	28.61	15.22	n.d	11.12	n.d	14.39	n.d	n.d	n.d	n.d	n.d	n.d	n.d	n.d
Shwezetaw	A2-41	n.d	n.d	2.61	n.d	9.37	10.89	19.40	29.28	9.71	n.d	n.d	n.d	10.07	8.67	1.00	n.d	n.d	n.d	n.d	n.d	n.d
Shwezetaw	A2-45	n.d	1.75	18.05	5.39	n.d	6.86	14.12	7.48	5.49	3.41	32.25	0.64	1.85	2.72	0.77	0.81	1.17	6.55	2.54	0.80	0.22
Shwezetaw	A1-109	n.d	n.d	5.77	10.46	1.74	6.95	0.53	n.d	5.38	18.26	50.90	0.00	n.d	n.d	0.36	n.d	n.d	n.d	n.d	n.d	n.d
Shwezetaw	A1-111	n.d	n.d	n.d	n.d	1.54	1.87	2.04	9.04	10.65	1.40	38.11	6.38	22.12	6.85	n.d	n.d	n.d	n.d	n.d	n.d	n.d
Yaw	A2-58	n.d	n.d	n.d	n.d	n.d	8.37	11.07	33.28	14.33	n.d	n.d	n.d	19.87	13.08	n.d	n.d	n.d	n.d	n.d	n.d	n.d
Yaw	A1-100	n.d	n.d	n.d	n.d	n.d	n.d	n.d	5.82	n.d	n.d	94.18	n.d	n.d	n.d	n.d	n.d	n.d	n.d	n.d	n.d	n.d
Yaw	A1-99	n.d	n.d	0.51	1.58	0.50	0.67	0.37	6.21	1.24	0.69	82.76	n.d	3.83	1.64	0.24	n.d	n.d	n.d	n.d	n.d	n.d
Yaw	A1-98	n.d	n.d	0.92	2.64	0.43	0.56	0.43	2.98	1.45	3.49	84.17	n.d	2.93	n.d	0.26	n.d	n.d	n.d	n.d	n.d	n.d
Yaw	A1-96	n.d	n.d	0.53	3.16	0.28	1.52	1.25	4.86	2.82	0.60	76.38	1.76	4.19	2.65	0.14	n.d	n.d	n.d	n.d	n.d	n.d
Yaw	A1-95	n.d	n.d	0.57	1.92	0.45	2.14	1.39	7.88	2.20	1.28	76.27	2.34	1.79	1.77	0.23	n.d	n.d	n.d	n.d	n.d	n.d
Yaw	A1-93	n.d	0.12	0.70	2.30	0.17	0.44	1.08	4.86	0.64	3.43	82.29	1.76	1.42	0.78	0.23	0.24	1.74	0.72	0.55	0.76	1.56
Pondaung	A1-115	0.43	3.67	10.75	10.16	n.d	4.20	12.43	25.92	8.64	3.26	13.65	1.73	4.36	0.80	0.51	1.91	4.46	11.12	7.14	3.33	0.35
Pondaung	A1-117	n.d	0.09	6.39	8.14	n.d	1.92	6.31	9.49	7.08	2.16	36.16	1.02	9.42	11.81	0.44	0.22	0.36	1.03	0.81	0.70	0.32
Pondaung	A2-50	n.d	n.d	n.d	n.d	n.d	7.37	25.79	33.01	17.50	0.71	n.d	n.d	15.62	n.d	n.d	n.d	n.d	n.d	n.d	n.d	n.d

Table 4.8. continued-

Formation	Sample	Cad	P	Fla	Py	Ret	BaAn	Chry	Bflas	BePy	BaPy	Pery	InPy	BghiP	Cor	Fla/(Fla+Py)	3-MP	2-MP	9-MP	1-MP	1,7 DMP	MPI-3
Tabyin	A2-48	n.d	n.d	0.86	1.32	0.31	1.58	10.06	17.31	5.54	2.12	53.64	n.d	2.85	4.41	0.39	n.d	n.d	n.d	n.d	n.d	n.d
Tabyin	A1-123	n.d	0.852	4.96	5.88	5.02	6.14	9.09	21.48	8.70	7.09	n.d	8.24	5.98	16.58	0.46	n.d	n.d	n.d	n.d	n.d	n.d
Tabyin	A1-125	n.d	n.d	2.12	1.39	n.d	9.32	11.74	33.21	19.38	n.d	n.d	1.65	10.24	10.95	0.60	n.d	n.d	n.d	n.d	0.16	n.d
Tabyin	A1-126	n.d	n.d	n.d	n.d	11.25	n.d	n.d	59.21	29.53	n.d	n.d	n.d	n.d	n.d	n.d	n.d	n.d	n.d	n.d	n.d	n.d
Tabyin	A1-127	n.d	n.d	n.d	n.d	n.d	n.d	n.d	92.15	7.85	n.d	n.d	n.d	n.d	n.d	n.d	n.d	n.d	n.d	n.d	n.d	n.d
Tabyin	A1-129	0.31	2.40	4.82	6.30	2.41	7.99	5.46	10.35	10.54	1.50	17.26	4.56	13.27	12.84	0.43	0.81	0.98	1.71	1.21	1.28	0.61
Tabyin	A1-131	n.d	1.25	3.91	4.64	2.61	2.17	9.79	14.01	9.46	1.58	12.08	5.47	15.21	17.82	0.46	0.47	0.42	0.95	0.64	0.72	0.56
Tilin	A1-164	n.d	n.d	5.28	2.32	7.05	6.72	5.11	21.44	12.79	2.95	3.57	11.17	11.45	10.16	0.69	n.d	n.d	n.d	n.d	n.d	n.d
Laungshe	A1-162	n.d	n.d	n.d	n.d	0.23	8.58	9.30	30.43	16.80	n.d	n.d	7.90	8.43	18.33	n.d	n.d	n.d	n.d	n.d	n.d	n.d
Laungshe	A1-134	n.d	n.d	1.22	6.24	1.58	4.97	6.89	19.03	2.51	6.87	6.28	13.32	22.47	8.63	0.16	n.d	n.d	n.d	n.d	n.d	n.d
Laungshe	A1-135	n.d	1.29	14.14	17.69	n.d	6.90	8.47	9.83	6.33	5.08	20.54	1.88	5.47	2.39	0.44	2.83	2.43	6.57	4.32	2.11	0.48
Laungshe	A1-136	1.01	8.33	14.66	12.34	1.44	7.30	7.78	8.50	4.29	3.46	23.54	3.13	3.72	0.51	0.54	7.09	7.35	12.98	7.75	2.04	0.70
Laungshe	A1-160	1.27	1.33	13.23	10.28	3.96	15.96	16.92	11.26	18.07	n.d	n.d	n.d	2.49	5.22	0.56	0.90	0.95	0.85	0.76	2.14	1.15
Laungshe	A1-158	0.36	0.83	0.95	4.11	2.26	12.75	6.38	16.58	13.75	2.75	4.53	8.74	10.37	15.64	0.19	0.43	0.45	0.59	0.65	0.70	0.71
Laungshe	A1-157	n.d	n.d	3.17	1.83	0.99	12.26	7.55	23.15	17.86	n.d	n.d	10.20	10.20	12.80	0.63	n.d	n.d	n.d	n.d	0.36	n.d
Laungshe	A1-156	n.d	n.d	n.d	n.d	1.07	8.70	7.22	22.01	14.41	1.34	3.37	8.20	11.32	22.36	n.d	n.d	n.d	n.d	n.d	n.d	n.d
Laungshe	A1-153	n.d	n.d	2.43	2.49	0.63	4.95	12.91	15.20	6.85	4.56	11.45	7.40	16.65	14.45	0.49	n.d	n.d	n.d	n.d	1.23	n.d
Paunggyi	A1-137	n.d	n.d	n.d	n.d	1.70	5.43	8.55	33.87	14.49	6.54	1.34	9.55	11.68	6.86	n.d	n.d	n.d	n.d	n.d	n.d	n.d
Paunggyi	A1-140	n.d	n.d	n.d	n.d	8.89	n.d	n.d	73.97	13.57	n.d	3.58	n.d	n.d	n.d	n.d	n.d	n.d	n.d	n.d	n.d	n.d
Paunggyi	A2-69	n.d	n.d	n.d	n.d	n.d	3.67	5.74	48.49	15.45	0.39	0.51	5.32	8.02	12.41	n.d	n.d	n.d	n.d	n.d	n.d	n.d
Paunggyi	A1-152	n.d	n.d	n.d	n.d	2.69	5.34	3.33	27.87	21.93	0.97	1.82	11.28	7.23	17.55	n.d	n.d	n.d	n.d	n.d	n.d	n.d
Kabaw	A1-142	n.d	n.d	n.d	n.d	0.99	5.65	4.89	38.23	15.40	0.48	5.90	12.07	7.72	8.67	n.d	n.d	n.d	n.d	n.d	n.d	n.d
Kabaw	A2-77	n.d	1.59	3.96	7.11	0.24	15.34	5.59	18.64	20.19	2.04	1.44	2.65	12.33	8.86	0.36	8.98	12.63	17.72	15.69	13.19	0.65
Kabaw	A2-78	n.d	4.61	6.26	13.10	n.d	16.41	7.17	16.48	12.42	4.45	0.29	7.53	8.35	2.93	0.32	19.25	33.67	36.14	29.24	17.17	0.81
Kabaw	A2-74	n.d	3.47	4.37	11.23	0.42	20.42	7.78	17.88	16.21	2.70	n.d	4.72	6.85	3.97	0.28	18.65	24.49	33.12	23.22	13.43	0.77
Kabaw	A1-149	n.d	0.74	8.22	4.62	0.37	5.88	8.32	21.77	14.18	0.18	1.51	11.75	11.84	10.61	0.64	0.33	0.19	0.38	0.36	0.39	0.71
Kabaw	A1-145	n.d	n.d	n.d	n.d	n.d	2.11	6.58	63.93	14.35	2.29	10.74	n.d	n.d	n.d	n.d	n.d	n.d	n.d	n.d	n.d	n.d
Kabaw	A1-146	n.d	n.d	n.d	n.d	n.d	n.d	n.d	79.47	20.53	n.d	n.d	n.d	n.d	n.d	n.d	n.d	n.d	n.d	n.d	n.d	n.d
Kabaw	A1-150	n.d	n.d	n.d	n.d	2.21	3.21	3.50	52.60	10.81	0.70	2.47	4.25	3.63	16.61	n.d	n.d	n.d	n.d	n.d	n.d	n.d
Kabaw	A2-80	n.d	0.10	2.83	3.78	n.d	13.54	6.63	17.68	19.76	2.62	2.14	7.49	13.79	9.66	0.43	0.43	1.06	1.81	1.66	1.33	0.43
Kabaw	A2-72	0.53	12.55	2.48	9.66	2.12	14.94	6.85	16.01	13.39	1.88	2.57	5.49	7.98	3.55	0.20	9.66	11.74	13.70	9.85	9.00	0.91
Kabaw	A2-71	0.07	1.22	3.13	10.28	2.03	8.84	8.26	18.41	17.78	0.66	4.63	9.27	11.25	4.17	0.23	5.57	7.56	8.44	7.42	7.60	0.83
Kabaw	A2-70	8.69	15.60	4.16	7.79	0.85	6.94	2.48	9.90	13.49	0.55	0.05	12.25	14.29	2.95	0.35	6.16	5.01	2.10	3.04	3.24	2.17

4.2 Inorganic Geochemistry

Average contents of major and trace elements for all mudstone and sandstone samples by formations and mean values of major elements in the upper continental crust (UCC) and average Post-Archaean Australian Shale (PAAS) (Taylor and McLennan, 1985) are listed in (Table 4.9).

4.2.1 Mudstones and Sandstone Compositions

The upper Cretaceous and Paleocene mudstones and sandstones have SiO_2 contents ranging from 61 to 70 wt% and 62 to 67 wt%, respectively, and Al_2O_3 contents ranging from 16 to 21 and 19–26 wt% wt% respectively. Eocene samples contain have SiO_2 and Al_2O_3 contents varying between 60 and 71 wt%, and 13 and 24 wt% respectively. The Pegu Group (Oligocene and Miocene) sediments have SiO_2 varying from 62 to 76 wt%, and Al_2O_3 from 12 to 22 wt%. Average contents of CaO are higher greater in sandstones (<4%) than in the mudstones (<3%) samples . (Table 4.9).

Sandstone samples in the lower to middle Eocene (Laungshe and Tilin Fm.) have relatively higher SiO_2 (79.14 and 73.91 wt%) contents than the single upper Cretaceous sandstone analyzed (67.40 wt%).

By plotting all major elements analyzed on Harker were plotted on variation diagrams against Al_2O_3, to examine the, potential effects of sorting, and any dilution affects by carbonate or quartz concentration. Correlations are relatively weak in the dataset overall, a feature suggesting weak to moderate sorting in immature sediments (Roser 2000, Kiminami and Fujii, 2007; Purevjav and Roser, 2013).

Table 4.9. Average geochemical compositions of mudstones and sandstones from CMB, Myanmar. (a) Major elements (wt%) (b) Trace elements (ppm).

Age	Miocene	Oligocene	Eocene	Paleocene	Late Cretaceous	PAAS T&M (1985)	UCC R&G (2005)
n	9	17	35	4	12		
(a) Major elements (wt%)							
SiO_2	66.10	66.70	63.66	64.17	64.74	62.80	66.60
TiO_2	0.84	0.76	0.87	1.06	0.90	1.00	0.64
Al_2O_3	19.03	17.46	18.79	22.86	18.27	18.90	15.40
Fe_2O_3T	6.88	6.52	7.90	6.25	7.69	7.22	5.60
MnO	0.05	0.07	0.09	0.01	0.05	0.11	0.10
MgO	3.01	3.24	3.53	1.92	2.93	2.20	2.48
CaO	0.68	1.32	1.77	1.03	1.38	1.30	3.59
Na_2O	0.63	1.21	1.14	0.53	1.18	1.20	3.27
K_2O	2.69	2.58	2.11	2.12	2.70	3.70	2.80
P_2O_5	0.10	0.13	0.14	0.05	0.14	0.16	0.15
SUM	100	100	100	100	100	98.59	100.63
(b) Trace elements (ppm)							
Ba	289	326	211	252	234	650	628
Ce	62	62	55	62	59	80	63
Cr	215	210	213	125	168	110	92
Ga	22	20	22	30	23	20	17.5
Nb	13	12	10	11	11	19	12
Ni	131	127	162	57	98	55	47
Pb	21	22	18	14	14	20	17
Rb	139	119	91	87	107	160	84
Sc	14.5	13.8	17.5	21.0	16.9	16.0	14.0
Sr	128	174	156	119	162	200	320
Th	12.7	12.9	9.1	8.3	9.1	14.6	10.5
V	157	137	163	189	181	150	97
Y	24	24	25	28	24	27	21
Zr	183	185	173	219	188	210	193
CIA	80	72	73	82	72	70	51
PIA	89	78	78	89	80	79	52
LOI (wt%)	9.64	8.28	10.61	12.11	8.39	6	

note: n= number of samples; PAAS= post Archaean Australian Shale; UCC= upper continental crust; LOI= loss of ignition; CIA= chemical index of alternation; PIA= plagioclase index of alternations)

Among the major elements, SiO_2 and Na_2O show clear negative correlation with Al_2O_3 (Fig. 4.19), a feature typical of hydrodynamic separation of quartz, feldspar and lithic fragments from clays (Roser, 2000). Conversely, both TiO_2 and Fe_2O_3 show a weak positive correlation with Al_2O_3 overall. Other major elements (MgO, CaO, MnO and K_2O) show very weak correlations, but differing patterns in parts of the succession. TiO_2, Fe_2O_3, MnO, show a positive correlation whereas SiO_2, MgO, and CaO, show a negative correlation MgO, MnO and CaO contents in the Eocene sediments are often higher, and K_2O markedly lower at given Al_2O_3 content, than in the rest of the sequence (Fig. 4.19). This suggests some variation in provenance occurred.

Similar patterns can be observed among the trace elements. Barium contents are generally low (<400 ppm) and no sorting trend is evident (Fig. 4.20a). However, contents in the Eocene sediments are typically lower (<200 ppm) in the rest of the succession. This is also the case for the incompatible element Nb, which displays a positive correlation for all except the Eocene sediments, which have characteristically lower Nb contents at given Al_2O_3 (Fig. 4.20a).

A second incompatible element, Ce, shows remarkably uniform abundances overall (30 – 70 ppm), but almost no variation with Al_2O_3, although contents are again typically lower (30 – 50 ppm) in the Eocene sediments (Fig. 4.20a).

As expected, Ga, which is geochemically coherent with Al, shows a marked linear trend overall, although two trends may be present (Fig. 4.20a). The Cretaceous, Paleocene and Miocene samples lie along a trend that runs towards the origin, suggestive of quartz dilution of a clay-rich sediment, whereas the Eocene sediment forms a trend that intersects the abscissa at about 5 wt% Al_2O_3. This suggests that feldspar remains a significant component of the Eocene mudstones.

Two compatible elements (Ni and Cr) that are typically enriched in mafic source rocks and contained in ferromagnesian minerals show very poor correlation overall, with considerable scatter (Fig. 4.20a). However, both are clearly enriched in most Eocene mudrocks relative to the rest of the succession, implying a more mafic source. Conversely, two other compatible elements (Sc and V), which are also often contained in ferromagnesian minerals, do not show the same pattern, forming weak positive correlations, with little clear contrast with age. This suggests that the Cr and Ni enrichment in the Eocene may thus not result from higher proportions of source rocks such as basalt and andesite. Cryptic contributions from ultramafic rocks (e.g. obducted ophiolite) may be the responsible for the Cr and Ni enrichments.

Three more mobile elements (Pb, Rb, and Sr) also show very weak correlations with Al_2O_3 (Fig. 4.20b). Of the three, Rb is the only element to show any contrast with age, with a tendency for lower and more scattered abundances in the Eocene, similar to the plot for K_2O. The remaining samples form a weak positive trend for Rb, suggesting association with clay fraction (Roser, 2000).

The three remaining incompatible elements analyzed (Th, Y, and Zr) show weak correlations, but slightly differing distributions (Fig. 4.20b). Yttrium shows a broad and weak positive correlation, with no clear contrasts between the age groups. Thorium shows little overall correlation, but abundances in the Cretaceous, Paleocene and Eocene mudrocks are distinctly lower at given Al_2O_3 than in the upper part of the sequence, similar to Nb. Finally, Zr abundances show little consistent variation with age, although a few Cretaceous and Miocene samples have contents ~50% greater than the majority. Contents are generally low overall (<250 ppm), and nearly all Eocene samples have contents <UCC (190 ppm). This and several other features described above suggest a less evolved source.

The major and trace elements abundances overall and the lack of linear correlations are typical of poorly-sorted and mineralogically immature sediments (e.g. Roser, 2000; Kiminami and Fujii, 2007; Purevjav and Roser, 2013), such as those that can be expected in arc settings. However, contrasting abundances of some elements in differing ages (e.g. MgO, K_2O, Rb, Ba, Ce, Nb, Th, Cr, and Ni) point to subtle changes in provenance, paleoweathering or diagenesis within the succession. These contrasts will be discussed in the following sections.

Geochemical maturity was calculated using the Index of Compositional Variability (ICV) = $(Fe_2O_3+K_2O+Na_2O+CaO+MgO+MnO+TiO_2)/Al_2O_3$ (Cox et al., 1995). Taylor and McLennan (1985) mentioned for post Archaean Australian Shale (PAAS) that the ICV values are greater than 0.85 for major rock-forming minerals such as feldspars, amphiboles, and pyroxenes, while values less than 0.89 reflect for alteration minerals such as kaolinite, illite, and muscovite. Average ICV values are ranging from 0.81 to 0.92 in the Late Cretaceous to Miocene samples, showing that they are mostly immature (Fig. 4.23).

4.2.2 Geochemical Classification

The Chemical Index of Alteration (CIA) values in the mudstones are relatively high, varying between 61 and 79 (mean: 71.4) in the upper Cretaceous; 75 and 86 (mean: 82.1) in the Paleocene; 54 and 86 (mean: 71.7) in the Eocene; 57 and 87 (mean: 73.7) in the Pegu Group (Table 4.9). Average CIA values are high in the Paleocene and Miocene mudstones (82% and 78%).

The log Na_2O/K_2O ratio (Pettijohn et al., 1987) indicate an index of chemical maturity while the and log Fe_2O_3/ K_2O ratios (Herron, 1988) have often been used to reflect the classify sedimentary rocks and hence to evaluate their maturityication of arkoses, as these ratios vary systematically between immature sediments such as wackes and litharenites, and more mature sediments including arkoses and arenites.

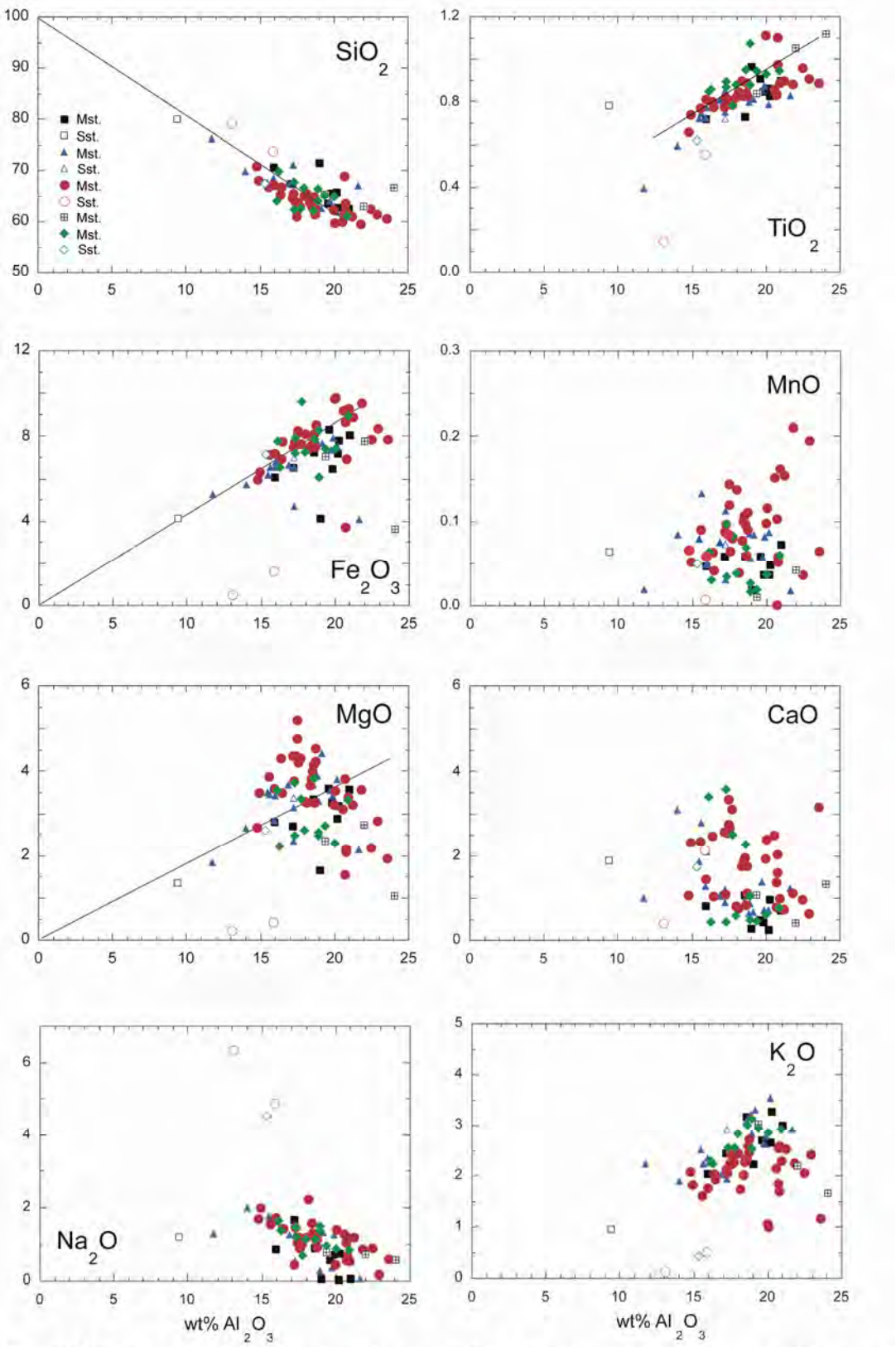

Fig. 4.19. Plots of selected major elements- Al_2O_3 for Upper Cretaceous to Miocene mudstones and sandstones from CMB.

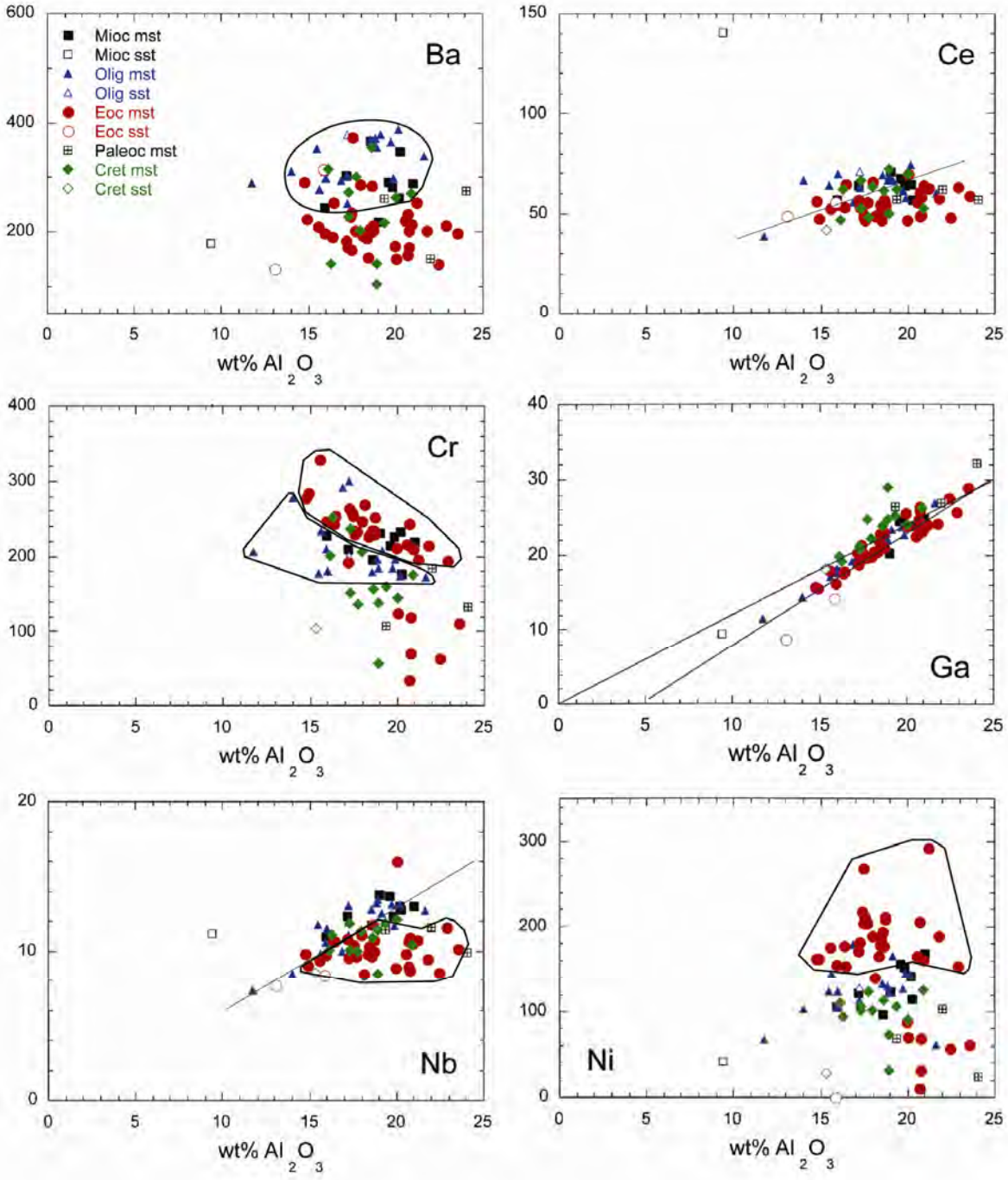

Fig. 4.20a. Plots of selected trace elements- Al_2O_3 for Upper Cretaceous to Miocene mudstones and sandstones from CMB.

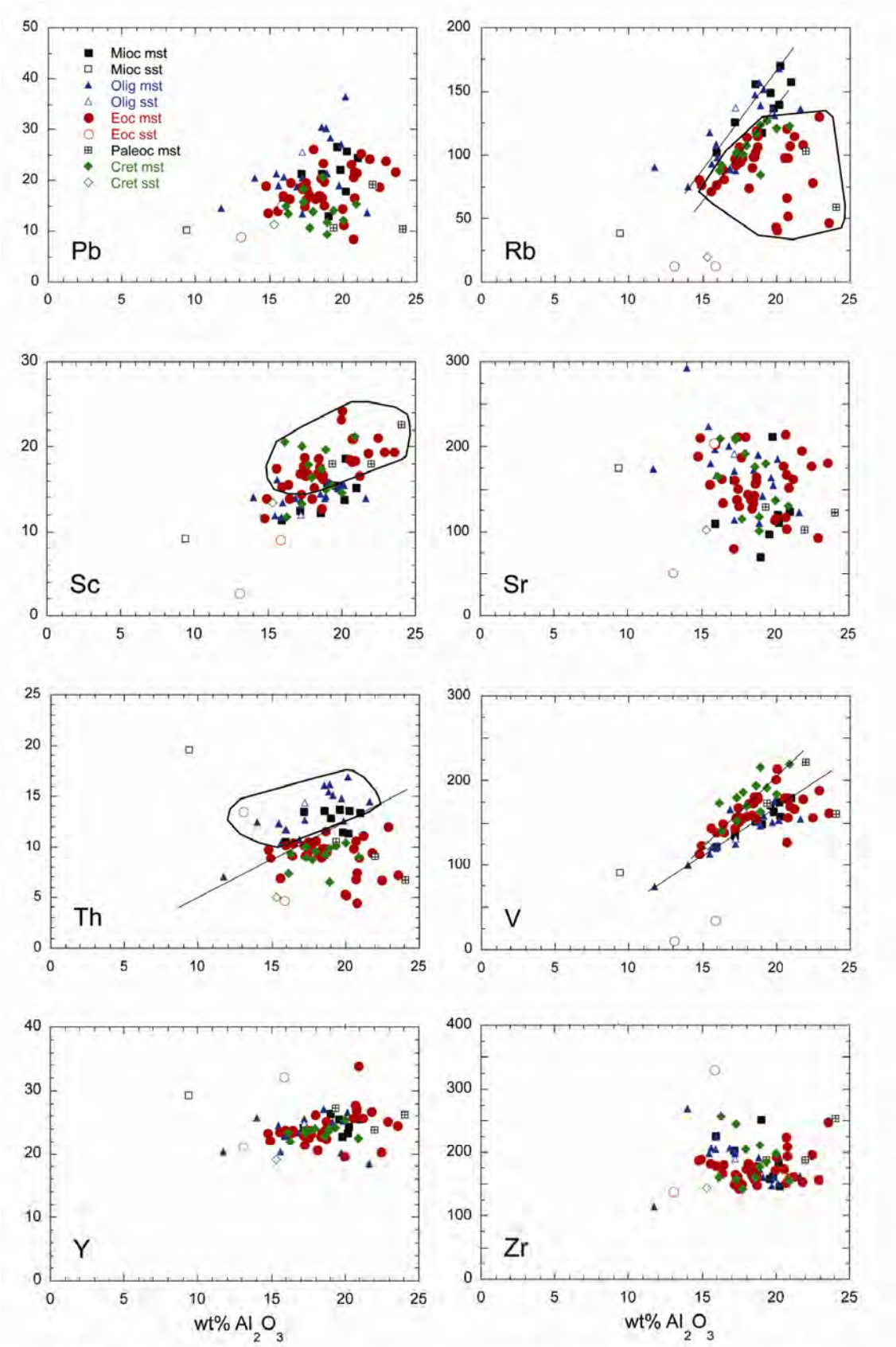

Fig. 4.20b. Plots of selected trace elements- Al_2O_3 for Upper Cretaceous to Miocene mudstones and sandstones from CMB.

On the basis of the Pettijohn et al. (1987) diagram (Fig. 4.21), the sandstones of the Pegu Group and the Eocene are classified as Greywacke and Litharenite, and hence are immature. Although this diagram is not designed for muddy rocks, mudstones of the upper Cretaceous, Eocene and Oligocene are identified classified as Greywackes, Litharenites, and Arkose, and those in the Paleocene and Miocene are as Litharenites and Arkoses (Fig. 4.21). Similar classifications were identified for arc-derived mudrocks elsewhere (Purevjav and Roser, 2013). On the Herron (1988) diagram, all mudstones and sandstones are classified as the Fe-shales and Fe-sands (Fig. 4.22). This classification is unusual, as most mudrocks from accretionary margin greywackes (e.g. Shimanto terrane, Japan; Torlesse terrane New Zealand) are classed as shales, rather than as Fe-shales (B.P. Roser, pers. comm., 2013). This suggests relative iron enrichment in the CMB sediments.

Geochemical maturity was calculated using the Index of Compositional Variability (ICV) = $(Fe_2O_3+K_2O+Na_2O+CaO+MgO+MnO+TiO_2)/Al_2O_3$ (Cox et al., 1995). Taylor and McLennan (1985) mentioned for post Archaean Australian Shale (PAAS) that the ICV values

are greater than 0.85 for major rock-forming minerals such as feldspars, amphiboles, and pyroxenex, while values less than 0.89 reflect for alteration minerals such as kaolinite, illite, and muscovite (Cox et al., 1995).

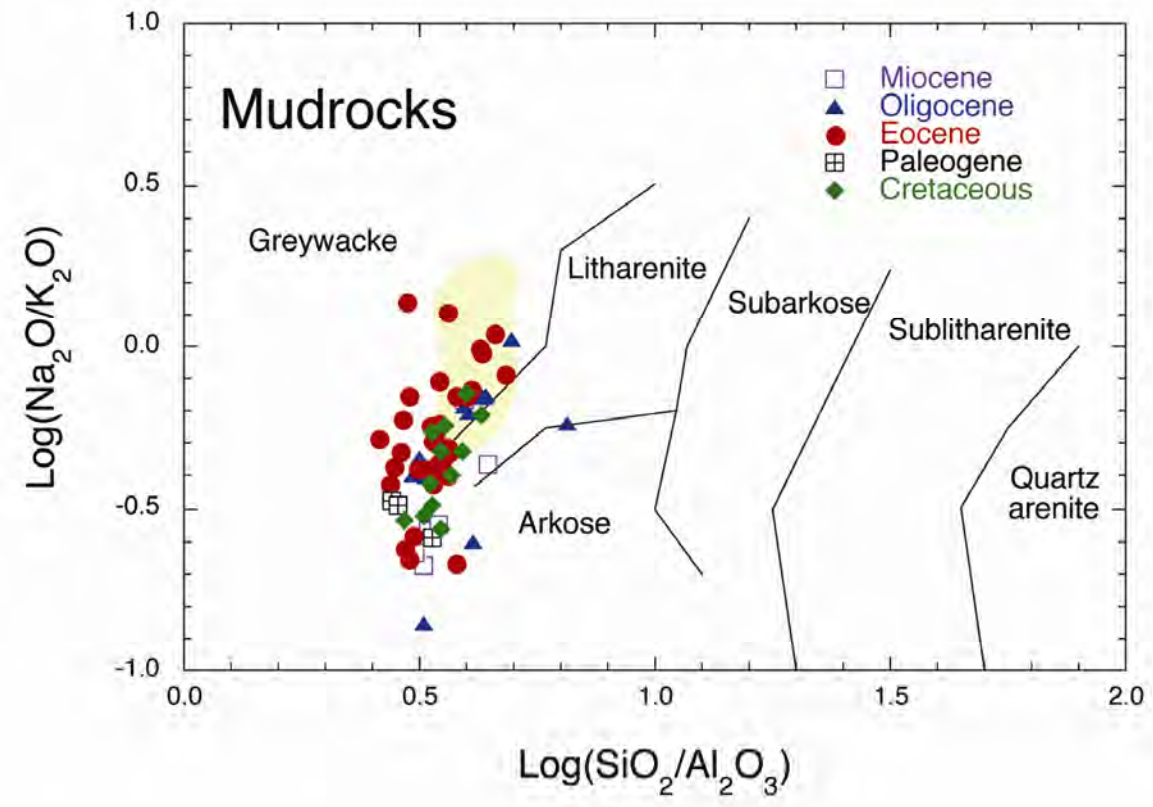

Fig. 4.21. Log (Na_2O/K_2O) vs. Log (SiO_2/Al_2O_3) for Upper Cretaceous to Miocene mudstones and sandstones from CMB. (Pettijohn et al., 1987)

The ICV value of post-Archaean Australian Shale (PAAS) of Taylor and McLennan (1985) is 0.84, and this can be taken as the break between immature sediments (ICV >0.85) and mature sediments (ICV <0.85). Average ICV values for the upper Cretaceous to Miocene formations are ranginge from 0.81 to 0.92 in the upper Cretaceous to Miocene samples, showing that they are mostly immature. In the plot ICV vs. the Chemical Index of Alteration (CIA), the CMB sediments show a linear trend from ICV ~0.80 through to ICV ~0.7 (Fig. 4.23), although most samples have ICV <0.85. Most of the samples with lower ICV come from the upper Cretaceous, Oligocene and Miocene parts of the succession, suggesting some change of maturity within the CMB with time.

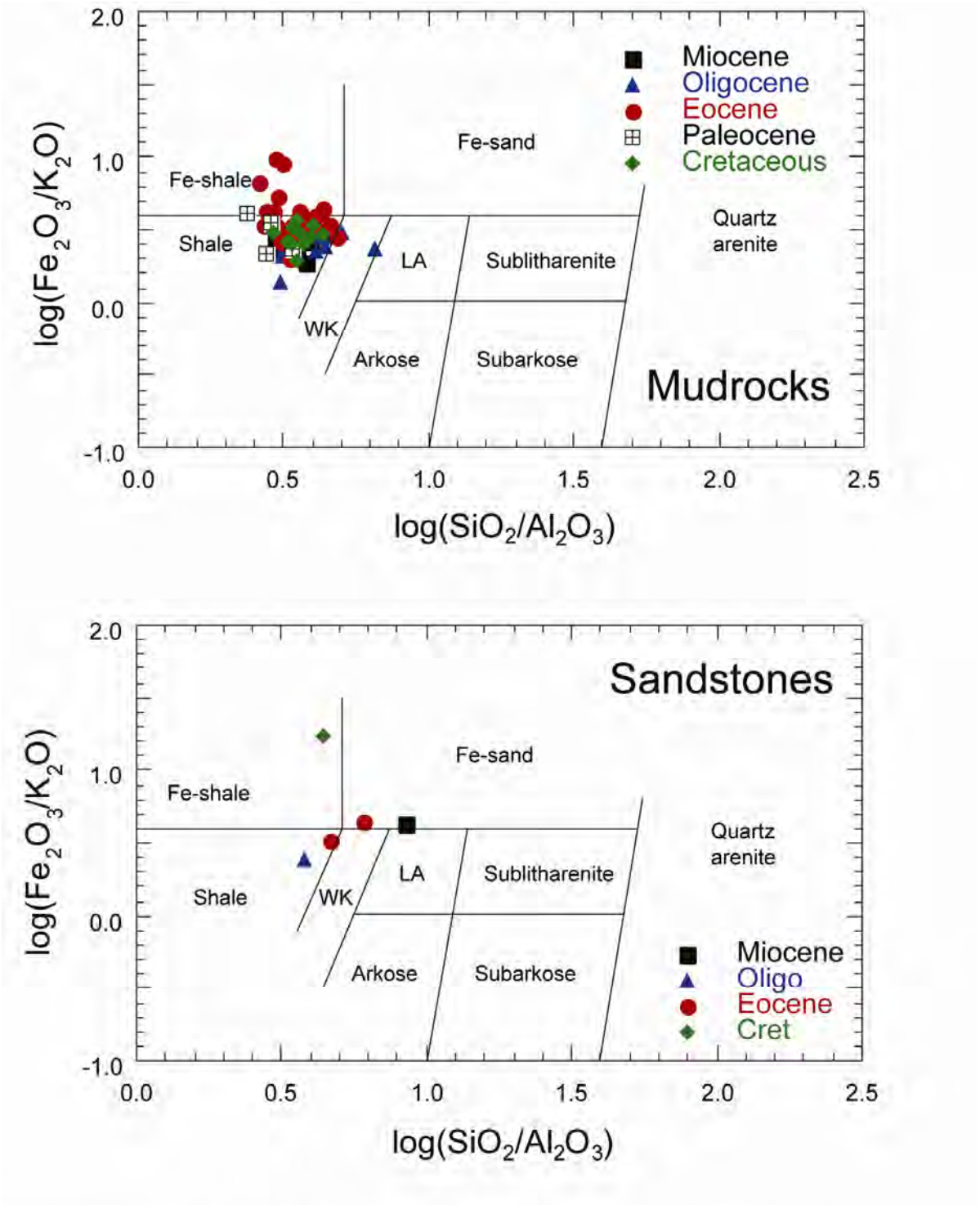

Fig. 4.22. Log (Fe_2O_3/K_2O) vs. Log (SiO_2/Al_2O_3) for upper Cretaceous to Miocene mudstones and sandstones from CMB. (Herron, 1988)

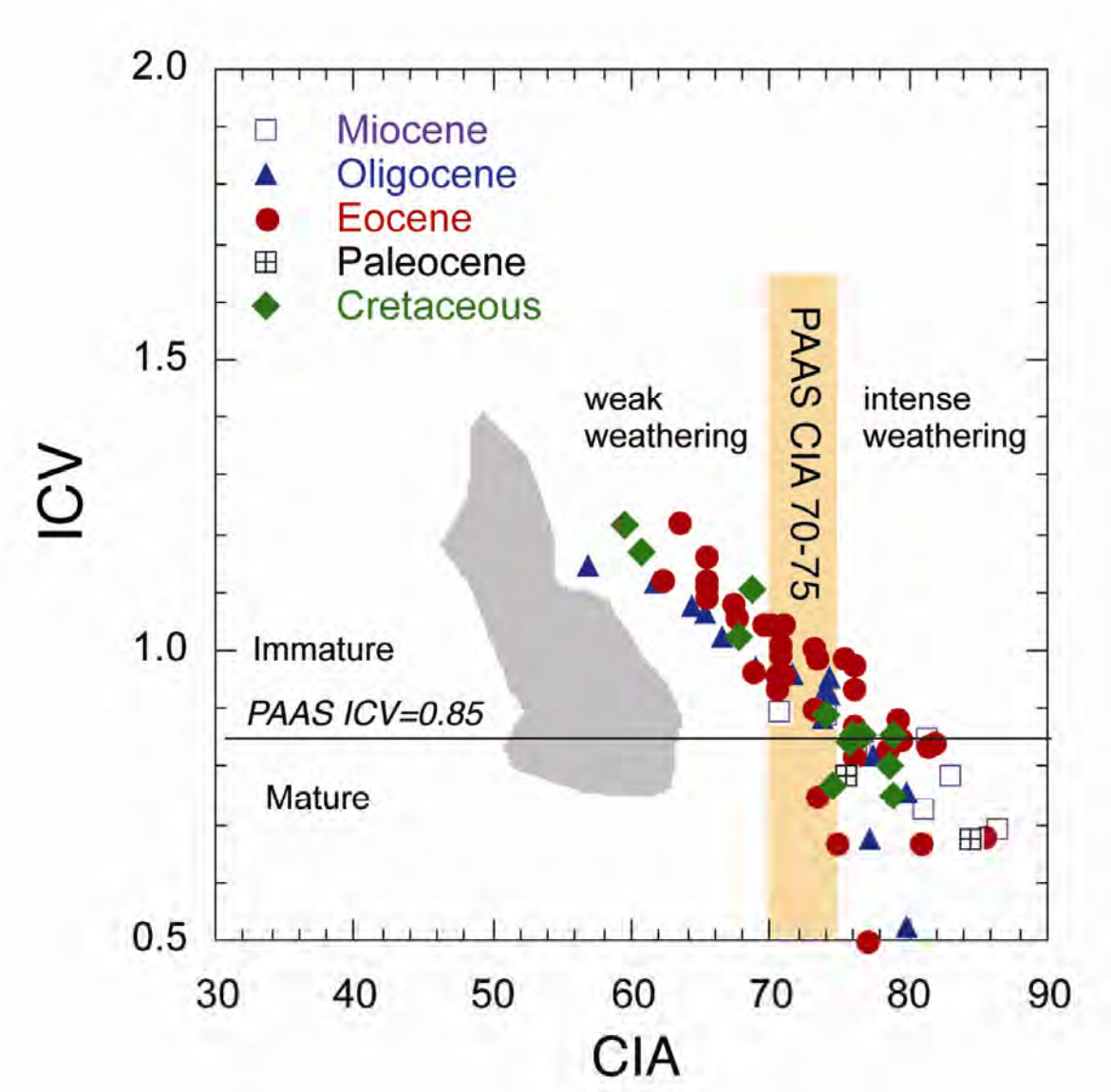

Fig. 4.23. Cross-plot of CIA vs. ICV for mudstones and sandstones from CMB. CIA= Chemical Index of Alteration, ICV= Index of Compositional Variability.

4.3 Basin Modelling

4.3.1 One-dimensional maturity modeling

Burial depths generally increase from north to south in the IMTB (Wandrey, 2006). Based on organic geochemical data, Basin Mod (1D) modeling software was used for reconstructing the maturity and burial history of the studied succession in the western margin of the Central

Myanmar Basin. The stratigraphic succession starts the Obogon Formation (Upper Miocene). The stratigraphic data was provided by present studied report and previous stratigraphic study (Pivnik et al., 1998). For basin modeling, petrophysical properties such as porosity, density, heat capacity and thermal conductivity of rocks were calculated using lithological information. These parameters are available within the software package. We constructed the geological time scale and Formation periods based on the work published by Walker and Geissman (2009) and unpublished Than htut (2008).

The constructed burial and temperature histories of the studied area are shown in Fig. 4.24. Reconstruction of burial history illustrates non-steady subsidence and sedimentation during the Cenozoic, especially from the beginning of Eocene. No major tectonic events may have occurred during upper Cretaceous to Paleocene, showing gentle subsidence. Major tectonic may bagin during the middle Eocene (Fig. 4.24). In this study the actual measured vitrinite reflectance (Ro%) and sterane (C_{29}) data available for upper Cretaceous to Miocene age can be considered that late stage of oil and gas generation might be in the upper Cretaceous and lower Eocene age (Fig. 4.25). Both present day surface temperature and present day heat flow data were used to calibrate the burial history model. Based on the measured vitrinite reflectance data, figure 4.26 shows that a variable heat flow throughout the upper Cretaceous to Miocene age in the western margin of the Central Myanmar basin.

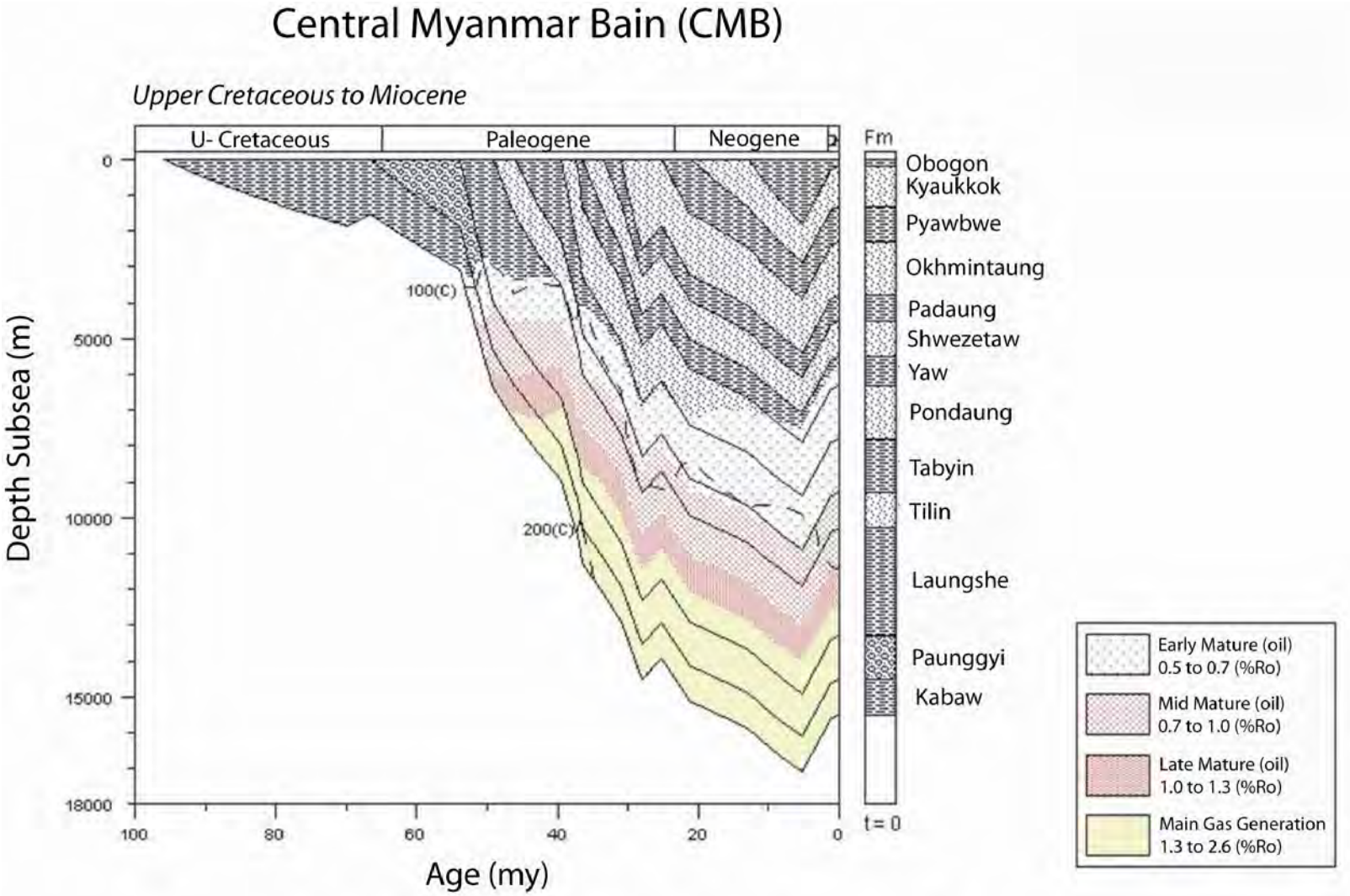

Fig. 4.24. Burial history of the Central Myanmar Basin.

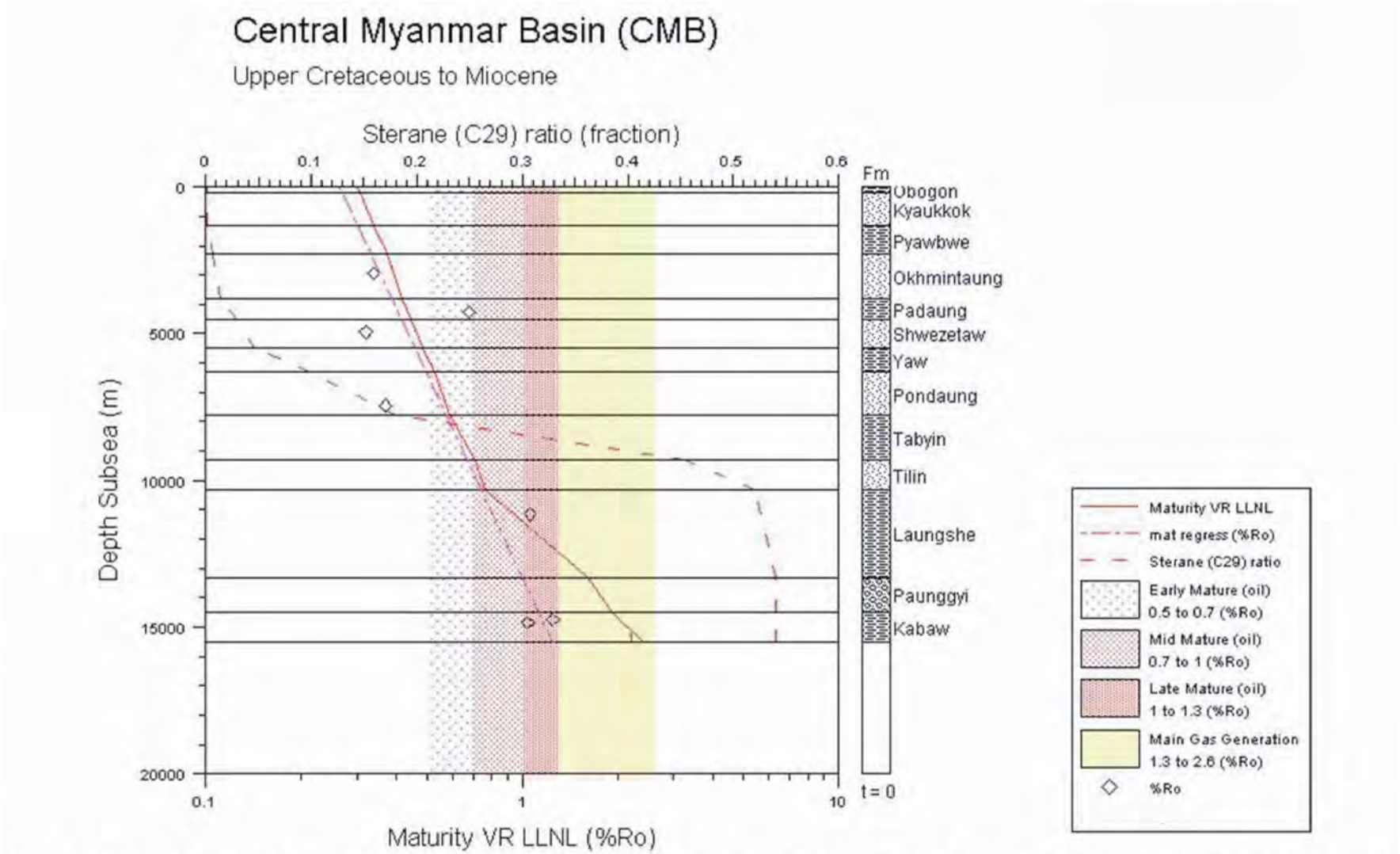

Fig. 4.25. Vitrinite reflectance (% Ro) and Sterane (C29), showing maturity throughout the Upper Cretaceous to Miocene in the Central Myanmar Basin.

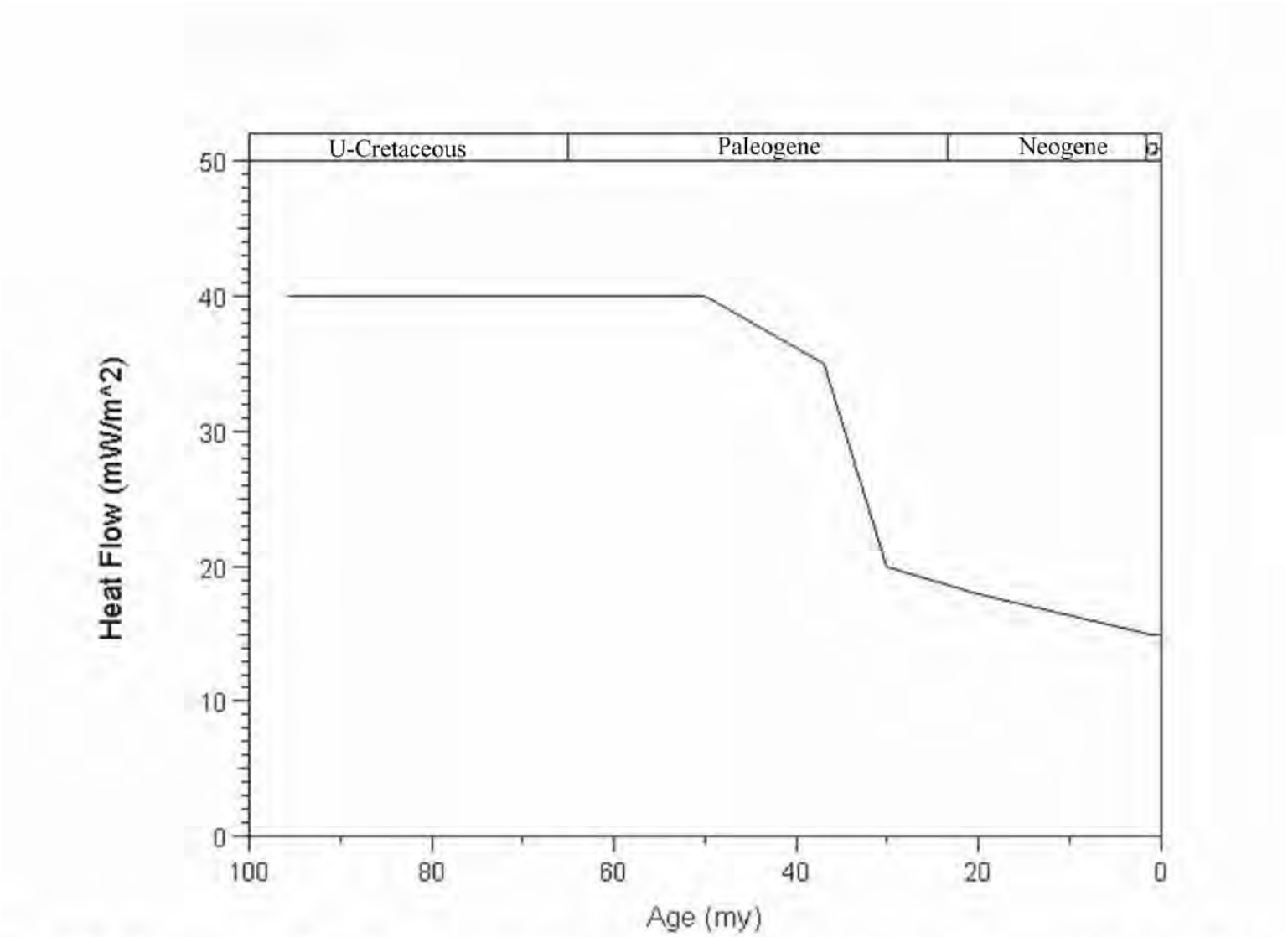

Fig. 4.26. Showing heat flow throughout the Upper Cretaceous to Miocene in the Central Myanmar Basin.

CHAPTER 5. DISCUSSION

5.1 Organic geochemical compositions

There are four major sources of sedimentary organic matter, namely, phytoplankton, higher plants, bacteria and zooplankton. Fungi are important organisms in non-marine environment, whereas they are much less in marine environment due decomposition is primarily carried out by bacteria. (Killops and Killops, 2005)

5.1.1 Coal and coaly shale (Upper Eocene)

5.1.1.1 Moderate weathering processes

The compositions of three coaly shale samples (A2-54, A2-52A, A1-120) have been moderately altered by oxidation and weathering in the humid tropical climate of central Myanmar, which has a mean annual rainfall of 1000 mm, and an average temperature of more than 27˚C. Microscopic investigation identified many thin, irregular micro-fissures and dark oxidation rims on the edges of oxidized vitrinite particles (Fig. 5.1). The weathered samples are brownish-black and partly brown color, and are characteristically more friable than the unweathered coals. This color feature also indicates progressive alteration of coal to soil (Copard et al., 2002). Petsch et al. (2000) showed that if carbonaceous shales are permeable, this condition can favour oxidation of the surface of organic matter, which is subsequently degraded during weathering. This feature is supported by the pair of fresh (A2-52) and weathered (A2-52A) coaly shales collected from the same seam in the Pondaung Formation. These show obvious loss of TOC (from 8.6 wt to 2.1 wt%, respectively) due to weathering. Increased permeability in the coaly shales thus favours chemical weathering along the micro-fissures.

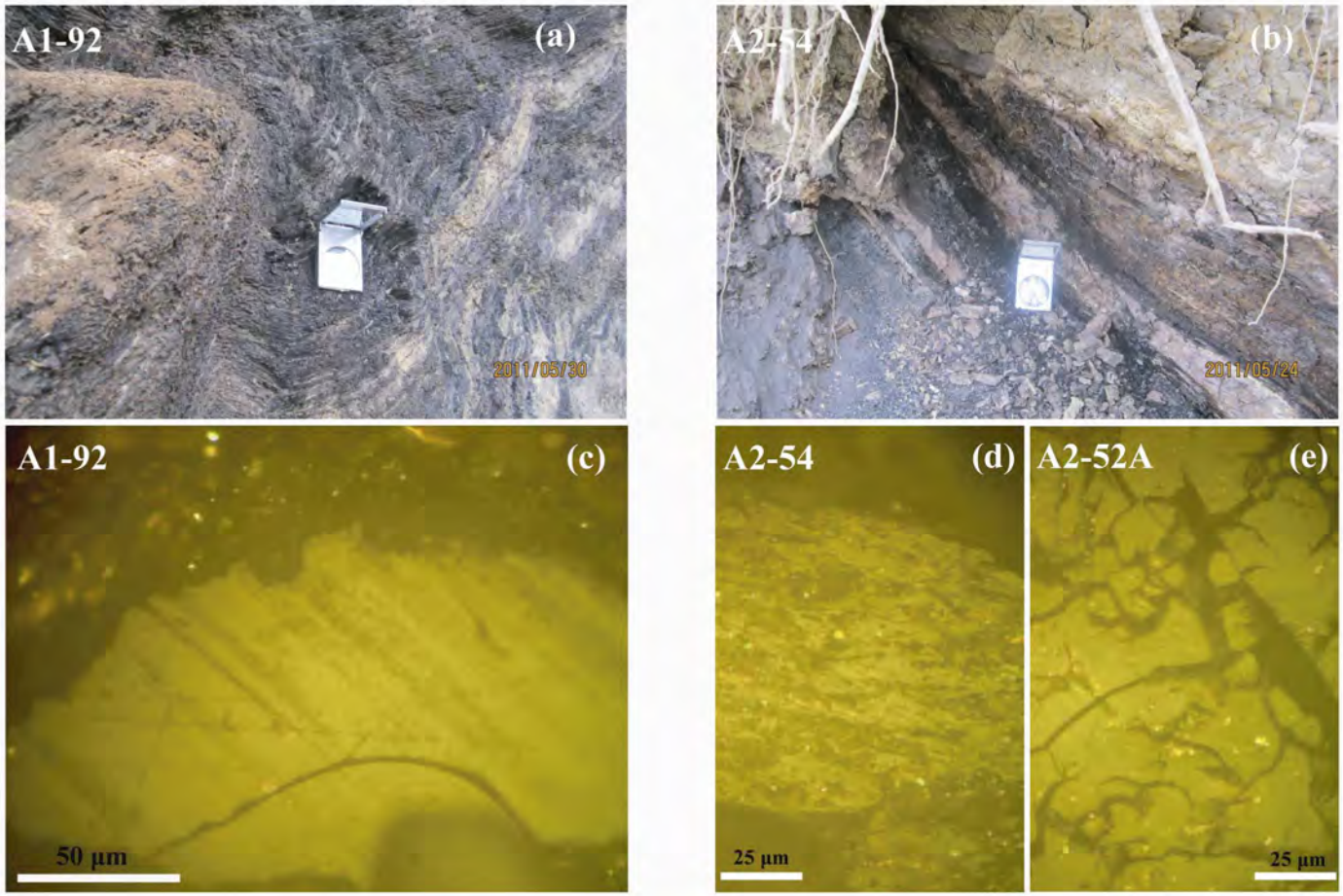

Fig. 5.1. Outcrop photographs of (a) unweathered coal and (b) weathered coaly shales; photomicrographs of (c) A1-92, illustrating thin micro-fissures in vitrinite (d) A2-54, dark oxidized rims along irregular micro-fissures in vitrinite (e) A2-52A, showing dark oxidized rims along irregular micro-fissures in vitrinite particles.

T_{max} has been used as a parameter to determine not only maturation, but also the oxidation process (Copard et al., 2002). The T_{max} values of 451˚C in the weathered coal shale (A2-52A) are clearly greater than the 425˚C determined for the fresh coal shale (A2-52), even though R_o of these samples are similar, at 0.30 and 0.39 %, respectively, showing immaturity. The three weathered coaly shales analyzed here are characterized by high T_{max} values (435–451˚C) related to their very high OI values (137–212 mg CO_2/g TOC), low Pr/Ph ratios (0.23–0.69) and low HI values (12–26 mg HC/g TOC). Copard et al. (2000) considered that anomalously high T_{max} (500–575˚C) and OI (50–80 mg CO_2/g TOC) values in immature or slightly mature samples showed the effects of oxidation of organic matter at high temperature. The low Pr/Ph ratios may be produced by decreased concentrations due to the effect of water washing, and the loss of light molecular weight hydrocarbons which are partly soluble in water (e.g. Martínez and Escobar, 1995). The py-GCMS compositions of the weathered samples show marked decrease in long chain *n*-alkanes (>*n*-C_{20}) bonded to kerogen (Fig. 5.2e, h, and i).

This suggests that bonded hydrocarbons may be lost due to change in pH to acidic conditions, because acid hydrolysis could decrease the bonded long fatty acids (e.g. Martínez and Escobar, 1995). The PAHs in the weathered samples (mostly 3- to 5-ring compounds), are either decreased significantly in concentration or are totally lost . Perylene, P, BaPy and BePy are unstable during oxidation (e.g. Kawka and Simoneit, 1990), and all have been reduced or lost in these samples. Methyl derivatives of PAHs such as MPs have also been lost from all three weathered samples.

Nevertheless, the fresh and weathered sample pair (A2-52 and A2-52A) shows no notable differences in free *n*-alkane content, biomarkers such as distributions of steranes and triterpanes, and kerogen $\delta^{13}C$ isotopic ratio, despite the moderate weathering.

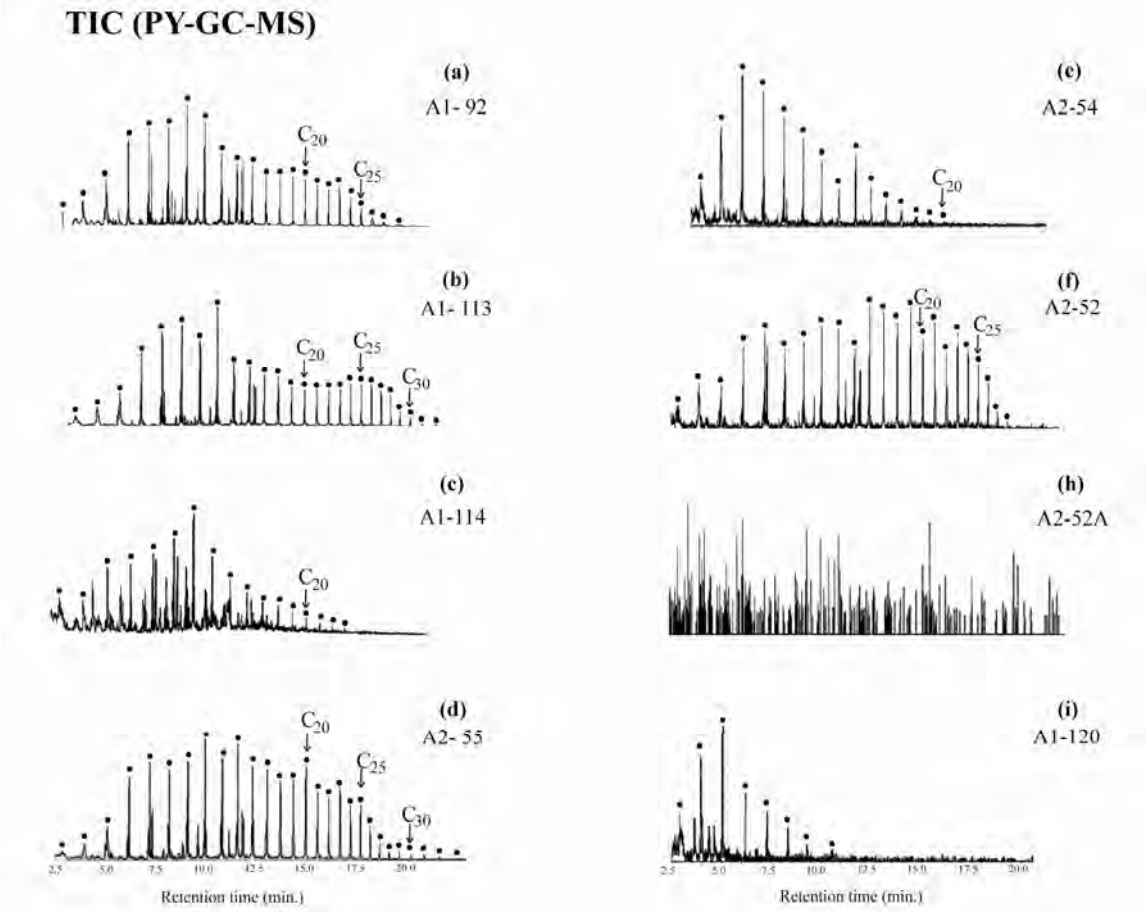

Fig. 5.2. Total ion chromatograms for pyrolysis GC-MS of Upper Eocene coals and coaly shales, CMB.

Results of kerogen samples which are acid-treatment using Rock-eval analysis, yield high S_3 values at 300-400˚C and S_3´ values at 400-650˚C. Although the S_3 values thus show a strong relationship with the S_3´ values in all kerogen samples, the ratio of S_3´ to S_3 is higher in the weathered samples, indicating an increase in S_3´ or a decrease in S_3 values.

Furthermore, py-GC-MS results showed that lighter *n*-alkanes/alkenes (<*n*-C_{10}) and methyl/dimethyl phenols are relatively decreased in the weathered kerogens. Similarly, FT-IR analysis indicate decreased peak of C-H methylene group and relatively constant and/or increased esters or ether groups including C=O (1716 cm^{-1})/C-O (1000-1300 cm^{-1}) peaks in

the weathered kerogens. This association can be considered that C-C methylene structures in the weathered kerogens have been cleaved and the alkyl chain moieties in the kerogen samples might be considerably released by weathering. Oxygen-containing moieties such as methyl/dimethyl phenolics in kerogen are also decreased due to weathering. In general, the oxygen-containing moiety in geomacromolecule is thought to be easily decomposed during oxidation and oxic biodegradation except peculiar cases as reported by e.g. Jenisch-Anton et al. (1999) and Guo and Bustin (1998). The oxygen-containing group in organic matter can be readily released and difficult to be preserved, although such organic oxygen in geomacromolecule has been poorly understood. The results of present study could indicate that rapid decomposition of alkyl chain moieties in kerogen by weathering faster than that of organic oxygen group had caused an increase in OI, because OI is a relative value based on organic oxygen to organic carbon in kerogen.

FT-IR analyses of the weathered kerogens indicate low peaks of aliphatic bonding at 2925-2850 cm^{-1}, and relatively constant and/or increased peaks of C=O and C-O bonds at 1716 $cm^{-1}$and 1000-1300 cm^{-1}, respectively.

5.1.1.2 Origin of organic matter

Change in sedimentary facies from the coaly shale layers to the coal layers seems to be accompanied by change in the origin of the organic matter. C/N values less than 10 are characteristic of algal-derived OM, whereas terrestrial source of OM have greater than 20 (Meyers and Ishiwatari, 1993; Meyers, 1994).The coals have C/N ratios greater than 30 (39.3–66.8), indicating higher vascular plant sources. C/N ratios of the coaly shales range from 16.0 to 30.57, and are clearly lower than those of the vascular plant-derived coals.

In general, short chain *n*-alkanes (*n*-C_{12}–C_{19}) are derived from plankton (Meyers, 1997), algae, and microorganisms (Cranwell, 1977; Cranwell et al., 1987), whereas long chain *n*-

alkanes (n-C_{20}–C_{35}) are derived from terrestrial land plant waxes (Tissot and Welte, 1984). Dominance in mid-chain n-alkanes (C_{20}–C_{26}) reflects origin from bacteria and aquatic plants (Davis, 1968; Ficken et al., 2000; Nott et al., 2000). Submerged and floating aquatic plants commonly show maxima at n-alkanes C_{21}, C_{23}, and C_{25} (de Souza et al., 2011). In my present study, the relative abundance of n-C_{20}–n-C_{33} alkanes and maxima at C_{21} in coals A1-114 and A2-55 and at n-C_{22} in A1-92 suggest that the OM mainly originated from terrestrial higher plants, along with a contribution from aquatic plants. Ficken et al. (2000) proposed that submerged and/or floating aquatic plants have ratios of mid-chain to long chain n-alkanes (P_{aq} = (C_{23}+C_{25})/(C_{23}+C_{25}+C_{29}+C_{31})) of 0.4 – 1.0.

The coals have P_{aq} values ranging from 0.40 to 0.89, indicating that they contain a contribution of submerged/floating aquatic plants. Furthermore, the coaly shales clearly exhibit predominance of odd-over-even carbon numbers in wax-derived long-chain n-alkanes (n-C_{27} – C_{33}). The average CPI value of 1.9 of the coaly shales is greater than the 1.7 average of the coals, suggesting a slightly more abundant contribution of vascular plant waxes in the former relative to the latter.

Similarly, Zheng et al. (2007) suggested P_{wax}= (C_{27}+C_{29}+C_{31})/ (C_{23}+C_{25} +C_{27}+C_{29}+C_{31}) as a proxy to evaluate the distributions of vascular plant waxes. Higher average value of P_{wax} in coaly shales (0.56) than in coals (average 0.47) is also consistent with higher plant wax input. High Pr/Ph ratios in the unweathered coaly shales (9.1 in A2-52) can indicate not only inputs of vascular plant waxes, but also an oxic depositional environment (e.g. Fabiańska et al., 2013). In addition, most samples contain relatively high concentrations of moretanes, implying a contribution from mosses or grasses, since the moretanes in peat are partly derived from lower plants such as mosses and ferns (e.g. Quirk et al., 1984).

Tm (22,29,30 -Trinorhopane) and Ts (22,29,30 -Trisnoneohopane) have been known to be related with the characteristics of both maturity and type of organic matter (e.g. Seifert and

Moldowan, 1978; Moldowan et al., 1986). Slightly high values of Ts over Tm (Ts/Tm) in the coals (A1-113, A1-114) and coaly shale (A2-52) can be speculated that it may be associated with an influence of depositional environment than the impact of maturity.

Retene has been identified as a biomarker for many higher land plants such as gymnosperms, especially resinous conifers (Noble et al., 1986; Simoneit et al., 1986; Otto et al., 1997; Otto and Simoneit, 2001; Otto et al., 2003; Piedad-Sánchez et al., 2004), whereas tripernoids are markers of angiosperms (Moldowan et al., 1994; Nakamura et al., 2010).

Similarly, the presence of oleananes has been considered as a molecular fossil for higher land plants, mostly angiosperms vegetation (Phlip and Gilbert, 1986; Peters and Moldowan, 1993).

Presence of retene and related compounds including dehydroabietins (18-*nor*-abieta-8,11,13-triene (*m/z* 241)), dehydroabietane (*m/z* 255), and 7-isopropyl-1 methyl-1,2,3,4-tetrahydrophenanthrene (*m/z* 223) in trace concentration in the coals can be attributed to be a small contribution of gymnosperms to their sedimentary OM. Retene can be transformed to 1,7-DMP (pimanthrene) (Simoneit et al., 1986; Armstroff et al., 2006; Nakamura et al., 2010), which itself originates mainly from pine resin abietic acid (Wakeham et al., 1980; Radke et al., 1982; Simoneit et al., 1986; Budzinski et al., 1997).

The low abundances of 1,7-DMP (pimanthrene) in the coals (0.03–0.21 μg/g TOC) also suggest limited contribution from resinous higher plants, especially conifers (e.g. Del Rio et al., 1992). In contrast, the higher 1,7-DMP content in coaly shale A2-52 (0.53 μg/g TOC) suggests a greater contribution of resinous materials in the coaly shales. The presence of oleanane/C_{30}-hopane in the coals indicates an increase in angiosperm vegetation, according to the accepted origin of oleanane (Philp and Gilbert, 1986; Peters and Moldowan, 1993; Moldowan et al., 1994).

The upper Eocene carbonaceous sediments in CMB are thus characterized by mixed inputs of angiosperm and gymnosperm vegetation during peat accumulation. The coaly shales reflect mixed inputs of abundant resinous conifers (i.e. gymnosperms) and lesser angiosperm plants, whereas the paleo-vegetation supplying the coals was mainly dominated by angiosperms, with a minor gymnosperm component.

Cadalene ($C_{15}H_{28}$) is one of the precursors of the cyclic sesquiterpenoidal hydrocarbons in vascular land plant resins (Simoneit et al., 1986; Otto et al., 1997; Killops and Killops, 2005) and is a product of diagenetic transformation of sesquiterpenoid biomarkers (Simoneit, 2005; cf. Stefanova et al., 2013). Sesquiterpenoid precursors are characterized by resinous materials (Simoneit et al., 1986; Otto et al., 1997), but types of vegetation can be identified based on diverse plant groups (e.g. Cupressaceae or Dipterocarpaceae). Dipterocarpaceae (angiosperms) has been found in Southeast Asia during the Paleogene (Prasad, 1993).

Widodo et al. (2009) detected that aromatic sesquiterpenoids (e.g. cadalene, tetrahydrocadalene, calamenene) compounds are associated with the occurrence of angiosperms containing dammer resin in ombrogenous tropical lowland peat swamp of Indonesia. However, the obviously presence of gymnosperm derived diterpenoid markers (e.g. retene, 1MP, pimarane) in most carbonaceous samples, especially coaly shale (A2-52), revealed that there was a small contribution of resinous higher plants (i.e. hymnosperms) during peat accumulation.

Cadalene is abundant in coaly shale A2-52 (9.1 μg/g TOC) and coal A1-92 (3.1 μg/g TOC). The relatively high concentrations of ses- and tri-terpenoids markers (e.g. cadalene and oleanane) in the coals thus suggest that their OM mainly contains inputs of angiosperms, with a small contribution from resinous conifers. The coaly shales are characterized by higher portions of diterpenoid compounds relative to triterpenoid compound markers, indicating more significant gymnosperm-dominated paleo-vegetation relative to angiosperms. Lücke et

al. (1999) showed that angiosperms had lighter $\delta^{13}C$ values of about -26‰ than gymnosperms (about -24‰).

Bechtel et al. (2003) also indicated that angiosperms average $\delta^{13}C$ of -25.5‰ to -26.6‰, whereas gymnosperm vegetation averages between -22.7‰ and -25.1‰. The coaly shales have $\delta^{13}C$ values ranging from -24.5‰ to -26.0‰ (Table 1, avg. -25.2‰), suggesting influence of changes in peat-forming vegetation, with both gymnosperm and angiosperm contributions. On the other hand, the coals have $\delta^{13}C$ values ranging between -24.8‰ and -26.5‰ (avg. -25.8‰), suggesting that the depositional environment was more influenced by angiosperm vegetation, with a minor gymnosperm contribution. The two uppermost coals (-26.5‰) clearly show an abundant contribution of angiosperms, whereas the lowermost coaly shale (A1-120, -24.6‰) reflects greater gymnosperm contribution.

The C_{27} steranes were likely originated from algae (Robinson et al., 1984), while C_{28} steranes from yeast, fungi, phytoplankton (e.g. diatoms) (Volkman, 2003) and C_{29} steranes from terrestrial higher plants (Huang and Meinschein, 1978) and brown and green algae (Volkman, 2003). In addition, the distribution of C_{29} sterols has been demonstrated as the presence of numerous microalgae such as diatoms and freshwater algae (Volkman et al., 1998) and C_{27} and C_{28} steranes may also generate from algae in swamp or lacustrine environments (Volkman, 2003; Piedad-Sánchez et al., 2004). Decreased C_{29} steranes derived mainly from terrestrial higher plants (Huang and Meinschein, 1978, 1979) in the coals also suggest an increase in algae/phytoplankton contribution relative to fungi/terrestrial plants.

The respective C_{27}- C_{28}- C_{29} ternary diagram (Fig. 5.3) reflects that the possible sources of OM for Upper Eocene coals and coaly shales are from terrestrial higher plants with lesser amounts of aquatic materials. One coal (A1-92) from the uppermost Eocene Yaw Formation can indicate algal inputs in swamp or lacustrine.

Similarly, fungi-derived perylene decreases from the coaly shales to the coals. In addition, high hopane/sterane ratios can be attributed to inputs of prokaryotic bacteria organisms (Peters et al., 2005; Mrkić et al., 2011). The wide range of hopane concentrations (0.22–36.26 µg/g TOC) in the analyzed samples suggests extensive inputs of bacterial organic matter (e.g. Böcker et al., 2013). However, average concentrations in the coaly shales (16.1 µg/g TOC) are almost double those of the coals (8.9 µg/g TOC), suggesting that bacterial activity may have decreased in the anoxic conditions (low Pr/Ph ratios in Fig. 4.6a) of coal deposition.

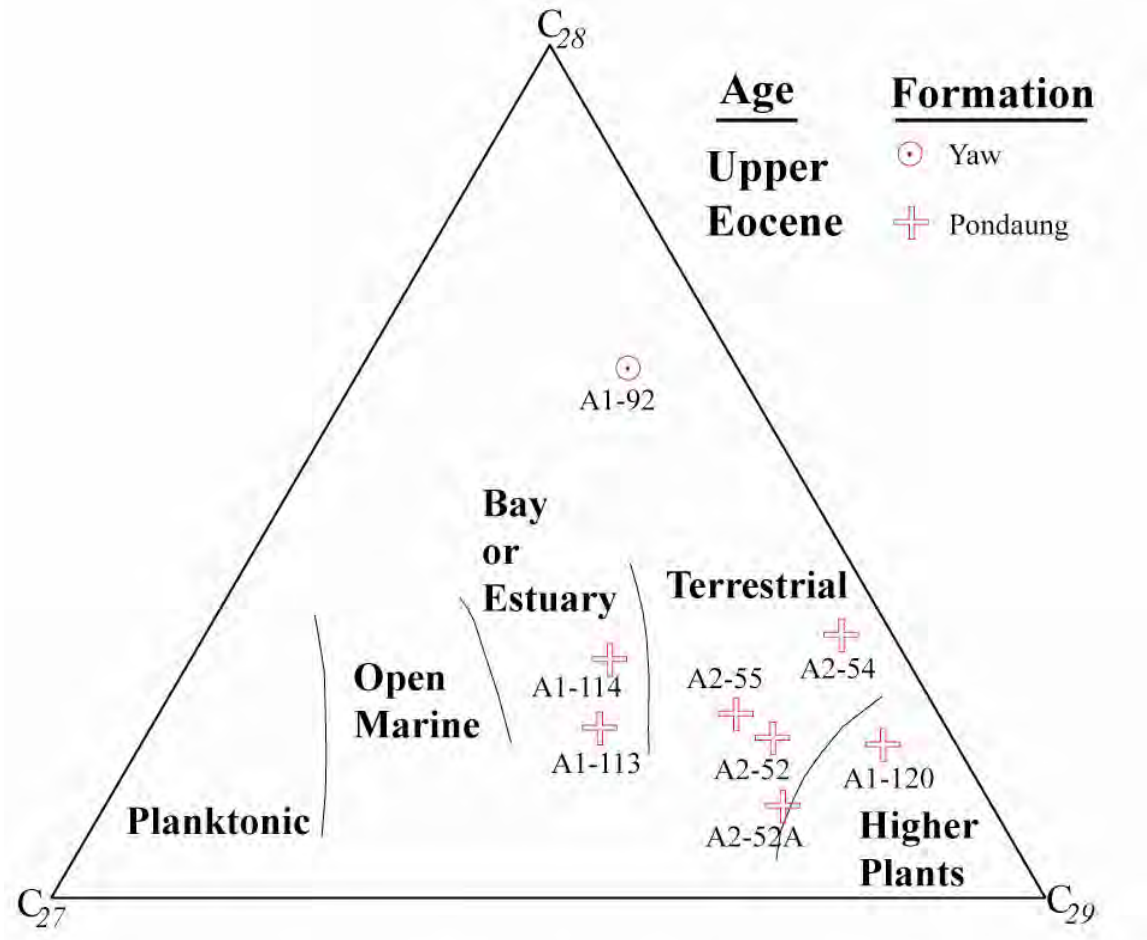

Fig. 5.3. Ternary diagram of C_{27} - C_{28} - C_{29} steranes for coal and coaly shales showing source of OM and depositional environments.

5.1.1.3 Depositional environments

The ratio of TOC to TS (C/S ratio) in all upper Eocene samples is greater than 6 (Table 1), implying oxic marine or non-marine environments (marine C/S <5; Berner, 1984; Berner and Raiswell, 1984). Three coals (A1-113, A1-114, A2-55) are characterized by low sulphur contents (0.09–0.47 wt%) and very high C/S ratios (49-612), implying that they were deposited in non-marine fresh water environments, such as those associated with fluvial-deltaic settings and coastal plains. The remaining coal (A1-92) has a high sulphur content (3.95wt%) and moderate C/S ratio (6.7), suggesting deposition in an oxygen-poor environment inundated by seawater fluctuation during peat accumulation (e.g. near-shore and tidal-influenced deltaic plain).

The coaly shale A2-52 also has a slightly elevated sulphur content (1.14 wt%) and moderate C/S ratio (7.5), and thus its OM may also have been deposited in a peat swamp in a fluvial-deltaic setting influenced by sea level fluctuations.

Likewise, low S/C ratio may indicate an evidence of fresh water non-marine environment (Berner, 1984; Raiswell and Berner, 1984). The S/C ratios in upper Eocene sediments are relatively lower than 0.2, indicating fresh water non-marine environment.

Ts/Tm (22,29,30 -Trinorhopane to 22,29,30 -Trisnoneohopane) ratios in the upper Eocene sediments support the above interpretations. Ts/Tm ratios are known to be related to the characteristics of both maturity and contribution of marine organic matter (e.g. Seifert and Moldowan, 1978).

Higher Ts/(Ts+Tm) ratios in the upper part of the coals suggest an increase in marine OM at that stage. These interpretations are consistent with the proposal of Chhibber (1934), who suggested that the Yaw Formation (upper Phase-II) was frequently influenced by marine waters, as based on the presence of marine vertebrate fossils. According to Haq et al. (1987), cyclic sea level fluctuations of +90 m increasing to +150 m occurred in the period from 36.5

to 39.4 million years ago, which is consistent with the age of the upper Eocene Pondaung and Yaw Formations.

Low to high Pr/Ph values of the fresh samples in these upper Eocene Formations indicate that the sediments were deposited in oxic to oxygen-poor environments. Pr/Ph ratio is useful as a geochemical indicator to evaluate the redox condition of the depositional environment (Didyk et al., 1978). Low Pr/Ph ratios (<1) are associated with anoxic conditions, values between 1 and 3 indicate sub-oxic conditions, and high Pr/Ph ratios (>3) indicate oxic environments containing inputs of terrestrial land plants (Didyk et al., 1978; Powell, 1988; Peters and Moldowan, 1993). The Pr/Ph ratios in the coals (0.71 – 4.63) suggest a spectrum from oxygen-poor to oxic environments, whereas the single fresh Phase-I coaly shale (9.09 in A2-52) indicates an oxic environment. Furthermore, low concentrations of pristane and phytane may indicate immature OM (e.g. Dzou et al., 1995; Hughes et al., 1995; Koopmans et al., 1999).

Slightly elevated homohopane oxic-anoxic index values (0.01–0.24) in the coals further suggest a range from oxic to oxygen-poor environments, because homohopane ratio generally increases with decrease in oxygen in water (anoxia >0.2; Waseda and Nishita, 1998). The homohopane index values of the fresh samples show a curvilinear negative correlation with Pr/Ph. Therefore, the Pr/Ph ratios of fresh coals and coaly shales are effective as an oxic/anoxic indicator.

The C_{31}-C_{33} homohopanes are enriched in all samples with very low C_{35} homohopane. The Phase-II coals are slightly richer in C_{35} homohopane, indicating oxygen-poor fresh water environment (fresh water C/S ratio>5), whereas the Phase-I coaly shale shows oxic condition. In the unweathered samples the Pr/Ph ratios exhibit negative correlation with *n*-C_{20-25}/total *n*-alkanes, and positive correlation with sterane $C_{29}/(C_{27}+C_{28}+C_{29})$ and HI (Fig. 5.4). These

relationships imply that aquatic plants and land higher plant material with high HI was deposited under oxic conditions.

Very high Pr/*n*-C_{17} values (4.80 – 9.86) in the unweathered coals and coaly shale imply that they were deposited in inland peat swamps and/or in high-biodegradation conditions, because Pr/*n*-C_{17} values >1 generally indicate inland peat swamp environments (Amijaya and Littke, 2005) and active biodegradation (e.g. Waseda and Nishita, 1998).

All of the studied samples may have been deposited in inland peat swamps, with associated oxic to oxygen-poor fresh water environments.

The cross-plot diagram of regular steranes $C_{27}/(C_{27}+C_{29})$ ratio versus Pr/Ph ratio (Fig. 5.5) illustrated the depositional environment of Late Eocene sediments, showing oxic to anoxic environments (e.g. Waseda and Nishita, 1998).

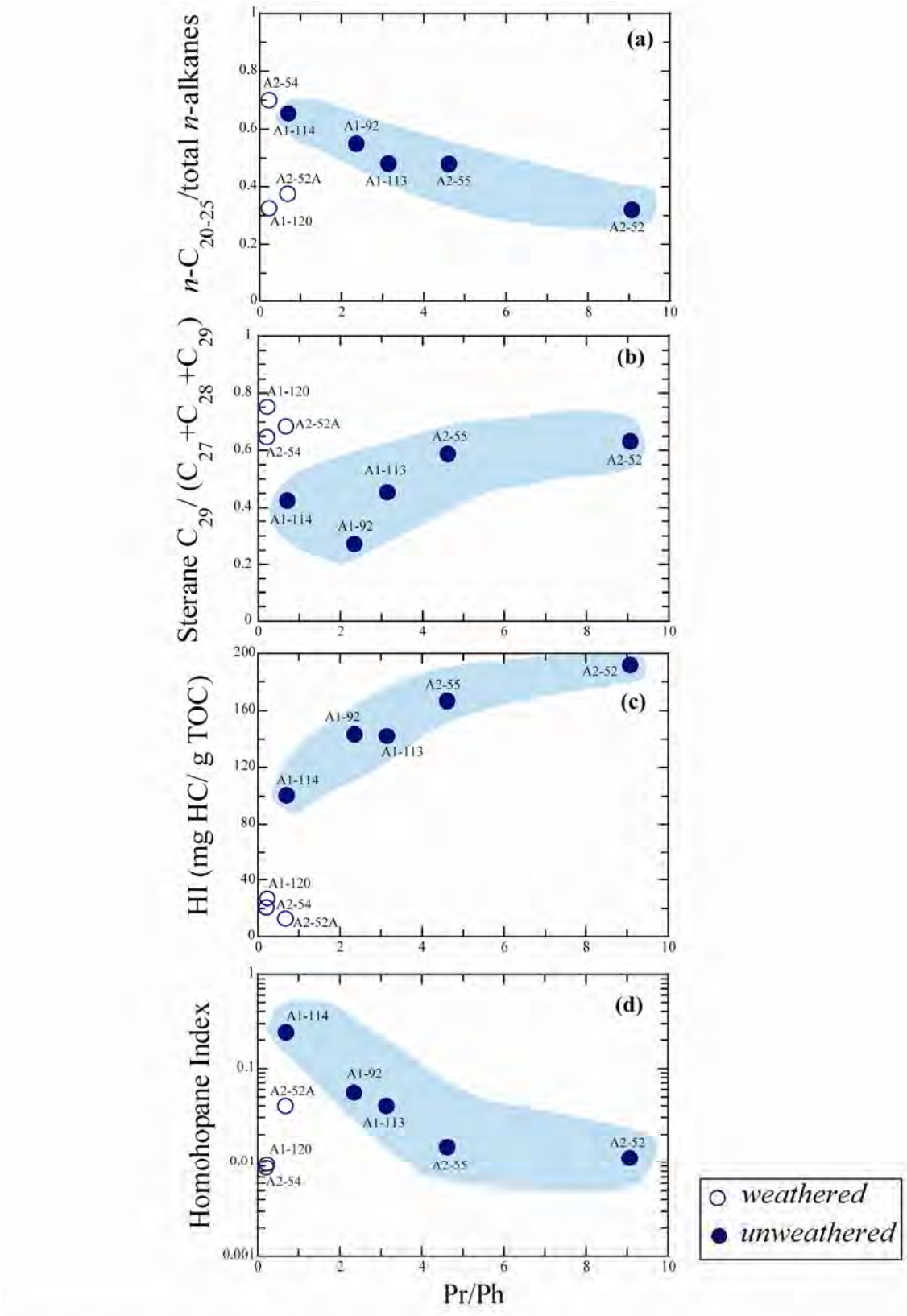

Fig. 5.4. Cross plots of (a) Pr/Ph vs. *n*-$C_{20\text{-}25}$ /total *n*-alkanes (b) Pr/Ph vs. sterane C29/(C27+C28+C29) (c) Pr/Ph vs. HI, and (d) Pr/Ph vs. homohopane index, showing hydrocarbon generation, source of OM, and depositional environments for the Upper Eocene coals and coaly shales. Open Circles indicate weathered samples; shaded zones illustrate the broad correlation in unweathered samples.

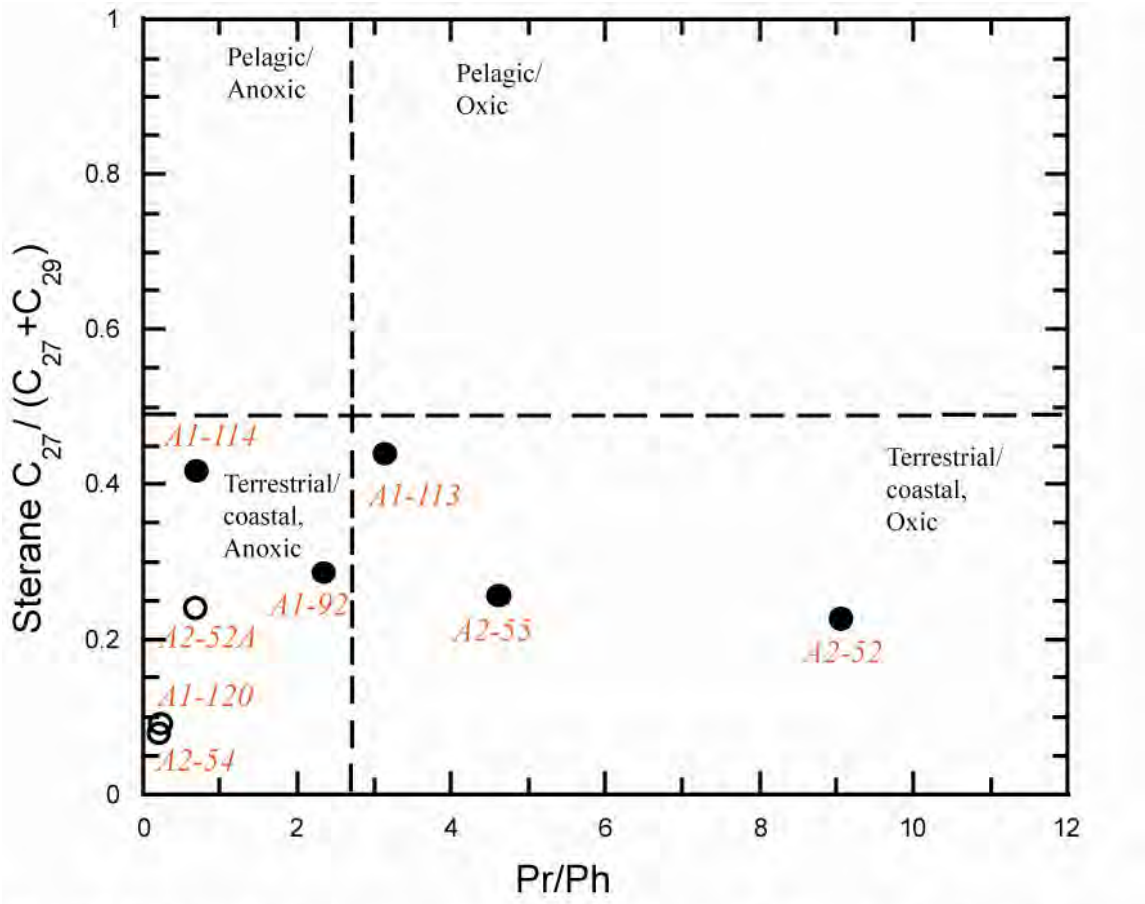

Fig. 5.5. Relationship between sterane $C_{27}/(C_{27}+C_{29})$ and Pr/Ph ratios for Upper Eocene coal and coaly shales in the western margin of the CMB showing source of OM and depositional environments. Open circles indicate weathered coaly shale samples.

5.1.1.4 Thermal maturity and type of organic matter

The Upper Eocene sediments have R_o values ranging from 0.26 to 0.42 %, indicating immature OM. T_{max} values of 413 to 429 °C for the fresh samples also suggests immaturity, in agreement with the immature R_o values (<0.5%). Peters (1986) stated that T_{max} values of less than 435˚C indicated immature OM. The sterane C_{29} 20S/(20S+20R) ratio is used as a maturity indicator; values here also indicate thermally immature OM (0.03 – 0.37). High Carbon Preference Index (CPI) values of more than 1 (1.2 – 2.3) further indicate immaturity. Moretane/C_{30} hopane ratios in the upper Eocene samples vary from 0.32 to 0.87, within the range of 0.15–0.8 that indicates immaturity (Peters and Moldowan, 1993).

The modified van Krevelen diagram showed that the unweathered coaly shale is characterized by a mixture of Type II and Type III kerogens. According to FTIR results, unweathered kerogen samples show rather abundant of ester groups, suggesting that it may indicate type II kerogen because ester groups (–COOR: R is any organic combining group) have not been detected in type III kerogen despite acids (carboxyl group: –COOH) and ketones (C=O) are abundant in type III (e.g. Tissot and Welte, 1984). Ester, derived from carboxylic acids, can produce alcohols and organic or inorganic acids when it reacts with water. Carboxylic acids are predominant in all studied sampls. This association can be likely considered that all fresh coals and coaly shale samples are characterized by a mixture of type II and III kerogens. Potential of hydrocarbon generation for coals and coaly shales may be reasonably good for gas-prone, based on the value of nearly 200 mg HC/g TOC. Generally, OM is categorized as Type II (oil prone) on the basis of HI values with 300 – 600 mg HC/g TOC, Type III (gas prone) with HI of 200 – 300 mg HC/g TOC, and Type IV (inertinite) when HI is <50 mg HC/g TOC (Peters, 1986).

5.1.1.5 Source rock quality and hydrocarbon Potential

Coal is known to be a source rock with gas-generating potential (Tissot and Welte, 1984). The gas-source potential may be more favourable in oxidizing facies than in the oil source. The OM in the Late Eocene sediments of the present study is characterized as immature, as noted above (R_o = 0.26–0.42 %). We determined the potential of hydrocarbon generation as source rocks by pyrolysis S_2 yields, according to Peters and Cassa (1994). The S_2 values are relatively high (16.4–57.3 mg HC/g rock) in the fresh upper Eocene coals and coaly shale, suggesting good to excellent hydrocarbon generating potential (Fig. 5.6).

According to Hunt (1991), hydrocarbon-rich coals containing resinous plants can generate liquid hydrocarbons, whereas hydrocarbon-poor coals can generate gas. Although

most samples of the present study are probably related to gas-prone type III and gas/oil-prone type II-III kerogens, the high HI and low OI values for the coals (A1-92, A1-113 and A2-55) and the fresh coaly shale (A2-52) suggest the potential to generate some volumes of liquid hydrocarbons as well as gas. The Upper Eocene samples show good source rock quality, with potential generation of liquid/gas hydrocarbons (Fig. 5.6).

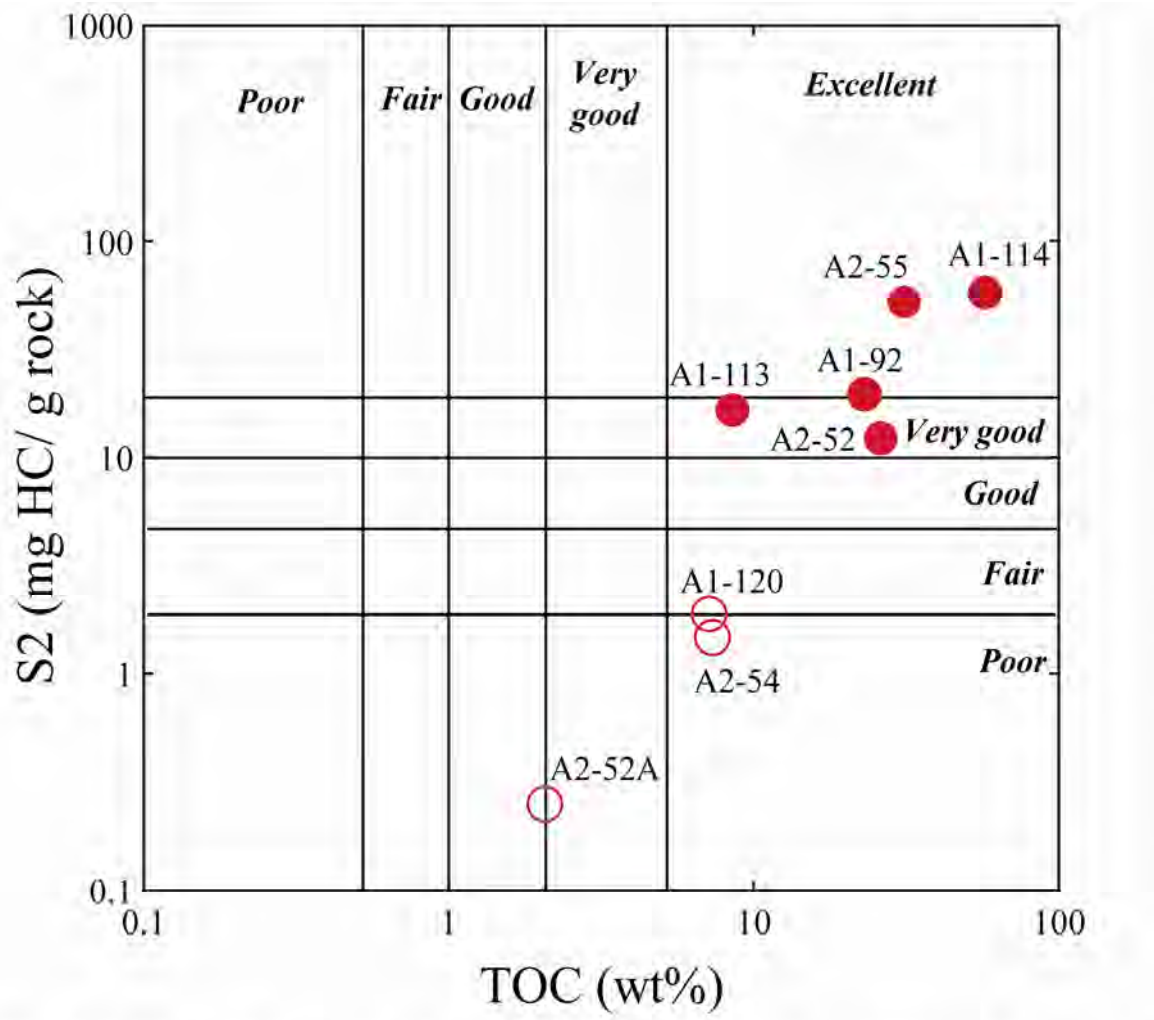

Fig. 5.6. Plot of Pyrolysis S2 versus total organic carbon (TOC), illustrating potential generative source rock for Upper Eocene coals and coaly shales. Open Circles indicate weathered coaly shale samples.

The weathered samples with low HI (12 –26 mg HC/g TOC) and very high OI (137 – 212 mg CO_2/g TOC) compared to the unweathered samples with high HI (100 – 191mgHC/g TOC) and low OI (28 – 107 mg CO_2/g TOC) indicate that hydrocarbon generation potential was decreased to about one tenth of the original value by moderate weathering. The weathered coaly shales, therefore, may have had good potential for hydrocarbon generation before weathering.

Khin (1991) reported that source rocks in the CMB must lie deeper than ca. 3km, because samples taken from the basin at about that depth have low maturity, with R_o values of 0.5%. Curiale et al. (1994) suggested that Paleogene and Early Oligocene source rocks in the deeply-buried parts of the CMB have probably reached the minimum thermal maturity for hydrocarbon generation. Consequently, upper Eocene sediments which are even more favourable for hydrocarbon generation may thus occur in the deeper parts of the basin, compared to those present at its margins.

5.1.1.6 Paleovegetation, Paleoclimate, and Paleowilfire

Aliphatic and aromatic terpenoid biomarkers have been used as a measurement to investigate not only paleo-vegetation but also paleo-climate (Killops et al., 1992; van Aarssen et al., 2000). Diterpenoids have been formed as the source of alphatic and aromatic hydrocarbons at the end of diagenesis (Killops and Killops, 2005).

Significantly dominant distribution of gymnosperms derived diterpenoids markers (e.g. retene and 1,7 DMP) in the coaly shales and coal (A2-55) indicates that these sediments have been influenced by a contribution of higher plants such resinous conifer trees.

In addition, coaly shales have the $\delta^{13}C$ values varying from -24.5‰ to -26‰ can be considered that there was an influence of changes in peat-forming vegetation with both gymnosperms and angiosperms contributions. Other hand, lowermost coals (A1-114 and A2-

55) yield $\delta^{13}C$ values ranging between -24.8‰ and -26.5‰ can be suggested that depositional environment was influenced by angiosperm vegetations with a minor gymnosperm contribution.

The non-hopanoid triterpenoids markers can indicate a contribution of angiosperms to the OM. The coals are characterized by angiosperm rich herbaceous type flora with a predominance of mid-chain n-alkanes, while coaly shales have a significance of both mid- and long-chain n-alkanes, illustrating mainly inputs of higher plant, especially resinous conifers (i.e. gymnosperms).

The Upper Eocene coals and coaly shales contain relatively abundant perylene, which is regarded as a biogenic product generated from perylenequinone pigments during early diagenesis (Wakeham et al., 1980; Budzinski et al., 1997; Silliman et al., 1998; Jiang et al., 2000). Perylene is also considered to originate from wood-degrading fungi (Grice et al., 2009; Suzuki et al., 2010; Marynowski et al., 2013), and is predominantly found in humid and minimum-oxygen environments (Aizenshtat, 1973). Perylene is thus recognized as a useful marker of humid/wet climatic conditions (Suzuki et al., 2010).

Grice et al. (2009) reported that the high concentration of perylene in OM has been related with the activity of wood degrading fungi and during deposition the oxidizing condition could be responsible to occur the decomposition of lignin in the wood by the activities of fungi and bacteria.

Bertrand et al. (2013) suggested that strongly abundant concentration of perylene have been associated with the intense accumulation of woody plants comprising perylene precursors such perylene quinones, which were degraded by the activities of fungi and insects during deposition under oxidizing condition and after deposition, increased accumulation of woody materials could be favourable to occur the transformation of perylene quinones into perylene with decreasing oxygen content.

In the present study, the coaly shale A2-52 contains abundant gymnosperm markers, and is also enriched in perylene. This perylene could thus have been generated from wood-degrading fungi in a humid climate. Moist conditions also favour the growth of coniferous trees and widespread contributions of subtropical rain forests. Perylene concentrations gradually decrease in the coals, suggesting that climatic condition changed from humid to relatively dry. Shift of climate from wet (humid) to dry (warm) could also account for the change in origin of the OM from gymnosperm-rich coaly shales to angiosperm-rich coals.

Values of > 0.5 for the ratio Fla/(Fla+Py) are representative indicators of wildfire (e.g. Yunker et al., 2002). Only the uppermost coal (A1-92) has a Fla/(Fla+Py) ratio greater than 0.5, suggesting the occurrence of wildfire in this part of the succession. This is compatible with the estimation of dry climate in Phase-II. The other non-alkylated PAHs such as BaAn, Chry, Tpn, Bflas, BePy and BaPy could be diagenetic products formed from original coals and coaly shales, because they show positive correlation with MP (R=0.67, Fig. 5.6). Alkyl-substituted PAHs such as MP are largely dominated by those produced by diagenesis rather than by fire (Liu et al., 2005).

5.1.2 Mudstones (Late Cretaceous to Miocene)

5.1.2.1 Origin of organic matter

Biomarker has been mostly considered as a molecular source indicator for source of organic matter and paleo-depositional environments (Peters et al., 1993; Meyers, 1997) and also for maturity in ancient sediments (Killop and Killop, 1991).

The presence of an odd-over-even numbered predominance in *n*-alkanes $>C_{22}$ is characteristic of terrestrial higher plants (Eglinton and Hamilton, 1967), whilst odd-numbered *n*-alkanes $<C_{22}$ are from planktons (Blumer et al.,1971).

Short chain n-alkanes (<C_{20}) are originated from planktons (Meyers, 1997), algae and microorganisms (Cranwell, 1977; Cranwell et al, 1987) and long chain ones (*n*-C_{20} – *n*-C_{35}) are from terrestrial land plant waxes (Tissort and Welte, 1984). Similarly, the mid-chain (*n*-C_{20} – *n*-C_{26}) *n*-alkanes were sourced from bacteria and aquatic plants (Davis, 1968; Nott et al, 2000; Ficken et al, 2000).

Generally, short chain n-alkanes are enrichment in the upper Cretaceous to Paleocene, and lower to middle Eocene, indicating partly source of planktons or microorganisms. Upper Eocene (Yaw Fm.) and Pegu Group mudstones show less distribution of short chain *n*-alkanes. The mid- and long chain *n*-alkanes are mostly abundant throughout the upper Cretaceous to Miocene succession, illustrating that the OM was likely originated from terrestrial higher land plants with lesser inputs of aquatic/bacteria.

Furthermore, the *n*-alkane distributions with maxima at C_{27} or C_{29} show inputs of deciduous wood, while at C_{31} indicate abundances of grass vegetation (Zdravkov et al., 2011). Generally, all studied mudstones exhibit the distribution of n-alkanes with maxima at C_{23} and C_{29} and/or C_{31}, showing inputs of deciduous woody plants and grasses.

The distribution of C_{20} – C_{35} n-alkanes with maxima at C_{23} or C_{25}, C_{29}, and C_{31} in most samples can be speculated that the OM is partly derived from submerged and floating aquatic plants, grasses, mosses because submerged and floating aquatic plants are characterized by dominant mid-chain n-alkanes with maximum at C_{21}, C_{23}, and C_{25} (de Souza et al, 2011).

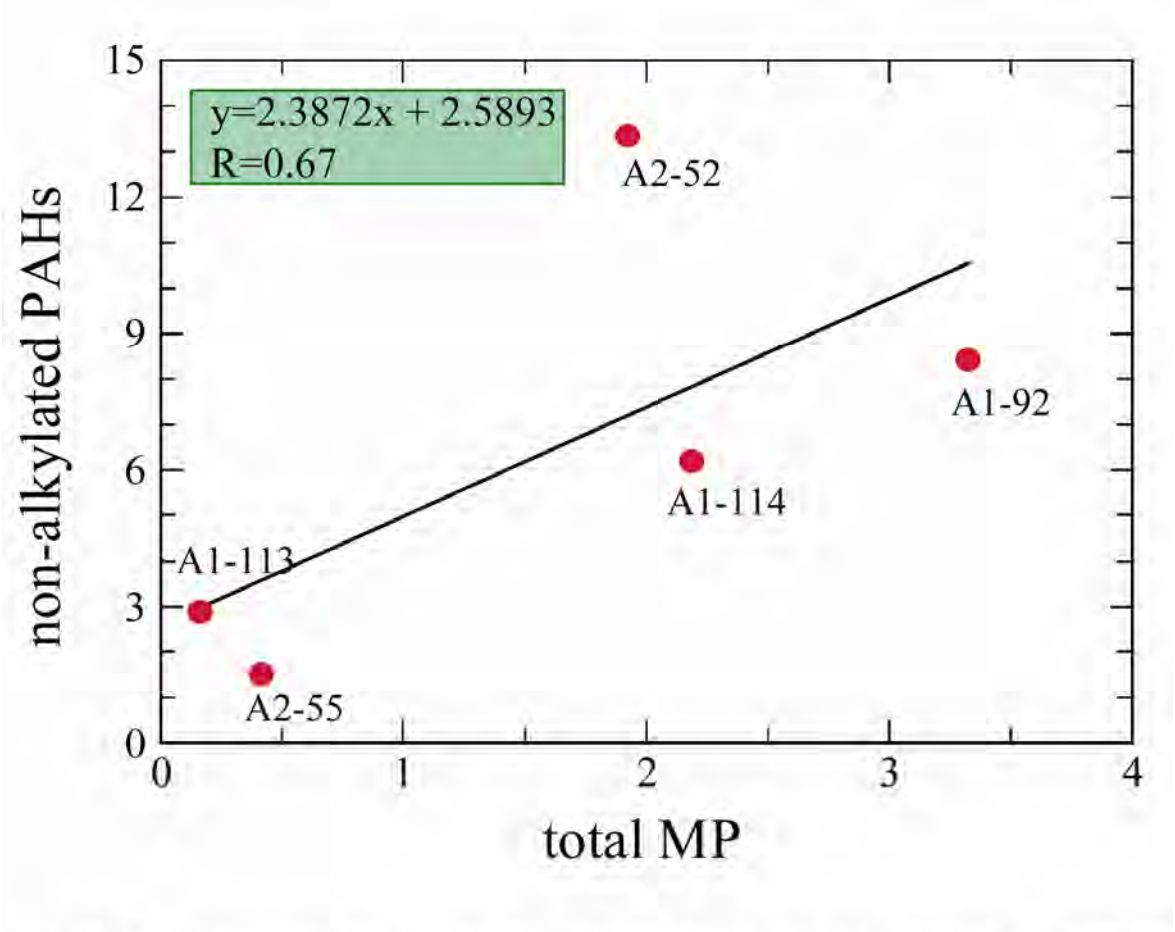

Fig. 5.7. Cross-plot of the non-alkylated hydrocarbons against the total MP (alkylated hydrocarbons) for the unweathered coals and coaly shale.

Most studied mudstone samples have the values of P_{aq} with greater than 0.4, showing partly inputs of aquatic plants. Similarly, the abundant contributions of hopanes and moretanes in all mudstone samples can suggest sources of lower plants such as mosses, grasses, and ferns (e.g. Quirk et al., 1984; Ramanampisoa et al., 1990).

In addition, all studied mudstones exhibit the predominance of odd-over- even carbon number in long-chain n-alkanes (n-C_{27} – n-C_{33}), suggesting a wide contribution of vascular plants wax (Killop and Killop, 2005). The carbon preference index (CPI) values are greater than 1, showing mainly inputs of higher plant wax throughout the studied succession (Killop and Killop, 2005).

Generally, the sterane C_{29}/C_{27} ratios are higher in the late Cretaceous, Eocene (Laungshe, Tabyin, Pondaung, Yaw Fm.), and Pegu Group (Shwezetaw, Okhmintaung, Obogon Fm.), indicating mainly inputs of terrestrial higher plants (Huang and Meinschein,1978; Killop and Killop, 2005). Other hand, steranes C_{27} and C_{28} may also generate from algae in swamp or lacustrine environments (Volkman, 2003; Piedad-Sánchez et al., 2004). The ratios of sterane C_{27}/C_{29} are relatively abundant in the upper Cretaceous to Paleocene, Eocene (Tilin, Yaw Fm.), and Pegu Group mudstones, showing partly inputs of algae and planktons. These values are lesser amounts in the Eocene (Laungshe, Tabyin, Pondaung Fm.), implying a small contribution of aquatic materials.

Furthermore, the respective C_{27} - C_{28} - C_{29} ternary diagram (Fig. 5.8) reflects that the possible sources of OM in the upper Cretaceous, and Eocene (Tilin, Yaw Fm.) are from terrestrial higher plants with lesser amounts of aquatic materials whereas that in the Paleocene, Eocene (Laungshe, Tilin, Tabyin and Pondaung Formations) was mainly sourced from terrestrial land plant inputs. In contrast, the OM in the Pegu Group mudstones was generated from both aquatic materials and terrestrial higher plants.

In this process, less abundant of short chain n-alkanes and low Pr/Ph ratios in Pegu Group may be considered that their concentrations would be decreased due to the effect of water washing because these would be partly soluble in water (e.g. Martínez and Escobar, 1995).

Sterane/ hopane ratio was identified to distinguish different inputs of organisms such as eukaryotic (algae and higher plants) and prokaryotic (bacteria) (Peter et al., 2005; Mrkić et al., 2011). Hopane/sterane ratios are widely ranging from 0.49 to 159.54 and low to slightly high sterane/hopane ratios (0.02 – 1.44) in all studied samples may exhibit both inputs of prokaryotic and eukaryotic organisms to the OM. Likewise, hopane concentrations vary with a wide range (0.95 – 209.24 μg/g TOC), indicating extensive occurrences of bacterial organic matter (e.g. Böcker et al., 2013).

Bacteria and fungi were useful indicators of hopanoid biomarkers (Zdravkov et al., 2011) and bacteria can be highly produced in aquatic environments (Killop and Killop, 2005).

Moreover, pentacyclic hydrocarbon such as perylene concentrations are significant in the middle to upper Eocene (Tabyin, Pondaung, Yaw), and Pegu Group mudstones, showing inputs of fungi, higher plants and insects because perylene originated from fungi, higher plants, and insects (Jiang et al., 2000; Suzuki et al., 2010).

The Ts/ (Ts+Tm) ratios are relatively increasing in the Eocene mudstones (0.19 – 0.84), can be suggested that it may be affected by differences in the sources of OM than maturity.

Non-hopanoid triterpenoids including structures of the oleanane skeleton, the ursane skeleton, or the lupane skeleton has been known to be molecular fossils for higher land plants, mostly angiosperms (Phlip and Gilbert, 1986; Peters and Moldowan, 1993; Rullikötter et al., 1994; Bechtel et al., 2005; Killop and Killop, 2005). Contents of oleanane concentration and oleanane/C_{30}hopane ratios are relatively dominant throughout the Central Myanmar succession, indicating a wide contribution of angiosperm dominated paleo-vegetation.

The Pr/*n*-C17 values may reflect not only maturity of OM but also biodegradation of hydrocarbons (e.g. Waseda and Nishita, 1998). Low to High values of Pr/*n*-C_{17} (0.22 –16.19) in most mudstone samples, indicating a wide range in biodegradation of hydrocarbons. This association can be agreement with the high UCM (unresolved complex mixture) contents throughout the studied succession. Other hand, most sediments (Pr/*n*-C17= >1) have been accumulated under inland peat swamp environment (e.g. Amijaya and Littke, 2005).

The C/N ratio has been useful as an indicator to identify the source of OM (Meyers, 1997; Sampei and Matsumoto, 2001). C/N ratios between 4 to 10 indicate planktonic materials, whereas greater than 15 show terrestrial OM (Meyers,1997). Generally, low C/N values with less than 4 in some samples can be speculated that it was affected by inorganic N as ammonia absorbed by clay minerals (Müller, 1977; Sampei and Matsumoto, 2001).

The aspect of C/N ratios in the CMB was unavailable to identify as a source indicator of OM due to the effect of inorganic nitrogen.

5.1.2.2 Depositional environments

Upper Cretaceous to Paleocene, mudstones have high C/S values varying from ca.5 to more than hundreds, suggesting non- marine fresh water oxic/sub-oxic environment with a periodic marine water fluctuation.

Lower to upper Eocene mudstones have high C/S values varying from ca.0.3 to more than hundreds, suggesting oxic and anoxic fresh water environments with a periodic marine water fluctuation. These values can be aggrement with sedimentary features (Aung and Myint, 1974; Myint and Soe, 1977; Bender, 1983) as Eocene sediments have been affected by marine water fluctuation due to sea level rises.

Low to high values of C/S ratios (ca. 0.6 to >600) in the Pegu Group mudstones can be ascribed that it was accumulated under alternating shifts of fresh and marine water environments dominated by oxic and anoxic conditions. It can be provided by the numerous reports because Pegu Group strata were deposited under shallow marine, shore marine to outer shelf, coastal swamp (Aung and Myint, 1974; Myint and Soe, 1977; Bender, 1983).

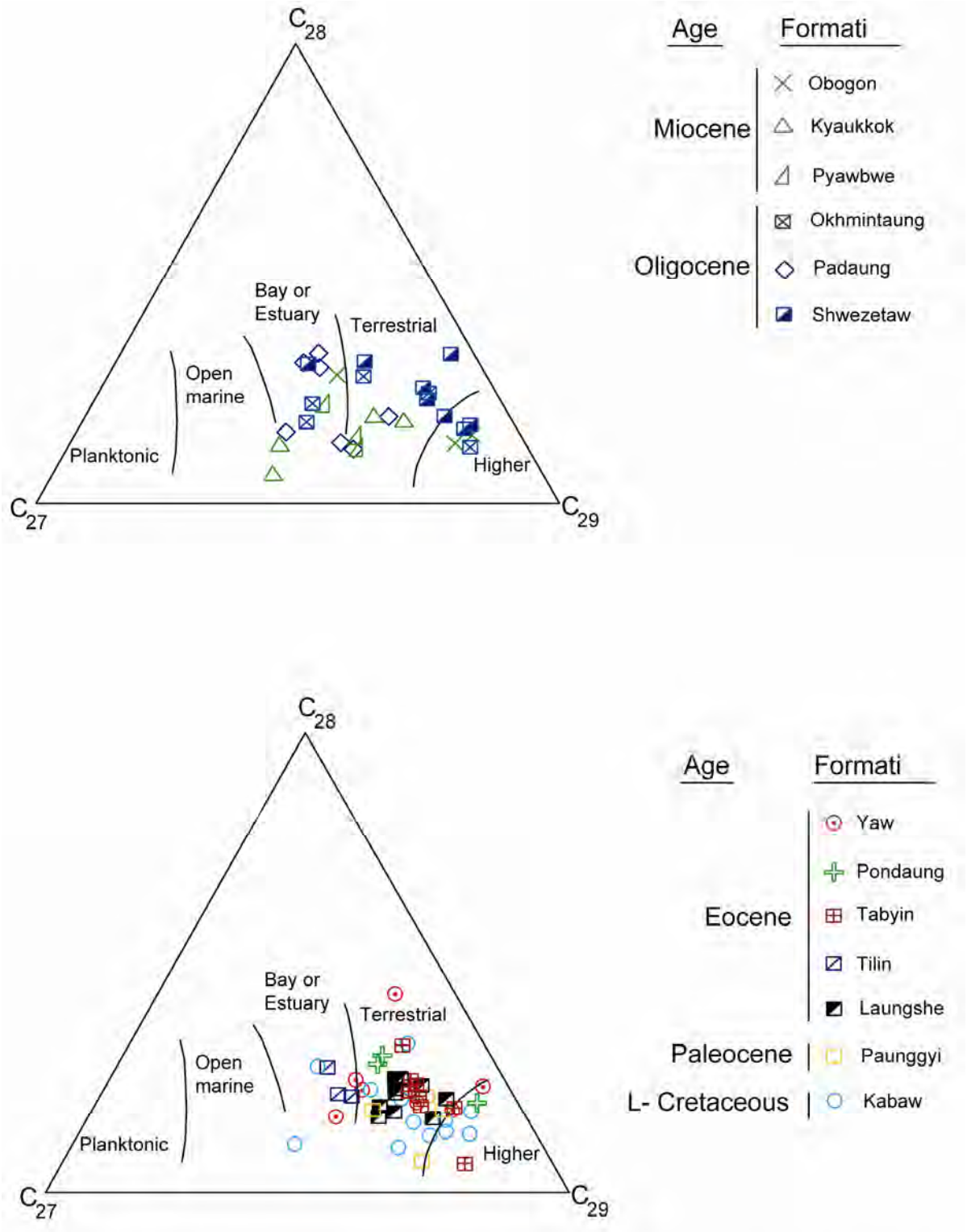

Fig. 5.8. Ternary diagram of C_{27}- C_{28}- C_{29} steranes for Upper Cretaceous to Miocene mudstones from CMB, showing sources of OM and depositional environments (Huang and Meinschein, 1979).

On the other hand, Hall & Morley (2004) suggested that the CMB was formed as a subsiding sub-basin in the IMTB and the great depth of the CMB may be considered due to the tectonic subsidence by sediment loading. Depositional environments have been associated with the relationship between the rates of sedimentation and subsidence. Chhibber (1934) reported that there was an interrupted occurrence between the rates of sedimentation and subsidence during Tertiary period and the rapid rate of subsidence than sedimentation can be favourable that marine deposits (e.g. Yaw Fm.) would be laid down over non-marine sediments (e.g. Pondaung Fm.). Moreover, he mentioned that the great thickness of sandstones in Pondaung formation can indicate a regression of the sea. Therefore, sedimentation in the CMB during Tertiary period (especially Eocene to Miocene in the study area) has been experienced with alternating shifts of marine transgression and regression processes.

The values of Pr/Ph with less than 1 exhibit anoxic environmental condition, whereas those with greater than 3 imply oxic environments (Powell, 1988; Peters and Moldowan, 1993). Similarly, values less than 0.8 would be associated with anoxic conditions in hypersaline or carbonate environments (Peters et al., 2005). In addition, Didyk et al. (1978) suggested that the Pr/Ph values with around 1 can reflect alternating oxic and anoxic environmental condition.

The Pr/Ph values are varying from 0.03 to 5.53 throughout the Late Cretaceous to Miocene succession, showing alternating oxidizing to reducing conditions. These values were under limited detection in the Miocene mudstone samples. The Pr/*n*-C_{17} values ranging from 0.22 to 16.19 in the upper Cretaceous to Miocene mudstones imply that they were deposited in inland peat swamps and/or in high-biodegradation conditions, because Pr/*n*-C_{17} values >1 generally indicate inland peat swamp environments (Amijaya and Littke, 2005) and active biodegradation (e.g. Waseda and Nishita, 1998) (Fig. 5.9). Similarly, low to high

homohopane index in the Late Cretaceous to Miocene succession can be speculated that their OM was accumulated under alternating oxic and oxygen poor conditions.

Generally, homohopane index may reflect both oxidizing and reducing conditions in the Miocene period although Pr/Ph values were under limited detection. Ts (22,29,30 -Trisnoneohopane) and Tm (22,29,30 -Trinorhopane) have been known to be relavent parameters to identify for depositional environments (Moldowan et al., 1986; Peters and Moldowan, 1993) and also for maturation (e.g Waseda and Nishita, 1998).

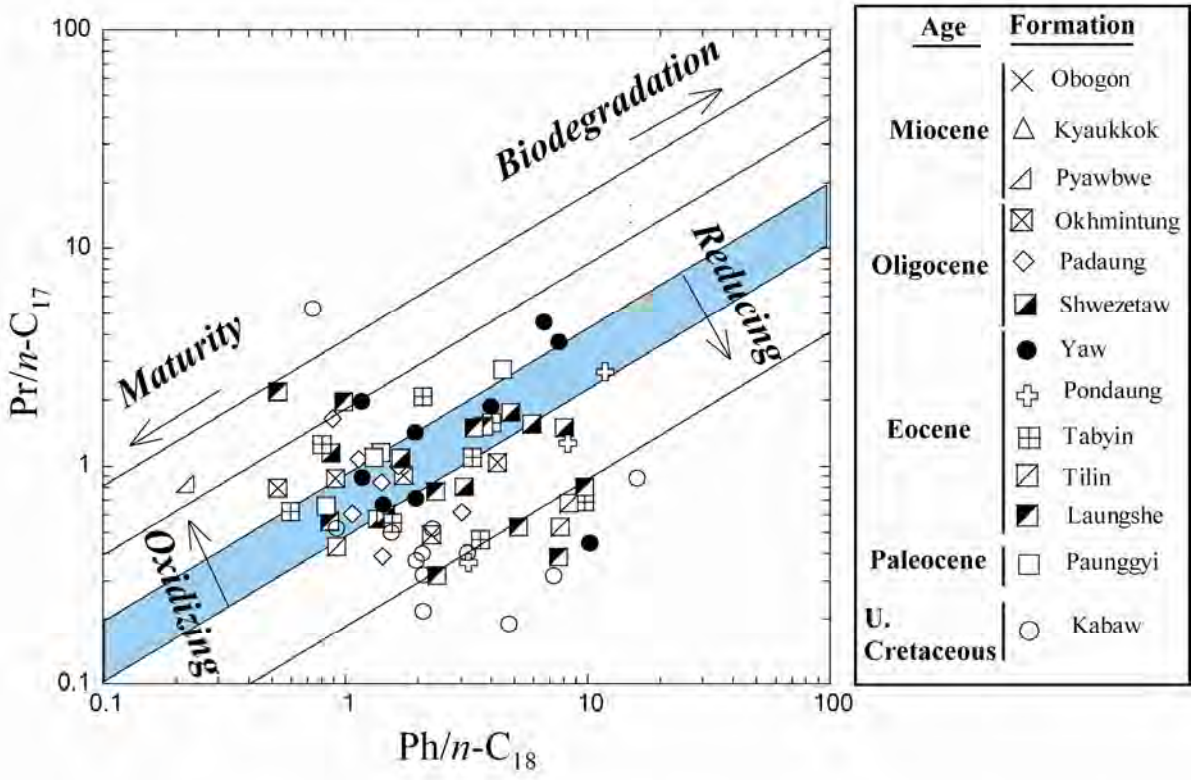

Fig. 5.9. Cross plot of Pr/*n*-C_{17} vs. Ph/ n-C_{18}, showing depositional environment for Upper Cretaceous to Miocene mudstones, CMB.

Likewise, high Ts/Tm (2.33 – 11.77; Table 2) values in the upper Cretaceous may indicate reducing environment provided by terrigenous OM inputs (e.g. Moldowan et al., 1986; Peters and Moldowan, 1993). Low to high Ts/Tm values (0.24 – 5.26; Table 2) in the Eocene and Pegu Group can indicate both oxic and oxygen poor conditions with inputs of terrigenous OM.

Pentacyclic hydrocarbon such as Perylene may originate from terrestrial and aquatic OM under oxygen poor environmental conditions (Aizenshtat, 1973; Wakeham et al., 1979; Silliman et al., 2000; Suzuki et al., 2010). The formation of perylene can be rapidly decayed under oxic environmental condition (Marynowski, et al., 2011). Lesser contents of perylene in the late Cretaceous to Paleocene, early to middle Eocene (Laungshe and Tilin Fm.) mudstones can be suggested that OM would be mostly accumulated under oxidizing condition. Late Cretaceous to Paleocene mudstones would be deposited under both oxic and anoxic conditions as high Ts/Tm values. Perylene contents are slightly low to higher in the upper Eocene and Pegu Group mudstones, showing an alternating oxic to oxygen poor condition.

5.1.2.3 Thermal maturity of organic matter

Vitrinite reflectance values (0.32 -1.25%) indicate that upper Cretaceous to lower Eocene sediments have reached early mature stage while upper Eocene to Miocene sediments exhibit immature. Despite the Ts/(Ts+Tm) parameter seems to depend on sedimentary facies of the depositional environment (Moldowan et al., 1986), it can be commonly useful for maturity assessment (e.g. Seifert and Moldowan, 1978;Waseda and Nishita, 1998). Ts (18α (H)-22,29,30-trisnorneohopane) is more stable to thermal maturity than Tm (17α(H)-22,29,30-trisnorhopane) (Seifert and Moldowan, 1978).

Ts/ (Ts+Tm) values are increasing with close to 1 in the upper Cretaceous mudstones, indicating that it may be due to increasing thermal maturity with burial depth (e.g Waseda and Nishita, 1998). In contrast, the 20S/(20S+20R) ratio at C-20 in the C_{29} 5a(H), 14a(H), 17a(H)- steranes is less dependent on inputs of organic matter source than the Ts/(Ts + Tm) ratio. These values are relatively increased in the upper Cretaceous (0.1 – 0.51), suggesting very early mature stage.

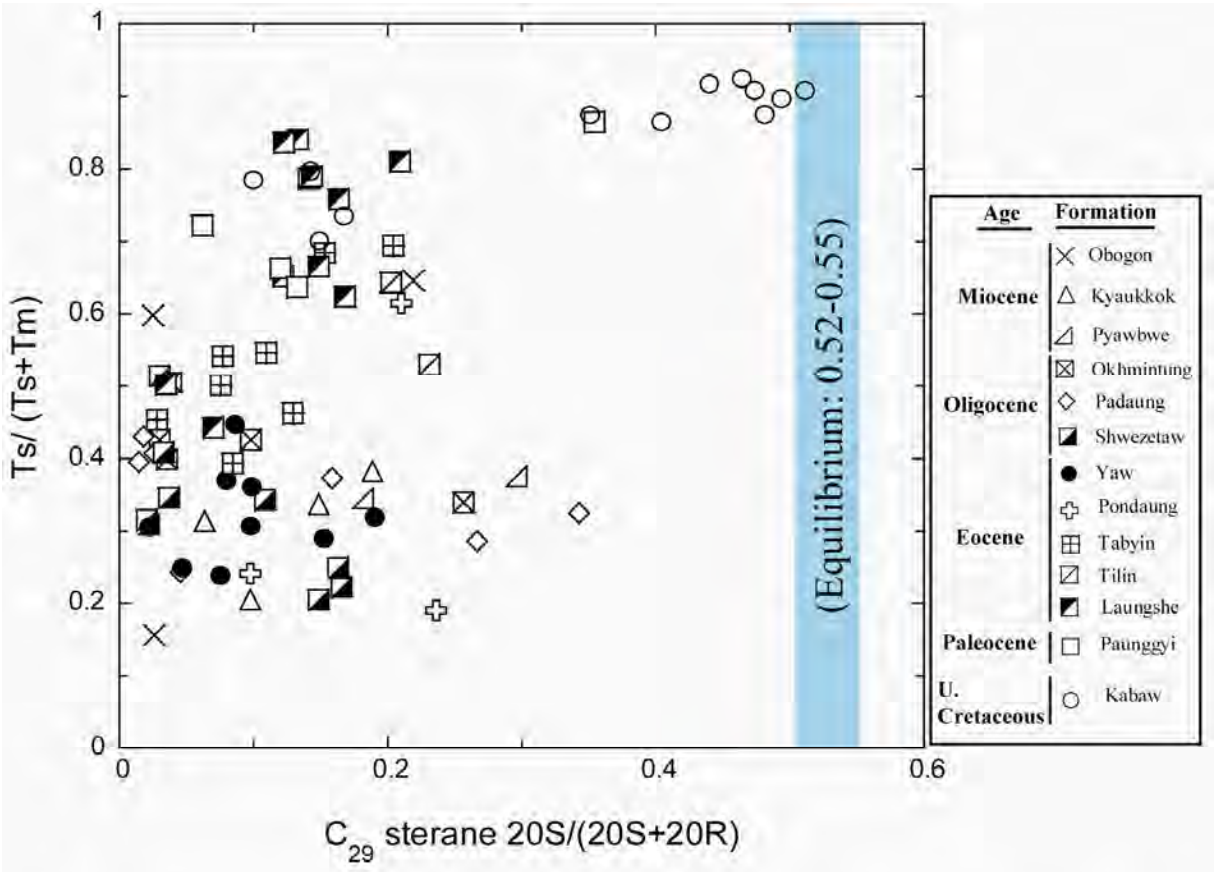

Fig. 5.10. Cross-plot of Ts/ (Ts+Tm) and C29 sterane 20S/(20S+20R) ratios, illustrating maturity and source of OM for Upper Cretaceous to Miocene mudstones from CMB. Upper Cretaceous mudstone samples approach to equilibrium, showing early mature stage.

The cross-plot of Ts/ (Ts+Tm) and C_{29} sterane 20S/(20S+20R) ratios illustrates maturity and source of OM (Fig. 5.10). The 20S/(20S+20R) ratios in the upper Cretaceous mudstones have approached to equilibrium (0.52 – 0.55; Seifert and Moldowan, 1986) and the Ts/ (Ts+Tm) values close to 1 indicate it has reached to the oil threshold window (Peters and Moldowan, 1993).

The moretane/C_{30} hopane ratios ranging from 0.21 to 3.35 in the Paleocene to Miocene succession can suggest an immature level, but these values in the late Cretaceous (0.10–0.51) may show very early mature stage because these ratios range from 0.8 in immature source rocks to 0.15 in mature source rocks (Peters and Moldowan, 1993).

The phenanthrene and alkylphenanthrene have been commonly known due to their different distributions with increasing maturity (Radke et al., 1982a; Radke and Welte, 1983; Sampei et al., 1994; Budzinski et al., 1995). The MP isomers 2-MP and 3-MP (β isomers) are thermodynamically more stable than 1-MP and 9-MP (α isomers) (Killop and Killop, 2005; Szczerba et al., 2010). Similarly, 1-MP and 9-MP isomers are significance in the immature sediments (Radke et al., 1982a).

The dominant distributions of 9-MP and 1-MP in the Eocene and Pegu group can indicate thermally low maturity, while in the late Cretaceous with dominant distribution of 2-MP and 3-MP isomers may reflect very early mature stage because 2MP and 3MP are more predominant when maturity increases (Killop and Killop, 2005). Similarly, the predominance of 9- and 1-MP over 2- and 3-MP isomers in the Eocene and Pegu group may exhibit immature organic matter, whereas upper Cretaceous samples containing decreased distribution of these isomers ratios may indicate very early mature stage (e.g Szczerba et al., 2010). In addition, the MPI 3 values in the studied samples are mostly ca. 1, indicating low maturity to very early mature stage (Radke, 1987).

5.1.2.4 Paleovegetation, Paleoclimate, and Paleowildfires

Biomarkers have been known as useful indicators for reconstruction of paleovegetation and past climatic assessment (Ficken et al., 1998; Nott et al., 2000; Hautevelle et al., 2006; Zheng et al., 2007).

The abundant contributions of angiosperms in tropical region thoughout the Tertiary have been reported (Lidgard and Crane, 1988). The presence of oleanane could exhibit high abundances of inland plant OM (Phlip and Gilbert, 1986) and it has been known as a marker of the angiosperms (Rullkötter et al., 1994). Murray et al (1994) reported the presence of oleanane in the fluvio-deltaic and Tertiary-age marine samples from Southeast Asia.

The oleanane/C_{30} hopane values are relatively low to high (0.02–0.60) throughout the studied succession, suggesting a widespread occurrence of angiosperms vegetation forests. The concentrations of oleanane derived from angiosperms are more predominant in the late Cretaceous to Paleocene, Eocene (Laungshe, Tabyin and Yaw Fm.), and Pegu Group (Shwezetaw, Padaung, Kyaukkok, and Obogon Fm.), showing abundant contributions of angiosperm vegatations.

Relatively higher contents of retene (i.e gymnosperms) in the Paleocene, middle Eocene and Pegu Group (Shwezetaw, Padaung, Okhmintaung) mudstones, indicating the widespread dissemination of resinous higher plants (i.e gymnosperms) because retene derived from aromatic diterpenoids has been identified as a typical biomarker of higher land plants originated from resinous conifers, mostly gymnosperms (Noble et al., 1986; Simoneit et al., 1986; Otto et al., 1997; Otto and Simoneit, 2001; Otto et al., 2003).

Similarly, upper Cretaceous, early and upper Eocene, and Pegu Group (Pyawbwe, Kyaukkok, Obogon) have lesser amounts of retene abundances, suggesting small contributions of resinous higher land plants at that time. Less concentrations of pimathrene (1,7 Dimethyl phenanthrene) in the upper Cretaceous, Eocene (Laungshe, Tabyin, Pondaung, Yaw), and

lower - middle Oligocene (Shwezetaw) mudstones can show a contribution of gymnosperm vegetations. This compound is below detection limits in other mudstone samples.

The occurrence of fungi-originated perylene formation in wet condition has been established (Grice et al., 2009; Suzuki et al., 2010). Less contents of perylene in the upper Cretaceous to Paleocene and middle Eocene (Tilin Fm.) may suggest dry (warm) climate. Low and high distributions of fungi-derived perylene in the mudstones of middle to upper Eocene and the Pegu Group can be speculated that the climatic condition became warmer and/or hot and wet (humid/seasonal) conditions. This association can be agreement with the abundances of retene (i.e. gymnosperms) because wet condition can be favourable to induce the widespread growth of resinous conifer trees and rain forests, although retene abundances are independent on climate changes.

High molecular weight *n*-alkanes (C_{31}) are significant in the mudstones of the Paleocene, Eocene (Laungshe, Tilin, Tabyin, Yaw), and Pegu Group (Shwezetaw, Padaung, Pyawbwe, and Obogon) mudstones, suggesting that it may exhibit warm climate (e.g. Simoneit et al., 1991). However, upper Cretaceous to Miocene succession would be characterized by mainly inputs of angiosperms with lesser amounts of gymnosperms dominated vegetations with alternating changes of climates. Especially, Paleocene, middle Eocene (Tabyin Fm.), and Oligocene mudstones might be influenced by both gymnosperm and angiosperm dominated paleo-vegetations. D`Arrigo, et al. (2011) mentioned that climate has been associated with the monsoon rainfall during three centuries of Myanmar because the growth of teak increased with rainfall.

The non-alkylated PAHs such as Fla, Py, BaAn, Bflas, BePy, BaPy, InPy, BghiP, and Cor have been commonly known to be generated from incomplete combustion process (Prahl and Carpenter, 1983; Grice et al., 2007; Yunker et al., 2002, 2011a). Furthermore, Fla, Py, BaAn, Bflas, BePy, BaPy, InPy, BghiP and Cor are commonly useful to indicate primarily of

combustion origin (Youngblood and Blumer, 1975; Hites et al., 1977; Laflamme and Hites, 1978; Wakeham et al., 1980a; Prahl and Carpenter, 1983; Killops and Massoud, 1992; Bence et al., 1996; Jiang et al., 1998; Grimalt et al., 2004; Grice et al., 2007; Yunker et al., 2002, 2011a). Yunker et al. (2002) mentioned that Fla, Py, BaAn, InPy and BghiP are often affected by catagenetic changes of the same PAHs from petroleum and matured kerogen.

3- to 5 rings combustion-derived PAHs such as Fla, Py, Chry and BePy are dominant in the upper Cretaceous, early Eocene, upper Eocene (Pondaung Fm.), and Pegu Group (Shwezetaw Fm.), indicating wildfires frequently occurred. Bflas, BePy and Cor are least degraded during transportation, alteration and biodegradation (Prahl and Carpenter, 1983; Jiang et al., 1998), whileas BaAn and BaPy are more easily degraded during those processes (Sicre et al., 1987; Yunker et al., 2002, 2011a, b; Stout and Emsbo-Mattingly, 2008). According to Yunker et al. (2002, 2011a), low abundances of BaAn and BaPy can be considered that could be soluble or biodegradable in an oxic water, or prolonged exposure in an oxic environmental condition. High temperature wildfire markers such as BghiP, InPy, and Cor (Finkelstein et al., 2005; Denis et al., 2012; Hossain et al., 2013) are enrichment in the upper Cretaceous to lower Eocene, suggesting that the intensity of wildfires would be high. These markers are slightly decreased in the middle to upper Eocene and Pegu Group mudstones, indicating that huge wildfires occasionally occurred with a dry season but sometimes small under wet condition because humid climate marker pery contents was increased at that time. Low contents of BaAn and BaPy in the upper Cretaceous to Eocene samples reflect strong oxidation/weathering in the air and on land before deposition and/or in oxic water within the basin.

Pery reflects a negative correlation with normal wildfire indicators (Fla and Py) and high temperature wildfires such as BghiP, InPy, and Cor in all mudstones (Fig. 5.11). This association can indicate that all wildfires were decreased with increasing in wet condition

throughout the studied succession as wet climate could be favourable to decrease frequency of the wildfires. Two- and three dimentional schematic diagrams (Fig. 5.12 a & b) indicate the relationships between paleovegetations and paleoclimates throughout the upper Cretaceous to Miocene succession in the CMB.

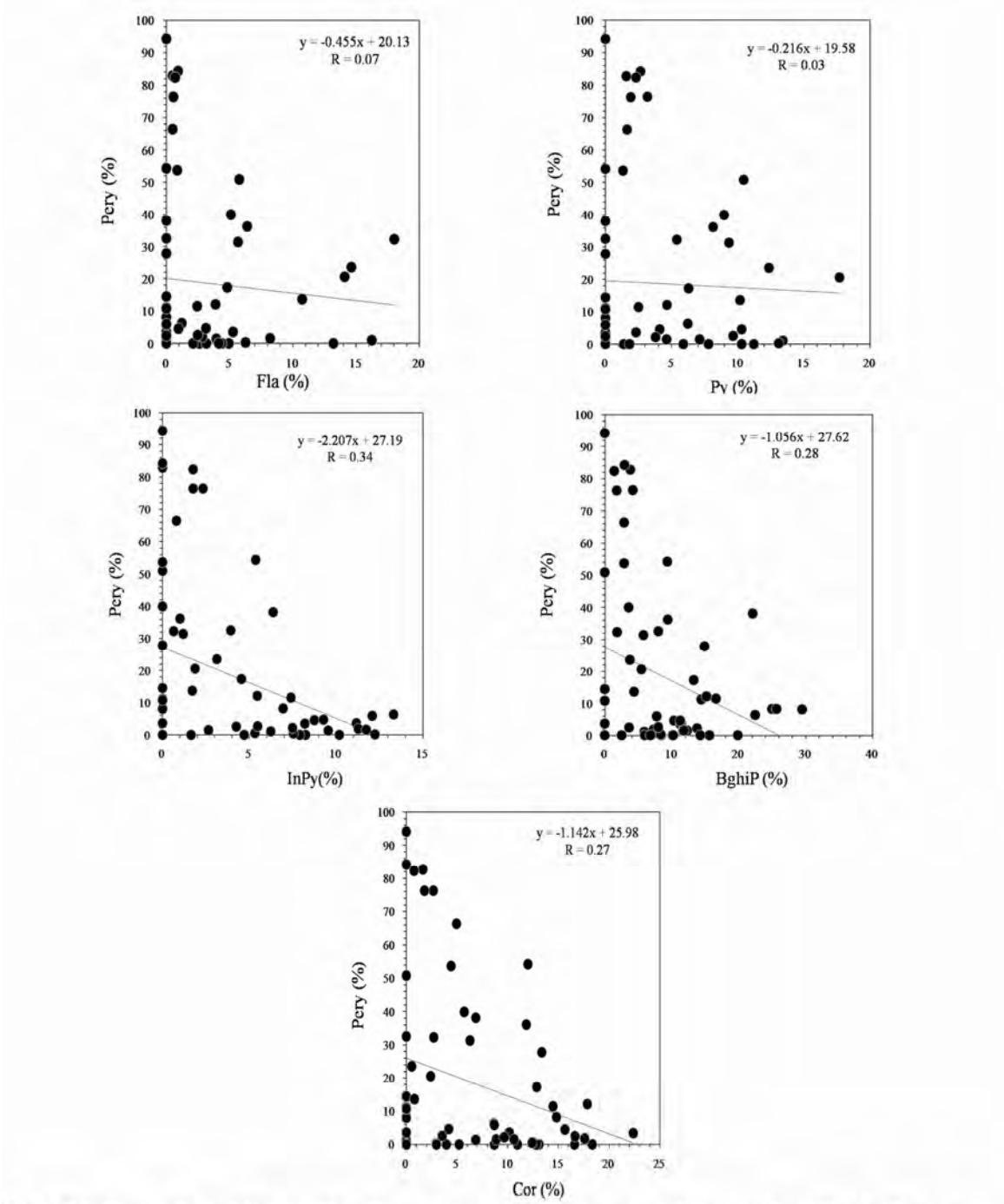

Fig. 5.11. Cross-plot of the humid indicator perylene (Pery) against the normal wildfire indicators (Fla, Py) and high temperaturemarkers (InPy, BghiP, Cor) for Late Cretaceous to Miocene mudstones from CMB.

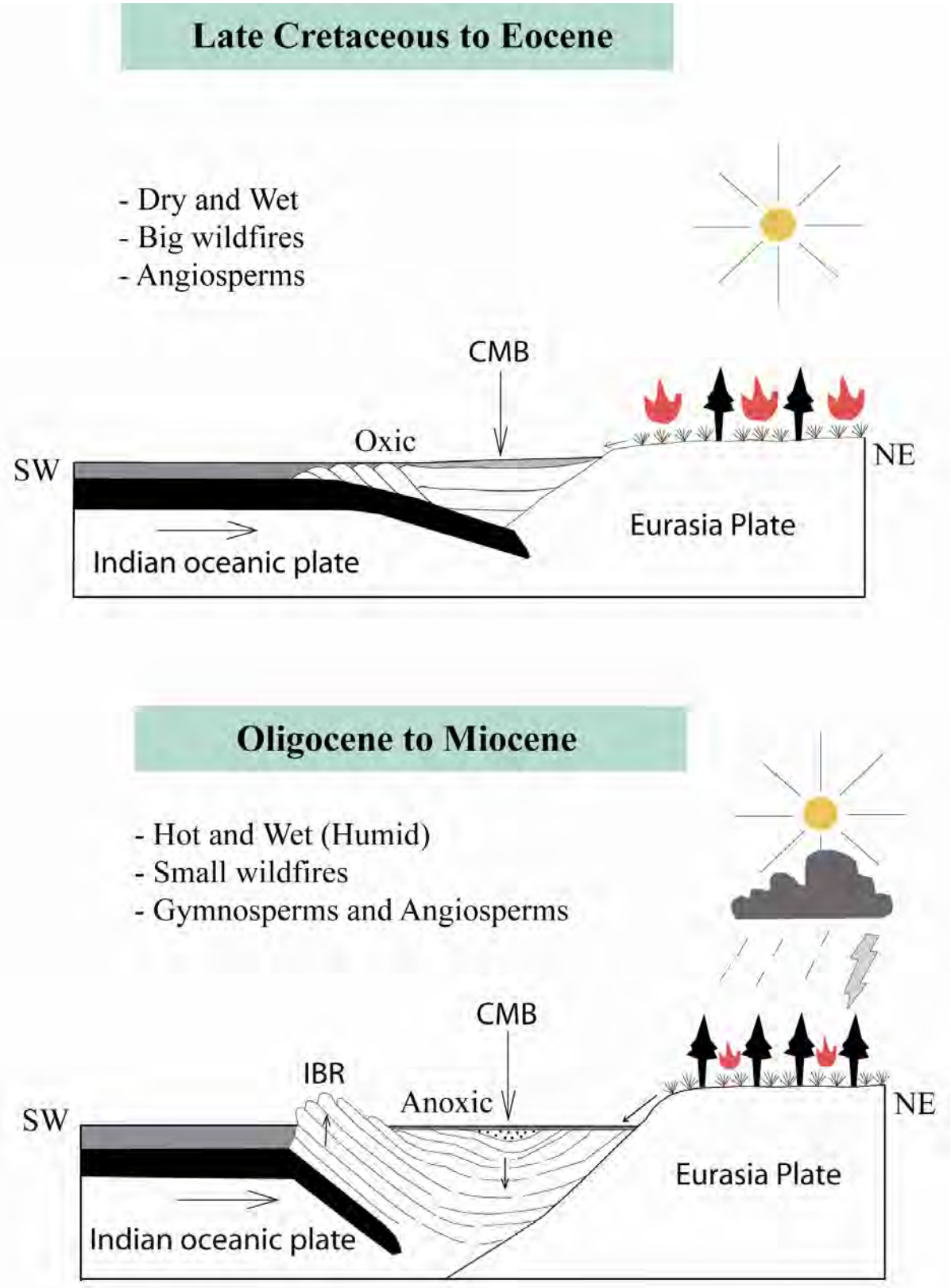

Fig. 5.12a. Two-dimentional schematic diagrams show the relationship between paleovegetation and paleoclimate throughout the Upper Cretaceous to Miocene succession in the CMB.

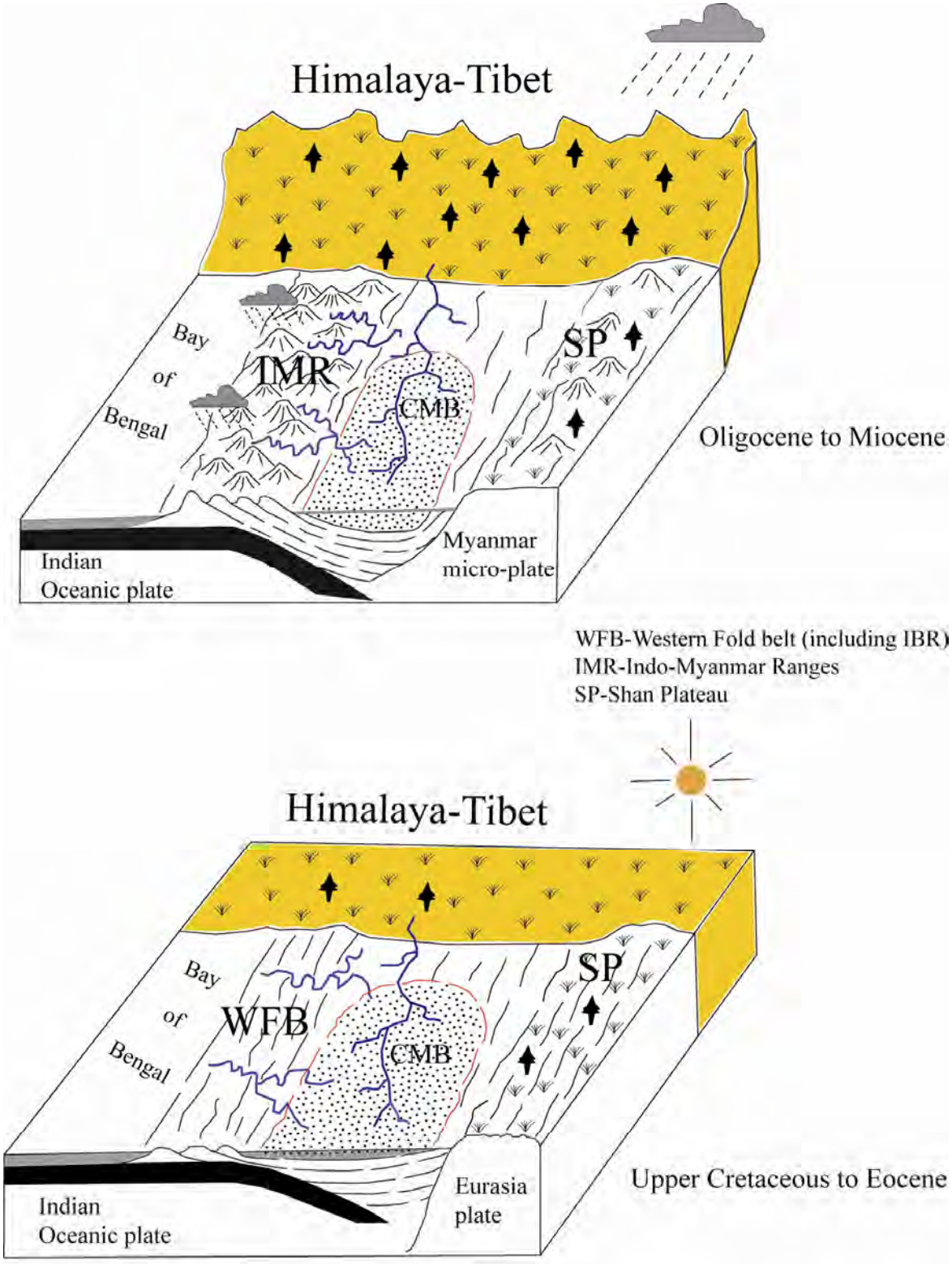

Fig. 5.12 b. Three-dimentional schematic diagrams show the relationship between paleovegetation and paleoclimate throughout the Upper Cretaceous to Miocene succession in the CMB.

5.2 Inorganic Geochemistry compositions

5.2.1 Mudstones and sandstones (Upper Cretaceous to Miocene)

5.2.1.1 Source Area Weathering and Paleoclimate

The Chemical Index of Alternation (CIA; Nesbitt and Young, 1984) and Plagioclase Index of Alteration (PIA) (PIA; Fedo et al., 1995) have been useful parameters to determine the intensity of source weathering for sedimentary rocks (Fig. 5.13). These indices are calculated based on relative molecular proportions using the following equations:

$$CIA= [Al_2O_3/(Al_2O_3+ CaO^*+ Na2O+ K_2O] \times 100$$

$$PIA= [(Al_2O_3- K2O)/(Al_2O_3+ CaO^*+ Na_2O] \times 100$$

In the above equations, CaO* represents the CaO content in the silicate fraction. Mudstones with high CaO contents (>4 wt%) were not used in this study as contamination of carbonate contents can be misleading in determining the source of CIA values. The CIA parameter examines the progressive conversion of plagioclase and potassium feldspars to clay minerals. Also, CIA has also been used to identify the reconstruction of past climatic conditions (Nesbitt and Young, 1982, 1984).

The intensity of chemical weathering has been categorized into incipient (CIA- 50-60), intermediate (CIA- 60-80), and intense (CIA >80) chemical weathering processes (Fedo et al., 1995). According to Nesbitt and Young (1982, 1984), fresh shales (e.g. PAAS) have averagely values varying from 70-75, whereas intensely weathered rocks and soils have values closer to 100, due to formation of aluminous phases such as kaolinite and gibbsite, and the loss of Na, Ca and K in solution..

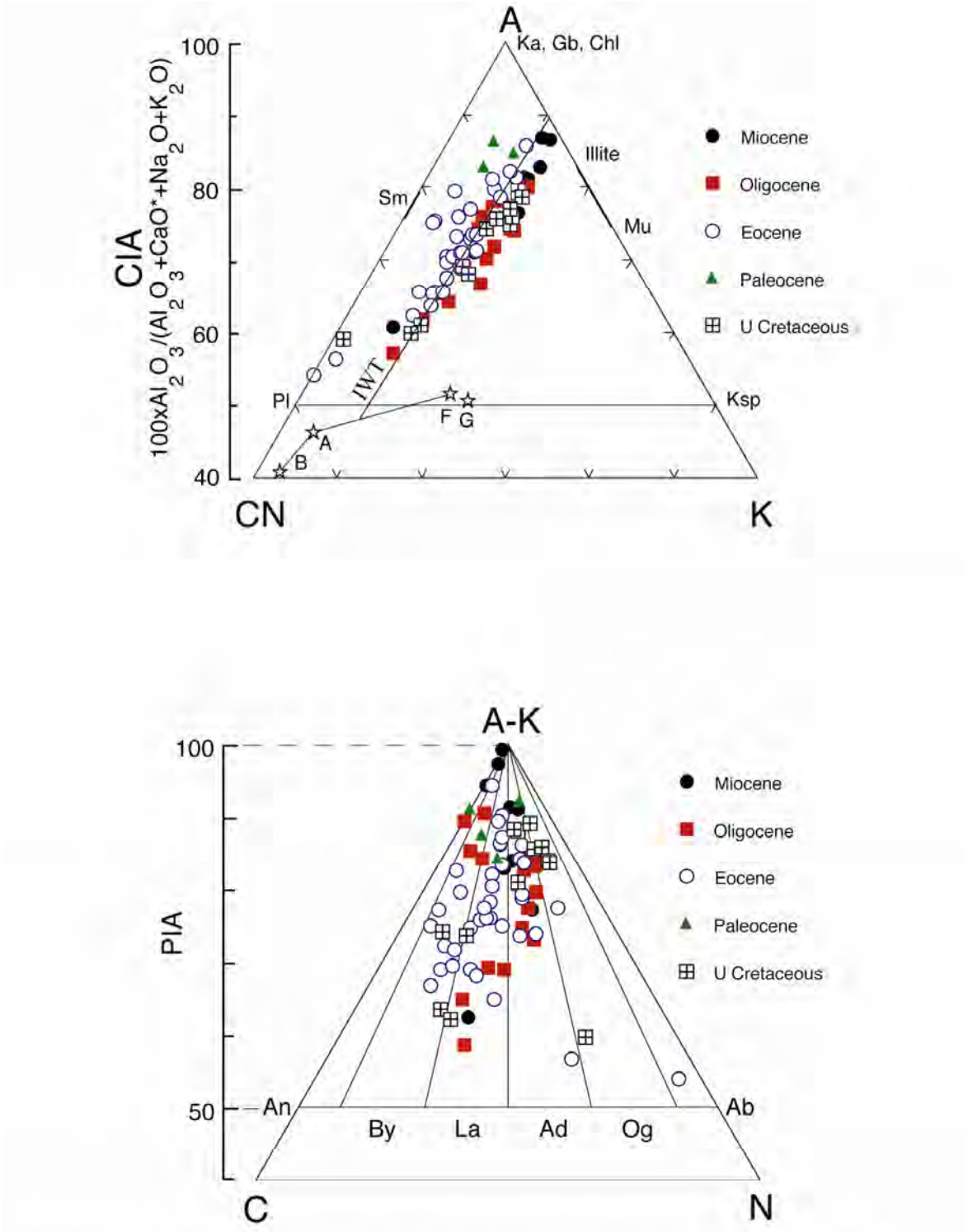

Fig. 5.13. (a) A-CN-K plot and (b) (A-K)-C-N plot for mudstones and sandstones from Central Myanmar Basin. A= Al_2O_3, CN= CaO+Na_2O, K= K_2O, N= Na_2O, Ka= kaolinite, Gb= Gibbsite, Chl= Chlorite, Mu= Muscovite, Pl= Plagioclase, Ksp= K- feldspar, Sm= smectite, B= basalt, A= andesite, F= felsic volcanic, G= granite (Condis, 1993); UCC= upper continental crust composition (Taylor and McLennan, 1985); IWT= ideal weathering trend; An= Anorthite, By= Bytownite, La= Labradorite, Ad= Andesine, Og= Oligocene, Ab= Albite.

The Chemical Index of Alteration (CIA) values in the CMB mudstones are relatively high, varying from 61 – 79 (mean: 71.4) in the upper Cretaceous; 75 – 86 (mean: 82.1) in the Paleocene; 54 – 86 (mean: 71.7) in the Eocene; 57 – 87 (mean: 73.7) in the Pegu Group (Table 4.9). Average CIA values are high in the Paleocene and Miocene mudstones (82% and 78%).

Average CIA values are relatively moderate to high in the mudstones from the upper Cretaceous (mean CIA = 71), Eocene (CIA 68-77), and Oligocene (CIA 68-76), implying intermediate (moderate) chemical weathering in the source region. Paleocene and Miocene mudstones have higher CIA values of ~82, indicating intense source weathering. Eroded materials from the northern Naga Hills, central Chin Hills, and southern Rakhine mountains along the Arakan Yoma in the north and NW northwest, and also continental materials from the northeast, were transported by river systems, rain falls and then and deposited throughout the Inner-Myanmar Tertiary Basin, including the Central Myanmar Basin. The development of uplifteding areas along the Burmese margins after the Miocene (Bender, 1983) could be responsible for change to occur tropical climate changes. High CIA values showing severe source weathering in the Miocene mudstones could be due to climate effects. In addition, these higher values at this time can be in aggrement with the report of Clift and Plumb (2008) that the evolution of East Asia Monsoon began at 23 Ma.

Similarly, chemical weathering has been associated with the past climate: high chemical weathering can reflect warm and humid climatic condition, and low chemical weathering cool and dry climates (Nesbitt and Young, 1982; Nesbitt et al., 1996). Nevertheless, CIA values can also be affected by grain size (CIA ratios of sandstones are typically lower in companion mudrocks), and by uplift.

Nesbitt et al. (1996) noted the effect of tectonism on CIA, in which steady-state weathering (uplift equal to or less than weathering rate) produces mudstones with uniform

CIA. In contrast, active tectonism during nonsteady-state weathering (uplift and erosion > weathering rate) produces sediments with varying CIA. This and other features can be illustrated on a ternary A–CN–K plot (Fig. 4.19). The CMB sediments form a linear trend running from a primary source line defined from igneous rock averages, suggesting nonsteady-state weathering, as could be expected for sediments deposited in a forearc pull-apart basin within the Myanmar arc system. However, there is a gap between the primary source line and the last weathered samples, suggesting that all detritus supplied to the basin was relatively weathered. The high maximum CIA ratios in almost all age ranges further suggest that weathering was relatively intense throughout, although CIA ratios are highest in the small number of Paleocene samples analyzed, and the Miocene, implying most intense weathering at these times.

The general trend of the CMB data on the A-CN-K plot runs parallel to the A–CN edge, and originates from a position between average andesite and felsic volcanic rock (Fig. 5.13). This suggests general lack of K-metasomatism in the sediments (Fedo et al., 1995), despite their thickness, and a geochemically intermediate source compatible with arc origin. There are, however, some slight differences in trend with age, with Eocene samples lying at the left (more mafic) side of the distribution, and Oligocene and Miocene samples to the right (more felsic). This also points to some change in source within the succession.

PIA values also reflect weathering in the source, and indicate the extent to which plagioclase, the more reactive of the feldspars, has been destroyed during weathering and/or transport and alluvial storage. High values of PIA in the mudstones of the upper Cretaceous (62-88; average 79.5), Paleocene (84-92; average 88.5), and Miocene (17-98; average 80.0), indicating indicate near-total destruction of plagioclase in these intervals (Fig. 5.13).

Climatic conditions may also be identified based on a new cross-plot of Ga/Rb vs. K_2O/Al_2O_3 (Roy et al., 2013) (Fig. 5.14). Relatively high Ga/Rb ratios combined with low

K_2O/Al_2O_3 ratios suggest dry (hot) to wet (humid/seasonal) conditions were maintained throughout the Central Myanmar succession. This is compatible with the generally high maximum CIA and PIA ratios observed.

Moderate source weathering in the upper Cretaceous, Eocene, and Oligocene mudstones may exhibit dry (warm) and wet (humid/seasonal) climatic conditions. Very severe chemical weathering in the Paleocene and middle to late Miocene mudstones (CIA- av. 82) can indicate hot and wet (humid/seasonal) climates (e.g. Nesbitt and Young, 1982). There were no significant mountains in the hinterland during the upper Cretaceous, because the Shan Plateau in the east and Arakan Yoma in the west, were elevated as a swelling at that time (Chhibber, 1934). This association may indicate that it might be under arid/semi-arid climate.

This condition may be in agreement with the lesser abundances of humid-indicator perylene. The topographic relief associated with the tectonic activities could be responsible for the initiation the of climatice changes with the influence of monsoon winds during the Oligocene-Miocene. It is consistent with the abundant contents of perylene, an indicator of humid conditions, is abundant in this part of the succession, indicating humid condition, supporting such a change in climate.

Generally, weathering process can be identified based on cross-plot of Ga/Rb vs. K_2O/Al_2O_3 (Roy et al., 2013) (Fig. 5.14). It reflects dry (hot) to wet (humid/seasonal) throughout the Central Myanmar Myanmar succession.

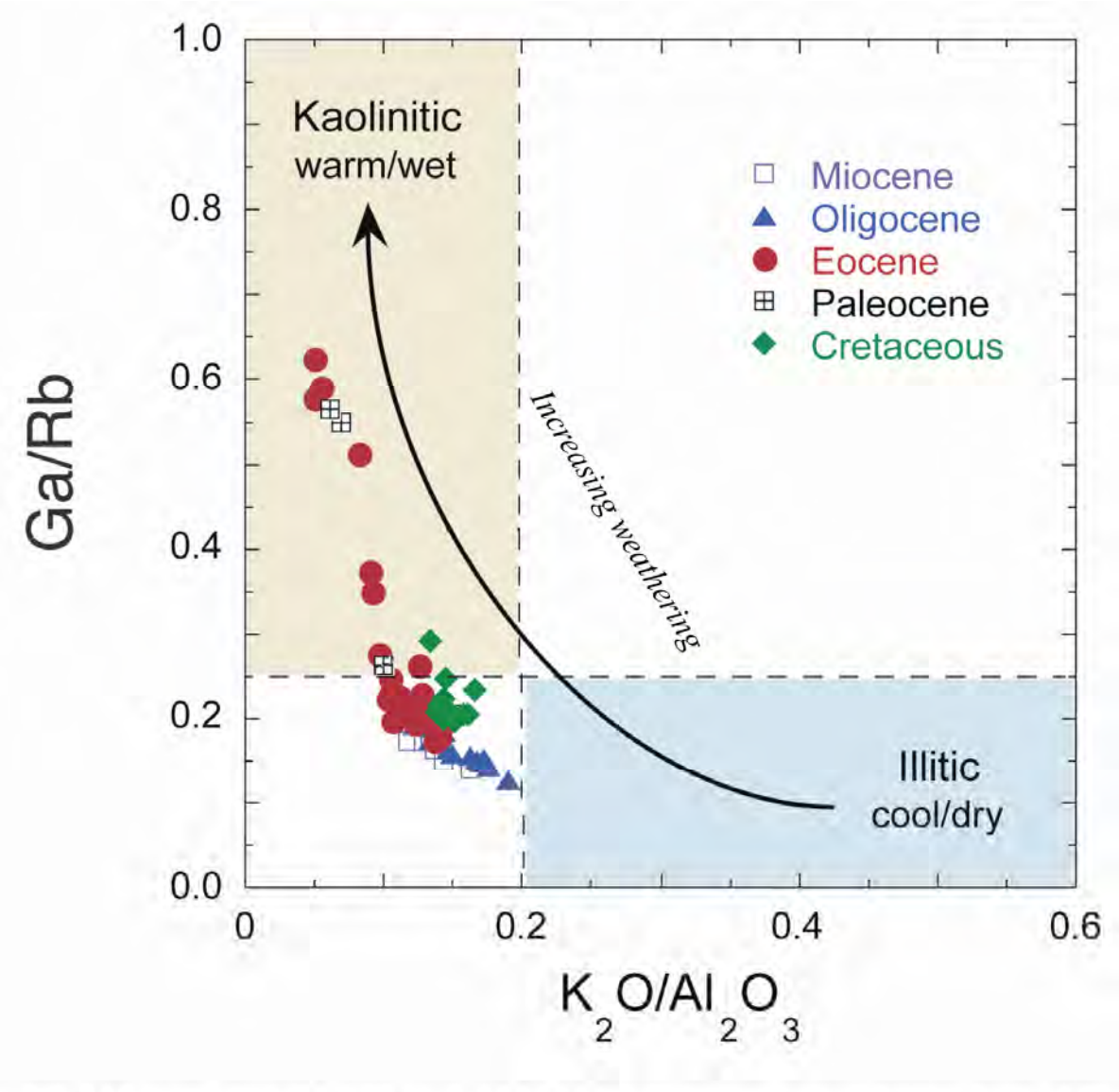

Fig. 5.14. Cross-plot of Ga/Rb vs. K_2O/Al_2O_3 for mudstones and sandstones from CMB.

5.2.1.2 Geochemical Provenance Signatures

We determined the Provenance signatures were determined using both major elements, and trace elements and the rare earth element (REE) data. According to Roser and Korsch (1988), there are four provenances, namely mafic (P1), intermediate (P2), felsic (P3), and quartzose recycled (P4) can be identified from major element compositions, suing a set of established discriminant functions.

Upper Cretaceous, Paleocene, and Eocene mudstones fall in the P1 (mafic) field and some are close to the P1-P4 boundary (Fig. 5.15). Most mudstones of the Pegu Group (Oligocene and Miocene) lie in the P4 (quartzose recycled). These classifications are anomalous with respect to the indication from the A–CN–K plot (Fig. 5.13) of an intermediate source, and a P2 classification should be expected. However, the classification of the mudstones as Fe-mudstones (Fig. 4.17) indicates unusual enrichment in Fe, which would lower F2 scores and hence produce a P1 classification. The origin of this Fe enrichment is unknown, but contribution of Fe-rich clays from weathered ophiolites in the source is a possibility, as signaled by the anomalous Cr and Ni contents of the Eocene rocks. This component would not be detectable on the A–CN–K plot.

Ratios of compatible and incompatible elements have been known to be useful indicators to distinguish felsic and mafic sources of sedimentary rocks (Wronkiewicz and Condie, 1987; McLennan et al., 1993; Cox et al., 19955).

A cross-plot of Th/Sc-Zr/Sc reflects that upper Cretaceous, Paleocene, and Eocene mudstones lie between average dacite (DAC) and UCC, whereas Pegu Group mudstones are close to UCC and fall between UCC and average rhyolite (RHY) (Fig. 5.16).

The upper Cretaceous to Eocene deposits were mostly generated from mafic too intermediate sources , based on Th/Sc ratios of less than 1, and Zr/Sc ratios which are typical of primary sources rocks (Fig. 5.16) and the The Pegu Group mudstones (Oligocene-Miocene) have consistently high Th/Sc ratios, and hence were derived from a more felsic source, with the possibility of contributions are from recycled materials. Ratio of Th/Sc less than 1 in the upper Cretaceous to Eocene mudstones and sandstones can suggest a mafic source.

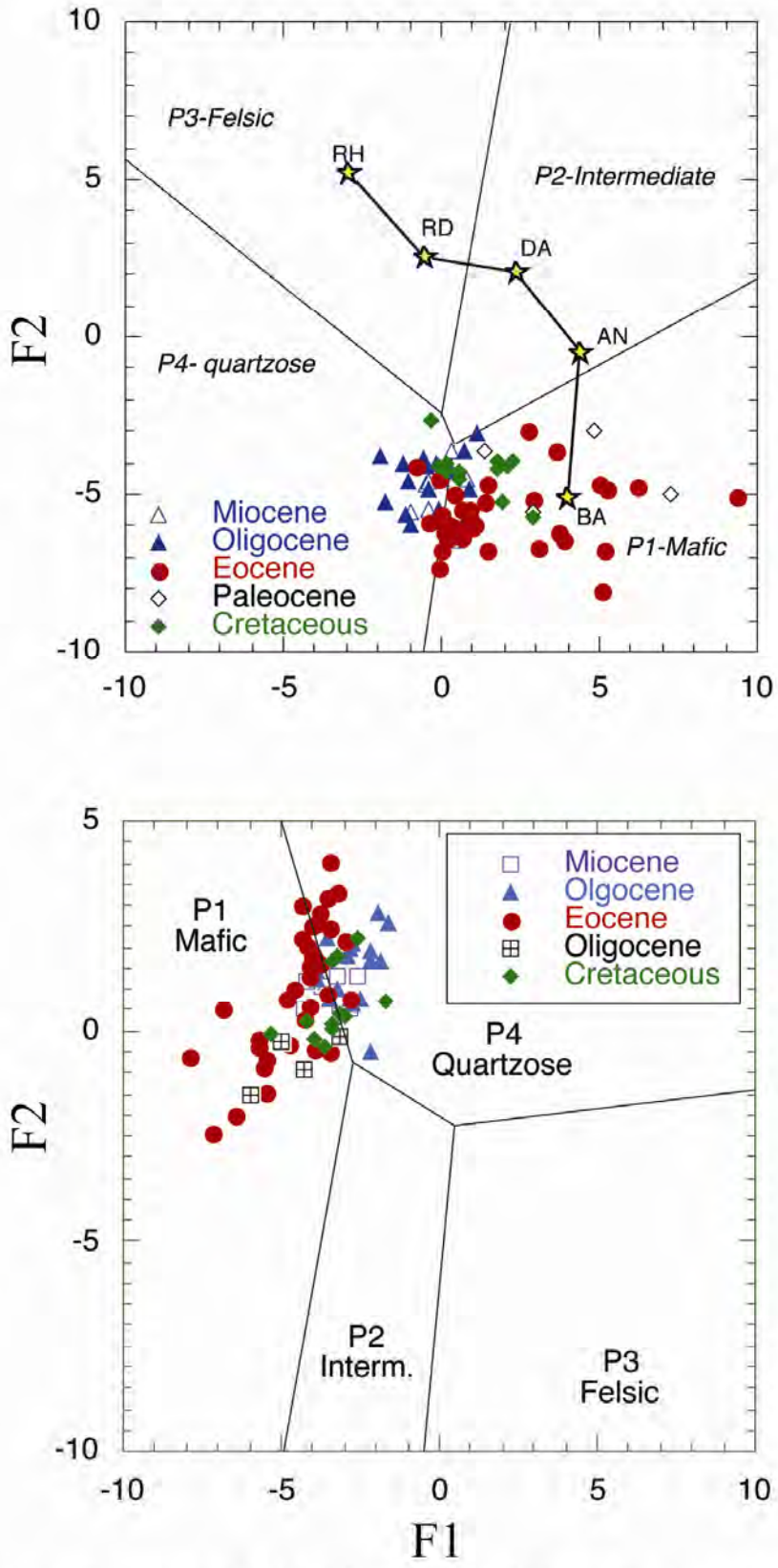

Fig. 5.15. Showing prvenance for Late Cretaceous to Miocene mudstones and sandstones from CMB. BA- basalt, AN- andesite, DA- dacite, RD- rhyodacite, RH- rhyolite. (Roser and Korsch, 1988)

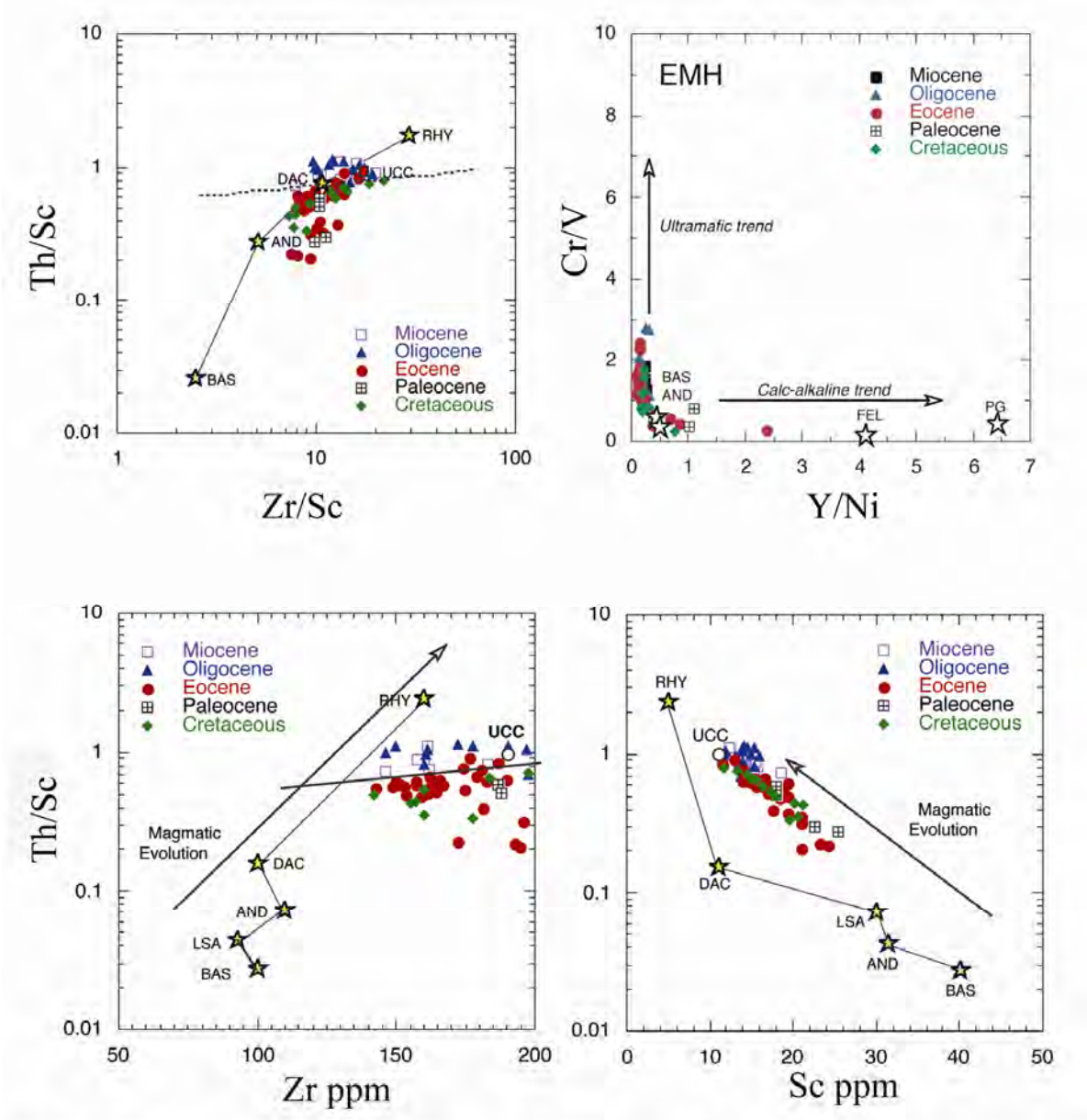

Fig. 5.16. Plots of Th/Sc vs. Zr/Sc, Th/Sc vs. Zr ppm, and Th/Sc vs. Sc ppm, showing mafic and felsic contributions for Late Cretaceous to Miocene from CMB. (McLennan et al., 1993)

Mafic to intermediate materials were most likely derived from the Myanmar (Burmese) magmatic arc. However, the Myanmar margins pull-apart basins have have been filled with continental materials, volcanic and magmatic rocks from the continents in the northern parts

(Bender, 1983; Mitchell, 1993; Mitchell, 2012), and this source could have provided felsic material to the uppermost part of the succession.

Th/Sc versus Zr/Sc (Mclennan et al., 1993) relationships can indicate provenance and these ratios increase during magmatic evolution.

Presence of an ultramafic component is also indicated by a Y/Ni-Cr/V plot (Fig. 5.16), on which the CMB sediments trend vertically, with Cr/V ratios of up to 3, at Y/Ni of <1. Arc sediments normally trend horizontally at Cr/V <1, as shown by the igneous rock averages. Addition of Cr- and Ni-bearing phases from obducted ophiolites that occur within the Myanmar magmatic arc could thus have increased Cr/V and lowered Y/Ni ratio in the samples analyzed here.

Cross-plots of Th/Sc-Zr/Sc, Th/Sc-Zr ppm, Th/Sc-Sc ppm reflect that late Cretaceous, Paleocene, and Eocene mudstones lie between average dacite (DAC) and UCC, whereas Pegu Group mudstones are close to UCC and fall between UCC and average rhyolite (RHY) (Fig. 5.16).

5.2.1.3 Tectonic Setting

Tectonic setting of the Central Myanmar Basin (CMB) succession was classified based on major elements compositions. An SiO_2- K_2O/Na_2O diagram (Roser and Korsch, 1986) illustrated the tectonic settings for the CMB succession (Fig. 5.17).

Late Cretaceous and Paleocene mudstones fall between the active continental margin (ACM) - passive margin (PM) boundaries, whereas Eocene sediments lie mainly in the ACM and partly in the PM field. Oligocene and Miocene mudstones lie mainly in the PM and partly in the ACM. Although this suggests ACM setting, a less-developed ARC setting cannot be excluded based on these data. In the original definition of this plot by Roser and Korsch (1986), it was noted that ARC mudstones trended towards and plotted within the ACM field,

whereas ARC sandstones defined the ARC field. This pattern has also been identified in the continental island arc Murihiku terrane of New Zealand (Roser et al., 2002). These authors also noted that continuous transition between CIA and ACM settings must be expected. The paucity of sandstones in this present study means clear distinction between ARC and ACM cannot be made. Clearly, however, the CMB sediments were mainly derived from a subductive margin.

High CIA values may indicate an influence of tectonism reflecting steady-state weathering and stable tectonism (Nesbitt et al., 1997).

Active tectonic condition can be considered as non-steady state weathering. Moderate to High hhigh CIA values in the mudstones of the Late Cretaceous to Miocene showed that these sediments were generated from non-steady state weathering during active tectonism and partly from steady state weathering.

The CIA and PIA values are high in the Late Cretaceous and Paleocene mudstones, can be possibly suggesting that it would could be mainly sourced from the both tectonically tectonically-stable Eurasia Plate, including the Myanmar (Burma) micro-Plate, and the active continental margin. Those values are moderate in the mudstones of Eocene, and Oligocene mudstones, showing suggesting that it has been the CMB sediments were generated from the tectonically active Myanmar (Burmese) active margin, with inputs of fresh materials from the Myanmar marginsthat source and partly from the Himalaya. These sediments have been eaffected by tropical climate changes after Oligocene time. High values of both indices in the Miocene materials can could be considered that it wasto have been partly sourced from a PM and the Himalaya during active tectonism, and additionally strongly eaffected by tropical climate after the middle Miocene. This is supported by the fact that Myanmar (Burmese) margins in the north and Indo-Myanmar Ranges were obviously emerged after the middle Miocene, and it this could be favourable to occur induce tropical climate changes.

In addition, upper cretaceous Cretaceous to Eocene materials are also partly mainly originated from the Myanmar magmatic arc, as they their composition indicate mafic-intermediate source. This feature can be provided by the proposal of Mitchell et al. (1993), as he suggested that Andean-type granite magmatism widely deposited occurred along the Myanmar margin prior to Indian collision. Southern part of Asia prior to collision comprises calc-alkaline and magmatic rocks related with to subduction of the Indian Oceanic plate.

The Pegu Group (Oligocene and Miocene) mudstones and sandstones were probably generated from both the Myanmar margins and Himalayan detritus. The Pegu Group shows more felsic composition, and Eocene sediments may have had some inputs of recycled materials.

Trace elements can also be used to evaluate tectonic setting. Although designed for sandstones, the The Th-Sc-Zr plot of Bhatia and Crook (1986) clearly shows some contrast in composition between the upper and lower parts of the succession (Fig. 5.18). Almost all the mudstones fall within the continental island arc (CIA) field.

However, the upper Cretaceous to Eocene samples fall in the lower part of the field, whereas the Pegu Group samples are displaced towards active continental compositions. This supports mafic to intermediate CIA arc source in the lower part of the succession, and a more felsic mixed arc-continental source in the upper part.

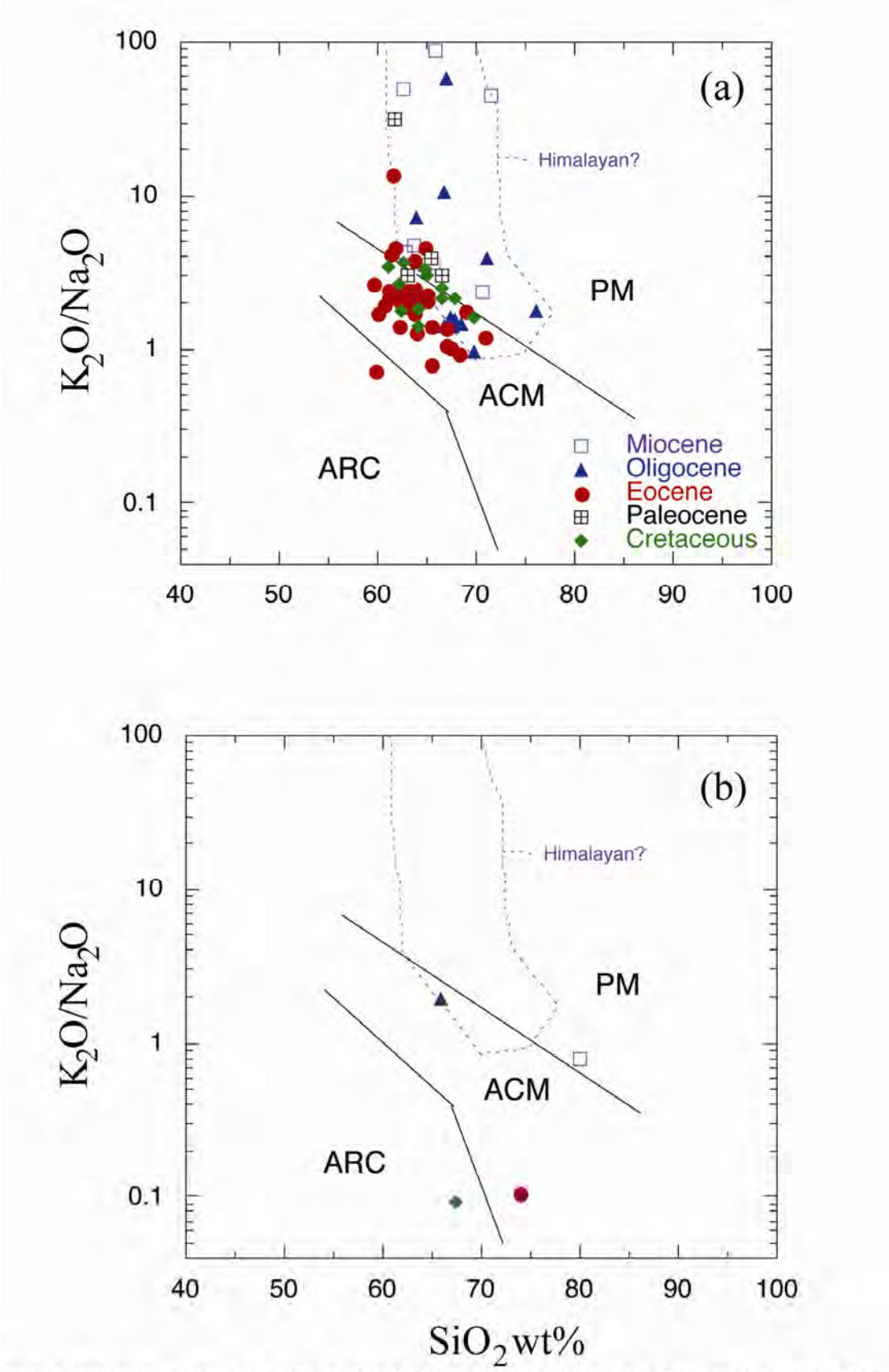

Fig. 5.17. Plots of Si_2O vs. K_2O/Na_2O for (a) mudstones and (b) sandstones of the Late Cretaceous to Miocene succession from CMB. ARC= volcanic island arc; ACM= active continental margin; PM= passive margin.

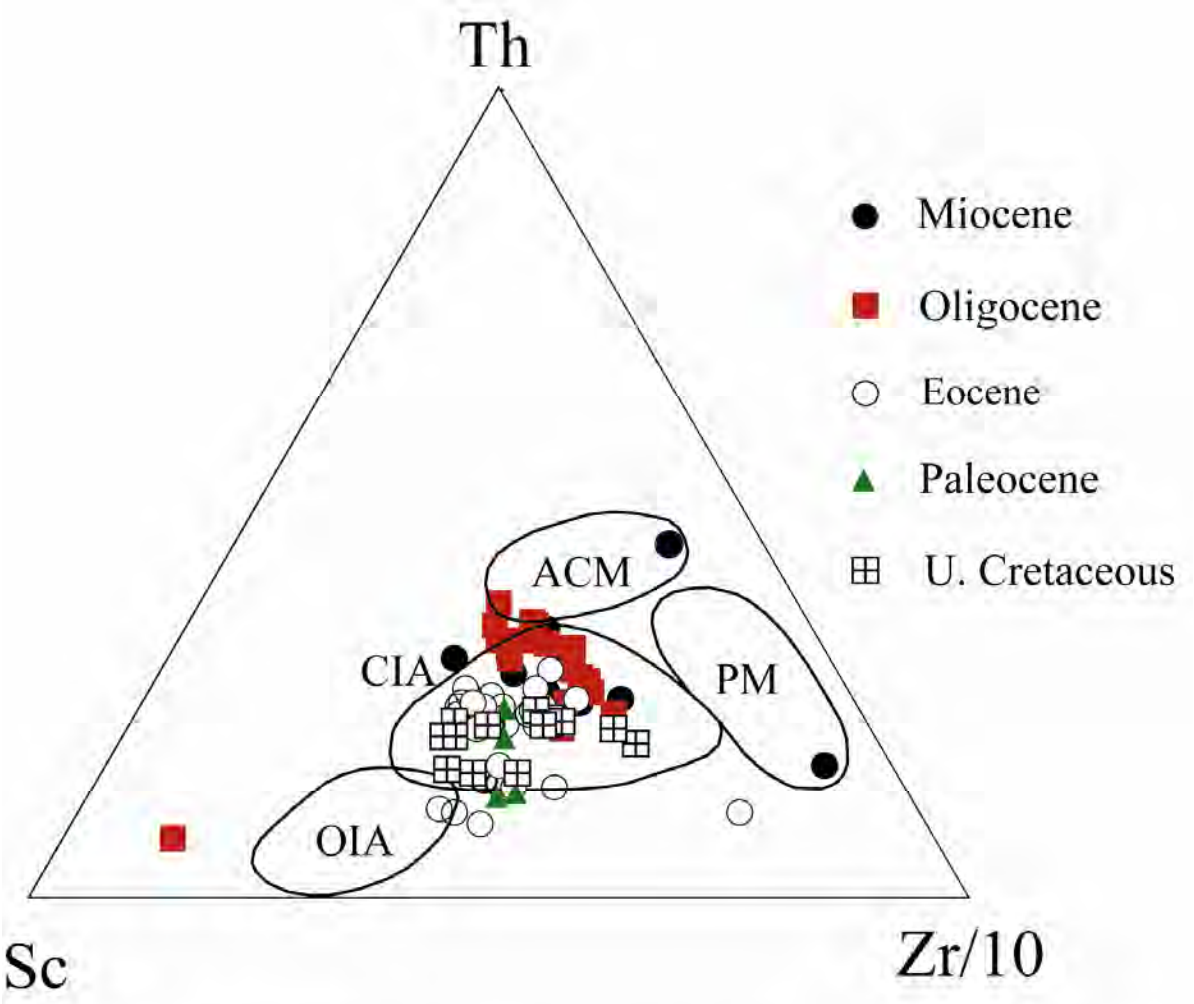

Fig. 5.18. Th-Sc-Zr/10 diagram, illustrating tectonic sttings for mudstones and sandstones from the CMB. OIA= oceanic island arc; CIA= continental island arc; ACM= active continental margin; PM= passive margin.

CHAPTER 6. CONCLUSIONS

6.1 Oigin and the effect of weathering of the upper Eocene coal and coaly shale

Moderate weathering was recognized in Late Eocene coaly shales (A2-54, A2-52A, A1-120), based on microscopic identification of weathering rims, fine cracks, and hole structures in vitrinite. The weathered coaly shale samples are characterized by very low Pr/Ph values (0.23–0.69), high T_{max} values (435–451˚C), low HI values (12–26 mg HC/g TOC), very high OI values (136–212 mg CO_2/g TOC) and decreased long chain *n*-alkanes (>*n*-C_{20}) bonded to kerogens. These results suggest that hydrocarbon generation potential of oil/gas source rocks can be decreased to about one tenth of the original value by moderate weathering.

However, free *n*-alkanes, biomarkers such as steranes and triterpanes, and $\delta^{13}C$ ratios of kerogen were not affected. According to FTIR results, unweathered kerogens yield rather abundant ester groups, suggesting that it may indicate type II kerogen because type III kerogen has no ester groups despite containing abundant acids and ketones. However, it can be considered that upper Eocene fresh coal and coaly shale samples are characterized by a mixture of Type II and Type III kerogens. Hydrocarbon generation potential for these gas-prone coals and coaly shales in the CMB is reasonably good, based on values of almost 200 mg HC/g TOC (HI). The coaly shales contain abundant gymnosperm biomarkers such as retene and pimarane (1,7-DMP).

During peat accumulation in the upper Eocene Pondaung Formation, the source of the OM was mainly derived from terrestrial waxy plant materials with a minor input of bacteria and aquatic plants, and deposited in oxic to oxygen-poor environments in peat swamps associated with the coastal plain, estuarine/fluvial-deltaic setting. The Yaw coal was probably affected by subsequent sea level rise.

$\delta^{13}C$ values of all upper Eocene carbonaceous samples range from -24.6‰ to -26.5‰, suggesting variable contributions of gymnosperm and angiosperm vegetation. High hydrocarbon generation potential in the coaly shales can be attributed to resinous higher plant origin.

Higher perylene abundances in the coaly shales decreasing into the coals suggest a slowly alternating shift of climate from wet (humid/seasonal) to dry (warm) in the western margin of the CMB in the upper Eocene, leading to floral changes. Vitrinite reflectance and biomarker maturity parameters for upper Eocene samples yield thermally immature organic matter.

Results form Rock-eval analysis on kerogens and bitumens (with acid treatment) suggest that the weathered kerogens exhibit low HI (29 – 42 mg HC/g TOC) and high OI (96 –168 mg CO_2/g TOC), whereas those from unweathered kerogen samples have higher HI (86 – 250 mg HC/g TOC) and lower OI (25 – 115 mg CO_2/g TOC), respectively. S_3' (mg CO_2/g rock, released during 400 – 650˚C) is more significant in the weathered kerogens. Lighter *n*-alkanes/alkenes less than *n*-C_{10} and methyl/dimethyl phenols in py-GC-MS results are relatively decreased in the weathered kerogens. FT-IR analysis indicate that the weathered kerogens have a decreased peak of C-H methylene group and relatively constant (or somewhat increased) C=O (1716 cm^{-1}) and/or C-O (1000-1300 cm^{-1}) peaks from esters or ether groups.

These results suggest that C-C methylene structures in the weathered kerogens have been cleaved and the alkyl chain moieties in the kerogen might be considerably reduced by weathering. Oxygen-containing moieties such as methyl/dimethyl phenolics in kerogen are also decreased by the weathering. In general, the oxygen-containing moiety in geomacromolecule is thought to be easily decomposed during oxidation and oxic biodegradation except peculiar cases as reported by e.g. Jenisch-Anton et al. (1999) and Guo and Bustin (1998). The oxygen-containing group in organic matter is commonly thought to be

labile and difficult to be preserved, although such organic oxygen in geomacromolecule has been poorly understood. The results of present study could indicate that rapid decomposition of alkyl chain moieties in kerogen by weathering faster than that of organic oxygen group had caused an increase in OI because OI is a relative value based on oxygen-containing compounds in kerogen.

6.2 Reconstruction of watershed environment influenced by collision of the Indian Plate

The western margin of the Central Myanmar succession contain low to moderate TOC contents (0.11 to 0.92%), with the exception of two carbonaceous mudstone in Padaung and Shwezetaw Formations (1.65% and 8.09%). Less preservation of OM (<0.5%) throughout the studied succession may be due to highly dilution of OM by largely inputs of inorganic materials/ organic-poor fluvial deposits. Furthermore, if sedimentation was under continental margins, the OM might be poor due to the effects of oxidation with very low sedimentation rates.

Generally, the CMB was classified into three units on the basis of biological markers.

In the first unit (upper Cretaceous to Paleocene), OM contains inputs of terrigenous higher plants and minor amounts of aquatic plants, mostly angiosperms (herbaceous type), accumulated under fresh water dominated oxic and anoxic conditions with a periodic marine water influence. The occurrences of phytoplanktons are more significant in the late Cretaceous. The contributions of combustion derived PAHs (Fla, Py) are enrichment in the late Cretaceous and absence in the Paleocene. But, high temperature wildfires indicators (BghiP, InPy, and Cor), are relatively abundant, showing that big wildfires frequently occurred in the late Cretaceous and Paleocene. Less abundances of Ret and Pery can suggest small contributions of resinous conifers and arid/semi-arid climatic condition.

The second unit (lower to upper Eocene) contains highly inputs of terrigenous higher plants with lesser amounts of aquatic plants, accumulated under fresh water oxic and anoxic conditions influenced by marine water fluctuation due to eustasic sea level rises in the Eocene. A small contribution of phytoplanktons occurred in the early to middle Eocene and late Eocene (Yaw Fm.). Resinous conifers are slightly abundant. The combustion derived PAHs (Fla, Py), and big wildfires indicators (BghiP, InPy, and Cor) are relatively abundant, indicating intensity of wildfires would be high with a dry season while decreased in the late Eocene suggests wildfires were occasionally lesser frequency due to wet climatic condition. Ret abundances are more significant in the middle Eocene and Pery contents are enrichment in the middle to upper Eocene. This association can indicate less abundant contributions of resinous conifers (i.e. gymnosperms) and warm (dry) to wet (humid/seasonal) climates.

The third unit (Pegu Group: lower Oligocene to upper Miocene) consists of OM having a mixture of terrestrial higher plant materials and aquatic plants deposited in alternating marine and non-marine environments dominated by oxic and anoxic conditions. Planktonic OM are abundant. Gymnosperm vegetations are more significance in the Oligocene mudstones and slightly abundant in the Miocene mudstones. The distribution of combustion derived PAHs (Fla, Py) are relatively abundant in the Oligocene mudstones and scare in the Miocene mudstones. 5- or 6-ring combustion derived PAHs are relatively increasing in the Oligocene (Shwezetaw Fm., Okhmintaung Fm.) and Miocene (Kyaukkok Fm., Obogon Fm.) mudstones. This association can indicate high temperature wildfires occurred in a dry season but occasionally intensity of wildfires would be small under wet condition. Fungi derived Pery are more predomianant in the Oligocene and Miocene (Kyaukkok Fm., Obogon Fm.) mudstones, showing dry (warm) to wet (humid/seasonal) climates. Wet climatic condition could be favourable not only to decrease the occurrence of wildfires but also to occur the widespread growth of conifer trees and tropical rain forests. Ret and Pery are low to high

abundances in the Pegu Group, implying an influence of gymnosperm vegetations under wet condition at that time. The progressively elevated Indo-Myanmar Ranges and Myanmar margins due to collision of Indian with the Eurasia plates after Oligocene would be more potential feature to induce significantly the tropical climate. Therefore, there was a significant shift of climate in the Central Myanmar succession after Oligocene. The climate was dry (warm) in the upper Cretaceous to lower Eocene, whereas middle to upper Eocene and Pegu Group mudstones were under alternating shifts of hot and humid/ seasonal climates.

During the Oligocene -Miocene, it may be due to significantly changes in topographic reliefs affected by collision of Indian plate relative to the Asia plate. On the basis of geochemical data, moderate to high source weathering in the Upper Cretaceous to Miocene mudstones may exhibit alternating shifts of dry (hot) and wet (humid/seasonal) climatic conditions.

Various biomarker maturity parameters indicate that the OM was immature. Vitrinite reflectance data exhibit that upper Cretaceous and lower Eocene (Laungshe Fm.) mudstones have been reached at the mature stage.

On the basis of burial history model, upper Cretaceous - upper Miocene petroleum system can be considered that oil generation may have been started during upper Eocene (approximately 36-39 Ma) and late oil and gas generation would be in the upper Cretaceous to lower Eocene. The subsidence of the Indian oceanic plate beneath the Asia Plate may begin at the end of Plaoecene.

6.3 Source rock compositions, tectonic setting and Paleoclimates

Geochemically, upper Cretaceous to Eocene deposits were mostly generated from mafic to intermediate arc sources, and whereas the Pegu Group represents a from mixture of recycled materials associated with continental island arc (CIA) detritus.

Upper Cretaceous and Paleocene mudstones would be mainlywere sourced from both the tectonically-stable Eurasia Plate and the Myanmar active continental subductive margins. Eocene and Oligocene mudstones have been generated from active continental margins such as uplifted Myanmar (Burmese) margins and Himalaya and partly from passive margin (i.e. Eurasia Plate). Some Oligocene and Miocene mudstones were sourced from both passive margin and Himalaya during active tectonism.

Upper Cretaceous to Eocene materials mainlyare also partly originated from the Myanmar magmatic arc, as they indicate mafic to intermediate sources with CIA signature.

The Pegu Group (Oligocene and Miocene) mudstones and sandstones were probably generated from both Myanmar margins and Himalayan detritus.

Moderate to high intense source weathering in the upper Cretaceous to Miocene mudstones may exhibit reflect alternating shifts of dry (hot) and wet (humid/seasonal) climatic conditions.

REFERENCES

Aizaeshtat, A., 1973. Perylene and its geochemical significance. *Geochim. Cosmochim. Acta* **37**, 559–567.

Alam, M., Alam, M. M., Curray, J. R., Chowdhury, M. L. R. and Gani, M. R., 2003. An overview of the sedimentary geology of the Bengal Basin in relation to the regional tectonic framework and basin─fill history. *Sedimentary Geology* **155**, 179-208.

Amijaya, H. and Littke, R., 2005. Microfacies and depositional environment of Tertiary Tanjung Enim low rank coal, South Sumatra Basin, Indonesia. *International Journal of Coal Geology* **61**, 197–221.

Armstroff A., Wilkes H., Schwarzbauer J., Littke R. and Horsfield B., 2006. Aromatic hydrocarbon biomarkers in terrestrial organic matter of Devonian to Permian age. *Palaeogeography, Palaeoclimatology, Palaeoecology* **240**, 253–274.

Aung, T. T. and Myint, T., 1974. The Stratigraphy of the Western Outcrops- Salin Area: Myanma Oil corporation Report, T.T.A.5, T.Mt.1.

Bauluz, B., Mayayo, M. J., Fernandez-Nieto, C. and Lopez, J. M. G., 2000. Geochemistry of Precambrian and Paleozoic siliciclastic rocks from the Iberian range (NE Spain): implications for source-area weathering, sorting, provenance, and tectonic setting. *Chemical Geology* **168**, 135–150.

Baumard, P., Budzinski, H., Michon, Q., Garrigues, P., Burgeot, T. and Bellocq, J., 1998. Origin and bioavailability of PAHs in the Mediterranean Sea from mussel and sediment records. *Estuarine, Coastal, and Shelf Science* **47**, 77–90.

Bechtel, A., Gruber, W., Sachsenhofer, R. F., Gratzer, R., Lücke, A. and Püttmann, W., 2003. Depositional environment of the Late Miocene Hausruck lignite (Alpine Foreland Basin): insights from petrography, organic geochemistry, and stable carbon isotopes. *International Journal of Coal Geology* **53**, 153–180.

Bender, F., 1983. Geology of Burma. Borntraeger, Berlin, 293 pp.

Berner, R. A., 1984. Sedimentary pyrite formation: An update. *Geochimica et Cosmochimica Acta* **48**, 605–615.

Berner, R. A. and Raisewell, R., 1984. C/S method for distinguishing freshwater from marine sedimentary rocks. *Geology* **12**, 365–368.

Bertrand, O., Montargès-Pelletier, E., Mansuy-Huault, L., Losson, B., Faure, P., Michels, R., Pernot, A. and Arnaud, F., 2013. A possible terrigenous origin for perylene based on a sedimentary record of a pond (Lorraine, France). *Organic Geochemistry* **58**, 69–77.

Bence, A.E., Kvenvolden, K. A., Kennicutt, M. C., 1996. Organic geochemistry applied to environmental assessments of Prince William Sound, Alaska, after the Exxon Valdez oil spill – a review. *Organic Geochemistry* **24**, 7–42.

Bhatia, M. R. and Taylor, S. R., 1981. Trace-element geochemistry and sedimentary provinces: a study from the Tasman geosyncline Australia. *Chemical Geology* **33**, 115–125.

Bhatia, M. R. and Crook, K. A. W., 1986. Trace element characteristics of greywackes and tectonic setting discrimination of sedimentary basins. *Contributions to Mineralogy and Petrology* **92**, 181–193.

Blumer, M., Guillard, R. R. L., Chase, T., 1971. Hydrocarbons of marine phytoplankton. *Marine Biology* **8**, 183–9.

Böcker, J., Littke, R., Hartkopf-Fröder, C., Jasper, K. and Schwarzbauer, J., 2013. Organic geochemistry of Duckmantian (Pennsylvanian) coals from the Ruhr Basin, western Germany. *International Journal of Coal Geology* **107**, 112–126.

Bhatia, M. R. and Crook, K. A. W., 1986. Trace elements characteristics of greywackes and tectonic setting discrimination of sedimentary basins. *Contributions and Mineralogy and Petrology* **92**, 181–93.

Blob A. K., Rulkotter J. and Welte D. U., 1988. Direct determination of the aliphatic carbon content of individual macerals in petroleum source rocks by near-infrared microspectroscopy. *Organic Geochemistry* **13**, 1073-1077.

Budzinski, H., Garrigues, P., Connan, J., Devillers, J., Domine, D., Radke, M. and Oudin, J. L., 1995. Alkylated phenanthrene distributions as maturity and origin indicators in crude oils and rock extracts. *Geochimica et Cosmochimica Acta* **59**, 2043–2056.

Budzinski, H., Jones, I., Bellocq, J., Piérard, C. and Garrigues, P., 1997. Evaluation of sediment contamination by polycyclic aromatic hydrocarbons in the Gironde estuary. *Marine Chemistry* **58**, 85–97.

Cervantes-Uc J. M., Cauich-Rodríguez J. V., Vázquez-Torres H. and Licea-Claveríe A. (2006) *Polymer Degradation and Stability* **91**, 3312-3321.

Chhibber, H. L., 1934. The Geology of Burma. Macmillan, London, 538 pp.

Christiansen J. V., Feldthus A. and Carlsen L., 1995. Flash pyrolysis of coals. Temperature-dependent product distribution. *Journal of Analytical and Appied Pyrolysis* **32**, 51-63.

Clift, P. D. and Plumb, R. A., 2008. The Asian Monsoon: Causes, History and effects. Cambridge University Press, Cambridge 270p.

Cox, R., Lowe, D. R. and Cullers, R. L., 1995. The influence of sediment recycling and basement composition on evolution of mud rock chemistry in the southwestern United States. *Geochimica et Cosmochimica Acta* **59**, 2919–2940.

Copard, Y., Disnar, J. R., Becq-Giraudon, J. F. and Boussafir, M., 2000. Evidence and effects of fluid circulation on organic matter in intramontane coalfields (Massif Central, France). *International Journal of Coal Geology* **44**, 49–68.

Copard, Y., Disnar, J. R., Becq-Giraudon, J. F. and Boussafir, M., 2002. Erroneous maturity assessment given by T_{max} and HI Rock-Eval parameters on highly mature weathered coals. *International Journal of Coal Geology* **49**, 57–65.

Cranwell, P. A., 1977. Organic geochemistry of Camloch (Sutherland) sediments. *Chemical Geology* **20**, 205–221.

Cranwell, P. A., Eglinton, G. and Robinson, N., 1987. Lipids of aquatic organisms as potential contributors to lacustrine sediments-II. *Organic Geochemistry* **11**, 513–527.

Clift, P. D. and Plumb, R. A., 2008. The Asian Monsoon: Causes, History and Effects. Cambridge University Press, Cambridge, 270.

Cox, R., Lowe, D. R. and Cullers, R. L., 1995. The influence of sediment recycling and basement composition on evolution of mudrock chemistry in the southwestern United States. *Geochimica et Cosmochimica Acta* **59**, 2919–40.

Cullers, R. L., Chaudhuri, C., Kilbane, N. and Koch, R., 1979. REE in size fractions and sedimentary rocks of Pennsylvanian-Permian age from the mid-continent of the USA. *Geochimica et Cosmochimica Acta* **43**, 1285–1301.

Cullers, R. L. and Stone, J., 1991. Chemical and mineralogical composition of the Pennsylvanian Mountain, Colorado, USA, (an uplifted continental block) to sedimentary rock from other tectonic environments. *Lithos* **27**, 115–131.

Curiale, J. A., Pe Kyi, Collins I. D., Aung Din, Kyaw Nyein, Maung Nyunt and Stuart, C. J., 1994. The central Myanmar (Burma) oil family – composition and implications for source. *Organic Geochemistry* **22,** 237–255.

Davis, J. B., 1968. Paraffinic hydrocarbons in the sulfate-reducing bacterium *Desulfovibrio desulfuricans*. *Chemical Geoogy* **3**, 155–160.

Del Rio, J. C., Gonzalez-Vila, F. J. and Martin, F., 1992. Variation in the content and distribution of biomarkers in two closely situated peat and lignite deposits. *Organic Geochemistry* **18**, 67–78.

Denis, E. H., Toney, J. L., Tarozo, R., Anderson, R. S., Roach, L. D. and Huang, H., 2012. Polycyclic aromatic hydrocarbons (PAHs) in lake sediments record historic fire events:

validation using HPLC-fluorescence detection. *Organic Geochemistry* **45**, 7–17.

De Souza, D. B., Machado, K. S., Froehner, S., Scapulatempo, C. F. and Bleninger, Y., 2011. Distribution of n-alkanes in lacustrine sediments from subtropical lake in Brazil. *Chemie der Erde* **71**, 171–176.

Didyk, B. M., Simoneit, B. R. T., Brassel, S. C. and Eglinton, G., 1978. Organic geochemical indicators of palaeonvironmental conditions of sedimentation. *Nature* **272**, 216–222.

Dzou, L. I. P., Noble, R. A. and Senftle, J. T., 1995. Maturation effects on absolute biomarker concentration in a suite of coals and associated vitrinite concentrates. *Organic Geochemistry* **23**, 681–697.

Eglinton, G., Hamilton R. J.,1967. Leaf epicuticular waxes. *Science* **156**, 1322–1335.

Everett, J. R., Russell, O. R., Staskowski, R. J., Loyd, S. P., Tabbutt, V. M., Dolan, P. and Stein, A., 1990, Regional tectonics of Myanmar (Burma) and adjacent areas: *American Association of Petroleum Geologists Bulletin*, v. 74, no. 5, p. 651.

Fabiańska, M. J., Ćmiel, S. R. and Misz-kennan, M., 2013. Biomarkers and aromatic hydrocarbons in bituminous coals of Upper Silesian Coal Basin: Example from 405 coal seam of the Zaleskie Beds (Poland). *International journal of Coal Geology* **107**, 96–111.

Faure P., Landais P. and Griffault L., 1999. Behavior of organic matter from Callovianshales during low-temperature air oxidation. *Fuel* **78**, 1515-1525.

Fedo, C. M., Nesbitt, H. W. and Young, G. M., 1995. Unraveling the effects of potassium metasomatism in sedimentary rocks and paleosols, with implications for paleoweathering conditions and provenance. *Geology* **23**, 921–924.

Ficken, K. J., Barber, K. E. and Eglinton, G., 1998. Lipid biomarker and plant macrofossil stratigraphy of a Scottish montane peat bog over the last two millennia. *Organic Geochemistry* **28**, 217–237.

Ficken, K. J., Li, B., Swain, D. L. and Eglinton, G., 2000. An n-alkane proxy for the sedimentary input of submerged/floating freshwater aquatic macrophytes. *Organic Geochemistry* **31**, 745–749.

Finkelstein, D. B., Pratt, L. M., Curtin, T. M. and Brassell, S. C., 2005. Wildfires and seasonal aridity recorded in Late Cretaceous strata from south-eastern Arizona, USA. *Sedimentology* **52**, 587–599.

Fujii S., Dsawa Y. and Sugimura H., 1970. Infrared spectra of Japanese coal: the absorption bands at 3030, 2920, and 1600 cm^{-1}. *Fuel* **43**, 48-75.

Ganz, H., Kalkreuth, W., 1987. Application of infrared spectroscopy to the classification of kerogen-types and the evolution of source rock and oil–shale potentials. *Fuel* **66**, 708–711.

Grice, K., Lu, H., Atahan, P., Asif, M., Hallmann, C., Greenwood, P., Maslen, E., Tulipani, S., Williford, K. and Dodson, J., 2009. New insights into the origin of perylene in geological samples. *Geochimica et Cosmochimica Acta* **73**, 6531–6543.

Grice, K., Nabbefeld, B. and Maslen, E., 2007. Source and significance of selected polycyclic aromatic hydrocarbons in sediments (Hovea-3 well, Perth Basin, Western Australia) spanning the Permian-Triassic boundary. *Organic Geochemistry* **38**, 1795–1803.

Grimalt, J. O., Drooge, B. L. V., Ribes, A., Fernández, P., Appleby, P., 2004. Polycyclic aromatichydrocarboncompositioninsoilsandsedimentsofhighaltitudelakes. *Environmental Pollution* **131**, 13–24.

Guo Y. and Bustin R. M., 1998. Micro-FTIR spectroscopy of liptinitemacerals in coal. *International Journal of Coal Geology* **36**, 259-275.

Hadden, R. L., 2008. The Geology of Burma (Myanmar): An annotated Bibliography Burma's Geology, Geography and Earth Science. Topographic Engineering Center,

Engineer Research and Development Center 7701 Telegraph Road Alexandria, Virgina 22315.

Herron, M. M., 1988. Geochemical classification of terrigenous sands and shales from core or log data. *Journal of Sedimentary Petrology* **58**, 820–9.

Haq, B. U., Hardenbol, J. and Vail, P. R., 1987. Chronology of fluctuating sea levels since the Triassic. *Science* **235**, 1156–1167.

Hall, R. and Morley, C. K., 2004. Sundaland Basins. Continent Ocean Interactions within East Asian Marginal Seas (Clift, P., Wang, X., Kuhnt, W. and Hayes, D., eds), Amer. Geophys. Union, *Geophysical Monograph Series* **149**, 55–85.

Hautevelle, Y., Michels, R., Malartre, F. and Trouiller, A., 2006. Vascular plant biomarkers as proxies for palaeoflora and palaeoclimatic changes at the Dogger/Malm transition of the Paris Basin (France). *Organic Geochemistry* **37**, 610–625.

Hites, R. A., Laflamme, R. E., Farrington, J. W., 1977. Sedimentary polycyclic aromatic hydrocarbons: the historical records. *Science* **198**, 829–831.

Hossain, H. M. Z., Sampei, Y. and Roser, B. P., 2013. Polycyclic aromatic hydrocarbons (PAHs) in late Eocene to early Pleistocene mudstones of the Sylhet succession, NE Bengal Basin, Bangladesh: Implications for source and paleoclimate conditions during Himalayan uplift. *Organic Geochemistry* **56**, 25–39.

Huang, W. Y., and Meinschein, W. G., 1978. Sterols in sediments from Baffin Bay, Texas. *Geochimica et Cosmochimica Acta* **42**, 1391–1396.

Huang, W. Y. and Meinschein, W. G., 1979. Sterols as ecological indicators. *Geochimica et Cosmochimica Acta* **43**, 739–745.

Hughes, W. B., Holba, A. G. and Dzou, L. I. P., 1995. The ratios of dibenzothiophene to phenanthrene and pristane to phytane as indicators of depositional environment and lithology of petroleum source rocks. *Geochimica et Cosmochimica Acta* **59**, 3581–3598.

Hunt, J. M., 1991. Generation of gas and oil from coal and other terrestrial organic matter. *Organic Geochemistry* **17**, 673–680.

Ibarra J. V., Muňoz E. and Moliner R., 1996. FTIR study of the evolution of coal structure during the coalification process. *Organic Geochemistry* **24**, 725-735.

Jackson W. R., Bongers G. D., Redlich P. J., Favas G., Fei Y., Patti A. F. and Johns R. B., 1996. Characterization of brown coals, humid acids, and modified humid acids using GCMS and other techniques. *International Journal of Coal Geology* **32**, 229-240.

Jenisch-Anton A., Adam P., Schaeffer P. and Albrecht P., 1999. Oxygen containing subunits in sulfur-rich nonpolar macromolecules. *Geochimica et Cosmochimica Acta* **63**, No7/8 , 1059-1074.

Jiang, C., Alexander, R., Kagi, R. I., Murray, A. P., 1998. Polycyclic aromatic hydrocarbons in ancient sediments and their relationships to paleoclimate. *Organic Geochemistry* **29**, 1721–1735.

Jiang, C., Alexander, R., Kagi, R. I. and Murray, A. P., 2000. Origin of perylene in ancient sediments and its geological significance. *Organic Geochemistry* **31**, 1545–1559.

Katz B. J., 1983. Limitations of 'Rock-Eval'pyrolysis for typing organic matter. *Organic Geochemistry* **4**, 195-199.

Kawka, O. E. and Simoneit, B. R. T., 1990. Polycyclic aromatic hydrocarbons in hydrothermal petroleums from the Guaymas Basin spreading center. *Applied Geochemistry* **5**, 17–27.

Khin, J. A., 1991. Hydrocarbon-producing formations of Salin, Irrawaddy, and Martaban Basins, Myanmar (Burma): Society of Petroleum Engineers Asia-Pacific Conference, Perth, Australia, November 4–7, 1991; Conference Proceedings, p. 245–258.

Killops, S. and Killops, V., 2005. Introduction to Organic Geochemistry. 2nd ed. Blackwell Publishing, 393 pp.

Killops, S. D. and Massoud, M. S., 1992. Polycyclic aromatic hydrocarbons of pyrolytic origin in ancient sediments: evidence for Jurassic vegetation fires. *Organic Geochemistry* **18**, 1–7.

Koopmans, M. P., Rijpstra, W. I. C., Klapwijk, M. M., de Leeuw, J. W., Lewan, M. D. and Sinninghe Damsté, J. S., 1999. A thermal and chemical degradation approach to decipher pristane and phytane precursors in sedimentary organic matter. *Organic Geochemistry* **30**, 1089–1104.

Kuder T., Kruge M. A., Shearer J. C. and Miller S. L., 1998. Environmental and botanical controls on peatification—a comparative study of two New Zealand restiad bogs using Py-GC/MS, petrography and fungal analysis. *International Journal of Coal Geology* **37**, 3-27.

Laflamme, R. E. and Hites, R. A., 1978. The global distribution of polycyclic aromatic hydrocarbons in recent sediments. *Geochimica et Cosmochimica Acta* **42**, 289–303.

Licht, A., Cojan, I., Caner, L., A. N. Soe, Jaeger, J. J. and France-Lanord, C., 2013. Role of permeability barriers in alluvial hydromorphic palaeosols: The Eocene Pondaung Formation, Myanmar. *Sedimentology* 1–21.

Licht, A., Cojan, I., Caner, L., A. N. Soe, Jaeger, J. J. and France-Lanord, C., 2013. A paleo Tibet -Myanmar connection? Reconstructing the Late Eocene drainage system of central Myanmar using a multi-proxy approach. *Journal of the Geological Society, London* 1–11.

Lidgard, S. and Crane P. R., 1988. Quantitative analyses of the early angiosperm radiation. *Nature* **331**, 344–346.

Liu, G. Q., Zhang, G., Li, X. D., Li, J., Peng, X. Z. and Qi, S. H., 2005. Sedimentary record of polycyclic aromatic hydrocarbons in a sediment core from the Pearl River Estuary, South China. *Mar. Poll. Bull.* **51**, 912–921.

Lücke, A., Helle, G., Schleser, G. H., Figueiral, I., Mosbrugger, V., Jones, T. P. and Rowe, N. P., 1999. Environmental history of the German Lower Rhine Embayment during the Middle Miocene as reflected by carbon isotopes in brown coal. *Palaeogeography, Palaeoclimatology, Palaeoecology* **154**, 339–352.

Mae K., Maki T., Okutsu H. and Miura K., 2000. Examination of relationship between coal structure and pyrolysis yields using oxidized brown coals having different macromolecular networks. *Fuel* **70**, 417-425.

Martínez, M. and Escobar, M., 1995. Effect of coal weathering on some geochemical parameters. *Organic Geochemistry* **23**, 253–261.

Marynowski, L., Smolarek, J., Bechtel, A., Philippe, M. and Kurkiewicz, S., 2013. Perylene as an indicator of conifer fossil wood degradation by wood-degrading fungi. *Organic Geochemistry* **59**, 143–151.

Marynowski, L., Szeląg, E., Jędrysek, M. O. and Simoneit, B. R. T., 2011. Effects of weathering on organic matter. Part II: Fossil wood weathering and implications for organic geochemical and petrographic studies. *Organic geochemistry* **42**, 1076–1088.

Matsumoto, G. I., Akiyama, M., Watanuki, K. and Torii, T., 1990. Unusual distribution of long-chain n-alkanes and n-alkanes in Antarctic soil. *Organic Geochemistry* **15**, 403–412.

McLennan, S. M., Hemming, S., McDaniel, D. K. and Hanson, G. N., 1993. Geochemical approaches to sedimentation, provenance, and tectonics. *Geological Society of America Special Paper* **284**, 21–40.

Mello, M. R., Koutsoukos, E. A. M., Hart, M. B., Brassell, S. C. and Maxwell, J. R., 1989. Late Cretaceous anoxic events in the Brazilian continental margin. *Organic Geochemistry* **14**, 529–542.

Meng, J., Wang, C., Zhao, X., Coe, R., Li, Y. and Finn, D., 2012. India-Asia collision was at 24˚N and 50 Ma: palaeomagnetic proof from southernmost Asia. Scientific Reports 2, 925 *Sedimentary Geology* **155**, 209–226

Me´ties, G., Soe, A. N. and Ducrocq, S., 2006. A new basal tapiromorph (Perissodactyla, Mammalia) from the middle Eocene of Myanmar. *Geobios* **39**, 513–519.

Meyers, P. A., 1994. Preservation of elemental and isotopic source identification of sedimentary organic matter. *Chemical Geology* **113**, 289–302.

Meyers, P. A., 1997. Organic geochemical proxies of paleoceanographic, paleolimnologic, and paleoclimatic processes. *Organic Geochemistry* **27**, 213–250.

Meyers, P. A. and Ishiwatari, R., 1993. Lacustrine organic geochemistry – an overview of indicators of organic matter sources and diagenesis in lake sediments. *Organic Geochemistry* **20**, 867–900.

Mitchell, A. H. G., 1993. Cretaceous- Cenozoic tectonic events in the western Myanmar (Burma)- Assam region. *Journal of the Geological Society*, London **150**, 1089–1102.

Mitchell, A. H. G., Chung, S. L., OO, T., Lin, T. H. and Hung, C. H., 2012. Zircon U-Pb ages in Myanmar: magmatic-metamorphic events and the closure of a Neo-Tethys Ocean? *Journal of Asian Earth Sciences* **56**, 1–23.

Moldowan, J. M. et al., 1994.. The molecular fossil record of oleanane and its relation to angiosperms. *Science* **265**, 768–771.

Moldowan, J. M., Dahl, J., Huizinga, B. J., Fago, F. J., Hickey, L. J., Peakman, T. M. and

Taylor, D. W., 1994. The molecular fossil record of oleanane and its relation to angiosperms. *Science* **265**, 768–771.

Moldowan, J. M., Sundararaman, P. and Schoell, M., 1986. Sensitivity of biomarker properties to depositional environment and/or source input in the Lower Toarcian of SW-Germany. *Organic Geochemistry* **10**, 915–926.

Mrkić, S., Stojanović, K., Kostić, A., Nytoft, H. P. and Šajnović, A., 2011. Organic geochemistry of Miocene source rocks from the Banat Depression (SE Pannonian Basin, Serbia). *Organic Geochemistry* **42**, 655–677.

Müller, P. J., 1977. C/N ratios in Pacific deep-sea sediments: effect of inorganic ammonium and organic nitrogen compounds sorbed by clays. *Geochimica et Cosmochimica Acta* **41**, 765–776.

Murray, A. P., Summons, R. E., Boreham, C. J. and Dowling, L. M., 1994. Biomarker and n-alkane isotope profiles for Tertiary oils: relationship to source rock depositional setting. *Organic Geochemistry* **22**, 521–542.

Myint, K. K. and Soe, K., 1977. Geology report on Tilin-Gangaw Area: Myanma Oil Corporation Report, K. K. M. 2, K. S. 1.

Najman, Y., Appel, E., Boudagher-Fadel, M., Bown, P., Carter, A., Garzanti, E., Godin,L., Han, J., Liebke, U., Oliver, G., Parrish, R. and Vezzoli, G., 2010.TimingofIndia-Asia collision: geological, biostratigraphic and palaeomagnetic constraints. *Journal of Geophysical Research* **115**, B12416

Nakamura, H., Sawada, K. and Takahashi, M., 2010. Aliphatic and aromatic terpenoid biomarkers in Cretaceous and Paleogene angiosperm fossils from Japan. *Organic Geochemistry* **41**, 975–980.

Nesbitt, H. W. and Young, G. M., 1982. Early Proterozoic climates and plate motions inferred from major element chemistry lutites. *Nature* **299**, 715–717.

Nesbitt, H. W. and Young, G. M., 1984. Prediction of some weathering trends of plutonic and volcanic rocks based on thermodynamic and kinetic considerations. *Geochimica et Cosmochimica Acta* **48**, 1523–1534.

Nesbitt, H. W., Young, G. M., McLennan, S. M. and Keays, R. R., 1996. Effects of chemical

Weathering and sorting on the petrogenesis of siliciclastic sediments, with implications for provenance studies. *Journal of Geology* **104**, 525–542.

Noble, R. P., Alexander, R., Kagi, R. I. and Knox, J., 1986. Identification of some diterpenoid hydrocarbons in petroleum. *Organic Geochemistry* **10**, 825–829.

Nott, C. J., Xie, S., Avsejs, L. A., Maddy, D., Chambers, F. M. and Evershed, R. P., 2000. n-Alkane distributions in ombrotrophic mires as indicators of vegetation change related to climate variation. *Organic Geochemistry* **31**, 231–235.

Otto, A. and Simoneit, B. R. T., 2001. Chemosystematics and diagenesis of terpenoids in fossil conifer species and sediment from the Eocene Zeitz Formation, Saxony, Germany. *Geochim. Cosmochim. Acta* **65**, 3505–3527.

Otto, A., Walter, H. and Püttmann, W., 1997. Sesqui- and diterpenoid biomarkers preserved in *Taxodium*-rich Oligocene oxbow lake clays, Weisselster basin, Germany. *Organic Geochemistry* **26**, 105–115.

Otto, A., Simoneit, B. R. T. and Rember, W. C., 2003. Resin compounds from the seed cones of three fossil conifer species from the Miocene Clarkia flora, Emerald Creek, Idaho, USA, and from related extant species. *Rev. Palaeobot. Palynol.* **126**, 225–241.

Painter P. C., Coleman M. M., Jenkins R. G. and Walker P. L., 1978. Fourier transform infrared studies of acid-demineralized coal. *Fuel* **57**, 125-126.

Pettijohn, F. J., Potter, P.E. and Siever, R. 1987. Sand and Sandstone. Springer-Verlag, New York.

Petsch, S. T., Berner, R. A. and Eglinton, T. I., 2000. A field study of the chemical weathering of ancient sedimentary organic matter. *Organic Geochemistry* **31**, 475–487.

Peters, K. E., 1986. Guidelines for evaluating petroleum source rock using programmed pyrolysis. *AAPG Bull.* **70**, 318–329.

Peter, K. E. and Cassa, M. R., 1994. Applied source rock geochemistry. In: Magoon, L. B., Dow, W. E. (Eds.). The Petroleum System – From Source to Trap. *AAPG Memoir* **60**, 93–120.

Peters, K. E. and Moldowan, J. M., 1993. The Biomarker Guide: Interpreting Molecular Fossils in Petroleum and Ancient Sediments. Prentice Hall, New Jersey, 363 pp.

Peters, K. E., Walters, C. C. and Moldowan, J. M., 2005. The Biomarker Guide, 2nd ed., Prentice Hall, New Jersey, 1155 pp.

Philp, R. P. and Gilbert, T. D., 1986. Biomarker distributions in Australian oils predominantly derived from terrigenous source material. *Organic Geochemistry* **10**, 73–84.

Piedad-Sánchez, N., Suárez-Ruiz, I., Martínez, L., Izart, A., Elie, M. and Keravis, D., 2004. Organic petrology and geochemistry of the Carboniferous coal seams from the Central Austrian Coal Basin (NW Spain). *International Journal of Coal Geology* **57**, 211–242.

Pivnik, D. A., Nahm, J., Tucker, R. S., Smith G. O., Nyein K., Nyunt M. and Maung P. H., 1998. Polyphase deformation in a fore-arc/back-arc basin, Salin sub-basin, Myanmar (Burma). *AAPG Bull.* **82**, 1837–1856.

Powell, T. G., 1988. Pristane /phytane ratio as environmental indicator. *Nature* **333**, 604.

Prasad, M., 1993. Siwalik (Middle Miocene) woods from the Kalagarh area in the Himalayan foot hills and their bearing on palaeoclimate and phytogeography. *Review of Paleobotany and Palynology* **76**, 49–82.

Prahl, F. G. and Carpenter, R., 1983. Polycyclic aromatic hydrocarbon (PAH)-phase associations in Washington coastal sediments. *Geochimica et Cosmochimica Acta* **47**, 1013–1023.

Quirk, M. M., Wardroper, A. M. K., Wheatley R. E. and Maxwell J. R., 1984. Extended hopanoids in peat environments. *Chemical Geology* **42**, 25–43.

Radke, M. and Welte, D. H., 1983. The Methylphenanthrene Index (MPI): a maturity parameter based on aromatic hydrocarbons. In: Bjorøy M. et al. (Eds.), *Advances on Organic Geochemistry* 1981. John Wiley and Sons, New York, pp. 504–512.

Radke, M., Welte, D. H. and Willsch, H., 1982a. Geochemical study on a well in the Western Canada Basin: relation of the aromatic distribution pattern to maturity of organic matter. *Geochimica et Cosmochimica Acta* **46**, 1–10.

Radke, M., Willsch H. and Leythaeuser D., 1982. Aromatic components of coal: relation of distribution pattern to rank. *Geochimica et Cosmochimica Acta* **46**, 1831–1848.

Ramanampisoa, L., Radke, M., Schaefer, R. G., Littke, R., Rullkötter, J. and Horsfield, B., 1990. Organic-geochemical characterization of sediments from the Sakoa coalfield, Madagascar. *Organic Geochemistry* **16**, 235–246.

Robinson, N., Cranwell, P. A., Finlay, B. J. and Eglinton, G., 1984. Lipids of aquatic organisms as potential contributors to lacustrine sediments. *Organic Geochemistry* **6**, 143–152.

Rochdi A. and Landais P., 1991. Transmission micro-infrared spectroscopy: an efficient tool for microsample characterization of coal. *Fuel* **70**, 367-371.

Roser, B. P. and Korsch, R. J., 1986. Determination of tectonic setting of sandstone and mudstone suites using SiO_2 and K_2O/Na_2O ratio. *Journal of Geology* **94**, 635–50.

Roser, B. P. and Korsch, R. J., 1988. Provenance signatures of sandstones-mudstone suites determined using discriminant function analysis of major-element data. *Chemical Geology* **67**, 119–139.

Roy, D. K. and Roser, B. P., 2013. Climatic control on the composition of Carboniferous–Permian Gondwana sediments, Khalaspir basin, Bangladesh. *Gondwana Research* **23**, 1163–1171.

Rullikötter, J., Peakman, T. M. and ten Haven, H. L., 1994. Early diagenesis of terrigenous triterpenoids and its implications for petroleum geochemistry. *Organic Geochemistry* **21**, 215–233.

Sampei, Y. and Matsumoto, E., 2001. C/N ratios in a sediment core from Nakaumi lagoon, southwest Japan─usefulness as an organic source indicator. *Geochemical Journal* **35**, 189–205.

Sampei Y., Suzuki, N., Mori, K., Nakai, T. and Sekiguchi K., 1994. Methylphenanthrenes from MITI Takadaheiya well and thermally altered Kusanagi shales by dolerite intrusion in Northeast Japan. *Geochemical Journal* **28**, 317–331.

Seifert, W. K. and Moldowan, J. M., 1978. Applications of steranes, terpanes, and monoaromatics to the maturation, migration, and source of crude oils. *Geochimica et Cosmochimica Acta* **42**, 77–95.

Seifert, W. K. and Moldowan, J. M., 1986. Use of biological markers in petroleum exploration. In R.B. Johns (Ed). *Methods in Geochemistry and Geophysics*, (Vol.24) (pp. 261–290).

Sicre, M. A., Marty, J. C., Saliot, A., 1987. Aliphatic and aromatic hydrocarbons in different sized aerosols over the Mediterranean Sea: occurrence and origin. *Atmospheric Environment* **21**, 2247–2259.

Silliman, J. E., Meyers, P. A. and Eadie, B. J., 1998. Perylene: an indicator of alternation processes or precursor materials? *Organic Geochemistry* **29**, 1737–1744.

Silliman, J. E., Meyers, P. A., Ostrom, P. H., Ostrom, N. E. and Eadie, B. J., 2000. Insights into the origin of perylene from isotopic analyses of sediments from Saanich Inlet,

British Columbia. *Organic Geochemistry* **31**, 1133–1142.

Simoneit, B. R. T., 1998. Biomarker PAHs in the environment. In: Neilson, A. (Ed.), The Handbook of Environmental Chemistry, Vol. 3, Part I. Springer Verlag, Berlin, pp.175–221.

Simoneit, B. R. T., 2005. A review of current applications of mass spectrometry for biomarker/molecular tracer elucidation. *Mass Spec. Rev.* **24**, 719–765.

Simoneit, B. R. T., Grimalt, J. G., Wang, T. G., Cox, R. E., Hatcher, P. G. and Nissenbaum, A., 1986. Cyclic terpenoids of contemporary resinous plant detritus and fossil woods, ambers and coals. *Organic Geochemistry* **10**, 877–889.

Soe, A. N., Myitta, S. T., Tun, A. K., Aung, T., Thein, B., Marandat, S., Ducrocq, J.-J, Jaeger., 2002. Sedimentary facies of the Late Middle Eocene Pondaung Formation (central Myanmar) and the paleoenvironments of its Anthropoid Primates. C.R. Palevol 1, 153–160.

Stamp, L. D., 1934. Natural gas fields of Burma. *AAPG Bull.* **18**, 315–326.

Standley, L. J. and Simoneit, B. R. T., 1994. Resin diterpenoids as tracers for biomass combustion aerosols. *Journal of Atmospheric Chemistry* **18**, 1–15.

Stefanova, M., Kortenski, J., Zdravkov, A. and Marinov, S., 2013. Paleoenvironmental settings of the Sofia lignite basin: Insights from coal petrography and molecular indicators. *International Journal of Coal Geology* **107**, 45–61.

Stout, S. A., Emsbo-Mattingly, S. D., 2008. Concentration and character of PAHs and other hydrocarbons in coals of varying rank – implications for environmental studies of soils and sediments containing particulate coal. *Organic Geochemistry* **39**, 801–819.

Suzuki, N., Yessalina, S. and Kikuchi, T., 2010. Probable fungal origin of perylene in Late Cretaceous to Paleogene terrestrial sedimentary rocks of northeastern Japan as indicated from stable carbon isotopes. *Organic Geochemistry* **41**, 234–241.

Szczerba, M. and Rospondek, M. J., 2010. Controls on distribution of methyl-phenanthrenes in sedimentary rock extracts: Critical evaluation of existing geochemical data from molecular modeling. *Organic geochemistry* **41**, 1297–1311.

Takeda N. and Asakawa T., 1988. Study of petroleum generation by pyrolysis─ I. Pyrolysis experiments by Rock-Eval and assumption of molecular structural change of kerogen using ^{13}C-NMR. *Applied Geochemistry* **3**, 441-453.

Tissot, B. P. and Welte, D. H., 1984. Petroleum Formation and Occurrence, 2nd ed. Springer-Verlag, Berlin, 699 pp.

Trevena, A. S. and Varga, R. J., 1991. Tertiary tectonics sedimentation in the Salin (fore-arc) basin, Myanmar (abs): *AAPG bulletin*, v.75, p. 683.

Htut, T., 2008. Generalized Central Myanmar Basin Reference section based on MOGE field and Lab data (1997).

Tun, P., 1968. Stratigraphic measurements of Western outcrops – Kyauktu-Laungshe Area: Myanma Oil Corporation Report, P. T. 1.

van Aarssen, B. G. K., Alexander, R. and Kagi, R. I., 2000. Highrt plant biomarkers reflect palaeovegetation changes during Jurassic times. *Geochimica et Cosmochimica Acta* **64**, 1417–1424.

Van Krevelen, D.W., 1961. Coal: typology-chemistry-physics-constitution: Elsevier Science, Amsterdam, 514 p.

Volkman, J. K., Barrett, S. M., Blackburn, S. I., Mansour, M. P., Sikes, E. L. and Gelin, F., 1998. Microalgal biomarkers: a review of recent research developments. *Organic Geochemistry* **29**, 1163–1179.

Volkman, J. K., 2003. Sterols in microorganisms. *Applied Microbiology and Biotechnology* **60**, 496–506.

Wakeham, S. G., Schaffner, C. and Giger, W., 1980. Polycyclic aromatic hydrocarbons in Recent lake sediments—II. Compounds derived from biogenic precursors during early diagenesis. *Geochimica et Cosmochimica Acta* **44**, 415–429.

Wang, B., Fan, S., Xu, F., Jiang, S., Fu, J., 1983. A preliminary organic geochemical study of the Fushan depression, A tertiary basin of eastern China. In: Advances in Organic Geochemistry 1981, pp. 108–113.

Wang S., Tang Y., Schobert H. H., Guo Y. and Lu X., 2013. FTIR and simultaneous TG/MS/FTIR study of Late Permian coals from Southern China. *Journal of Analytical and Applied Pyrolysis* **100**, 75–80.

Waseda, A. and Nishita, H., 1998. Geochemical characteristics of terrigenous- and marine-sourced oils in Hokkaido, Japan. *Organic Geochemistry* **28**, 27–41.

Widodo, S., Bechtel, A., Anggayana, K. and Püttmann, W., 2009. Reconstruction of floral changes during deposition of the Miocene Embalut coal from Kutai Basin, Mahakam Delta, East Kalimantan, Indonesia by use of aromatic hydrocarbon composition and stable carbon isotope ratios of organic matter. *Organic Geochemistry* **40**, 206–218.

Wronkiewicz, D. J. and Condie, K. C., 1987. Geochemistry of Archean shales from the Witwatersrand Supergroup, South Africa: Source-area weathering and provenance. *Geochimica et Cosmochimica Acta* **51**, 2401–2416.

Waseda, A. and Nishita, H., 1998. Geochemical characteristics of terrigenous- and marine-sourced oils in Hokkaida, Japan. *Organic Geochemistry* **28**, 27–41.

Youngblood, W. W., Blumer, M., 1975. Polycyclic aromatic hydrocarbons in the environment: homologous series in soils and recent sediments. *Geochimica et Cosmochimica Acta* **39**, 1303–1314.

Yunker, M. B., Macdonald, R. W., Vingarzan, R., Mitchell, R. H., Goyette, D. and Sylvestre, S., 2002. PAHs in the Fraser River basin: a critical appraisal of PAH ratios as indicators

of PAH source and composition. *Organic Geochemistry* **33**, 489–515.

Yunker, M. B., Macdonald, R. W., Snowdon, L. R. and Fowler, B. R., 2011a. Alkane and PAH biomarkers as tracers of terrigenous organic carbon in Arctic Ocean sediments. *Organic Geochemistry* **42**, 1109–1146.

Zdravkov, A., Bechtel, A., Sachsenhofer, R. F., Kortenski, J. and Gratzer, R., 2011. Vegetation differences and diagenetic changes between two Bulgarian lignite deposits-Insights from coal petrology and biomarker composition. *Organic Geochemistry* **42**, 237–254.

Zheng, Y., Zhou, W., Meyers, P. A. and Xie, S., 2007. Lipid biomarkers in the Zoige-Hongyuan peat deposit: indicators of Holocene climate changes in West China. *Organic Geochemistry* **38**, 1927–1940.